IL
NUOVO CIMENTO
ORGANO DELLA SOCIETÀ ITALIANA DI FISICA
SOTTO GLI AUSPICI DEL CONSIGLIO NAZIONALE DELLE RICERCHE

VOL. III, N. 2 *Serie decima* 1° Febbraio 1956

Hydrodynamical Description of the Dirac Equation.

T. TAKABAYASI

Physical Institute, Nagoya University - Nagoya (Japan)

(ricevuto il 26 Maggio 1955)

Summary. — By suppressing ψ-spinor and γ-matrices completely, the Dirac field is shown to be equivalent with a non-linear vector field, which is fully interpreted as defining a new kind of relativistic hydrodynamics of a spinning fluid. In this hydrodynamics, there appears, besides spin, an additional internal degree of freedom θ, which specifies the disparatenesses between rest charge density and proper mass density and also between velocity and momentum. The theory is described for the case of Dirac field under the action of Maxwell field, manifesting also the gauge-independent feature of the formulation.

1. – Introduction.

From the point of view of cultivating the meaning of quantum theory or the concept of spinor field, it would be in itself an important problem to reformulate the Dirac field in a tensor form completely and thereby to bring to light the picture in classical sense underlying the Dirac field.

Such formulation will push forward a new aspect of the Dirac field, and as a result may provide also a useful method for practical applications to certain sort of problems. Furthermore we might expect that it would give some suggestions for the future progress of the quantum theory itself.

Various investigations [1-3] related to the above mentioned problem have

(1) E. T. WHITTAKER: *Proc. Roy. Soc.*, A **158**, 38 (1937).
(2) W. KOFINK: *Ann. der Phys.*, **38**, 421, 436, 565, 583 (1940).
(3) O. COSTA DE BEAUREGARD: *Thèse* (Paris, 1943).

been done in the last decades, yet, as far as the author knows, none of them is sufficient for the present purpose. They did not arrive at any formulation which is mathematically closed and physically fully interpreted.

However, the goal has been reached in our previous note ([4]) where it has been shown that the Dirac field can be formulated in a definite hydrodynamical form. In the present note we shall enlarge the method.

In the first place we extend our formulation previously described for free Dirac equation to the case with interaction. The extension is extremely simple: the equations of motion are not at all altered in form. In other words, our formulation has a remarkable feature that it is not only *explicitly gauge-invariant* but also here the electromagnetic field quantities perfectly *disappear* from the equations of motion for our hydrodynamical field.

In the second, the physical meaning of the formalism is made clearer, especially through considerations in which the energy momentum tensor is concerned. The complicated structure of our hydrodynamics is interpreted on the basis of the assumptions of the *spin* distribution (*) and the *disparity* between velocity and momentum.

For the deductions of our results, the mathematical preliminaries furnished by the former investigation ([2,5-7]) had also to be developed in various respects (+), though we do not enter into them here.

The present formulation may be regarded as the extension of the hydrodynamical methods, developed for the cases of relativistic scalar equation ([8]) (Klein-Gordon equation) on the one hand and of non-relativistic spinor equation ([9]) on the other, to the case of Dirac equation.

For the present we treat the Dirac field in c-number theory, corresponding to the quantum mechanics of a single Dirac particle.

2. – Formalism ([4]).

The Dirac spinor wave function ψ can be represented by the set of following gauge-invariant tensor quantities. Namely, ten bilinear quantities

---

([4]) T. TAKABAYASI: *Prog. Theor. Phys.*, **13**, 222 (1955).

(*) In our formulation « spin » means intrinsic angular momentum which is considered to distribute in space.

([5]) W. PAULI: *Ann. Inst. H. Poincaré*, **6**, 109 (1936).

([6]) G. PETIAU: *Journ. Math. pures et appl.*, **25**, 335 (1946); **26**, 1 (1947).

([7]) T. TAKABAYASI: *Prog. Theor. Phys.*, **13**, 106 (1955).

(+) For instance, the presence of the kinematical identity (6), which is essential for our formulation, has been overlooked by other authors.

([8]) T. TAKABAYASI: *Prog. Theor. Phys.*, **9**, 187 (1953).

([9]) T. TAKABAYASI: *Prog. Theor. Phys.*, **12**, 810 (1954).

without differentiation (+):

$$\begin{cases} \Omega = \bar{\psi}\psi\,, & \hat{\Omega} = i\bar{\psi}\gamma^5\psi\,, \\ S_\mu = i\bar{\psi}\gamma^\mu\psi\,, & \hat{S}_\mu = i\bar{\psi}\gamma^5\gamma^\mu\psi\,, \end{cases}$$

and four bilinear quantities involving differentiation $\partial_\mu = \partial/\partial x_\mu$:

$$J_\mu = \frac{i}{2\varkappa}(\partial_\mu\bar{\psi}\cdot\psi - \bar{\psi}\partial_\mu\psi) - \varepsilon A_\mu\Omega\,, \tag{2}$$

$$(\varkappa = mc/\hbar,\ \varepsilon = e/mc^2)$$

where A_μ is the electromagnetic potential.

In place of (1) we may also adopt the quantities:

$$\begin{cases} a)\ \text{scalar} & P = (\Omega^2 + \hat{\Omega}^2)^{\frac{1}{2}}\,, \\ b)\ \text{pseudoscalar} & \theta = \operatorname{tg}^{-1}(\hat{\Omega}/\Omega)\,, \\ c)\ \text{vector} & v_\mu = S_\mu/P\,, \\ d)\ \text{pseudovector} & w_\mu = \hat{S}_\mu/P\,, \end{cases} \tag{3}$$

where v_μ and w_μ satisfy the kinematical identities:

$$\begin{cases} a) & v_\mu v_\mu = -1\,, \qquad (v_0 \equiv v_4/i > 0)\,, \\ b) & w_\mu w_\mu = 1\,, \\ c) & v_\mu w_\mu = 0\,. \end{cases} \tag{4}$$

Likewise, in place of (2), we may take the vector:

$$k_\mu = (\Omega J_\mu + \hat{\Omega}\hat{J}_\mu)/P^2\,, \tag{5}$$

where $\hat{J}_\mu = -1/2\varkappa(\partial_\mu\bar{\psi}\gamma^5\psi - \bar{\psi}\gamma^5\partial_\mu\psi) - \varepsilon A_\mu\bar{\Omega}$. The k_μ's satisfy the kinematical identities:

$$\partial_\mu k_\nu - \partial_\nu k_\mu = -\frac{i}{2\varkappa}\varepsilon_{\alpha\beta\gamma\delta}v_\alpha w_\beta(\partial_\mu v_\gamma\partial_\nu v_\delta - \partial_\mu w_\gamma\partial_\nu w_\delta) - \varepsilon F_{\mu\nu}\,, \tag{6}$$

(+) Greek suffix means tensor suffix running from 1 to 4. We also use Latin suffix running from 1 to 3, afterwards.

where $\varepsilon_{\alpha\beta\gamma\delta}$ is the completely antisymmetric unit pseudotensor of the fourth rank, and $F_{\mu\nu} = \partial_{[\mu}A_{\nu]}$ is the electromagnetic field strength. The six equations of (6) are not all independent of each other, as the Curl of each side of (6) vanishes identically.

The spinor ψ is thus represented by the basic tensor quantities

$$(7) \qquad (P, \theta, v_\mu, w_\mu, k_\mu)$$

restricted by the subsidiary conditions (4) and (6), hence every physical relation concerning the Dirac field must be expressible in terms of (7). Especially we can show that the Dirac equation:

$$(8) \qquad \left\{\gamma_\mu\left(\partial_\mu - \frac{ie}{\hbar c}A_\mu\right) + \varkappa\right\}\psi = 0$$

can be replaced equivalently by the set of following 12 equations of motion for our basic quantities (7)

$$(\mathrm{I}) \quad \begin{cases} (9) & \partial_\mu(Pv_\mu) = 0\,, \\ (10) & \partial_\mu(Pw_\mu) = -2\varkappa P\sin\theta\,, \\ (11) & w_\mu\partial_\mu\theta + 2\varkappa v_\mu k_\mu + i\varepsilon_{\alpha\beta\gamma\delta}v_\alpha w_\beta\partial_\gamma v_\delta = -2\varkappa\cos\theta\,, \\ (12) & v_\mu\partial_\mu\theta + 2\varkappa w_\mu k_\mu + i\varepsilon_{\alpha\beta\gamma\delta}v_\alpha w_\beta\partial_\gamma w_\delta = 0\,, \\ (13) & v_\nu\partial_\nu(Pv_\mu)\; w_\nu\partial_\nu(Pw_\mu) = \\ & \qquad = -\partial_\mu P - P(v_\mu w_\nu - v_\nu w_\mu)w_\varrho\partial_\nu v_\varrho + 2i\varkappa P\varepsilon_{\mu\nu\varkappa\lambda}v_\nu w_\varkappa k_\lambda\,, \\ (14) & v_\nu\partial_\nu w_\mu = w_\nu(\partial_\nu v_\mu - \partial_\mu v_\nu) + i\varepsilon_{\mu\nu\varkappa\lambda}v_\nu w_\varkappa\partial_\lambda\theta\,. \end{cases}$$

The set (I) consists of 2 scalar equations (9) and (11), 2 pseudoscalar equations (10) and (12), a vector equation (13), and a pseudovector equation (14), and really contains 8 independent equations, since each of (13) and (14) involves only 2 linearly independent ones on account of (4).

(I) contains no electromagnetic field quantities, which in our formalism only appear in the second subsidiary condition (6).

3. – Physical Meaning—Density, Velocity and Spin.

The formalism above stated implies a new sort of relativistic hydrodynamics which differs from those already known, and has a more complicated structure.

First, the factorization (3*c*) with the constraint (4*a*) for the current vector S_μ satisfying the continuity equation (9), shows that we can assume v_μ as clas-

sical 4-velocity and P (or eP) as particle density (or charge density) in the *rest frame.*

This interpretation is also justified from the following. Introducing the 3-dimensional velocity $\mathfrak{v}$ corresponding to v_μ:

$$\mathfrak{v}_i = cv_i/v_0\,, \qquad v_0 = (1 - \mathfrak{v}^2/c^2)^{-\frac{1}{2}}\,, \tag{15}$$

the density in the ordinary reference system

$$P(1 - \mathfrak{v}^2/c^2)^{-\frac{1}{2}} = Pv_0 = S_0\,, \qquad (S_0 \equiv S_4/i), \tag{16}$$

just coincides with the quantum-mechanical probability density (*), and also the mean velocity agrees with the quantum-mechanical expectation value of velocity, since $\int S_0 \mathfrak{v}_i \,\mathrm{d}^3x = c\int P v_i \,\mathrm{d}^3x = c\int S_i \,\mathrm{d}^3x$.

Now the fluid with the distributions of rest charge density eP and velocity v_μ should be assumed also to carry *spin density* distribution, $(\hbar/2)\hat{S}_i$. This is required for our picture to give the quantum-mechanical expectation value of particle spin $(\hbar/2)\int \hat{S}_i \,\mathrm{d}^3x$, correctly.

Further we define 3-dimensional *axial vector* $\mathfrak{w}$ from the spatial part of (3*d*) by

$$\mathfrak{w}_i = \frac{\hbar}{2}\frac{w_i}{v_0}\,, \tag{17}$$

which is regarded as *spin vector* distributed in space, since it is related to the spin density by $S_0\mathfrak{w}_i = (\hbar/2)\hat{S}_i$. Corresponding to (4*c*) and (4*b*), we have relations:

$$\frac{\hbar}{2} w_0 = v_0 \mathfrak{v}\mathfrak{w}/c\,, \tag{18}$$

$$\left(\frac{2}{\hbar}\mathfrak{w}\right)^2 + \left(\frac{1}{c}\mathfrak{v}\right)^2 = 1 + \left(\frac{2}{\hbar c}\mathfrak{v}\mathfrak{w}\right)^2\,, \tag{19}$$

the former of which exhibits the meaning of the fourth component of w_μ, while the latter implies kinematical condition connecting $\mathfrak{w}$ and $\mathfrak{v}$, involving $|\mathfrak{w}| \leqq \hbar/2$.

Now, eq. (10) shows that the quantity $\hat{\Omega} = P\cdot\sin\theta$ implies the source density for the quantity $-\mathfrak{v}\mathfrak{w}/mc^3$ (multiplied by particle number); and then (12) is regarded as the hydrodynamical equation of motion for θ, taking into account that $v_\mu\partial_\mu = \mathrm{d}/\mathrm{d}\tau$, ($\tau$: proper time), is substantial derivative.

Further, eq. (13) means the Euler equation of flow and (14) the equation of motion for the spin field.

(*) Provided that normalization condition $\int S_0 \,\mathrm{d}^3x = 1$ be imposed.

4. – Physical Meaning—Energy-Momentum Tensor.

The meaning of our hydrodynamics is made clearer by considering the energy-momentum tensor of this field given by

$$T_{\mu\nu} = cP\left\{mck_\mu v_\nu + \frac{\hbar}{2}(\partial_\mu\theta\cdot w_\nu + i\varepsilon_{\nu\alpha\beta\gamma}v_\alpha w_\beta\partial_\mu v_\gamma)\right\}. \tag{20}$$

This form is obtained by re-expressing, in terms of the quantities (7), the canonical energy-momentum tensor for the original ψ-field:

$$T_{\mu\nu} = -\frac{\hbar c}{2}(\partial_\mu\bar{\psi}\gamma^\nu\psi - \bar{\psi}\gamma^\nu\partial_\mu\psi) - eA_\mu S_\nu .$$

We regard (20) as the energy-momentum tensor of our field, because, in the first place, it satisfies the conservation law:

$$\partial_\nu T_{\mu\nu} = eF_{\mu\nu}S_\nu , \tag{21}$$

and in the second the momentum density $\mathcal{G}_i = T_{i4}/ic$ and the energy density $\mathcal{H} = -T_{44}$ belonging to this tensor, when integrated throughout over space, yield the quantum-mechanical expectation values of kinetic momentum $p_i - (e/c)A_i$, and kinetic energy $H - eA_0$, correctly (*).

The *mass density* of our hydrodynamical field is to be given by $\mu = \mathcal{H}/c^2$. Then, by the transformation of this quantity to the rest frame, we can obtain the *proper mass density* to be

$$\mu^0 = T_{\mu\nu}v_\mu v_\nu/c^2 = -mPv_\mu k_\mu = \tag{22}$$

$$= mP\left\{\cos\theta + \frac{1}{2\varkappa}(w_\mu\partial_\mu\theta + i\varepsilon_{\alpha\beta\gamma\delta}v_\alpha w_\beta\partial_\gamma v_\delta)\right\}.$$

Thus in our hydrodynamics we must assume the proper mass density which is not positive definite. In the classical limit it becomes proportional to the rest charge density: $\mu_0 \to mP$ (see the next note [10]).

In terms of $T_{\mu\nu}$ eq. (11) is expressed as

$$\sum_\mu T_{\mu\mu} = -mc^2P\cos\theta \tag{11'}$$

(*) The underlined quantities mean the quantum-mechanical operators; especially, H the particle hamiltonian.

(10) T. TAKABAYASI: *Nuovo Cimento*, **2**, 242 (1956).

defining the meaning of θ once more. We have also the relation

$$mcPk_\mu = -T_{\mu\nu}v_\nu/c\,, \tag{23}$$

which shows the physical meaning of k_μ: that is, $mcPk_\mu$ implies the component of the energy momentum tensor in the velocity direction (a time-like direction).

When we use the 3-dimensional quantities, the energy and momentum densities are also written (+)

$$T_{\mu 4} = iS_0\left(mc^2k_\mu + \partial_\mu\theta\cdot\mathfrak{v}\mathfrak{w} - \frac{1}{c(1-\mathfrak{v}^2/c^2)}\varepsilon_{lmn}\mathfrak{v}_l\mathfrak{w}_m\partial_\mu\mathfrak{v}_n\right), \tag{24}$$

accordingly we may look upon mcS_0k_μ as that part of the energy and momentum densities which is not due to the coupling between the orbital motion and spin, and which may survive as $\mathfrak{v}\to 0$. Also taking into account that S_0 is particle density, we may call mck_μ « proper » momentum-energy vector. The disparity of this vector from v_μ expresses a characteristic of the Dirac field.

However, if we use the equations of motion, k_μ can be solved in terms of the other quantities to be

$$k_\mu = v_\mu\cos\theta + \frac{1}{2\varkappa}\left\{(v_\mu w_\nu - w_\mu v_\nu)\partial_\nu\theta - \frac{i}{P}\varepsilon_{\mu\alpha\beta\gamma}\partial_\alpha(Pv_\beta w_\gamma)\right\}, \tag{25}$$

accordingly in the classical limit we have $k_\mu\to v_\mu$, (see the next note). By the way, it is to be noted that the relation (25) is equivalent with the set of the equation of motion, (11), (12) and (13), and therefore the fundamental set of equations of motion (I) may be replaced by the set

$$\text{(9), (10), (14), (25)}\,. \tag{II}$$

Now the energy-momentum conservation relation (21) is nothing but the equation of motion for the proper momentum vector:

$$mcv_\nu\partial_\nu k_\mu = -\frac{\hbar}{2P}\,\partial_\nu\left\{P(\partial_\mu\theta\cdot w_\nu + i\varepsilon_{\nu\alpha\beta\gamma}v_\alpha w_\beta\partial_\mu v_\gamma)\right\} + \frac{e}{c}F_{\mu\nu}v_\nu\,. \tag{26}$$

The second term on the right hand side is the usual Lorentz force and the

(+) ε_{lmn} denotes the 3-dimensional Levi Civita symbol.

first term implies the « quantum force » in the present case; that is, we are to assume an extra elastic stress (« quantum stress ») $(\hbar/2)P(\partial_\mu\theta\cdot w_\nu+i\varepsilon_{\nu\alpha\beta\gamma}v_\alpha w_\beta\partial_\mu v_\gamma)$ inside the fluid.

For the derivation of (21) i.e. (26) from the fundamental equations of our formalism, it is essential to make use of the second subsidiary condition (6), besides the equations of motion. The conservation law (21) consists of 4 equations involving second order derivatives, and is not equivalent with the equations of motion (I) which consist of 8 independent equations containing merely first order derivatives. This is a situation different from the cases of ordinary relativistic hydrodynamics or of the hydrodynamics representing the Klein-Gordon field ([8]).

We can show, however, that the set of equations (12), (13), (14)) is equivalent with the tensor equation without differentiation on $T_{\mu\nu}$:

$$T_{\mu\nu}-T_{\nu\mu}=-\frac{i}{2}\hbar c\varepsilon_{\mu\nu\varkappa\lambda}\partial_\varkappa\hat{S}_\lambda\,, \tag{27}$$

and therefore (I) may also be replaced by the set of equations:

$$\text{(III)}\qquad (9),\ (10),\ (11'),\ (27)\,. \tag{III}$$

Eq. (27) indicates that the symmetrical energy momentum tensor is given by

$$\Theta_{\mu\nu}=T_{\mu\nu}+\frac{i}{4}\hbar c\varepsilon_{\mu\nu\varkappa\lambda}\partial_\varkappa\hat{S}_\lambda\,. \tag{28}$$

This relation fits with that the quantity $(\hbar/2)\hat{S}_i$ has been interpreted as the spin angular momentum density. Speaking more explicitly, the total angular momentum density tensor $M_{\nu\nu'\mu}=x_\nu\Theta_{\nu'\mu}-x_{\nu'}\Theta_{\nu\mu}$ for our hydrodynamical field, satisfying its conservation law, is equal, aside from a divergenceless term, to

$$M'_{\nu\nu'\mu}=(x_\nu T_{\nu'\mu}-x_{\nu'}T_{\nu\mu})-\frac{i}{2}\hbar c\varepsilon_{\nu\nu'\mu\lambda}\hat{S}_\lambda\,,$$

whose $(ij4)$ component $M'_{ij4}/ic=(x_i\mathcal{G}_j-x_j\mathcal{G}_i)+(\hbar/2)\hat{S}_{i\times j}$ being the total angular momentum density, contains the spin part $(\hbar/2)\hat{S}_{i\times j}$.

Our formulation is thus defined by the set of quantities all of which can be interpreted mechanically. i.e., the particle rest density P, the proper mass density μ^0, velocity $\mathfrak{v}_i$, proper momentum mck_i, spin $\mathfrak{w}_i$, and θ related to the source density for $(\mathfrak{v}\mathfrak{w})$. They obey the hydrodynamical equations of motion in which the orbital and spin motions are intimately coupled to each other, and at the same time coupled to the momentum field and also to the

gradients of the rest density and θ fields. In our fundamental equations the electromagnetic field acting on the hydrodynamical field appears solely in the subsidiary condition (6) which connects the Curl of the k_μ-field with the velocity and spin fields. $F_{\mu\nu}$ also appears in the equation of motion for k_μ, (26), but merely in the form of Lorentz force $(e/c)F_{\mu\nu}v_\nu$, so that in our formulation we are not needed to attribute magnetic and electric moment density distributions to the fluid.

A more detailed account of the same subject, including calculations, will be published elsewhere.

RIASSUNTO (*)

Sopprimendo completamente le matrici dello spinore ψ e la matrice γ si dimostra che il campo di Dirac è equivalente ad un campo vettoriale non lineare che si interpreta compiutamente come la definizione di una nuova specie di idrodinamica relativistica di un fluido in rotazione. In tale idrodinamica, oltre allo spin, appare un addizionale grado di libertà θ che caratterizza la differenza tra la densità di carica a riposo e la densità di massa vera e propria ed anche tra velocità e quantità di moto. Si enuncia la teoria per il caso di un campo di Dirac sotto l'azione di un campo di Maxwell, ponendo in evidenza anche l'aspetto della formulazione indipendente dal « gauge ».

(*) *Traduzione a cura della Redazione.*

IL NUOVO CIMENTO Vol. III, N. 2 1° Febbraio 1956

New Classical Spin Theory as the Limit of the Dirac Equation.

T. TAKABAYASI

Physical Institute, Nagoya University - Nagoya (Japan)

(ricevuto il 26 Maggio 1955)

Summary. — By taking the classical limit in the tensor formulation of the Dirac equation, which was established in our preceding article, a new classical relativistic spin theory is obtained, which is different from the one due to KRAMERS, coinciding with it only in non-relativistic approximation substantially. The theory yields the classical limit for Dirac particle, which is different from that due to PAULI.

In the foregoing note [1] (which will be cited as A hereafter), we have established a complete tensor formulation of the Dirac equation. In the present note we study the classical limit of the formulation. The procedure leads to the *classical relativistic theory of spin* which should be regarded as the legitimate classical limit for a Dirac particle. The classical spin theory thus obtained is different from the ones formerly considered by KRAMERS [2] and others [3]. This theory also serves to improve the « *new classical theory of electron* » of Dirac [4] in such a way that the electron has spin.

We take the classical limit (*) $\hbar \to 0$ (i.e., $\varkappa \to \infty$) in the fundamental equations of the tensor formulation stated in A, which consist of the subsidiary conditions (A-4) and (A-6), and the equations of motion (A-9)–(A-14) (+):

---

[1] T. TAKABAYASI: *Nuovo Cimento*, **2**, 233 (1956).

[2] H. A. KRAMERS: *Physica*, **1**, 825 (1934); *Zeeman Verhandelingen* (Nijhoff, 1935), p. 403; *Quantentheorie des Elektrons und der Strahlung* (Leipzig, 1938), p. 227.

[3] J. WEYSSENHOFF: *Acta Phys. Polon.*, **9**, 8 (1947).

[4] P. A. M. DIRAC: *Proc. Roy. Soc.*, A **209**, 291 (1951); **212**, 330 (1952).

(*) In the limiting process we assume k_μ to be of the same order with the other variables.

(+) (A.n) means the equation (n) in A.

From (A-10)–(A-13) we get

$$\theta \to 0\,, \qquad k_\mu \to v_\mu\,, \tag{1}$$

so we are left with (P, v_μ, w_μ). The subsidiary condition (A-4) remains the same, while (A-6) becomes

$$\partial_\mu v_\nu - \partial_\nu v_\mu = -\varepsilon F_{\mu\nu}\,, \qquad (\varepsilon = e/mc^2), \tag{2}$$

The equations of motion now consist of (A-9) and

$$\frac{\mathrm{d}w_\mu}{\mathrm{d}\tau} = v_\nu \partial_\nu w_\mu = \varepsilon F_{\mu\nu} w_\nu\,, \tag{3}$$

only. From (2) we get

$$\frac{\mathrm{d}v_\mu}{\mathrm{d}\tau} = \varepsilon F_{\mu\nu} v_\nu\,, \tag{4}$$

which is the purely classical Euler-Lorentz equation of motion. The relation (2) further restricts the velocity field to being *quasi-irrotational*.

We thus have the fundamental equations in the classical limit:

$$\text{(A-4), (A-9), (2), (3)}\,. \tag{a}$$

This includes

$$\text{(A-4}a\text{), (A-9), (2)}\,, \tag{b}$$

which coincides with the system of equations of the hydrodynamics corresponding to the Klein-Gordon field in its classical limit (*). But (a) contains, besides (b), the equations (A-4b), (A-4c), and (3), which determine the spin motion, though the latter does not react upon the orbital motion. It is also to be noted that (a) contains the specific charge ε as the unique natural constant.

In this way a Dirac particle in the classical limit is represented by an ensemble of mutually independent motions of classical particle *with spin* under Lorentz force.

This classical limit theory is essentially *different from the WKB-like approximation* for the Dirac particle given by PAULI and others [5,6]. In the latter

(*) See reference [8] in A.

[5] W. PAULI: *Helv. Phys. Acta*, **5**, 179 (1932); *Die allgemeine Prinzipien der Wellenmechanik* (1933), p. 241.

[6] L. DE BROGLIE: *La Théorie des particules de spin* $\frac{1}{2}$ (Paris, 1952), p. 117.

procedure, the first approximation led to an ensemble of classical relativistic motions of particle *without spin*, and the next approximation brought about the effect of spin jumbled with the wave-mechanical interference effects, whereas our procedure takes out the classical spin motion separated from the interference effects.

The theory here obtained, on the other hand, presents a consistent classical spin theory which is different from those already known. To see more intimately the motion of spin in our case, we rewrite the spin equation (3) in terms of the spin vector $\mathfrak{w}$. Making use of (A-18) and (4) also, we obtain

$$\frac{\mathrm{d}\mathfrak{w}}{\mathrm{d}\tau} = \frac{e}{mc}\left\{[\mathfrak{w}\times\boldsymbol{H}] + \frac{1}{c}[\mathfrak{v}\times[\boldsymbol{E}\times\mathfrak{w}]]\right\}, \tag{5}$$

where $\boldsymbol{H}$ and $\boldsymbol{E}$ are magnetic and electric field strengths respectively. This equation differs from the Kramers' equation of motion for spin ([2]):

$$\frac{\mathrm{d}\mathfrak{w}^k}{\mathrm{d}\tau} = \frac{e}{mc}\left\{[\mathfrak{w}^k\times\boldsymbol{H}] + \frac{1}{c}[\boldsymbol{E}\times[\mathfrak{w}^k\times\mathfrak{v}]]\right\}, \tag{6}$$

in the second terms of the right sides.

In non-relativistic approximation, however, we have (*)

$$[\boldsymbol{E}\times[\mathfrak{w}\times\mathfrak{v}]] \cong -\frac{1}{2}[\mathfrak{w}\times[\mathfrak{v}\times\boldsymbol{E}]] + \frac{m}{2e}\frac{\mathrm{d}\boldsymbol{V}}{\mathrm{d}t}, \tag{7}$$

with

$$\boldsymbol{V} = [\mathfrak{v}\times[\mathfrak{w}\times\mathfrak{v}]],$$

and accordingly also

$$[\mathfrak{v}\times[\boldsymbol{E}\times\mathfrak{w}]] \cong -\frac{1}{2}[\mathfrak{w}\times[\mathfrak{v}\times\boldsymbol{E}]] - \frac{m}{2e}\frac{\mathrm{d}\boldsymbol{V}}{\mathrm{d}t}. \tag{8}$$

Furthermore, in atomic problems the $\mathrm{d}\boldsymbol{V}/\mathrm{d}t$ term may be omitted approximately (*). Hence in such cases (5) becomes equivalent with (6), and also gives the Thomas term (the first term in the right hand side of (8)). The fact that our theory contains the correct Landé factor for spin, e/mc, (as is seen in (5)), is necessary in order that the spin equation (3) be compatible with the Lorentz equation (4) under the condition (A-4c).

Our spin vector $\mathfrak{w}$ obeys, besides the equation of motion (5), the subsidiary condition (+),

$$\mathfrak{w}^2 - (\mathfrak{v}\mathfrak{w}/c)^2 = (w^0)^2(1 - (\mathfrak{v}/c)^2), \tag{9}$$

corresponding to (A-19).

(*) See reference ([2]).

(+) Here the constant w^0 should be $w^0 \cdot \hbar/2$ according to (A.19), but may well be an arbitrary constant from the viewpoint of the classical spin theory in general.

We thus have a classical spin theory defined by the fundamental equations

$$(c) \qquad \text{(A-4), (4), (3)} \quad \text{or} \quad \text{(9), (4), (5)}\,.$$

The difference between this theory and Kramers', as was indicated between (5) and (6), arises primarily from the fact that in our theory $\mathfrak{w}$ is an axial vector obtained from the spatial part of a pseudovector w_μ, while Kramers' spin was assumed to be an axial vector dual to the spatial part of an antisymmetric tensor of the second rank (7).

Finally, if we again supplement the set (*c*) with the continuity equation (A-9), we have the set of equations,

$$(d) \qquad \text{(A-4), (A-9), (4), (3)}\,,$$

describing the motion of continuous spinning fluid without internal stress. This gives just the « *new classical theory of electron* » of Dirac (1) improved in such a way that the electron carries spin. In the equations (*d*) the constant e implies the specific charge for the continuous matter and we are not required to separate it into the particle constants e and m.

* * *

The author would like to thank Prof. S. Sakata and Prof. Z. Koba for interest taken in this work.

(7) Other classical spin theories were considered by Weyssenhoff (3) and also by A. Proca (*Journ. Phys. et Rad.*, **15**, 65 (1954)). In these theories again spin is defined by an antisymmetric tensor.

RIASSUNTO (*)

Prendendo il limite classico nella forma tensoriale dell'equazione di Dirac ricavata nel nostro precedente lavoro, si ottiene una nuova teoria relativistica classica dello spin, differente da quella dovuta a Kramers, con la quale coincide sostanzialmente solo in approssimazione non relativistica. La teoria dà il limite classico per la particella di Dirac, limite differente da quello dovuto a Pauli.

(*) *Traduzione a cura della Redazione.*

Ingoing Waves in the Final State of Ionization Problems.

S. ALTSHULER

The Ramo-Wooldridge Corporation - Los Angeles, California

(ricevuto l'8 Agosto 1955)

Summary. — The Ionization Problem is re-formulated to show how the ingoing wave modification of final states may be directly deduced. The analysis is general and includes interactions which are explicitly time dependent.

It is well known that the final state in the matrix element for the transition probability corresponding to the ejection of a particle must represent a plane plus ingoing scattered wave. While confirming reasons based upon some interesting visualization have been recently given [1], a formal demonstration, without approximation, encompassing all ionization processes including those which are explicitly time dependent still remains desirable. It is the intent of the present note to provide a straightforward deduction leading automatically to this modification on the final continuum state of the system which is undergoing ionization.

To begin, we write down the time dependent Schrödinger equation in integral form. Linear operation algebra will be used and only the time exhibited explicitly. Therefore,

$$\psi_a(t) = \Phi_a(t) + \frac{1}{i\hbar}\int_{-\infty}^{\infty} \exp\left[\frac{i}{\hbar} H_0(t'-t)\right] \eta(t'-t) V(t') \psi_a(t')\, \mathrm{d}t', \tag{1}$$

where H_0 is the Hamiltonian for a system being disturbed in a perfectly general

---

[1] BREIT and BETHE: *Phys. Rev.*, **93**, 888 (1954); also contains references to related discussions for special cases.

way by $V(t)$ which may or may not contain time explicitly. Also,

$$\eta(t'-t) = 1\,, \qquad t' < t$$
$$= 0\,, \qquad t' > t$$

and $\psi_a(t)$ satisfies $(i\hbar(\partial/\partial t) - H_0)\psi_a(t) = V(t)\psi_a(t)$, while $\Phi_a(t)$ describes the time development of the system in the absence of interaction. That is, $\Phi_a(t) = \exp[(-i/\hbar)H_0 t]\Phi_a(0)$ is a perfectly general state of the free system which may be represented as any superposition of the stationary states of H_0, or $\Phi_a(0)$ may be an eigenfunction of any Hermitian operator.

Upon making a measurement on a system in the state $\psi_a(t)$, the amplitude which corresponds to observing a state $\Phi_b(t)$ is given by

$$(2) \qquad a_b(t) \equiv \Phi_b^\dagger(t)\psi_a(t) = \Phi_b^\dagger(t)\Phi_a(t) +$$
$$+ \frac{1}{i\hbar}\int_{-\infty}^{t} \Phi_b^\dagger(0)\exp\left[\frac{i}{\hbar}H_0 t\right]\exp\left[\frac{i}{\hbar}H_0(t'-t)\right]V(t')\psi_a(t')\,dt' =$$
$$= \Phi_b^\dagger(0)\cdot\Phi_a(0) + \frac{1}{i\hbar}\int_{-\infty}^{t}\Phi_b^\dagger(t')\cdot V(t')\psi_a(t')\,dt' = \frac{1}{i\hbar}\int_{-\infty}^{t}\Phi_b^\dagger(t')V(t')\psi_a(t')\,dt'\,.$$

Here, we have adopted the point of view that our measuring apparatus is ultimately capable of discriminating between the free motion, $\Phi_a(t)$, and that part of $\psi_a(t)$ which depends upon $V(t)$, so that we do not necessarily assume $\Phi_a(0)$ and $\Phi_b(0)$ to be members of an orthonormal set of functions corresponding to some operator. If, in (2), the Φ's are specialized to be the stationary state solutions, $\exp[(-i/\hbar)\varepsilon_n t]\varphi_n$, then $a_b(t)$ becomes the amplitude obtained from the standard Dirac method of variation of constants.

We now inquire as to the specific behavior of $\Phi_b(t')$ in (2) when a particle is ejected by means of some perturbing agency, $V(t)$. Since (1) represents a complete description of the motion including the boundary conditions, it is clear that the answer should be unambiguously deducible. To accomplish this, we ask for the amplitude describing the ionizing event in a way that does not depend upon the scattering which is contained in the positive energy states of the target. For example, suppose the target is a single bound electron and let us assume further that the ionized state is a stationary one so that $\Phi_b = \varphi_b \exp[-(i/\hbar)\varepsilon_b t]$ with asymptotic behavior

$$(3) \qquad \varphi_b \sim \exp[i\boldsymbol{k}_b\cdot\boldsymbol{r}] + \frac{\exp[\pm ik_b r]}{r} f(\theta)\,.$$

We wish to avoid committing ourselves at the outset in forming $\Phi_b^\dagger\psi_a$ as to

the choice of sign in (3) corresponding to outgoing or ingoing scattered waves. Instead, we separate H_0 into $H_0 = L + v$ and form a packet, $W(t) = \exp[(-i/\hbar)Lt]W(0)$, which is appropriate for describing the ejected particle. In the case of our simple example, L would be the kinetic energy operator. The amplitude for ionization is now expressed as

$$W^{\dagger}(t)\psi_a(t) = W^{\dagger}(t)\int_{-\infty}^{\infty}\frac{1}{i\hbar}\exp\left[\frac{i}{\hbar}H_0(t'-t)\right]\eta(t'-t)V(t')\psi_a(t')\,dt' , \tag{4}$$

so that the aforementioned ambiguity of sign is circumvented.

Next, the property of the kernel, $G(t/t') = (1/i\hbar)\exp[(i/\hbar)H_0(t'-t)]\eta(t'-t)$, in (4) is stated explicitly as follows:

$$\left(i\hbar\frac{\partial}{\partial t} - H_0\right)G(t/t') = \left(i\hbar\frac{\partial}{\partial t} - L - v\right)G(t/t') = \delta(t'-t) ,$$

or

$$\left(i\hbar\frac{\partial}{\partial t} - L\right)G(t/t') = \delta(t'-t) + vG(t/t') . \tag{6}$$

This first order differential equation leads at once to the following integral equation for $G(t/t')$:

$$G(t/t') = \frac{1}{i\hbar}\int_{-\infty}^{\infty}\exp\left[\frac{i}{\hbar}L(t''-t)\right]\eta(t''-t)\{\delta(t''-t') + vG(t''/t')\}\,dt'' = \tag{7}$$

$$= \frac{1}{i\hbar}\exp\left[\frac{i}{\hbar}L(t'-t)\right]\eta(t'-t) + \int_{-\infty}^{\infty}\frac{1}{i\hbar}\exp\left[\frac{i}{\hbar}L(t''-t)\right]\eta(t''-t)vG(t''/t')\,dt'' ,$$

where, now

$$\left(i\hbar\frac{\partial}{\partial t} - L\right)\frac{1}{i\hbar}\exp\left[\frac{i}{\hbar}L(t'-t)\right]\eta(t'-t) = \delta(t'-t) .$$

Since the boundary condition on the scattered wave requires the delta function property for G, the solution for the homogeneous part of (6) must be chosen as zero.

Upon incorporating (7) into (4), the amplitude for observing $W(t)$ becomes

$$W^{\dagger}(t)\psi_a(t) = \int_{-\infty}^{\infty}W^{\dagger}(0)\exp\left[\frac{i}{\hbar}Lt\right]\left\{\frac{1}{i\hbar}\exp\left[\frac{i}{\hbar}L(t'-t)\right]\eta(t'-t) + \right.$$

$$\left. \int_{-\infty}^{\infty}\frac{1}{i\hbar}\exp\left[\frac{i}{\hbar}L(t''-t)\right]\eta(t''-t)vG(t''/t')\,dt''\right\}V(t')\psi_a(t')\,dt' =$$

$$= \frac{1}{i\hbar}\int_{-\infty}^{\infty}\left[W^{\dagger}(t')\eta(t'-t) + \int_{-\infty}^{\infty}W^{\dagger}(t'')\eta(t''-t)vG(t''/t')\,dt''\right]V(t')\psi_a(t')\,dt'$$

and

$$\text{(8)} \qquad \lim_{t\to\infty} W^{+}(t)\,\psi_a(t) = \frac{1}{i\hbar}\int_{-\infty}^{\infty}\left[W^{+}(t') + \int_{\infty}^{\infty} W^{+}(t'')vG(t''/t')\,\mathrm{d}t''\right] V(t')\,\psi_a(t')\,\mathrm{d}t' =$$

$$= \frac{1}{i\hbar}\int_{-\infty}^{\infty}\chi^{+}(t')V(t')\psi_a(t')\,\mathrm{d}t' .$$

We now examine the meaning of the function

$$\text{(9)} \qquad \chi(t') = W(t') + \int_{\infty}^{\infty} G^{+}(t''/t')vW(t'')\,\mathrm{d}t'' , \quad (v \text{ is Hermitian}),$$

$$= W(t') + \int_{\infty}^{\infty}\frac{1}{(-i\hbar)}\exp\left[-\frac{i}{\hbar}H_0(t'-t'')\right)\eta(t'-t'')vW(t'')\,\mathrm{d}t'' =$$

$$= W(t') + \frac{1}{i\hbar}\int_{\infty}^{-\infty}\exp\left[\frac{i}{\hbar}H_0(t''-t')\right]\eta(t'-t'')vW(t'')\,\mathrm{d}t'' =$$

$$= W(t') - \frac{1}{i\hbar}\int_{\infty}^{t'}\exp\left[\frac{i}{\hbar}H_0(t''-t')\right]vW(t'')\,\mathrm{d}t'' .$$

The first observation concerning the wave packet $\chi(t')$ is that it obeys the time dependent Schrödinger equation for the free motion,

$$\left(i\hbar\frac{\partial}{\partial t'} - H_0\right)\chi(t') = 0 ,$$

a fact which is easily demonstrated. Secondly, (9) indicates that this wave packet is fully developed originally at $t' = -\infty$ and depreciates steadily to $W(t')$ as $t'\to\infty$. Such contrary temporal behavior is precisely what is meant by the ingoing wave solution. More specifically, let $\chi(t)$ be the stationary state, $\chi(t) = \exp[-(i/\hbar)Et]u$ rather than a wave packet. Then, upon re-writing (9), we obtain

$$\text{(10)} \qquad \exp\left[-\frac{i}{\hbar}Et\right]u = \exp\left[-\frac{i}{\hbar}Et\right]R +$$

$$+ \frac{1}{i\hbar}\int_{\infty}^{t'}\exp\left[\frac{i}{\hbar}H_0(t''-t')\right]v\exp\left[-\frac{\varepsilon}{\hbar}t''\right]\exp\left[-\frac{i}{\hbar}Et''\right]R\,\mathrm{d}t'',$$

where $(E - L)R = 0$ and the term $\exp[-(\varepsilon/\hbar)t'']$ is introduced in order to define the integral. This is an inevitable contingency whenever stationary states replace the more realistic but intractable wave packets and corresponds to Lippman's and Schwinger's [2] adiabatic decrease in the interaction strength. Upon performing the time integration (*) (10) becomes

$$u = R + \operatorname*{Lim}_{\varepsilon\to\infty} \frac{1}{E - H_0 - i\varepsilon} vR = R + G^{+}vR \,, \tag{11}$$

a stationary state of H_0 of energy E with ingoing scattered wave.

In order to reduce (11) to most familiar form, consider that this ionized state describes a single particle moving in the field v with energy $E = k^2$. Then $(\nabla^2 + k^2)R = 0$,

$$(\nabla^2 + k^2 - v)G^{+} = 1 \,, \tag{12}$$

or, $(\nabla^2 + k^2)G^{+} = 1 + vG^{+}$, and if the Green's function, g, for the operator $\nabla^2 + k^2$ is introduced, we may write an integral equation for G^{+}, namely

$$G^{+} = g^{+} + g^{+}vG^{+} \,.$$

Here, as in (7), the homogeneous solution to (12) vanishes in order to satisfy the boundary conditions. Then (11) becomes

$$\begin{cases} u = R + (g^{+} + g^{+}vG^{+})vR \\ \quad = R + g^{+}v(R + G^{+}vR) = R + g^{+}vu \end{cases} \tag{13}$$

or, in configuration representation, this eigenfunction of $H_0 = -\nabla^2 + v$ becomes

$$u(\boldsymbol{k}|\boldsymbol{r}) = \exp[i\boldsymbol{k}\cdot\boldsymbol{r}] + \int \frac{\exp[-ik|\boldsymbol{r} - \boldsymbol{r}'|]}{-4\pi|\boldsymbol{r} - \boldsymbol{r}'|} v(\boldsymbol{r}')u(\boldsymbol{k}|\boldsymbol{r}')\,\mathrm{d}\boldsymbol{r}' , \tag{14}$$

which at large distances from the origin behaves as

$$\exp[i\boldsymbol{k}\cdot\boldsymbol{r}] + \frac{\exp[-ikr]}{r} f(\theta) \,, \tag{15}$$

a plane plus ingoing scattered wave.

---

(2) B. A. Lippman and J. Schwinger: *Phys. Rev.*, **79**, 469 (1950).

(*) The procedure in treating the exponential as c numbers may be fully justified by regarding the exponential operator as defined by its Taylor expansion.

Referring back to (8), it is seen that what actually appears in the matrix element is $u^{\dagger} \equiv u^{*}$ which, in view of (14), represents a plane wave moving toward the origin away from the observer together with an outgoing scattered wave.

As a second example, consider the problem of ionization produced by particle impact, and for convenience we choose the prototype three-body scattering problem which can always be reduced to a problem in two vector coordinates, $\boldsymbol{r}_1$ (primary particle) and $\boldsymbol{r}_2$. V is no longer explicitly time dependent, and $H_0 = L + v(\boldsymbol{r}_2) = -\nabla_1^2 - \nabla_2^2 + v(\boldsymbol{r}_2)$. Equation (11) becomes

$$u(\boldsymbol{r}_1, \boldsymbol{r}_2) = \exp\left[i(\boldsymbol{k}_1 \cdot \boldsymbol{r}_1 + \boldsymbol{k}_2 \cdot \boldsymbol{r}_2)\right] + \tag{16}$$

$$+ \int\int \mathrm{d}\boldsymbol{r}_1' \mathrm{d}\boldsymbol{r}_2' \sum_n \int \mathrm{d}\boldsymbol{k} \exp\left| \frac{[i\boldsymbol{k} \cdot (\boldsymbol{r}_1 - \boldsymbol{r}_1')]\varphi_n(\boldsymbol{r}_2)}{E - \varepsilon_n - k^2 - i\varepsilon} \right| \varphi_n^{*}(\boldsymbol{r}_2' v)(\boldsymbol{r}_2') \exp\left[i(\boldsymbol{k}_1 \cdot \boldsymbol{r}_1' + \boldsymbol{k}_2 \cdot \boldsymbol{r}_2')\right]$$

$$= \exp\left[i\boldsymbol{k}_1 \cdot \boldsymbol{r}_1\right] \left\{ \exp\left[i\boldsymbol{k}_2 \cdot \boldsymbol{r}_2\right] + \int \mathrm{d}\boldsymbol{r}_2' G_{K_2}^{\dagger}(\boldsymbol{r}_2 - \boldsymbol{r}_2') v(\boldsymbol{r}_2') \exp\left[i\boldsymbol{k}_2 \cdot \boldsymbol{r}_2'\right] \right\}. \tag{17}$$

where $K_2^2 = E - K_1^2$, E is the total energy of the entire system,

$$G_{K_2}^{\dagger} \equiv G_{K_2}^{*} = \sum_n \frac{\varphi_n(\boldsymbol{r}_2)\varphi_n^{*}(\boldsymbol{r}_2')}{K_2^2 - \varepsilon_n - i\varepsilon}, \qquad \text{and} \qquad (-\nabla_2^2 + v(\boldsymbol{r}_2))\varphi_n = \varepsilon_n \varphi_n$$

The function in (17) is the spacial part of $\chi(t)$ in (8) which now represents the amplitude for observing the ejected particle moving with momentum $\boldsymbol{K}_2$ while the primary particle is scattered into the momentum state $\boldsymbol{K}_1$. The term in curly brackets is the target continuum state with the ingoing asymptotic behavior. It is to be observed that the transformation functions $\exp\left[i\boldsymbol{k} \cdot \boldsymbol{r}_1\right]\varphi_n(\boldsymbol{r}_2)$ which affect the transformation of (11) into configuration representation are complete regardless of outgoing or ingoing choice on the scattered part of the continuum $\varphi_n^{(1)}$.

RIASSUNTO (*)

Si riformula il problema della ionizzazione per mostrare come si possa direttamente dedurre la modificazione degli stati finali dovuta all'onda entrante. L'analisi è generale e comprende interazioni esplicitamente dipendenti dal tempo.

(*) *Traduzione a cura della Redazione.*

The Non Linear Theory of Betatron Oscillations in the Strong-Focusing Synchrotron (I).

Y. Orlov (*)

Academy of Sciences of the USSR - Moscow

(ricevuto il 20 Settembre 1955)

Summary. — A new method of the investigation of betatron resonances has been developed. The resonances due to errors in the field gradient have been examined.

1. – Equations of Motion.

Equations of betatron oscillations around the closed orbit in the strong-focusing synchrotron (1) are

$$(1)\qquad \frac{\mathrm{d}^2 r}{\mathrm{d}\theta^2}+\frac{P'_\theta}{P}r'_\theta+\frac{1}{P}\left(\frac{l}{2\pi}\right)^2\left(\frac{\partial H_z}{\partial r}\right)_0 r=\frac{1}{P}\left(\frac{l}{2\pi}\right)^2\left\{\frac{1}{\varrho}(P-\varrho H_{z0})-\delta\left(\frac{\partial H_z}{\partial r}\right)r-\right.$$
$$\left.-\frac{\partial H_z}{\partial z}z-\sum_{n\geq z}\left(\frac{\partial^n H_z}{\partial r^n}\right)\left[\frac{r^n}{n!}-\frac{r^{n-2}z^2}{2!(n-2)!}+\frac{r^{n-4}z^4}{4!(n-4)!}-\cdots\right]\right\}.$$

$$(2)\qquad \frac{\mathrm{d}^2 z}{\mathrm{d}\theta^2}+\frac{P'_\theta}{P}z'_\theta-\frac{1}{P}\left(\frac{l}{2\pi}\right)^2\left(\frac{\partial H_z}{\partial r}\right)_0 z=\frac{1}{P}\left(\frac{l}{2\pi}\right)^2\left\{H_{\varrho 0}+\delta\left(\frac{\partial H_z}{\partial r}\right)z-\right.$$
$$\left.-\frac{\partial H_z}{\partial z}r+\sum_{n\geq z}\left(\frac{\partial^n H_z}{\partial r^n}\right)\left[\frac{r^{n-1}z}{(n-1)!}-\frac{r^{n-3}z^3}{3!(n-3)!}+\cdots\right]\right\}.$$

(*) In the transliteration of Russian names we follow the international System of Transliteration of Cyrillic Characters (2nd Draft Iso Recommendation n°. 6, 1954), published at pag. 388 of the n°. 4 of the *Supplemento* to Vol. 1 (1955) of *Il Nuovo Cimento*.

(1) E. D. Courant, M. S. Livingston and H. S. Snyder: *Phys. Rev.*, 88, 1190 (1952).

where r denotes the horizontal displacement, z the vertical displacement, $\varrho(\theta)$ is the radius of the periodic orbit. An « angle » θ varies from zero to 2π on the length l of the periodic element, $1/P = e/cp$, where p is the momentum of the particle, $\partial H_z/\partial r$ is the field gradient, $\delta(\partial H_z/\partial r)$ is the error in the gradient. Some unessential terms in (1) and (2) are omitted: so, we neglected the influence of H_ϑ.

Now put

$$(3)\qquad \begin{cases} \left(\frac{P(\theta)}{P(0)}\right)^{\frac{1}{2}} r = x(\theta)\varphi_r^*(\theta)\exp[iv_r\theta] + x^*(\theta)\varphi_r(\theta)\exp[-iv_r\theta]\,, \\ \left(\frac{P(\theta)}{P(0)}\right)^{\frac{1}{2}} r_\theta' = x(\theta)\frac{\mathrm{d}\varphi_r^*}{\mathrm{d}\theta}\exp[iv_r\theta] + x^*(\theta)\frac{\mathrm{d}\varphi_r}{\mathrm{d}\theta}\exp[-iv_r\theta]\,. \end{cases}$$

$$(4)\qquad \begin{cases} \left(\frac{P(\theta)}{P(0)}\right)^{\frac{1}{2}} z = y(\theta)\varphi_z^*(\theta)\exp[iv_z\theta] + y^*(\theta)\varphi_z(\theta)\exp[-iv_z\theta]\,. \\ \left(\frac{P(\theta)}{P(0)}\right)^{\frac{1}{2}} z_\theta' = y(\theta)\frac{\mathrm{d}\varphi_z^*}{\mathrm{d}\theta}\exp[iv_z\theta] + y^*(\theta)\frac{\mathrm{d}\varphi_z}{\mathrm{d}\theta}\exp[-iv_z\theta]\,. \end{cases}$$

where $\varphi_{r,z}$ are Floquet functions, $\varphi_{r,z}(\theta+2\pi) = \varphi_{r,z}(\theta)\exp[2\pi i\nu_{r,z}]$; $\nu_{r,z}$ are the numbers of betatron oscillations on the length l.

This gives

$$(5)\qquad \frac{\mathrm{d}x}{\mathrm{d}\theta} - i\nu_r x = i\left(\frac{l}{2\pi}\right)^2\frac{1}{P\omega_r}\left(\frac{P(\theta)}{P(0)}\right)^{\frac{1}{2}} f_r(\theta)\left\{\frac{1}{\varrho}(P - \varrho H_{z0}) - \delta\left(\frac{\partial H_z}{\partial r}\right)\cdot\right.$$
$$\cdot\left(\frac{P(\theta)}{P(0)}\right)^{\frac{1}{2}}(xf_r^* + x^*f_r) - \frac{\partial H_z}{\partial z}\left(\frac{P(0)}{P(\theta)}\right)^{\frac{1}{2}}(yf_z^* + y^*f_z) - \sum_{n\geq 2}\left(\frac{\partial^n H_z}{\partial r^n}\right)\cdot$$
$$\left.\cdot\left(\frac{P(0)}{P(\theta)}\right)^{\frac{1}{2}}\left[\frac{(xf_r^* + x^*f_r)^n}{n!} + \ldots\right]\right\}.$$

$$(6)\qquad \frac{\mathrm{d}y}{\mathrm{d}\theta} - i\nu_z y = i\left(\frac{l}{2\pi}\right)^2\frac{1}{P\omega_r}\left(\frac{P(\theta)}{P(0)}\right)^{\frac{1}{2}} f_z(\theta)\left\{H_{\varrho 0} - \delta\left(\frac{\partial H_r}{\partial r}\right)\left(\frac{P(0)}{P(\theta)}\right)^{\frac{1}{2}}(yf_z^* + y^*f_z)\right.$$
$$\left.\frac{\partial H_z}{\partial z}\left(\frac{P(0)}{P(\theta)}\right)^{\frac{1}{2}}(xf_r^* + x^*f_r) - \sum_{n\geq 2}\left(\frac{\partial^n H_z}{\partial r^n}\right)\left(\frac{P(0)}{P(\theta)}\right)^{\frac{1}{2}}\left[\frac{(xf_r^* + x^*f_r)^{n-1}(yf_z^* + y^*f_z)}{(n-1)!} + \ldots\right]\right\}.$$

$$(7)\qquad -i\omega_{r,z} = \varphi_{r,z}\frac{\mathrm{d}\varphi_{r,z}^*}{\mathrm{d}\theta} - \varphi_{r,z}^*\frac{\mathrm{d}\varphi_{r,z}}{\mathrm{d}\theta}\,,$$

$$(8)\qquad \varphi_{r,z}(\theta) = f_{r,z}(\theta)\exp[i\nu_{r,z}\theta]\,; \qquad f_{r,z}(\theta) = f_{r,z}(\theta+2\pi)\,.$$

It is important to notice that all coefficients in equations (5) and (6) are periodical functions with maximum period $2\pi M$: M is the number of periodic elements.

2. – First " Resonance Approximation ".

On the $(\nu_r \nu_z)$ plane, $1/2M$ is the distance between linear resonances (see Fig. 1). One of the main problems of the theory is the definition of the boundaries of the so-called «safe region » inside the region between resonances. So the values of ν_r, ν_z approaching the resonances are of main interest. Analyzing the amplitudes $r_{\max}$, $z_{\max}$ near the resonances it is possible to leave in equations only resonance terms (in the first approximation). In fact, deviations $\delta(\partial H_z/\partial r)$, $\partial H_z/\partial z$, $(P - \varrho H_{z0})$ and nonlinearity of field are usually sufficiently small and the influence of their nonresonance harmonics is negligible.

The simple « resonance equations » obtained in such a way have a remarkable feature. Namely, by a proper choice of variables they can be written in the form of the Hamilton equations with an integral of motion independent of θ.

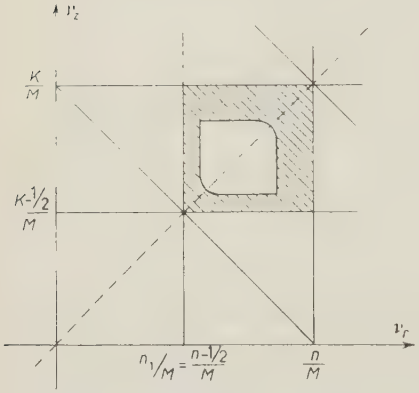

Fig. 1.

3. – Resonance Due to Gradient Errors.

With a good approximation, this resonance only acts on the left and the bottom boundaries of the safe region (Fig. 1).

Consider the left boundary for example. Then the Hamilton resonance equations are

$$\frac{\mathrm{d}A_r^2}{\mathrm{d}\theta} = 2g_r A_r^2 \cos\varphi_r = -\frac{\partial \mathcal{H}}{\partial \varphi_r}, \tag{9}$$

$$\frac{\mathrm{d}\varphi_r}{\mathrm{d}\theta} = 2(\varepsilon_r + \alpha_1 A_r^2 + \alpha_2 A_z^2 - g_r \sin\varphi_r) = \frac{\partial \mathcal{H}}{\partial A_r^2}, \tag{10}$$

where by definition

$$x = \frac{A_r \exp[-i(\varphi_r/2 + n_1\theta/2M + \gamma_r/2)]}{2|\varphi_r|_{\max}[P(0)/P(\theta)]^{\frac{1}{2}}}, \quad A_r = 2|\varphi_r|_{\max}\left(\frac{P(0)}{P(\theta)}\right)^{\frac{1}{2}}|x|, \tag{11}$$

$$\varepsilon_r = \nu_r^{(1)} - \frac{n_1}{2M}, \quad \nu_r^{(1)} = \nu_r + \frac{l^2}{8\pi^3 M\omega_r}\int_0^{2\pi M}|\varphi_r|^2\delta\left(\frac{\partial H_z}{\partial r}\right)\mathrm{d}\theta, \tag{12}$$

$$g_r \exp[i\gamma_r] = -\frac{il^3}{8\pi^3 M\omega_r}\int_0^{2\pi M}\delta\left(\frac{\partial H_z}{\partial r}\right) f_r^2(\theta)\exp[i(n_1\theta/M)]\,\mathrm{d}\theta \approx \tag{13}$$

$$\approx -\frac{il^2}{8\pi^3 M\omega_r}\int_0^{2\pi M}\delta\left(\frac{\partial H_z}{\partial r}\right)\varphi_r^2\,\mathrm{d}\theta,$$

$$\alpha_1 = \frac{l^2}{16\pi^3\omega_r}\,\frac{1}{4|\varphi_r|^2_{\max}}\,\frac{1}{P}\int_0^{2\pi}\frac{\partial^3 H_z}{\partial r^3}|\varphi_r|^4\,\mathrm{d}\theta\,, \tag{14}$$

$$\alpha_2 = -\frac{l^2}{8\pi^3\omega_r}\,\frac{1}{4|\varphi_z|^2_{\max}}\,\frac{1}{P}\int_0^{2\pi}\frac{\partial^3 H}{\partial r^3}|\varphi_r\varphi_z|^2\,\mathrm{d}\theta\,, \tag{15}$$

$$A_z = 2\,|\varphi_z|_{\max}\left(\frac{P(0)}{P(\theta)}\right)^{\frac{1}{2}}|y| \approx \mathrm{const}\left(\frac{P(0)}{P(\theta)}\right)^{\frac{1}{2}}, \tag{16}$$

A_r, defined by (11), is the amplitude of free betatron oscillations. In (9) and (10), the terms due to $\partial^{2k+1}H_z/\partial r^{2k+1}$, $k > 1$ are omitted: calculations show that usually they are of negligible influence. According to (9) and (10) the amplitude A_r varies with a period large as compared with that of free oscillations $2\pi/\nu_r$. Hence the derivative $(\mathrm{d}\varphi_r/\mathrm{d}\theta)/2$ is equal to the difference between some « effective » frequency ν_{eff} and its resonance value $n_1/2M$,

$$\nu_{\mathrm{eff}} = \nu_r^{(1)} + \alpha_1 A_r^2 + \alpha_2 A_z^2 - g_r \sin\varphi_r\,. \tag{17}$$

It should be noted that frequencies ν_r and ν_z are usually nearly equal: $|\nu_r - \nu_z| \lesssim 1/M \ll \nu_{r\,z}$. Then

$$\frac{\partial^3 H(\theta)}{\partial r^3} \approx -\frac{\partial^3 H(\theta+\pi)}{\partial r^3}\,, \qquad \int_0^{\pi}|\varphi_r\varphi_z|^2\,\mathrm{d}\theta \approx \int_{\pi}^{2\pi}|\varphi_r\varphi_z|^2\,\mathrm{d}\theta\,,$$

and $|\alpha_2| \ll |\alpha_1|$. Thus we neglect the term $\alpha_2 A_z^2$ in (10).

From (9) and (10)

$$\mathcal{H} = 2(\varepsilon_r - g_r\sin\varphi_r)A_r^2 + \alpha A_r^4 = \mathrm{const}\,. \tag{18}$$

Equations

$$\frac{\mathrm{d}A_r^2}{\mathrm{d}\theta} = 0\,, \qquad \frac{\mathrm{d}\varphi_r}{\mathrm{d}\theta} = 0\,,$$

define periodic solutions for x, since, according to (11), x is periodic if $A_r = \mathrm{const}$, $\varphi_r = \mathrm{const}$. Substituting these solutions into (18) we get the following formulae

$$\begin{cases} a) & -\dfrac{\alpha\mathcal{H}}{g_r^2} = \left(\dfrac{\varepsilon_r}{g_r}+1\right)^2 \\ b) & -\dfrac{\alpha\mathcal{H}}{g_r^2} = \left(\dfrac{\varepsilon_r}{g_r}-1\right)^2 \\ c) & \mathcal{H} \quad 0\,. \end{cases} \tag{19}$$

Apparently, (19) define three curves on the plane $(-\alpha\mathcal{H}/g_r^2,\ \varepsilon_r/g_r)$ which Divide it into regions, characterized by different types of phase diagrams $|\alpha| A_r^2/g_r = (|\alpha|/g_r)A_r^2(\varphi_r,\ -\alpha\mathcal{H}/g_r^2,\ \varepsilon_r/g_r)$. Simple analysis, here omitted, shows that in the region under *abed* (Fig. 2) the phase diagrams are infinite ($d\varphi_r/d\theta$

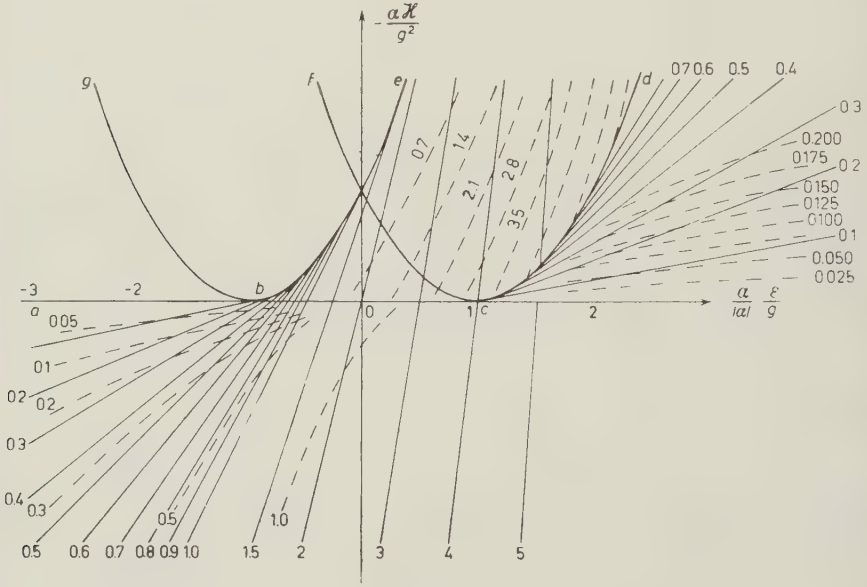

Fig. 2.

doesn't change its sign; see Fig. 3), while in the region within *ebcd* (assuming $\alpha < 0$), or within *fcbd* (assuming $\alpha > 0$), the phase diagrams are closed (Fig. 4). Above *abc* ($\alpha < 0$), or above *fcd* ($\alpha > 0$) there will be no motion. As to the points lying on the curves (19), the phase diagram on *eb* ($\alpha < 0$) or on *fc* ($\alpha > 0$) is a point, while on *bc* and *cd* (or *gb*) the motion is asymptotic:

$$A_r \to 0 \quad \text{by} \quad \mathcal{H} \equiv 0, \quad -1 < \frac{\varepsilon_r}{g_r} < 1, \tag{20}$$

$$-\frac{\alpha A_r^2}{g_r} \to \frac{\varepsilon_r}{g_r} - 1, \quad \sin\varphi_r \to 1 \quad \text{by} \quad -\frac{\alpha\mathcal{H}}{g_r^2} = \left(\frac{\varepsilon_r}{g_r} - 1\right)^2, \quad \frac{\varepsilon_r}{g_r} > 1, \quad \alpha < 0, \tag{21}$$

$$\frac{\alpha A_r^2}{g_r} \to -\left(1 + \frac{\varepsilon_r}{g_r}\right), \quad \sin\varphi_r \to -1 \quad \text{by} \quad -\frac{\alpha\mathcal{H}}{g_r^2} = \left(\frac{\varepsilon_r}{g_r} + 1\right)^2, \quad \frac{\varepsilon_r}{g_r} < -1, \quad \alpha > 0. \tag{22}$$

Knowing the type of the phase diagram, one can readily find the extreme values of the amplitude A_r.

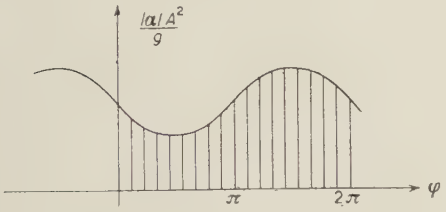

Fig. 3.

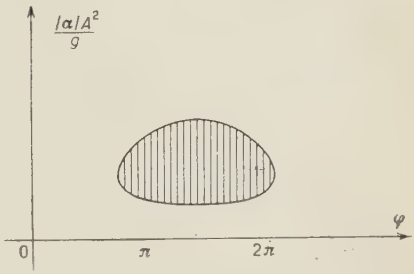

Fig. 4.

Fig. 2 shows parabolas (19) as well as lines $|\alpha| A^2_{\max}/g_r = \text{const}$ for $\alpha < 0$ (solid lines). These lines are defined by the formulae

$$(23)\qquad \varepsilon > g + |\alpha| A^2_{\max},\quad \alpha < 0,\quad \mathcal{H} > 0 \begin{cases} -\dfrac{\alpha\mathcal{H}}{g_r^2} = 2\dfrac{|\alpha| A^2_{\max}}{g_r}\left(\dfrac{\varepsilon_r}{g_r} - 1\right) - \left(\dfrac{\alpha A^2_{\max}}{g_r}\right)^2, \\ -\dfrac{\alpha\mathcal{H}}{g_r^2} = 2\dfrac{|\alpha| A^2_{\min}}{g_r}\left(\dfrac{\varepsilon_r}{g_r} + 1\right) - \left(\dfrac{\alpha A^2_{\min}}{g_r}\right)^2, \end{cases}$$

$$(24)\qquad \varepsilon < -g,\quad \alpha < 0,\quad \mathcal{H} < 0 \begin{cases} -\dfrac{\alpha\mathcal{H}}{g_r^2} = 2\dfrac{|\alpha| A^2_{\max}}{g_r}\left(\dfrac{\varepsilon_r}{g_r} + 1\right) - \left(\dfrac{\alpha A^2_{\max}}{g_r}\right)^2, \\ -\dfrac{\alpha\mathcal{H}}{g_r^2} = 2\dfrac{|\alpha| A^2_{\min}}{g_r}\left(\dfrac{\varepsilon_r}{g_r} - 1\right) - \left(\dfrac{\alpha A^2_{\min}}{g_r}\right)^2, \end{cases}$$

Other regions on $(\mathcal{H}, \varepsilon)$-plate by $\alpha < 0$ is of no practical interest. The simple reflection relative to the axis $\varepsilon/g = 0$ of the Fig. 2 gives the picture for $\alpha > 0$.

The value $\xi = A^2_{\max}/A^2_{\min}$ characterizes the magnitude of amplitude beatings Hence, an acceptable value of $\varepsilon = \varepsilon_{\text{boundary}}$ should be choosen depending on given value of $\xi_{\max}$. Corresponding formulae have a simple form

$$(25)\qquad \left(\frac{\varepsilon}{g}\right)_{\text{boundary}} = \frac{\xi+1}{\xi-1} + \frac{1}{2}\frac{|\alpha| A^2_{\max}}{g}\frac{\xi+1}{\xi},\quad \varepsilon > g + |\alpha| A^2_{\max},\ \alpha < 0,\ \mathcal{H} > 0,$$

$$(26)\qquad \left|\frac{\varepsilon}{g}\right|_{\text{boundary}} = \frac{\xi+1}{\xi-1} - \frac{1}{2}\frac{|\alpha| A^2_{\max}}{g}\frac{\xi+1}{\xi},\quad \varepsilon < -g,\ \alpha < 0,\ \mathcal{H} < 0.$$

Another criterium for the determination of the «safe region» boundary is that the value of $+ (\alpha/g^2)\sqrt{\mathcal{H}^2}$, computed with the account of gas scat-

tering, shouldn't correspond to amplitude greater than the greatest permissible value of A_{max}.

The Hamiltonian form of equations (9), (10) makes it possible to study the amplitude changes connected with adiabatic changes of parameters. Fig. 2 shows the curves (dashed curves)

$$J = \frac{|\alpha|}{g} \int A^2 \left(\varphi, \frac{\varepsilon}{g}, -\frac{\alpha \mathcal{H}}{g^2} \right) \mathrm{d}\varphi = \text{const} , \tag{27}$$

for $\alpha < 0$, when the integral in (27) numerically equals the shaded area shown in Figs. 3 and 4. Fig. 2 gives a clear picture of the amplitude beating, the parameters changing slowly. In particular the oscillations ε due to the synchrotron oscillations of the momentum are usually to be considered as adiabatic, which is permissible even at the start of acceleration cycle. It is quite obvious that by such oscillations ε shoudn't approach the resonance region *cbcd* (or *abef*) deformed by non linearity.

4. – The Resonance Theory of Perturbations.

To analyse the influence of nonresonance harmonics it is possible to use the so-called resonance theory of perturbations. This theory is based on the idea of the Ljapunov-substitution ([2,3]).

Let us suppose that equation

$$\frac{\mathrm{d}x}{\mathrm{d}\theta} + i\nu x = \mathcal{F}(\theta, x, x^*) , \tag{28}$$

contains linear, square and cubic terms representing small perturbation (the coefficients of (28) are periodic). Then we put

$$x = s + a_1(\theta)s + a_2(\theta)s^* + b_1(\theta)s^2 + b_2(\theta)ss^* + b_3(\theta)s^{*2} + \dots , \tag{29}$$

where $a(\theta)$, $b(\theta)$, ... are periodic functions of θ, to be found. It is necessary that s satisfies (with accuracy to second order terms) the equation of the first « resonance approximation ». This condition together with periodicity requirement defines the coefficients of (29). A and φ represent now the amplitude

([2]) A. M. LJAPUNOV: *Obščaja zadača ob usmojčivosti dviženija* (*The general problem of the stability of movement*), Moskva, 1950.

([3]) I. G. MALKIN: *Teorija ustojčivosti dviženija* (*Theory of the stability of movement*), Moskva-Leningrad, 1952.

and the « phase » of s but not of x. If the perturbations are not small, then $A_{r,s}$ doesn't represent the amplitude of free oscillations of r or s.

Additional terms to s in (29) express the direct action of the nonresonance harmonics. Next approximations give now supplementary resonances, because of the nonlinearity of equations. If the perturbations are sufficiently small, the influence of these high order resonances is negligible.

The first approximation in (29) and the second one in the resonance equation might be examined, but higher order approximation are practically incomputable because of rapid increase of the numbers of terms.

5. – Other Effects.

By means of the method described above, other boundaries of the safe region as well as nonlinear resonances were examined. The results of this work will be presented in the next parts of the paper.

* * *

I wish to thank Professor V. B. Berestecki, Dr. V. V. Vladimirski and Dr. L. L. Goldin for helpful discussions.

RIASSUNTO (*)

È stato sviluppato un nuovo metodo per lo studio delle risonanze di betatrone. Sono state esaminate le risonanze dovute ad errori nel gradiente del campo.

(*) *Traduzione a cura della Redazione.*

IL NUOVO CIMENTO Vol. III, N. 2 1° Febbraio 1956

On "Potentials" in the Theory of Quantized Fields.

W. Królikowski

Institute of Physics of the Polish Academy of Sciences - Warsaw

J. Rzewuski

Institute of Physics of the Polish Academy of Sciences - Wroclaw

(ricevuto il 6 Ottobre 1955)

Summary. — In the first part of this paper we discuss the problem of deriving the equations for the state vector of N_0 particles from the Schrödinger equation corresponding to a system of interacting fields. An inhomogeneous integro-differential equation is obtained in which the inhomogeneity is determined by the initial value of the state vector corresponding to N particles ($N \neq N_0$). In the case when this vector vanishes at a particular time, the equation for the state vector of N_0 particles becomes homogeneous and may be replaced by a stationary equation independent of the time and containing an interaction operator which is a function of the energy eigenvalue (non linear energy eigenvalue problem). A closed expression is obtained for the kernel of the integro-differential equation, valid for arbitrary values of the interaction constant. In the second part the integro-differential equation for the state vector of N_0 particles is replaced by an equivalent purely differential equation with respect to the time. In the homogeneous case this equation has the form of a Schrödinger equation (linear energy-eigenvalue problem) with a complex « potential ». The imaginary part of this potential is due to the instability of the state of N_0 particles and determines the life-time of this state. It is suggested that this equation describes —after time separation— the bound states of N_0 particles.

1. - Introduction.

Consider a system of two quantized fields interacting with each other and possibly with an external field. Assume one of the fields to obey the Fermi-Dirac and the other the Bose-Einstein statistics. Let $\overset{0}{H}$ denote that part of

the Hamiltonian which describes the energy of the free fields and, possibly, the interaction with external fields. In the case of electrodynamics we shall possibly include in $\overset{0}{H}$ also interactions by means of the longitudinal quanta. Let $\overset{1}{H}$ denote the remaining part of the Hamiltonian describing mutual interactions of the fields.

We introduce a representation by means of the basic vectors $|\lambda(N)\rangle$ being simultaneous eigenvectors of a complete system of commuting observables. These observables are chosen in such a way that their eigenvalues $\lambda(N)$ determine the state λ corresponding to $N = (f, a, b)$ particles, where f, a, b are the numbers of fermions, antifermions and bosons respectively. We assume for simplicity that $\overset{0}{H}$ is diagonal in this representation

$$\overset{0}{H}\,|\lambda(N)\rangle = E_{\lambda(N)}\,|\lambda(N)\rangle\,. \tag{1.1}$$

In particular, when there is no interaction with external fields, the representation $|\lambda(N)\rangle$ is just the momentum representation (of Fock's type).

Let us introduce further the notation

$$P_{\parallel} = \sum_{\lambda(N_0)} |\lambda(N_0)\rangle\langle\lambda(N_0)|\,, \qquad P_{\perp} = \sum_{N \neq N_0} \sum_{\lambda(N)} |\lambda(N)\rangle\langle\lambda(N)| \tag{1.2}$$

The operator $P_{\parallel}$ projects an arbitrary state Ψ of the system upon the subspace corresponding to N_0 particles, whereas the operator $P_{\perp}$ projects Ψ upon the subspace corresponding to all other numbers of particles $N \neq N_0$. Thus the vector $\Psi_{\parallel} = P_{\parallel}\Psi$ describes N_0 particles and the vector $\Psi_{\perp} = P_{\perp}\Psi$ describes all other numbers of particles occuring in the state Ψ of the system.

We note the relations

$$P_{\parallel} + P_{\perp} = 1\,, \qquad P_{\parallel}P_{\perp} = P_{\perp}P_{\parallel} = 0\,, \qquad P_{\parallel}^2 = P_{\parallel}\,, \qquad P_{\perp}^2 = P_{\perp}\,. \tag{1.3}$$

From the first of these relations there follows $\Psi = \Psi_{\parallel} + \Psi_{\perp}$. The operators $P_{\parallel}$ and $P_{\perp}$ commute, due to (1.1), with $\overset{0}{H}$. Thus

$$P_{\parallel}\overset{0}{H}P_{\perp} = P_{\perp}\overset{0}{H}P_{\parallel} = 0\,.$$

Further, due to the linearity of $\overset{1}{H}$ in the operators of the Bose-field, we have

$$P_{\parallel}\overset{1}{H}P_{\parallel} = 0\,.$$

The equation for the state vector Ψ has in the interaction picture the form

$$i\hbar\,\frac{\partial \Psi_{\mathrm{I}}}{\partial t} = \overset{1}{H}_{\mathrm{I}}(t)\Psi_{\mathrm{I}}\,. \tag{1.4}$$

To obtain an equation for the state vector $\Psi_{\parallel}$ we multiply (1.4) on the left with $P_{\parallel}$ or $P_{\perp}$ respectively.

$$\left\{\begin{array}{l} i\hbar\,\dfrac{\partial \Psi_{\mathrm{I}\parallel}}{\partial t} = P_{\parallel}\overset{1}{H}_{\mathrm{I}}\Psi_{\mathrm{I}\perp}\,, \\ i\hbar\,\dfrac{\partial \Psi_{\mathrm{I}\perp}}{\partial t} - P_{\perp}\overset{1}{H}_{\mathrm{I}}\Psi_{\mathrm{I}\perp} - P_{\perp}\overset{1}{H}_{\mathrm{I}}\Psi_{\mathrm{I}\parallel}\,. \end{array}\right. \tag{1.5}$$

where $\Psi_{\mathrm{I}\parallel} = P_{\parallel}\Psi_{\mathrm{I}} = \Psi_{\parallel\mathrm{I}}$, $\Psi_{\mathrm{I}\perp} = P_{\perp}\Psi_{\mathrm{I}} = \Psi_{\perp\mathrm{I}}$. The set (1.5) is, of course, equivalent with the original equation (1.4).

Integrating now the second equation (1.5) with respect to the time we obtain

$$\Psi_{\mathrm{I}\perp}(t) = \Psi_{\perp}(t_0) - \frac{i}{\hbar}\int_{t_0}^{t} \mathrm{d}t' P_{\perp}\overset{1}{H}_{\mathrm{I}}(t')\,\Psi_{\mathrm{I}\parallel}(t') - \frac{i}{\hbar}\int_{t_0}^{t} \mathrm{d}t' P_{\perp}\overset{1}{H}_{\mathrm{I}}(t')\Psi_{\mathrm{I}\perp}(t')\,. \tag{1.6}$$

We introduce this equation into the first equation (1.5) and repeat this procedure n times. Assuming

$$\lim_{n\to\infty}\int_{t_0}^{t}\mathrm{d}t_1\int_{t_0}^{t_1}\mathrm{d}t_2 \ldots \int_{t_0}^{t_{n-1}}\mathrm{d}t_n P_{\perp}\overset{1}{H}_{\mathrm{I}}(t_1)P\overset{1}{H}_{\mathrm{I}}(t_2)\ldots P_{\perp}\overset{1}{H}_{\mathrm{I}}(t_n)\Psi_{\mathrm{I}\perp}(t_n) = 0 \quad (*) \tag{1.7}$$

we get in this way in the limit $n \to \infty$ an equation which does not contain $\Psi_{\mathrm{I}\perp}(t)$ any more

$$i\hbar\,\frac{\partial \Psi_{\mathrm{I}\parallel}(t)}{\partial t} = P\overset{1}{H}_{\mathrm{I}}(t)P\; T\exp\left[-\frac{i}{\hbar}\int_{t_0}^{t}\mathrm{d}t' P\overset{1}{H}_{\mathrm{I}}(t')P\right]\Psi_{\perp}(t_0) - \frac{i}{\hbar}\int_{t_0}^{\infty}\mathrm{d}t' K_{\mathrm{I}}(t,t')\Psi_{\mathrm{I}\parallel}(t')\,, \tag{1.8}$$

where

$$K_{\mathrm{I}}(t,t') = P_{\parallel}\overset{1}{H}_{\mathrm{I}}(t)P_{\perp}\left[\theta^{+}(t-t') + \left(-\frac{i}{\hbar}\right)^{2}\int_{t_0}^{\infty}\mathrm{d}t_1\int_{t}^{\infty}\mathrm{d}t_2\,\theta^{-}(t-t_1)P\overset{1}{H}_{\mathrm{I}}(t_1)P\,\theta^{+}(t_1-t_2)P\overset{1}{H}_{\mathrm{I}}(t_2)P_{\perp}\theta^{+}(t_2-t') + \ldots\right]\cdot P_{\perp}\overset{1}{H}_{\mathrm{I}}(t')P_{\parallel}\,. \tag{1.9}$$

$$\theta^{-}(t) = \begin{cases} 1 & \text{for} \quad t > 0 \\ 0 & \text{for} \quad t < 0 \end{cases}$$

and the symbol T denotes the operator of chronological ordering.

(*) This equation will be justified presently by another direct method for the elimination of $\Psi_{\perp}$.

Formula (1.9) represents the kernel of equation (1.8) in the form of an expansion in powers of the coupling constant. The rule for the construction of higher order terms is evident from the first two terms in (1.9). It may be noted that in $K_I(t, t')$ only terms containing an even number of $\overset{1}{H}$ operators occur. This is a consequence of the relation

$$P_{\parallel} \text{ (product of an odd number of } \overset{1}{H}) \, P_{\parallel} = 0 \,,$$

which is due to the fact that the Bose-fields occur in $\overset{1}{H}$ linearly.

By means of the unitary transformation

$$\Psi_I(t) = \exp\left[\frac{i}{\hbar}\overset{0}{H}(t-t_0)\right]\Psi(t)\,, \qquad O_I(t) = \exp\left[\frac{i}{\hbar}\overset{0}{H}(t-t_0)\right] O \exp\left[-\frac{i}{\hbar}\overset{0}{H}(t-t_0)\right],$$

we may now go over to the Schrödinger picture in which the operators are time independent. Equation (1.8) takes in this picture the form

$$\left(i\hbar\frac{\partial}{\partial t} - \overset{0}{H}\right)\Psi_{\parallel}(t) =$$

$$= P_{\parallel}\overset{1}{H}P_{\perp} \exp\left[-\frac{i}{\hbar}\overset{0}{H}(t-t_0)\right] T \exp\left[-\frac{i}{\hbar}\int_{t_0}^{t} dt' P_{\perp}\overset{1}{H}_I(t')P_{\perp}\right]\Psi_{\perp}(t_0)$$

$$-\frac{i}{\hbar}\int_{t_0}^{\infty} dt'\, K(t, t')\Psi_{\parallel}(t')\,,$$

where

$$K(t, t') = P_{\parallel}\overset{1}{H}P_{\perp} \exp\left[-\frac{i}{\hbar}\overset{0}{H}(t-t_0)\right]\Big[\theta^+(t-t') +$$

$$+\left(-\frac{i}{\hbar}\right)^2\int_{t_0}^{\infty} dt_1 \int_{t_0}^{\infty} dt_2 \theta^+(t-t_1)P_{\perp}\overset{1}{H}_I(t_1)P_{\perp}\theta^+(t_1-t_2)P_{\perp}\overset{1}{H}_I(t_2)P_{\perp}\theta^+(t_2-t') + \ldots\Big]$$

$$\cdot \exp\left[\frac{i}{\hbar}\overset{0}{H}(t'-t_0)\right] P_{\parallel}\overset{1}{H}P_{\parallel} + P_{\parallel}\overset{1}{H}P_{\perp}\theta^+(t-t') \exp\left[-\frac{i}{\hbar}\overset{0}{H}(t-t')\right] P_{\perp}\overset{1}{H}P_{\parallel}$$

$$+ P_{\perp}\overset{1}{H}P_{\perp}\left(-\frac{i}{\hbar}\right)^2\int_{t_0}^{\infty} dt_1 \int_{t_0}^{\infty} dt_2 \theta^+(t-t_1) \exp\left[-\frac{i}{\hbar}\overset{0}{H}(t-t_1)\right] P_{\perp}\overset{1}{H}P_{\perp}\theta^+(t_1-t_2)\cdot$$

$$\cdot \exp\left[-\frac{i}{\hbar}\overset{0}{H}(t_1-t_2)\right] P_{\perp}\overset{1}{H}P_{\perp}\theta^+(t_2-t') \exp\left[-\frac{i}{\hbar}\overset{0}{H}(t_2-t')\right] P_{\perp}\overset{1}{H}P_{\parallel} + \ldots\,.$$

Equation (1.10) is the integro-differential equation (with respect to t) for the state vector $\Psi_{\parallel}(t)$ corresponding to a state with N_0 particles. It may be written in terms of the representatives in the representation determined by the basic vectors $|\lambda(N)\rangle$. It then becomes an integral equation with respect to the variables $\lambda(N)$ for the amplitude $\Psi(\lambda(N_0), t) = \langle\lambda(N_0)|\Psi_{\parallel}(t)\rangle$ depending upon the initial values of the amplitude $\Psi(\lambda(N,) t) = \langle\lambda(N)|\Psi_{\perp}(t)\rangle$ for $N \neq N_0$.

We note that the quantity $\langle\Psi(t)|\Psi(t)\rangle$ is a constant of the motion and, therefore, the normalization condition

$$1 = \langle\Psi(t)|\Psi(t)\rangle = \langle\Psi_{\parallel}(t)|\Psi_{\parallel}(t)\rangle + \langle\Psi_{\perp}(t)|\Psi_{\perp}(t)\rangle \tag{1.12}$$

is preserved in time. In particular if $\Psi_{\perp}(t_0) = 1$, equation (1.10) describes transitions from the state $\Psi_{\perp}(t)$ to the state $\Psi_{\parallel}(t)$. If $\Psi_{\perp}(t_0) = 0$ this equation describes transitions from the state $\Psi_{\parallel}(t)$ to the state $\Psi_{\perp}(t)$ and, therefore, between others, also the so called bound states of N_0 particles. Obviously the states corresponding to N_0 particles (even the bound states of N_0 particles) are in general not stationary, i.e. they are not eigenstates of the total Hamiltonian $H = \overset{0}{H} + \overset{1}{H}$. This is due to the fact that this Hamiltonian does not commute with the operator of the number of particles.

In the case when $\Psi_{\perp}(t_0) = 0$ and $t_0 \to -\infty$ one may separate in (1.10) the time by means of the substitution

$$\Psi_{\parallel E}(t) = \Phi_{\parallel E} \exp\left[-\frac{i}{\hbar} Et\right]. \tag{1.13}$$

In this case the kernel K becomes a function of the difference $t - t'$ (cf. (1.11)) and one gets for $\Phi_{\parallel E}$ the following equation

$$(E - \overset{0}{H})\Phi_{\parallel E} = U(E)\Phi_{\parallel E} \tag{1.14}$$

where

$$U(E) = -\frac{i}{\hbar}\int_{-\infty}^{+\infty} dt K(t) \exp\left[\frac{i}{\hbar} Et\right] = \tag{1.15}$$

$$= P_{\parallel}\overset{1}{H}P_{\perp}\left[P\frac{1}{E - \overset{0}{H}} - i\pi\delta(E - \overset{0}{H})\right]P_{\perp}\overset{1}{H}P_{\parallel} +$$

$$P_{\parallel}\overset{1}{H}P\left[P\frac{1}{E - \overset{0}{H}} - i\pi\delta(E - \overset{0}{H})\right]P_{\perp}\overset{1}{H}P_{\perp}\left[P\frac{1}{E - \overset{0}{H}} - i\pi\delta(E - \overset{0}{H})\right]\cdot$$

$$\cdot P_{\perp}\overset{1}{H}P_{\perp}\left[P\frac{1}{E - \overset{0}{H}} - i\pi\delta(E - \overset{0}{H})\right]P_{\parallel}\overset{1}{H}P_{\parallel} + \ldots$$

(The rule for constructing higher order terms in (1.15) is evident from the first two). Obviously an arbitrary linear combination of solutions of the type (1.13) is again a solution of (1.10)

$$\Psi_{\parallel}(t) = \sum_{E} \Phi_{\parallel E} \exp\left[-\frac{i}{\hbar} Et\right] c_E ,$$

(c_E. arbitrary constants). In deriving the second of the expressions (1.15) we have made use of the well known relation

$$-\frac{i}{\hbar}\int_{-\infty}^{\infty} dt \exp\left[\frac{i}{\hbar}(\overset{0}{H} - E)t\right] \theta^{-}(t) = -2\pi i\,\delta_{+}(\overset{0}{H} - E) = P\,\frac{1}{E - \overset{0}{H}} - i\pi\,\delta(E - \overset{0}{H}),$$

where the symbol P denotes that upon integration one has to take Cauchy's principal value of the integral.

Equation (1.14) written in terms of representatives in the representation given by the basic vectors $|\lambda(N)$ becomes an integral equation with respect to $\lambda(N_0)$ (we note that $U = P_{\parallel} U P_{\parallel}$ so that only matrix elements from the subspace $|\lambda(N_0)\rangle$ occur) for the amplitude $\Phi_E(\lambda(N_0)) = \langle \lambda(N_0) | \Phi_{\parallel E}\rangle$.

The method for the elimination of the component $\Psi_{\perp}(t)$ presented here is based on the assumption (1.7) and results in an equation for $\Psi_{\parallel}(t)$ in which the kernel $K(t, t')$ is an expansion in powers of the coupling constant. The method is, therefore, limited by the condition of convergence for this expansion.

We shall show now that the elimination of $\Psi_{\perp}(t)$ may be carried out in another direct way leading to an equation for $\Psi_{\parallel}(t)$ in which the kernel $K(t, t')$ is given by a closed expression. This derivation makes no use of the assumption (1.7) and does not involve expansions in powers of the coupling constant. It is not limited, therefore, by the convergence condition.

Let us transform the equation for the state vector in the Schrödinger picture

$$\left(i\hbar\frac{\partial}{\partial t} - \overset{0}{H}\right)\Psi = \overset{1}{H}\Psi ,$$

by means of the following unitary transformation:

$$\Psi_F(t) = \exp\left[\frac{i}{\hbar}(\overset{0}{H} + P_{\perp}\overset{1}{H}P_{\perp})(t - t_0)\right]\Psi(t) ,$$

$$O_F(t) = \exp\left[\frac{i}{\hbar}(\overset{0}{H} + P_{\perp}\overset{1}{H}P_{\perp})(t - t_0)\right] O \exp\left[-\frac{i}{\hbar}(\overset{0}{H} + P_{\perp}\overset{1}{H}P_{\perp})(t - t_0)\right] .$$

We note that the operators $P_{\parallel}$ and $P_{\perp}$ commute with $\overset{0}{H} + P_{\perp}\overset{1}{H}P_{\perp}$. In-

deed, we have

$$[P_{\parallel}, \overset{0}{H} + P_{\perp}\overset{1}{H}P_{\perp}] = [P_{\parallel}, P_{\perp}\overset{1}{H}P_{\perp}] = 0$$

(since $P_{\parallel}P_{\perp} = P_{\perp}P_{\parallel} = 0$) and

$$[P_{\perp}, \overset{0}{H} + P_{\perp}\overset{1}{H}P_{\perp}] = [P_{\perp}, P_{\perp}\overset{1}{H}P_{\perp}] = 0$$

(since $P_{\perp}^2 = P_{\perp}$). Another relation which we shall use in the derivation is

$$\overset{1}{H} = P_{\perp}\overset{1}{H}P_{\perp} + P_{\parallel}\overset{1}{H}P_{\perp} + P_{\perp}\overset{1}{H}P_{\parallel} .$$

It is a consequence of the equations $P_{\parallel} + P_{\perp} = 1$ and $P_{\parallel}\overset{1}{H}P_{\parallel} = 0$. Due to these relations, the equation for the state vector in the new picture takes the form

$$i\hbar \frac{\partial \Psi_F}{\partial t} = (P_{\parallel}\overset{1}{H}_F(t)P_{\perp} + P_{\perp}\overset{1}{H}_F(t)P_{\parallel})\Psi_F . \tag{1.4'}$$

Multiplying this equation by $P_{\parallel}$ or $P_{\perp}$ respectively, we get the equivalent system of two equations

$$\begin{cases} i\hbar \dfrac{\partial \Psi_{F\parallel}}{\partial t} = P_{\parallel}\overset{1}{H}_F(t)\Psi_{F\perp} , \\ i\hbar \dfrac{\partial \Psi_{F\perp}}{\partial t} = P_{\perp}\overset{1}{H}_F(t)\Psi_{F\parallel} , \end{cases} \tag{1.5'}$$

where $\Psi_{F\parallel} = P_{\parallel}\Psi_F = \Psi_{\parallel F}$, $\Psi_{F\perp} = P_{\perp}\Psi_F = \Psi_{\perp F}$. Eliminating now from the first equation (1.5') the component Ψ_F by means of the second of these equations, we get

$$i\hbar \frac{\partial \Psi_{F\parallel}(t)}{\partial t} = P_{\parallel}\overset{1}{H}_F(t)P_{\perp}\Psi_{\perp}(t_0) - \frac{i}{\hbar}\int_{t_0}^{\infty} dt' K_F(t, t')\Psi_{F\parallel}(t') , \tag{1.8'}$$

where

$$K_F(t, t') = P_{\parallel}\overset{1}{H}_F(t)P_{\perp}\theta^{+}(t - t')P_{-}\overset{1}{H}_F(t')P_{\parallel} . \tag{1.9'}$$

Going back to the Schrödinger picture and making use of the equality $P\overset{1}{H}P\Psi = 0$, we get for the component $\Psi_{\parallel}(t)$ of the state vector $\Psi(t)$ in the Schrödinger picture the following equation

$$\left(i\hbar \frac{\partial}{\partial t} - \overset{0}{H}\right)\Psi_{\parallel}(t) = P_{\parallel}\overset{1}{H}P_{\perp} \cdot$$

$$\cdot \exp\left[-\frac{i}{\hbar}(\overset{0}{H} + P\overset{1}{H}P)(t - t_0)\right]\Psi_{\perp}(t_0) - \frac{i}{\hbar}\int_{t_0}^{\infty} dt' K(t - t')\Psi_{\parallel}(t') ,$$

where

$$(1.11)' \qquad K(t-t') = P_{\parallel}\overset{1}{H}P_{\perp}\theta^{+}(t-t')\exp\left\{-\frac{i}{\hbar}(\overset{0}{H}+P_{\perp}\overset{1}{H}P_{\perp})(t-t')\right\}P_{\perp}\overset{1}{H}P_{\parallel}.$$

It is seen that the formula (1.11′) gives a closed expression for the kernel $K(t-t')$, whereas formula (1.11) was an expansion of this kernel in powers of the coupling constant. (1.11′) is valid independently of the assumption about the convergence of (1.11). We shall show presently that for $t_0 \to \infty$ and for sufficiently small values of the coupling constant, admitting convergent expansions in powers of this constant, formula (1.11′) is identical with (1.11) (cf. (1.15′) and (1.15)).

In the case when $\Psi_{\perp}(t_0) = 0$ and $t_0 \to -\infty$ we may go over from (1.10′) to the corresponding time-independent equation by means of the substitution (1.13). We get in this way equation (1.14) with

$$(1.15') \qquad U(E) = -\frac{i}{\hbar}\int_{-\infty}^{+\infty} dt\, K(t)\exp\left[\frac{i}{\hbar}Et\right] =$$

$$= P_{\parallel}\overset{1}{H}P_{\perp}\left\{P\frac{1}{E-\overset{0}{H}-P_{\perp}\overset{1}{H}P} - i\pi\delta(E-\overset{0}{H}-P_{\perp}\overset{1}{H}P_{\perp})\right\}P_{\perp}\overset{1}{H}P_{\parallel}.$$

The operator $P(1/(E-\overset{0}{H}-P_{\perp}\overset{1}{H}P_{\perp})) - i\pi\delta(E-\overset{0}{H}-P_{\perp}\overset{1}{H}P_{\perp})$ occuring in (1.15′) is one of the inverse operators to the operator $E-\overset{0}{H}-P_{\perp}\overset{1}{H}P_{\perp}$. We may write, therefore,

$$P\frac{1}{E-\overset{0}{H}-P_{\perp}\overset{1}{H}P} - i\pi\delta(E-\overset{0}{H}-P_{\perp}\overset{1}{H}P_{\perp}) = (E-\overset{0}{H}-P_{\perp}\overset{1}{H}P_{\perp})^{-1} =$$

$$= \left\{(E-\overset{0}{H})\left[1-\left(P\frac{1}{E-\overset{0}{H}} - i\pi\delta(E-\overset{0}{H})\right)P_{\perp}\overset{1}{H}P_{\perp}\right]\right\}^{-1} =$$

$$= \left[1-\left(P\frac{1}{E-\overset{0}{H}} - i\pi\delta(E-\overset{0}{H})\right)P_{\perp}\overset{1}{H}P_{\perp}\right]^{-1}\left(P\frac{1}{E-\overset{0}{H}} - i\pi\delta(E-\overset{0}{H})\right).$$

Here we have put $P(1/(E-\overset{0}{H}-P_{\perp}\overset{1}{H}P_{\perp})) - i\pi\delta(E-\overset{0}{H})$ for the inverse of $E-\overset{0}{H}$ and we have made use of the relation $(a\cdot b)^{-1} = b^{-1}a^{-1}$. It follows that in the case when a convergent expansion in powers of the coupling constants exists, we may expand (1.15′) into the series (1.15) and, therefore, (1.11′) into (1.11) with $t_0 = -\infty$.

Equation (1.14) is identical with the equation for the component $\Phi_{\parallel E} = P\Phi_E$ which one obtains from the eigenvalue problem for the total energy $H = \overset{0}{H} + \overset{1}{H}$:

$$(1.16) \qquad (E-\overset{0}{H})\Phi_E = \overset{1}{H}\Phi_E$$

(where $\Phi_E = |E\rangle$) by elimination of the component $\Phi_{\perp E} = P_\perp \Phi_E$. Indeed, multiplying (1.16) on the left with $P_\perp$ or $P_\parallel$ respectively, we get the equivalent set of two equations

$$\begin{cases} (E - \overset{0}{H})\Phi_{\parallel E} = P_\parallel \overset{1}{H}\Phi_{\perp E} + P_\parallel \overset{1}{H}\Phi_{\parallel E}, \\ (E - \overset{0}{H})\Phi_{\perp E} = P_\perp \overset{1}{H}\Phi_{\perp E} + P_\perp \overset{1}{H}\Phi_{\parallel E}. \end{cases} \tag{1.17}$$

From the second of these equations we get

$$\Phi_{\perp E} = (E - \overset{0}{H} - P_\perp \overset{1}{H} P_\perp)^{-1} P_\perp \overset{1}{H}\Phi_{\parallel E} = \tag{1.18}$$

$$= \left[P \frac{1}{E - \overset{0}{H} - P_\perp \overset{1}{H} P_\perp} - i\pi\delta(E - \overset{0}{H} - P_\perp \overset{1}{H} P_\perp) \right] P_\perp \overset{1}{H}\Phi_{\parallel E},$$

where the operator $P\big(1/(E - \overset{0}{H} - P_\perp \overset{1}{H} P_\perp)\big) - i\pi\delta(E - \overset{0}{H} - P_\perp \overset{1}{H} P_\perp)$ is taken as the inverse of $E - \overset{0}{H} - P_\perp \overset{1}{H} P_\perp$. Introducing (1.18) into the first equation (1.17) we get equation (1.14) with $U(E)$ given by formula (1.15′).

It follows that the parameter E in equation (1.14) represents the eigenvalue of the total energy of the system. This equation describes, therefore, the state $\Phi_{\parallel E} = P_\parallel \Phi_E$ corresponding to N_0 particles on the energy shell E. Since the total Hamiltonian H does not commute with the operator of the number of particles, this state $(\Phi_{\parallel E})$ is in general not stationary. There occur (on the energy shell E) transitions from the state $\Phi_{\parallel E}$ to the state $\Phi_{\perp E}$. Equation (1.14) together with the normalization condition

$$1 = \langle \Phi_E | \Phi_E \rangle \equiv \langle \Phi_{\parallel E} | \Phi_{\parallel E} \rangle + \langle \Phi_{\perp E} | \Phi_{\perp E} \tag{1.19}$$

describes these transitions if we disregard their temporal development.

Due to the dependence of $U(E)$ on E, equation (1.14) does not represent a linear eigenvalue problem with respect to the parameter E (cf. [1]). The operator $U(E)$ does not represent, therefore, the interaction energy of N_0 particles as would be the case if $U(E)$ were independent of E and hermitean.

Several approximative methods were developed for the elimination of E from the right hand side of equations of the type (1.14) (cf. [1] and [2]). In these methods the parameter E in the operator $U(E)$ is usually replaced in the first approximation by the rest-energy of N_0 particles. The resulting operator represents then the so called adiabatic potential.

---

[1] A. KLEIN: *Phys. Rev.*, **94**, 195 (1954).

[2] J. C. TAYLOR: *Phys. Rev.*, **96**, 1438 (1954).

It is seen from (1.15) that $U(E)$ is a real (= hermitean) operator only in the case when $\delta(E - \overset{0}{H}) = 0$, i.e. if E is different from all $E_{\lambda(N)}$ where N corresponds to the intermediate states occuring in formula (1.15). In general $U(E)$ will possess an imaginary (= antihermitean) part. The approximative procedure eliminating E from the right hand side of (1.14) must then be carried out in such a way as to yield from $U(E)$ a real interaction operator. Otherwise the result would be inconsistent with the real character of E following from equation (1.16).

We shall show in Section 2 of this paper that the integro-differential equation (1.10) may be replaced by an equivalent purely differential equation with respect to t. This differential equation takes in the case $\Psi(t_0) = 0$ the form of a Schrödinger equation with a complex « potential ». The appearance of an imaginary (= antihermitean) part of this potential is a consequence of the non-stationary character of the states corresponding to a fixed number of particles, i.e. a consequence of transitions which occur from the state $\Psi_1(t)$ to the state $\Psi_2(t)$. These results are obtained by means of a procedure developed by one of us [3] in connection with the theory of non-local interactions. The same procedure was later applied in [4] to convert the Bethe-Salpeter equation into an equivalent one-time equation possessing the form of a Schrödinger equation.

2. - The equation for the state vector corresponding to a fixed number of particles.

Equation (1.10) for the state vector of N_0 particles is integro-differential with respect to the time. It may be replaced by an equivalent purely integral equation (with respect to t) by means of an arbitrary particular solution $G(t)$ (the operator analogous to the Green function) of the equation

$$\left(i\hbar\frac{\partial}{\partial t} - \overset{0}{H}\right) G(t) = \delta(t)\,. \tag{2.1}$$

It is easily seen that the solution of (2.1) may be represented by the integral

$$G(t) = -\frac{1}{2\pi\hbar}\int_{-\infty}^{+\infty} \mathrm{d}\alpha\,(\overset{0}{H} + \alpha)^{-1} \exp\left|\frac{i}{\hbar}\,\alpha t\right|. \tag{2.2}$$

Choosing here a particular form for the inverse of the operator $\overset{0}{H} + \alpha$, e.g.

---

[3] J. Rzewuski: *Acta Phys Pol.*, **13**, 135 (1954); **14**, 121 (1955); *Bull. Acad. Pol. Sci., Cl. III*, **2**, 429 (1954).

[4] W. Królikowski and J. Rzewuski: *Nuovo Cimento*, **2**, 203 (1955).

$(\overset{0}{H} - \varkappa)^{-1} = P(1/(\overset{0}{H} + \varkappa)) - i\pi\delta(\overset{0}{H} + \varkappa)$ we fix the particular solution of (2.1). It may be noted that a representation of the type (2.2) is possible only in the Schrödinger picture, where the operators do not depend on time. $G(t)$ as a function of $\overset{0}{H}$ is a real operator commuting with $\overset{0}{H}$.

Assuming for simplicity $\Psi_\perp(t_0) = 0$ and $t_0 \to -\infty$, multiplying equation (1.10) on the left by $G(t' - t)$ and integrating with respect to t from $-\infty$ to $+\infty$ we get after a partial integration, due to (2.1) and to the commutability of G and $\overset{0}{H}$,

$$\Psi_\parallel(t) = \Psi^0_\parallel(t) - \frac{i}{\hbar}\int_{-\infty}^{+\infty} \mathrm{d}t'\, N(t - t')\Psi_\parallel(t')\,, \tag{2.3}$$

where $\Psi^0_\parallel(t)$ is a state of N_0 particles satisfying the unperturbed equation

$$\left(i\hbar\frac{\partial}{\partial t} - \overset{0}{H}\right)\Psi^0_\parallel(t) = 0 \tag{2.4}$$

and

$$N(t - t') = \int_{-\infty}^{+\infty} G(t - t'')\,\mathrm{d}t''\, K(t'' - t'). \tag{2.5}$$

Equation (2.3) is equivalent with (1.10) in the sense that each solution of (1.10) satisfies (2.3) with a particular $\Psi^0_\perp$ and vice versa each solution of (2.3) satisfies equation (1.10), $\Psi^0_\parallel$ being a general solution of (2.4).

Denoting by $R(t - t')$ the resolving kernel of equation (2.3), we may write the solution of this equation in the form

$$\Psi_\parallel(t) = \Psi^0_\parallel(t) - \frac{i}{\hbar}\int_{-\infty}^{+\infty} \mathrm{d}t'\, R(t - t')\Psi^0_\parallel(t')\,. \tag{2.6}$$

Now $\Psi^0_\parallel(t)$ is an arbitrary solution of (2.4) and we have, therefore,

$$\Psi^0_\parallel(t) = \exp\left[-\frac{i}{\hbar}\overset{0}{H}(t - t_0)\right]\Psi^0_\parallel(t_0)\,, \tag{2.7}$$

the initial value $\Psi^0_\parallel(t_0)$ being an arbitrary state corresponding to N_0 particles. Expressing in the integral in equation (2.6) $\Psi^0_\parallel(t')$ by means of $\Psi^0_\parallel(t)$ we get, according to (2.7),

$$\Psi_\parallel(t) = (1 - A)\Psi^0_\parallel(t)\,, \tag{2.8}$$

with

$$A = \frac{i}{\hbar}\int_{-\infty}^{+\infty} dt\, R(t) \exp\left[\frac{i}{\hbar}\overset{0}{H}t\right]. \tag{2.9}$$

Equation (1.10) may be reduced to an equivalent purely differential equation with respect to the time if we can find an operator V for which the following equation

$$-\frac{i}{\hbar}\int_{-\infty}^{\infty} dt'\, K(t-t')\Psi_{\parallel}(t') = V\Psi_{\parallel}(t)\,, \tag{2.10}$$

is satisfied identically in the solutions of (1.10) (cf. [3] and [1]). Introducing (2.8) into (2.10), making use of (2.7) and remembering that the initial value of the general solution $\Psi_{\parallel}^{0}$ at an arbitrary but fixed point may be chosen at will, we get the following equation for the operator V

$$V(1-A) = -\frac{i}{\hbar}\int_{-\infty}^{+\infty} dt\, K(t)(1-A)\exp\left[\frac{i}{\hbar}\overset{0}{H}t\right]. \tag{2.11}$$

This equation may be solved immediately by multiplication on the right with the operator $(1-A)^{-1}$

$$V = -\frac{i}{\hbar}\int_{-\infty}^{+\infty} dt\, K(t)(1-A)\exp\left[\frac{i}{\hbar}\overset{0}{H}t\right](1-A)^{-1}. \tag{2.12}$$

Conversely one may easily show, that equation (2.10) is a consequence of (2.11) or (2.12). The operator V is, therefore, uniquely determined by the operators K and G. It may be noted that, due to the relation $K = P_{\parallel}KP_{\parallel}$, we have $R = P_{\parallel}RP_{\parallel}$, $A = P_{\parallel}AP_{\parallel}$ and $V = P_{\parallel}VP_{\parallel}$.

The above method does not involve expansions in powers of the coupling constant. Assuming that such convergent expansions exist for the quantities $\Psi_{\parallel}$ and K (cf. (1.11))

$$K = \sum_{n=1}^{\infty} K^{(2n)}\,, \qquad \Psi_{\parallel} = \sum_{n=0}^{\infty}\Psi_{\parallel}^{(2n)} \tag{2.13}$$

and, therefore, also for the quantities R and A

$$R = \sum_{n=1}^{\infty} R^{(2n)}\,, \qquad A = \sum_{n=1}^{\infty} A^{(2n)} \tag{2.14}$$

we may calculate

$$V = \sum_{n=1}^{\infty} V^{(2n)} \tag{2.15}$$

up to an arbitrary order of approximation.

Introducing (2.13-15) into (2.12) we get e.g. for the first two approximations $V^{(2)}$ and $V^{(4)}$ (order 2 and 4 in the coupling constant)

$$V^{(2)} = -\frac{i}{\hbar}\int_{-\infty}^{+\infty} \mathrm{d}t\, K^{(2)}(t) \exp\left[\frac{i}{\hbar}\overset{0}{H}t\right], \tag{2.16}$$

$$V^{(4)} = -\frac{i}{\hbar}\int_{-\infty}^{+\infty} \mathrm{d}t \left\{K^{(4)}(t) \exp\left[\frac{i}{\hbar}\overset{0}{H}t\right] - \right. \tag{2.16'}$$

$$\left. - K^{(2)}(t) A^{(2)} \exp\left[\frac{i}{\hbar}\overset{0}{H}t\right] + K^{(2)}(t) \exp\left[\frac{i}{\hbar}\overset{0}{H}t\right] A^{(2)}\right\}$$

By virtue of (2.10) we may replace equation (1.10) in the case $\Psi_{\perp}(t_0) = 0$, $t_0 \to -\infty$ by the equivalent equation

$$\left(i\hbar\frac{\partial}{\partial t} - \overset{0}{H}\right)\Psi_{\parallel}(t) = V\Psi_{\parallel}(t) \tag{2.17}$$

with V given by the formula (2.12). This purely differential equation (with respect to the time) possesses the form of a Schrödinger equation with the «potential» V and determines the temporal development of the state $\Psi_{\parallel}$ of N_0 particles.

In the representation $|\lambda(N)\rangle$ (2.18) becomes an integral equation with respect to $\lambda(N_0)$ for the amplitude $\Psi(\lambda(N_0), t) = \langle\lambda(N_0)|\Psi_{\parallel}(t)$

$$\left(i\hbar\frac{\partial}{\partial t} - E_{\lambda(N_0)}\right)\Psi(\lambda(N_0), t) = \sum_{\lambda'(N_0)} \langle\lambda(N_0)|V|\lambda'(N_0)\rangle\Psi(\lambda'(N_0), t)\,. \tag{2.17'}$$

According to (2.16) and (1.15), we have in the lowest order of approximation

$$\langle\lambda(N_0)|V^{(2)}\ \lambda'(N_0)\rangle = \langle\lambda(N_0)|U^{(2)}(E_{\lambda'(N_0)})|\lambda'(N_0)\rangle = \tag{2.18}$$

$$= \sum_{N''\neq N_0}\sum_{\lambda''(N'')} \langle\lambda(N_0)|\overset{1}{H}|\lambda''(N'')\rangle \left[P\frac{1}{E_{\lambda'(N_0)} - E_{\lambda''(N'')}} - i\pi\,\delta(E_{\lambda'(N_0)} - E_{\lambda''(N'')})\right] \cdot$$

$$\cdot\ \lambda''(N'')|\overset{1}{H}|\lambda'(N_0)\rangle\,.$$

To calculate the higher approximations of $\lambda(N_0)\,V\,\lambda'(N_0)$ we must decide upon the particular form of $G(t)$. We get e.g. in the second approximation, due to (2.2), (2.9), (2.3-6) and (1.15),

$$\langle\lambda'(N')|\,A^{(2)}\,|\lambda''(N'')\rangle = -\langle\lambda'(N')(E_{\lambda''(N'')} - \overset{0}{H})^{-1}U^{(2)}(E_{\lambda''(N'')})\,|\lambda''(N'') \quad . \tag{2.19}$$

From (2.16′) and (2.19) it is seen that $V^{(4)}$ may be expressed by means of $U^{(2)}(E)$, $U^{(4)}(E)$ and the operator $(E - \overset{0}{H})^{-1}$. In general the $2n$-th approximation of $\langle\lambda'(N')|\,V\,|\lambda''(N'')\rangle$ involves all $U^{(2m)}(E)$ with $m = 1, 2, \ldots, n$. The inverse $(E - \overset{0}{H})^{-1}$ is so far arbitrary. It may be determined uniquely if we fix the initial conditions for the solution $\Psi_\parallel(t)$. Demanding e.g. that $\Psi_\parallel(t)$ coincides for $t = -\infty$ with $\Psi_\parallel^0$ (cf. (2.3)) we have to choose for $G(t)$ the retarded solution of (2.1). This may be achieved by fixing appropriately the integration path around the poles of the integrand in the matrix elements of $G(t)$ (cf. 2.2)).

It is seen already from the lowest approximation (2.18) that the potential V is, in general, a complex operator

$$V = V^{\mathrm{R}} + iV^{\mathrm{I}}\,,$$

where the real part V^{R} and the complex part V^{I} are real (= hermitean) operators, their lowest approximation being clearly exhibited by (2.18).

We may write the solution of (2.17) in the form

$$\Psi_\parallel(t) = \sum_W \Psi_{\parallel W}(t)b_W\,, \tag{2.20}$$

with arbitrary coefficients b_W, where

$$\Psi_{\parallel W}(t) = \chi_{\parallel W}\exp\left[-\frac{i}{\hbar}\,Wt\right] \tag{2.21}$$

and $\chi_{\parallel W}$ satisfies the time-independent equation

$$(W - \overset{0}{H})\chi_{\parallel W} = V\chi_{\parallel W} \tag{2.22}$$

(note that (2.20) is not an orthogonal expansion). The parameter W occuring in (2.20-22) is complex

$$W = \overline{E} - i\Gamma\,. \tag{2.23}$$

Its real part $\overline{E}$ may be considered, according to (2.22), as the expectation value of the energy of N_0 particles (not the total energy $\overset{0}{H} + \overset{1}{H}$) in the state $\chi_{\parallel W}$.

The real number $\Gamma/\hbar$ may be considered, according to (2.21) as the probability per unit time of the transition from the state $\chi_{\|W}$ to all other states. The number $\tau = \hbar/\Gamma$ is, therefore, the life-time of the state $\chi_{\|W}$.

We may treat equation (2.22) by means of the stationary perturbation method. In the first order approximation we get for Γ an expression of Weisskopf-Wigner's type (cf. e.g. [5]). Indeed replacing in (2.22) V by $V^{(2)}$ and treating this quantity as a perturbation we get

$$W = E_{\lambda(N_0)} + \langle \lambda(N_0) | V^{(2)} | \lambda(N_0) \rangle ,$$

where the correction $\langle \lambda(N_0) | V^{(2)} | \lambda(N_0) \rangle$ is given by formula (2.18) with $\lambda'(N_0) = \lambda(N_0)$. Comparison with (2.23) yields for Γ the expression

$$\Gamma = \pi \sum_{N' \neq N_0} \sum_{\lambda'(N')} | \langle \lambda(N_0) | \overset{1}{H} | \lambda'(N') \rangle |^2 \delta(E_{\lambda(N_0)} - E_{\lambda'(N')}) .$$

Equation (2.22) is neither an eigenvalue problem for the total energy of the system (in contradistinction to (1.16)) nor is it the eigenvalue problem of N_0 particles. It also differs from the equation (1.14) for the component $\Phi_{\|E}$ (corresponding to N_0 particles) of the eigenstate Φ_E of the total energy of the system. The state $\chi_{\|W}$ becomes an eigenstate of the total energy of the system corresponding to N_0 particles if $V^{\mathrm{I}}\chi_{\|W} = 0$. In this case $\chi_{\|W} = \Phi_{\|E}$.

The considerations of this Section suggest that (2.22) is the proper equation describing correctly (between others) the bound states of N_0 particles. Adopting this point of view we have the result, that a bound state of N_0 particles is stationary (i.e. is an eigenstate of the total energy of the system) only if $V^{\mathrm{I}}\chi_{\|W} = 0$ (it is then also an eigenstate of the energy of N_0 particles).

Assuming the normalization condition for $\chi_{\|W}$

$$\chi_{\|W} \cdot \chi_{\|W} = 1 ,$$

we get from (2.22), due to the hermitean character of the operators $\overset{0}{H} + V^{\mathrm{R}}$ and V^{I},

$$E = \langle \chi_{\|W} | \overset{0}{H} + V^{\mathrm{R}} | \chi_{\|W} \rangle , \tag{2.24}$$

$$\Gamma = -\langle \chi_{\|W} | V^{\mathrm{I}} | \chi_{\|W} \rangle . \tag{2.25}$$

It may be emphasized, however, that the $\chi_{\|W}$ are not simultaneous eigenstates

[5] P. A. M. DIRAC: *The Principles of Quantum Mechanics* (Oxford, 1947), p. 203.

of the operators $\overset{0}{H} + V^{R}$ and V^{I} since these operators do not commute with each other.

The operator $\overset{0}{H} + V^{R}$ commutes with the operator of the number of particles, due to the property $V^{R} = P_{\parallel} V^{R} P_{\parallel}$. This fact and the formula (2.24) suggest that $\overset{0}{H} + V^{R}$ may be considered as the proper operator, representing the energy of N particles.

RIASSUNTO (*)

Nella prima parte di questo lavoro si discute il problema della derivazione delle equazioni per il vettore di stato di N_0 particelle dell'equazione di Schrödinger corrispondente a un sistema di campi interagenti. Si ottiene un'equazione integro-differenziale non omogenea in cui la non omogeneità è determinata dal valore iniziale del vettore di stato corrispondente a N particelle ($N \neq N_0$). Nel caso in cui tale vettore si annulla in un determinato istante, l'equazione per il vettore di stato di N_0 particelle diventa omogenea e può essere sostituita da un'equazione stazionaria indipendente dal tempo e contenente un operatore di interazione funzione dell'autovalore dell'energia (problema non lineare di autovalore dell'energia). Si ottiene per il nocciolo dell'equazione integro-differenziale un'espressione chiusa, valida per valori arbitrari della costante di interazione. Nella seconda parte l'equazione integro-differenziale per il vettore di stato di N_0 particelle si sostituisce con un'equivalente equazione semplicemente differenziale rispetto al tempo. Nel caso omogeneo tale equazione ha la forma di un'equazione di Schrödinger (problema lineare di autovalore dell'energia) con un potenziale complesso. La parte immaginaria di tale potenziale è dovuta all'instabilità dello stato di N_0 particelle e determina la vita media dello stato stesso. Si postula che quest'ultima equazione descriva – dopo la separazione dei tempi – gli stati legati di N_0 particelle.

The Determination of the Scattering Potential from the Spectral Measure Function.

III. Calculation of the Scattering Potential from the Scattering Operator for the One-Dimensional Schrödinger Equation (*).

I. Kay and H. E. Moses

Institute of Mathematical Sciences, New York University - New York

(ricevuto il 27 Ottobre 1955)

Summary. — A procedure discussed in previous papers for the calculation of the scattering potentials from the spectral measure functions associated with certain eigenfunctions of the continuous spectrum of the perturbed Hamiltonian, has been adapted to the problem of obtaining the scattering potential from the scattering operator for the one-dimensional Schrödinger equation ($-\infty < x < \infty$). Examples are given to show how the procedure may be used.

---

1. – Introduction and Summary of Results.

Several writers [1,2,3] have recently discussed the problem of obtaining the scattering potential from the scattering phases for a variety of radial wave equations. Their work is characterized by the fact they require the perturbed eigenfunctions to approach the unperturbed eigenfunctions at the origin. From this boundary condition and from specific properties of the unperturbed Hamil-

---

(*) The research reported in this article was done at the Institute of Mathematical Sciences, New York University, and has been made possible through support and sponsorship extended by Geophysics Research Directorate, Air Force Cambridge Research Center under Contract No. AF19(122)-463.

(1) R. Jost and W. Kohn: *Det. Kgl. Danske Videnskabernes Selskab, Mathematisk-fysiske Meddelelser*, **27**, nr. 9 (1953).

(2) E. Corinaldesi: *Nuovo Cimento*, **11**, 468 (1954).

(3) R. G. Newton and R. Jost: *Nuovo Cimento*, **1**, 590 (1955).

tonians and of the perturbation, they then obtain the Gelfand-Levitan equation ([4,5]). In the special cases discussed in ([1-3]) this equation was used to obtain the scattering potential in terms of the spectral measure function. By showing how the spectral measure function can be obtained from the scattering phases, it is then possible to derive the potential in terms of the phases.

In a previous paper ([6]) the authors provided a more abstract formulation of the problem of obtaining the scattering potential from the spectral measure function. It is the objective of the present paper to illustrate the use of the theorems presented there by considering the one-dimensional wave equation ($-\infty < x < \infty$). By showing how the spectral measure function can be obtained from the scattering operator S one can then calculate the potential from suitable elements of S. Actually this one-dimensional problem has already been treated by KAY ([7]) using properties of the one-dimensional wave equation discussed by FRIEDRICHS ([8]). The advantage of the more general approach of the present paper is that it seems to indicate a way to tackle the more interesting problem of three-dimensional scattering from a general (i.e., non-symmetric) potential.

For conciseness we shall summarize the results below.

First, let us define the reflection coefficient $b(k)$. Let us consider solutions $\Psi_k(x)$ of the equation

$$\left[-\frac{\mathrm{d}^2}{\mathrm{d}x^2} + V(x)\right]\Psi_k(x) = k^2\Psi_k(x)\,, \tag{1.1}$$

which satisfy the condition that they represent the sum of an incident plane wave and an «outgoing wave», i.e., which satisfy the integral equation

$$\Psi_k^{\mathrm{out}}(x) = \exp\,[ikx] - \frac{i}{2k}\int_{-\infty}^{+\infty}\exp\,[ik|x-x'|]V(x')\Psi_k^{\mathrm{out}}(x')\,\mathrm{d}x'\,. \tag{1.2}$$

The reflection coefficient $b(k)$ is defined by considering the following asymptotic form for $\Psi_k(x)$ when $k > 0$

$$\lim_{x\to-\infty}\Psi_k^{\mathrm{out}}(x) = \exp\,[ikx] + b(k)\exp\,[-ikx] \qquad (k>0). \tag{1.3}$$

([4]) I. M. GELFAND and B. M. LEVITAN: *Izv. Akad. Nauk. SSSR, Math. Series*, **15**, 309 (1951).

([5]) N. LEVINSON: *Phys. Rev.*, **89**, 755 (1953).

([6]) I. KAY and H. E. MOSES: *Nuovo Cimento*, part I, 2, 917 (1955); part II, 3, 66 (1956).

([7]) I. KAY: *On the determination of a linear system from the reflection coefficient*: New York University, Institute of Mathematical Sciences, Division of Electromagnetic Research Report No. EM-74.

([8]) K. O. FRIEDRICHS: *Spectral representation of linear operators*: Lecture Notes, New York University, Institute of Mathematical Sciences, (Summer 1948).

The reflection coefficient gives the amplitude of the plane wave which is reflected toward the left when an incident wave of unit amplitude moves toward the right.

Though we have defined $b(k)$ for $k \geq 0$ only, one can define this function for $k < 0$. One can show by analytic continuation

$$b(-k) = b^*(k) \qquad \text{for } k \text{ real} \tag{1.4}$$

where the asterisk means complex conjugate.

We shall show that the potential $V(x)$ can be obtained from the knowledge of the reflection coefficient $b(k)$ alone if it satisfies certain sufficient conditions. (Some of these conditions are also necessary.)

Let $b(k)$ have the form

$$b(k) = g(k) \exp[-2ik\alpha] \qquad (\alpha > 0) \tag{1.5}$$

where

$$g(k) = 0(k^{-1}) \qquad \text{for } |k| \to \infty \tag{1.6}$$

Further let the analytic continuation of $g(k)$ have positive imaginary residues r_i at a finite number of poles $k_j = i\tau_j$, $(j=1, 2, ..., n)$ where $\tau_j > 0$. Then if the equation

$$\langle x|K|x'\rangle = -\langle x|\Omega|x'\rangle - \eta(x + x' + 2\alpha)\int_{-(2\alpha+x')}^{x} \langle x|K|x''\rangle \, dx'' \langle x''|\Omega|x'\rangle \,, \tag{1.7}$$

can be solved for $\langle x|K|x'\rangle$ $(x' < x)$, where

$$\langle x|\Omega|x'\rangle = \frac{1}{2\pi}\int_{-\infty}^{+\infty} b(k) \exp[-ik(x + x')] \, dk - i \sum_j r_j \exp[\tau_j(x + x' + 2\alpha)] \,, \tag{1.8}$$

and $\eta(x)$ is the usual Heaviside unit function

$$\eta(x) = \begin{cases} 1 & \text{for } x > 0, \\ 0 & \text{for } x < 0, \end{cases} \tag{1.8a}$$

then the scattering potential $V(x)$ is given by

$$V(x) = 2\frac{d}{dx}\langle x|K|x\rangle \,. \tag{1.9}$$

Furthermore

$$\langle x|K|x'\rangle \equiv V(x) = 0 \qquad \text{when } x < -\alpha \tag{1.10}$$

and the point eigenvalues of $-(\mathrm{d}^2/\mathrm{d}x^2) + V(x)$ will have the values τ_j^2. The reflection coefficient associated with $V(x)$ as obtained from (1.9) will be $b(k)$, as required by a consistent theory.

One will be able to obtain a unique set of eigenfunctions of $-(\mathrm{d}^2/\mathrm{d}x^2) + V(x)$ corresponding to the continuous spectrum. These are given by

$$\Psi_k(x) = \exp[ikx] + \int_{-\infty}^{x} \langle x|K|x'\rangle \exp[ikx']\,\mathrm{d}x' , \tag{1.11}$$

which satisfy the boundary condition

$$\lim_{x\to-\infty} \Psi_k(x) = \exp[ikx] . \tag{1.12}$$

The eigenfunctions corresponding to the point eigenvalue τ_j^2 denoted by $\Psi_{-i\tau_j}(x)$ are given by

$$\Psi_{-i\tau_j} = \exp[\tau_j x] + \int_{-\infty}^{x} \langle x|K|x'\rangle \exp[\tau_j x']\,\mathrm{d}x' . \tag{1.13}$$

The normalization of the eigenfunctions $\Psi_k(x)$ of the continuous spectrum given by (1.11) is

$$\frac{1}{2\pi}\int_{-\infty}^{+\infty} \Psi_k^*(x)\Psi_{k'}(x)\,\mathrm{d}x + \frac{b(-k)}{2\pi}\int_{\infty}^{+\infty} \Psi_{-k}^*(x)\Psi_{k'}(x)\,\mathrm{d}x = \delta(k-k') . \tag{1.14}$$

The bound states are orthogonal to eigenfunctions of the continuous spectrum. They satisfy the following orthogonality relation with respect to each other

$$\int_{-\infty}^{+\infty} \Psi_{-i\tau_m}(x)\Psi_{-i\tau_j}(x)\,\mathrm{d}x = i\delta_{mj} r_j^{-1} \exp[-2\tau_j\alpha] . \tag{1.15}$$

The eigenstates $\Psi_k(x)$ and $\Psi_{-i\tau_j}$ form a complete set and satisfy the completeness relationship

$$\frac{1}{2\pi}\left[\int_{\infty}^{+\infty} \Psi_k(x)\Psi_k^*(x')\,\mathrm{d}k + \int_{\infty}^{+\infty} \Psi_k(x)b(-k)\Psi_{-k}^*(x')\,\mathrm{d}k\right] - i\sum_j \Psi_{-i\tau_j}(x)\Psi_{-i\tau_j}(x')r_j \exp[2\tau_j\alpha] = \delta(x-x') . \tag{1.16}$$

2. The one-dimensional eigenfunctions; the scattering operator.

The unperturbed Hamiltonian H_0 is given by

$$H_0^x = -\frac{\mathrm{d}^2}{\mathrm{d}x^2}, \qquad -\infty < x < +\infty, \tag{2.1}$$

where the superscript x on H_0^x signifies that the operator is expressed in the x-representation. It is convenient to use the eigenfunction $|H_0, A_0; E, a\rangle$ given by

$$\langle x|H_0, A_0; E, a\rangle = \frac{(E)^{-\frac{1}{4}}}{2\sqrt{\pi}} \exp\left[ia\sqrt{E}x\right], \tag{2.2}$$

where a is restricted to having the values $+1$ or -1. It is easily verified from (2.2) that

$$\langle H_0, A_0; E', a'|H_0, A_0; E, a\rangle = \int_{-\infty}^{\infty} \langle H_0, A_0; E', a'|x\rangle \,\mathrm{d}x \langle x|H_0, A_0; E, a\rangle = \tag{2.3}$$

$$= \delta(E - E')\,\delta_{a,a'},$$

where $\delta_{a,a'}$ is the usual Kronecker δ. It can also be verified that

$$\sum_a \int_0^{\infty} |H_0, A_0; E, a\rangle \,\mathrm{d}E \langle H_0, A_0; E, a| = \eta(H_0), \tag{2.4}$$

where $\eta(H_0)$ is the identity operator in Hilbert space and maps remainder of the extended vector space into zero.

The perturbed Hamiltonian H is given by

$$H = H_0 + \varepsilon V. \tag{2.5}$$

Initially, we shall assume that $\langle x|V|x'\rangle$ is generally not diagonal. Later we shall give conditions under which $\langle x|V|x'\rangle$ is diagonal, i.e., has the form

$$\langle x|V|x'\rangle = V(x)\,\delta(x - x'). \tag{2.6}$$

We shall assume, however, that $\langle x|V|x'\rangle$ is such that a scattering operator exists.

The outgoing, and incoming eigenfunctions of H corresponding to the continuous spectrum satisfy the integral equations

(2.7) $\langle x|H, A; E, a\rangle_{\pm} = \langle x|H_0, A_0; E, a\rangle \pm$

$$\pm \frac{i}{2}\varepsilon(E)^{-\frac{1}{2}}\int_{-\infty}^{+\infty}\int_{-\infty}^{+\infty}\exp\left[\mp i\sqrt{E}|x-x'|\right]\mathrm{d}x'\langle x'|V|x''\rangle\,\mathrm{d}x''\langle x''|H, A; E, a\rangle_{\pm}\,.$$

In (2.7) we use the well-known result

(2.7a) $$\langle x|\gamma_{\pm}(E-H_0)|x'\rangle = \pm\frac{i}{2}(E)^{-\frac{1}{2}}\exp\left[\mp i\sqrt{E}|x-x'|\right].$$

The scattering operator and its inverse can be represented in the H_0-representation by (see [6], Part I, eqs. (4.12), (4.20), and [6], Part. II, Eqs. (3.7), (3.8))

(2.8) $$\langle H_0, A_0; E, a|S|H_0, A_0; E', a'\rangle = \delta(E-E')\langle a|S(E)|a'\rangle$$

and

(2.9) $$\langle H_0, A_0; E, a|S^{-1}|H_0, A_0; E', a'\rangle = \delta(E-E')\langle a|S^{-1}(E)|a'\rangle\,,$$

where

(2.10) $$\langle a|S(E)|a'\rangle = \delta_{a,a'} - 2\pi i\varepsilon\langle H_0, A_0; E, a|V|H, A; E, a'\rangle_- =$$

$$= \delta_{a,a'} - 2\pi i\varepsilon\int_{-\infty}^{+\infty}\int_{-\infty}^{+\infty}\langle H_0, A_0; E, a|x\rangle\,\mathrm{d}x\langle x|V|x'\rangle\,\mathrm{d}x'\langle x'|H, A; E, a'\rangle_-\,,$$

and

(2.11) $$\langle a|S^{-1}(E)|a'\rangle = \delta_{a,a'} + 2\pi i\varepsilon\langle H_0, A_0; E, a|V|H, A; E, a'\rangle_+ =$$

$$= \delta_{a,a'} + 2\pi i\varepsilon\int_{-\infty}^{+\infty}\int_{-\infty}^{+\infty}\langle H_0, A_0; E, a|x\rangle\,\mathrm{d}x\langle x|V|x'\rangle\,\mathrm{d}x'\langle x'|H, A; E, a'\rangle_+\,.$$

For future reference we note the reciprocity theorem

(2.12) $$\langle H_0, A_0; E, a|V|H, A; E, b\rangle_- = {}_+\langle H, A; E, a|V|H_0, A_0; E, b\rangle =$$

$$= \langle H_0, A_0; E, b|V|H, A; E, a\rangle_+^*\,,$$

where the asterisk means complex conjugate.

If $\langle x|V|x'\rangle$ dies down with sufficient rapidity, the asymptotic forms of $\langle x|H, A; E, a\rangle_+$ are related to $\langle a|S(E)|b\rangle$ and $\langle a|S^{-1}(E)|b\rangle$ by

(2.13) $$\lim_{x\to\pm\infty}\langle x|H, A; E, a\rangle_- = \langle x|H_0, A_0; E, a\rangle + \langle x|H_0, A_0; E, \pm 1\rangle\left[\langle \pm 1|S(E)|a\rangle - \delta_{\pm 1,a}\right]$$

$$\lim_{x\to\pm\infty}\langle x|H, A; E, a\rangle_{+} = \langle x|H_0, A_0; E, a\rangle + \langle a|H_0, A_0; E, \mp 1\rangle \tag{2.14}$$

$$[\langle \mp 1|S^{-1}(E)|a\rangle - \delta_{\mp 1,a}] ,$$

as can be shown from (2.10) and (2.11).

3. - Expression for the weight operator in terms of the scattering operator.

We shall now express in terms of S and S^{-1} the operators W_e, $M_{\pm}$ associated with those operators U such that the eigenfunctions of H given by

$$\langle x|H, A; E, a\rangle = \langle x|U|H_0, A_0; E, a \tag{3.1}$$

satisfy the boundary condition

$$\lim_{x\to\infty}\langle x|H, A; E, a\rangle - \langle x|H_0, A_0; E, a\rangle = 0 \tag{3.2}$$

or, symbolically,

$$\lim_{x\to\infty}\langle x|H, A; E, a\rangle = \langle x|H_0, A_0; E, a\rangle . \tag{3.2a}$$

Since we shall work in the continuous spectrum of H, we shall drop the factor $\eta(H_0)$ for the time being, since it will always act like the identity operator.

From $U = U_{-}M_{-}$ we can write

$$\langle x|H, A; E, a\rangle = \sum_{a'}\langle x|H, A; E, a'\rangle_{-}\langle a'|\mu_{-}(E)|a\rangle , \tag{3.3}$$

where $\langle a|\mu_{-}(E)|a'\rangle$ is given by (by cf. (6), Part I, Eq. (5.5))

$$\langle H_0, A_0; E, a|M_{-}|H_0, A_0; E', a'\rangle = \delta(E - E')\langle a|\mu_{-}(E)|a'\rangle . \tag{3.4}$$

From Eqs. (3.2a) and (2.13) we obtain an equation for $\langle a|\mu_{-}(E)|a'\rangle$, namely

$$\langle x|H_0, A_0; E, a\rangle = \sum_{a'}\langle x|H_0, A_0; E, a'\rangle\langle a'|\mu_{-}(E)|a\rangle + \tag{3.5}$$

$$+ \langle x|H_0, A_0; E, -1\rangle\sum_{a'}[\langle -1|S(E)|a'\rangle - \delta_{-1,a}]\langle a'|\mu_{-}(E)|a\rangle .$$

On multiplying (3.5) through by $\langle H_0, A_0; E', a''|x\rangle$ and integrating with respect

o x, and then using the orthogonality relation (2.3), one finds that

$$\delta(E'-E)\delta_{a'',a} = \delta(E''-E)\sum_{a'}\delta_{a'',a'}\langle a'|\mu_-(E)|a\rangle + \tag{3.6}$$

$$+\,\delta(E'-E)\delta_{a'',-1}\sum_{a'}[\langle -1|S(E)|a'\rangle - \delta_{-1,a'}]\langle a'|\mu_-(E)|a \quad .$$

which on renaming some of the variables, may be rewritten as

$$\delta_{a,a'} = \langle a|\mu_-(E)|a'\rangle + \delta_{a,-1}\sum_{a''}[\langle -1|S(E)|a''\rangle - \delta_{-1,a''}[\langle a''|\mu_-(E)|a' \quad . \tag{3.7}$$

Eq. (3.7) may be regarded as an equation for the matrix $\langle a|\mu_-(E)|a'$. The solution of (3.7) can be shown to be

$$\langle a|\mu_-(E)|a'\rangle = \begin{pmatrix} 1 & 0 \\ \dfrac{-\langle -1|S(E)|+1\rangle}{\langle -1|S(E)|-1\rangle} & \dfrac{1}{\langle -1|S(E)|-1\rangle} \end{pmatrix}, \tag{3.8}$$

where we adopt the convention that the first row and column are labeled by $+1$ and the second by -1, i.e., $\langle +1|\mu_-(E)|-1\rangle = 0$. Eq. (3.8) gives us M_- in the H_0-representation.

From ([6]), Part I, Eq. (5.9) we have

$$W_c = M_-^{-1}M_-^{*-1} \, . \tag{3.9}$$

To find W_c, therefore, we shall have to obtain M_-^{-1} and M^{*-1}. We shall express these operators in terms of the H_0-representation. Let us define $\langle a|\mu_-^{-1}(E)|a'\rangle$ by

$$\langle H_0, A_0; E, a|M_-^{-1}|H_0, A_0; E', a'\rangle = \delta(E-E')\langle a|\mu_-^{-1}(E)|a' \quad . \tag{3.10}$$

From $M_-^{-1}M_- = M_-M_-^{-1} = \eta(H_0)$, (where we recall $\eta(H_0)$ is the identity in Hilbert space) it can be shown that for fixed E the quantities $a|\mu_-^{-1}(E)|a'\rangle$ are just the elements of the matrix which is the inverse of the matrix whose elements are $\langle a|\mu_-(E)|a'\rangle$. It is then shown that

$$\langle a|\mu_-^{-1}(E)|a'\rangle = \begin{pmatrix} 1 & 0 \\ \langle -1|S(E)|+1\rangle & \langle -1|S(E)|-1\rangle \end{pmatrix} \tag{3.11}$$

Let us now define $\langle a|M^{*-1}(E)|a'\rangle$ by

$$\langle H_0, A_0; E, a|M_-^{*-1}|H_0, A_0; E', a'\rangle = \delta(E-E')\langle a|\mu_-^{*-1}(E)|a' \quad . \tag{3.12}$$

From the fact that $M_-^{*-1} = (M^*)^{-1} = (M^{-1})^*$ is the Hermitian adjoint of M^{-1} we have

$$\langle a|\mu_-^{*-1}(E)|a'\rangle = \langle a'|\mu_-^{-1}(E)a\rangle^* . \tag{3.13}$$

If, as in [6] we define $\langle a|\omega_c(E)|a'\rangle$ by

$$\langle H_0, A_0;\ E, a|W_c|H_0, A_0;\ E', a'\rangle = \delta(E - E')\langle a|\omega_c(E)|a'\rangle , \tag{3.14}$$

we have from (3.9)

$$\langle a|\omega_c(E)|a'\rangle = \sum_{a''} \langle a|\mu_-^{-1}(E)|a''\rangle\langle a''|\mu_-^{*-1}(E)|a'\rangle , \tag{3.15}$$

or, on using (3.13) and (3.11)

$$\langle a|\omega_c(E)|a'\rangle = \begin{pmatrix} 1 & \langle -1|S(E)|+1\rangle^* \\ \langle -1|S(E)|+1\rangle & 1 \end{pmatrix} . \tag{3.16}$$

In deriving (3.16) from (3.15) we have used the relation

$$|\langle -1|S(E)|-1\rangle|^2 + |\langle -1|S(E)|+1\rangle|^2 = 1 , \tag{3.17}$$

which follows from the fact that $S^* = S^{-1}$, i.e., $SS^* = \eta(H_0)$.

For the sake of completeness, we shall also give the expression for $\langle a|\mu^+(E)|a'\rangle$ defined by

$$\langle x|H, A;\ E, a\rangle = \sum_{a'} \langle x|H, A;\ E, a'\rangle \langle a'|\mu_+(E)|a\rangle , \tag{3.18}$$

where $\langle x|H, A;\ E, a\rangle$ satisfies the boundary condition (3.2a). The expression can be shown to be

$$\langle a|\mu_+(E)|a'\rangle = \begin{pmatrix} \dfrac{1}{\langle +1|S^{-1}(E)|+1\rangle} & -\dfrac{\langle +1|S^{-1}(E)|-1\rangle}{\langle +1|S^{-1}(E)|+1\rangle} \\ 0 & 1 \end{pmatrix} . \tag{3.19}$$

4. – The complex energy plane.

In this section we consider the analytic continuation of various quantities introduced above, and for this purpose we introduce the complex E-plane which shall have a cut along the positive real axis. The results obtained here will be useful in later sections.

Let us first introduce the function $\langle x|H_0, A_0; E, a\rangle$. This function is defined as the analytic continuation of $\langle x|H_0, A_0; E, a\rangle$ when E is on the upper part of the cut. From (2.2), we see that when E is in the lower part of the cut

$$\langle x|H_0, A_0; E, a\rangle^+ = -i\langle x|H_0, A_0; E, -a\rangle \quad . \tag{4.1}$$

One can also introduce $\langle x|H_0, A_0; E, a\rangle^-$ which defined as being equal to $\langle x|H_0, A_0; E, a\rangle$ when E is on the lower side of the cut. Hence, from (4.1)

$$\langle x|H_0, A_0; E, a\rangle^- = i\langle x|H_0, A_0; E, -a\rangle^+ \tag{4.2}$$

and

$$\langle x|H_0, A_0; E, a\rangle^- = i\langle x|H_0, A_0; E, -a\rangle \tag{4.3}$$

when E is on the upper side of the cut.

We can also introduce $\langle H_0, A_0; E, a|x\rangle^-$ which equals $\langle H_0, A_0; E, a|x\rangle$ when E is on the upper side of the cut. Then since

$$\langle H_0, A_0; E, a|x\rangle = \langle x|H_0, A_0; E, -a \tag{4.4}$$

we have

$$\langle H_0, A_0; E, a|x\rangle^+ = \langle x|H_0, A_0; E, -a\rangle^+ . \tag{4.5}$$

Similarly one can define $\langle H_0, A_0; E, a|x\rangle^-$ as being the analytic continuation of $\langle H_0, A_0; E, a|x\rangle$ when E is at the bottom of the cut, where from (4.4) it can be shown that

$$\langle H_0, A_0; E, a|x\rangle^- = \langle x|H_0, A_0; E, -a\rangle^- . \tag{4.6}$$

Now we define $\langle x|H, A; E, a\rangle^+_\pm$ as the analytic continuation of $\langle x|H, A; E, a\rangle_\pm$ when E is on the top of the cut. From the integral equation (2.7) it is clear that when E is at the bottom of the cut we have

$$\langle x|H, A; E, a\rangle^+_\pm = -i\langle x|H_0, A_0; E, -a\rangle \mp \frac{i}{2}\varepsilon(E)^{-\frac{1}{2}} \cdot \int_{-\infty}^{+\infty}\int_{-\infty}^{+\infty} dx'\,dx''\exp\left[\pm i\sqrt{E}|x-x'|\right]\langle x'|V|x''\rangle\langle x''|H, A; E, a\rangle^+_\pm , \tag{4.7}$$

from which it can be shown that

$$\langle x|H, A; E, a\rangle^+_\pm = -i\langle x|H, A; E, -a\rangle \tag{4.8}$$

when E is on the lower part of the cut.

Likewise one can introduce $\langle x|H, A; E, a\rangle_{\pm}^{-}$ which is the analytic continuation of $\langle x|H, A; E, a\rangle_{\pm}$ defined on the lower part of the cut. It is clear from (4.8) that

$$\langle x|H, A; E, a\rangle_{\pm}^{-} = i\langle x|H, A; E, -a\rangle_{\mp}^{+} \tag{4.9}$$

and that when E is at the top of the cut

$$\langle x|H, A; E, a\rangle_{\pm}^{-} = i\langle x|H, A; E, -a\rangle_{\mp} . \tag{4.10}$$

The analytic continuation of $\langle a|S(E)|a'\rangle$ when E is on the top of the cut will be denoted by $\langle a|S(E)|a'\rangle^{+}$. From (2.10), (4.8), (4.5), (4.1), (2.11), (2.12) we see that when E is at the bottom of the cut

$$\langle a|S(E)|a'\rangle^{+} = \delta_{a,a'} + 2\pi i \int_{-\infty}^{+\infty} \mathrm{d}x \int_{-\infty}^{+\infty} \mathrm{d}x' \cdot \tag{4.11}$$

$$\cdot \langle H_0, A_0; E, -a|x\rangle\langle x|V|x'\rangle\langle x'|H, A; E, -a'\rangle_{+} =$$

$$= \langle -a|S^{-1}(E)|-a'\rangle = \langle -a'|S(E)|-a\rangle^{*} ,$$

where, as usual, the asterisk means complex conjugate. We denote by $\langle a|S(E)|a'\rangle^{-}$ the analytic continuation of $\langle a|S(E)|a'\rangle$ when E is at the bottom of the cut. It can be shown that when E is at the top of the cut

$$\langle a|S(E)|a'\rangle^{-} = \langle -a|S^{-1}(E)|-a'\rangle = \langle -a'|S(E)|-a\rangle^{*} . \tag{4.12}$$

5. Extension of the unperturbed Hamiltonian. Diagonal form for the scattering potential.

In (6) we saw that it is necessary to extend the definition of the operator H_0 to a space larger than Hilbert space in order that the extended operator H_0 have the same spectrum as H. In (6), Part II the extension was carried out by introducing «eigenfunctions» of the extended operator H_0. Here we specialize this procedure to the present case.

In Hilbert space H_0 is defined by the way it acts in the x-representation, namely,

$$H_0^x = -\frac{\mathrm{d}^2}{\mathrm{d}x^2} . \tag{5.1}$$

We shall require that the extended space, H_0, be also given by (5.1). In

the notation of (6), Part II, H_0 is then an x-extended operator. With this extension the potential V has the desirable property that it is diagonal in the x-representation, as we shall show shortly. First, however, we shall obtain the additional eigenfunctions necessary to complete the extended space. In accordance with (6), Part II we shall look for solutions of

$$H_0 |H_0, A_0; E, a\rangle = E|H_0, A_0; E, a \tag{5.2}$$

for values of E in the vicinity of each E_i which is a point eigenvalue of H such that

$$\lim_{x\to-\infty} \langle x|H_0, A_0; E, a\rangle = 0 . \tag{5.3}$$

In terms of the x-representation Eq. (5.2) becomes

$$-\frac{d^2}{dx^2}\langle x|H_0, A_0; E, a\rangle = E\langle x|H_0, A_0; E, a\rangle . \tag{5.4}$$

For a fixed negative value of E, there is only one solution which satisfies (5.3). We conclude therefore that *the spectrum of the extended Hamiltonian H_0 and the point spectrum of H cannot be degenerate.*

Let us denote by $\langle x|H_0; E$ the suitable solutions of (5.4). Then we can write

$$\langle x|H_0; E\rangle = A(E)\frac{\exp[-i(\pi/4)]}{2\sqrt{\pi}}(-E)^{-\frac{1}{4}}\exp[\sqrt{-E}x] = \tag{5.5}$$
$$= A(E)\langle x|H_0, A_0; E, -1\rangle^{+}$$

where $A(E)$ is an arbitrary function of E which has no zeros or singularities for $E<0$. With this choice of $|H_0; E\rangle$ we take for the bi-orthogonal vector $|H_0; E\rangle_B$ another solution of (5.2) or (5.4) which satisfies

$${}_B\langle H_0, E|H_0, E'\rangle = \delta(E-E') . \tag{5.6}$$

It is clear that

$${}_B\langle H_0; E|x\rangle = [A(E)]^{-1}\frac{\exp[-i(\pi/4)]}{2\sqrt{\pi}}(-E)^{-\frac{1}{4}}\exp[\sqrt{-E}x] = \tag{5.5a}$$
$$H_0, A_0; E, \quad 1|x\rangle .$$

Also

$$\langle H_0; E|x\rangle = A^*(E)\frac{\exp[i(\pi/4)]}{2\sqrt{\pi}}(-E)^{-\frac{1}{4}}\exp[\sqrt{-E}x] = \tag{5.5b}$$
$$= iA^*(E)\langle H_0, A_0; E, +1|x\rangle .$$

In the general vector space all states $\langle x|\varphi\rangle$ will have the property that they are quadratically integrable from $x = -\infty$ to any finite limit.

We shall now prove V is diagonal in the x-representation. We have

$$(5.7)\qquad \varepsilon V = H - H_0 = UH_0U_0 - H_0UU_0 = (UH_0 - H_0U)U_0 = \\ = \varepsilon(KH_0 - H_0K) + \varepsilon^2(KH_0 - H_0K)K_0 .$$

We shall first calculate $(KH_0 - H_0K)$ in terms of the x-representation. Since K is triangular in the x-representation we can always write

$$(5.8)\qquad \langle x|K|x'\rangle = \eta(x - x')\langle x|P|x'\rangle ,$$

where

$$(5.9)\qquad \begin{cases} \langle x|P|x'\rangle = \langle x|K|x'\rangle & \text{for } x' \leqslant x, \\ \langle x|P|x'\rangle = \text{an arbitrary function,} & \text{for } x' > x, \end{cases}$$

We choose $\langle x|P|x'\rangle$ so that it is continuous at $x = x'$. Since H_0 is Hermitian, we have

$$(5.10)\qquad \langle x|KH_0|x'\rangle = -\langle x|K|x'\rangle \frac{\partial^2}{\partial x'^2} = -\frac{\partial^2}{\partial x'^2}\langle x|K|x'\rangle = \\ = -\frac{\partial^2}{\partial x'^2}\eta(x - x')\langle x|P|x'\rangle .$$

Now

$$(5.11)\qquad \frac{\partial}{\partial x'}\eta(x - x')\langle x|P|x'\rangle = -\delta(x - x')\langle x|P|x'\rangle + \eta(x - x')\frac{\partial}{\partial x'}\langle x|P|x'\rangle = \\ = -\delta(x - x')\langle x|P|x\rangle + \eta(x - x')\frac{\partial}{\partial x'}\langle x|P|x'\rangle ,$$

and

$$(5.12)\qquad \frac{\partial^2}{\partial x'^2}\eta(x - x')\langle x|P|x'\rangle = \delta'(x - x')\langle x|P|x\rangle - \delta(x - x')\frac{\partial}{\partial x'}\langle x|P|x\rangle + \\ + \eta(x - x')\frac{\partial^2}{\partial x'^2}\langle x|P|x'\rangle .$$

Likewise

$$(5.13)\qquad \langle x|H_0K|x'\rangle = -\frac{\partial^2}{\partial x^2}\langle x|K|x'\rangle = -\frac{\partial^2}{\partial x^2}\eta(x - x')\langle x|P|x'\rangle .$$

But

$$(5.14)\qquad \frac{\partial}{\partial x}\eta(x-x')\langle x|P|x'\rangle = \delta(x-x')\langle x|P|x\rangle + \eta(x-x')\frac{\partial}{\partial x}\langle x|P|x'\rangle ,$$

and

$$(5.15)\qquad \frac{\partial^2}{\partial x^2}\eta(x-x')\langle x|P|x'\rangle = \delta'(x-x')\langle x|P|x\rangle + \delta(x-x')\frac{\mathrm{d}}{\mathrm{d}x}\langle x|P|x\rangle +$$
$$+ \delta(x-x')\frac{\partial}{\partial x}\langle x|P|x\rangle + \eta(x-x')\frac{\partial^2}{\partial x^2}\langle x|P|x'\rangle .$$

In (5.15) the expression $(\mathrm{d}/\mathrm{d}x)\langle x|P|x\rangle$ means that after x' has been set equal to x in $\langle x|P|x'\rangle$, one takes the derivative of $\langle x|P|x\rangle$ with respect to x. In contrast, the expression $(\partial/\partial x)\langle x|P|x\rangle$ means that one has taken the derivative of $\langle x|P|x'\rangle$ with respect to x and then set x' equal to x. In (5.12) $(\partial/\partial x')\langle x|P|x\rangle$ means that one is to take the derivative of $\langle x|P|x'\rangle$ with respect to x' and then set x' equal to x. From (5.11)-(5.15), (5.8), and the fact that

$$\frac{\partial}{\partial x}\langle x|P|x\rangle + \frac{\partial}{\partial x'}\langle x|P|x\rangle = \frac{\mathrm{d}}{\mathrm{d}x}\langle x|P|x\rangle ,$$

one can write

$$(5.16)\qquad \langle x|KH_0 - H_0K|x'\rangle =$$
$$= 2\delta(x-x')\frac{\mathrm{d}}{\mathrm{d}x}\langle x|K|x\rangle + \eta(x-x')\left[\frac{\partial^2}{\partial x^2}\langle x|K|x'\rangle - \frac{\partial^2}{\partial x'^2}\langle x|K|x'\rangle\right].$$

Hence from (5.7) and the fact that K_0 is triangular in the x-representation we have

$$(5.17)\qquad \langle x|V|x'\rangle = 2\delta(x-x')\frac{\mathrm{d}}{\mathrm{d}x}\langle x|K|x\rangle + \eta(x-x')\cdot$$
$$\cdot\left\{\frac{\partial^2}{\partial x^2}\langle x|K|x'\rangle - \frac{\partial^2}{\partial x'^2}\langle x|K|x'\rangle + 2\varepsilon\frac{\mathrm{d}}{\mathrm{d}x}\langle x|K|x\rangle\cdot\langle x|K_0|x'\rangle -\right.$$
$$\left. + \varepsilon\int_{x'}^{x}\left[\frac{\partial^2}{\partial x^2}\langle x|K|x''\rangle - \frac{\partial^2}{\partial x'^2}\langle x|K|x''\rangle\right]\mathrm{d}x''\langle x''|K_0|x'\rangle\right\}.$$

Now from the general theory, V is Hermitian if the generalized Gelfand-Levitan equation of [6] can be solved. Furthermore, it will later be shown that $\langle x|K|x'\rangle$ is real. Therefore the right-hand side of (5.17) is the sum of a Hermitian operator which is diagonal in the x-representation, and an operator which, because it is triangular in the x-representation, cannot be Hermitian. Since the right-hand side must be Hermitian, the expression in

brackets must vanish and we are left with

$$\langle x|\,V\,|x'\rangle = \delta(x-x')V(x)\,, \tag{5.18}$$

where

$$V(x) = 2\,\frac{\mathrm{d}}{\mathrm{d}x}\langle x|\,K\,|x\quad. \tag{5.19}$$

Hence V is diagonal in the x-representation and can be obtained from K very simply, by means of (5.19).

6. – The weight operator and the Gelfand-Levitan equation.

We shall now develop expressions for the weight operator in terms of the H_0-representation. In accordance with the general theory, the equation for K is

$$\langle x|\,K\,|x'\rangle = -\langle x|\,\Omega\,|x'\rangle - \varepsilon\int_{-\infty}^{x}\langle x|\,K\,|x''\rangle\,\mathrm{d}x''\langle x''|\,\Omega\,|x'\rangle\,, \tag{6.1}$$

where

$$\varepsilon\Omega = W-\eta(H_0) = [W_c-\eta(H_0)]\eta(H_0) + W_d\sum_i \delta(E_i-H_0)\eta(-H_0)\,. \tag{6.2}$$

We have already expressed W in terms of the H_0-representation and have seen that it can be obtained in terms of the reflection coefficient of the scattering operator (Eqs. (3.14) and (3.16)). We shall now obtain the expression for W_d in terms of the H_0-representation.

From the general procedure discussed in [6], Part II, W_d as given in the H_0-representation has the form

$${}_B\langle H_0, A_0;\, E, a|\,W_d\,|H_0, A_0;\, E', b\rangle_B = \delta(E-E')\langle a|\,\omega_d(E)\,|b\rangle\,, \tag{6.3}$$

where ${}_B\langle H_0, A_0;\, E, a|$ are the bi-orthogonal eigenfunctions (5.5a) of H_0 defined for negative eigenvalues E in the neighborhoods of the point eigenvalues E_i of H. Since, in the present case, these eigenfunctions have no degeneracy, we shall write

$${}_B\langle H_0, E|\,W_d\,|H_0, E'\rangle_B = \delta(E-E')\omega_d(E) = \delta(E-E')[C(E)]^{-1}\,, \tag{6.4}$$

where, in accordance with [6], Part II, the $C(E_i)$ are the normalization constants of the proper eigenstates of H, that is,

$$\langle H, E_i | H, E_j \rangle = C(E_i)\delta_{ij} . \tag{6.5}$$

We shall now obtain $\varepsilon\langle x|\Omega|x'\rangle$ in the form

$$\varepsilon\langle x|\Omega|x'\rangle = \langle x|(W_c - \eta(H_0))\eta(H_0)|x'\rangle + \langle x|W_d \sum_i \delta(E_i - H_0)\eta(-H_0)|x'\rangle \tag{6.6}$$

We note that

$$\langle x|(W_c - \eta(H_0))\eta(H_0)|x'\rangle = \sum_{a,b} \int \langle x|H_0, A_0; E, a\rangle [\langle a|\omega_c(E)|b \quad \delta_{ab}] \cdot \eta(E) \mathrm{d}E \langle H_0, A_0; E, b \; x' \tag{6.7}$$

On using (3.16) and (2.2) we have

$$\langle x|(W_c - \eta(H_0))\eta(H_0)|x'\rangle = \tag{6.8}$$

$$= \int_0^\infty \mathrm{d}E \langle x|H_0, A_0; E, -1\rangle\langle -1|S(E) + 1\rangle\langle H_0, A_0; E, +1|x'\rangle +$$

$$+ \int_0^\infty \mathrm{d}E \langle x|H_0, A_0; E, +1\rangle\langle -1|S(E)| + 1\rangle^* \langle H_0, A_0; E, -1 \; x' =$$

$$= 2\mathrm{Re}\int_0^\infty \mathrm{d}E \langle x|H_0, A_0; E, -1\rangle\langle -1|S(E)| + 1\rangle\langle H_0, A_0; E, +1 \; x' ,$$

where Re means « real part ». Eq. (6.8) leads to

$$\langle x|(W_c - \eta(H_0))\eta(H_0)|x'\rangle = \tag{6.9}$$

$$= \mathrm{Re}\,\frac{1}{2\pi}\int_0^\infty \mathrm{d}E \; E^{-\frac{1}{2}} \exp[-i\sqrt{E}(x + x')]\langle -1|S(E)| + 1 .$$

We can simplify (6.9) by introducing the momentum variable defined by

$$E = k^2 . \tag{6.10}$$

Then

$$\langle x|(W_c - \eta(H_0))\eta(H_0)|x'\rangle = \mathrm{Re}\,\frac{1}{\pi}\int_0^\infty \mathrm{d}k \exp[-ik(x + x')]\langle -1|S(k^2)| \cdot 1 . \tag{6.11}$$

We also have

$$\langle x|W_a\sum_i\delta(E_i-H_0)\eta(-H_0)|x'\rangle = \tag{6.12}$$

$$= \sum_i\int \mathrm{d}E\langle x|H_0;\,E\rangle[C(E)]^{-1}\delta(E_i-E)\langle H_0;\,E|x'\rangle =$$

$$= \sum_i \langle x|H_0;\,E_i\rangle[C(E_i)]^{-1}\langle H_0;\,E_i|x'\rangle\,,$$

where the integration is over the intervals ΔE_i. On using (5.5) we have

$$\langle x|W_a\sum_i\delta(E_i-H_0)\eta(-H_0)|x'\rangle = \tag{6.13}$$

$$-\frac{1}{4\pi}\sum_i(\quad E_i)^{\frac{1}{2}}\exp\left[\sqrt{\quad}E_i(x\quad -x')\right][C(E_i)]^{-1}\,A(E_i)|^2 =$$

$$= i\sum_i[C(E_i)]^{-1}|A(E_i)|^2\langle x|H_0,A_0;\,E_i,-1\rangle^+\langle H_0,A_0;\,E_i,+1|x'\rangle^+.$$

Hence finally we have

$$\varepsilon\langle x|\Omega|x'\rangle = \tag{6.14}$$

$$= 2\mathrm{Re}\int_0^\infty \mathrm{d}E\langle x|H_0,A_0;\,E,-1\rangle\langle -1|S(E)|+1\rangle\langle H_0,A_0;\,E,+1|x'\rangle +$$

$$+ i\sum_i[C(E_i)]^{-1}|A(E_i)|^2\langle x|H_0,A_0;\,E_i,-1\rangle^+\langle H_0,A_0;\,E_i,+1|x'\rangle^+ =$$

$$= \mathrm{Re}\,\frac{1}{\pi}\int_0^\infty \mathrm{d}k\exp[ik(x+x')]\langle -1|S(k^2)|+1\rangle +$$

$$\frac{1}{4\pi}\sum_i(-E_i)^{-\frac{1}{2}}[C(E_i)]^{-1}|A(E_i)|^2\exp\left[\sqrt{-E_i}(x+x')\right].$$

Clearly $\langle x|\Omega|x'\rangle$ is real. Then from the uniqueness theorem it can be shown that $\langle x|K|x'\rangle$ is also real, as stated in Section 5.

7. – The conditions on the bound states and the reflection coefficient.

In accordance with the general theory of (6), we can generally find the operators $U = I+\varepsilon K$, $U_0 = I+\varepsilon K_0$, and therefore the complete set of eigenfunctions $|H, A; E, a\rangle = U|H_0, A_0; E, a\rangle$ and $|H; E_i\rangle = U|H_0; E_i\rangle$ corresponding to the continuous and the discrete spectrum of $H = UH_0U_0$ respectively whose normalization is given by the matrix elements of $W = \eta(H_0)+\varepsilon\Omega$.

where Ω is given by (6.14); these eigenfunctions satisfy the relations

$$\langle H, A; E, a | H, A; E', a' \rangle = \langle H_0, A_0; E, a | W^{-1}\eta(H_0) | H_0, A_0; E', a' \rangle = \langle a | \omega^{-1}(E) | a' \rangle \delta(E - E')\eta(E) , \tag{7.1}$$

$$\langle H, E_i | H, E_j \rangle = \delta_{ij} C_i , \tag{7.2}$$

$$\langle H, A; E, a | H, E_i \rangle = 0 . \tag{7.3}$$

However, in order to be interesting, our solution must be such that we are able to construct a scattering of S in which the reflection coefficient $-1|S(E)|+1\rangle$ is the one used to form the weight operator W. Toward this end we shall obtain some necessary conditions on the reflection coefficient, point eigenvalues, and normalization constants.

The necessary conditions follow from the requirements on the rapidity with which $V(x)$ must decay as x approaches $+\infty$ or $-\infty$.

Let us first discuss consequences of the decay of $V(x)$ as $x \to -\infty$. If $V(x)$ is to decay sufficiently rapidly to ensure the existence of a scattering operator, one can show that the outgoing wave $\langle x | H, A; E, a \rangle^{-}$ must be unique. As a consequence of this uniqueness it follows that we must have

$$\langle x | H, A; E, a \rangle^{-} \to \langle x | H_0, A_0; E, a \rangle \qquad \text{as } x \to -\infty. \tag{7.4}$$

In [6], Part I, Section 16 we have already discussed two requirements on $\langle x | \Omega | x' \rangle$ which ensure the validity of (7.4). However, in the present application of the general procedure, it turns out that because $\langle x | \Omega | x' \rangle$ is a function of $x+x'$ (see (6.14)) another approach is useful. A sufficient condition for the validity of (7.4) is that a positive number α exists such that

$$\langle x | K | x' \rangle \equiv 0 , \qquad x < -\alpha. \tag{7.5}$$

It is clear that a consequence of(7.5) is that

$$V(x) = 2\frac{\mathrm{d}}{\mathrm{d}x}\langle x | K | x \rangle = 0 , \qquad \text{for } x < -\alpha, \tag{7.6}$$

i.e., that $V(x)$ is cut-off from below.

We shall now show that a necessary and sufficient condition for (7.5) to hold is

$$\langle x | \Omega | 0 \rangle = 0 , \qquad x < -2\alpha, \tag{7.7}$$

and that a necessary condition for (7.7) and hence (7.5) to be valid is that

the point eigenvalues E_n be the poles of $\langle -1|S(E)|+1\rangle$, i.e., the analytic continuation of the reflection coefficient. A sufficient condition for (7.7) and (7.5) to hold is that $\langle -1|S(E)|+1\rangle$ be of the form $\exp[-i2\sqrt{E}\,\alpha]f(E)$ where $f(E)$ behaves like $0(E^{-\frac{1}{2}})$ for $|E|\to\infty$ in the cut complex plane.

Let us first prove that (7.7) is a necessary condition for (7.5) to hold. From (6.14) the following identity is obvious:

$$\langle x|\Omega|x'\rangle = \langle x+x'|\Omega\ 0\quad . \tag{7.8}$$

The Gelfand-Levitan equation (6.1) can then be written

$$\langle x|K|x'\rangle = -\langle x+x'|\Omega|0\rangle - \varepsilon\int_{-\infty}^{x}\langle x|K|x''\rangle dx''\langle x''+x'|\Omega|0\rangle \qquad (x>x') \tag{7.9}$$

Now let $x<-\alpha$. From (7.5) we have

$$\langle x+x'|\Omega|0\rangle = 0 \qquad \text{for } x<-\alpha,\ x'<x<-\alpha. \tag{7.10}$$

from which (7.7) follows as a necessary condition.

Let us now show the sufficiency of condition (7.7). If we use Eq. (7.7), then Eq. (7.9) becomes

$$\langle x|K|x'\rangle = -\langle x+x'|\Omega|0\rangle - \varepsilon\eta(x+2\alpha+x')\int_{-(2\alpha+x')}^{x}\langle x|K|x''\rangle dx''\langle x''+x'|\Omega|0\rangle\,, \qquad (x<x'). \tag{7.11}$$

When $x<-\alpha$, we have $x+x'<-2\alpha$ or, equivalently, $x<-(2\alpha+x')$; hence the right-hand side of (7.11) vanishes and we are left with (7.5).

To show the connection between the singularities of $\langle -1|S(E)|+1\rangle$ and the bound states we note that we can write the expression for $\varepsilon\langle x|\Omega|x'\rangle$ as an integral in the complex E-plane. On using (4.11), which gives the analytic continuation of the matrix elements of the scattering operator, we see that

$$\langle -1|S(E)|+1\rangle^{+} = \langle -1|S(E)|+1\rangle^{*}$$

where E is at the bottom of the cut.

Hence, using this fact and the fact that

$$\langle x|H_0, A_0; E, -1\rangle^{+}\ \langle H_0, A_0; E, +1|x'\rangle^{+} = \frac{E^{\frac{1}{4}}}{2\sqrt{\pi}}\langle x+x'|H_0, A_0; E, -1\rangle^{+}\,, \tag{7.12}$$

we have

$$(7.13)\quad \varepsilon\langle x|\Omega|x'\rangle = \frac{1}{2\sqrt{\pi}}\int_{\gamma}\langle -1|S(E)|+1\rangle^{+}(E)^{-\frac{1}{4}}\langle x+x'|H_0, A_0; E, -1\rangle^{+}\mathrm{d}E + \frac{1}{2\sqrt{\pi}}\exp[i\pi/4]\sum_i [C(E_i)]^{-1}|A(E_i)|^2(-E_i)^{-\frac{1}{4}}\langle x+x'|H_0, A_0; E_i, -1\rangle^{+},$$

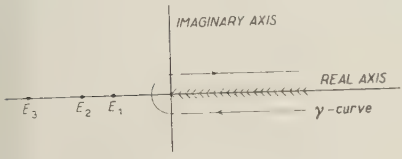

Fig. 1. – Complex E-Plane.

where the contour γ goes in a clockwise direction around the cut in the E-plane.

Let us introduce the momentum variable $k = \sqrt{E}$. The E-plane is then transformed to the upper k-plane. Let us write $b(k) = \langle -1|S(k^2)|+1\rangle$. From (4.11) it is clear that $b(-k) = b^*(k)$ for real k. We have

$$(7.14)\quad \varepsilon\langle x|\Omega|0\rangle = \frac{1}{2\pi}\int_{-\infty}^{+\infty}\mathrm{d}k\, b(k)\exp[-ikx]\,\mathrm{d}k + \frac{1}{2\sqrt{\pi}}\exp[i\pi/4]\sum_i [C(E_i)]^{-1}|A(E_i)|^2(-E_i)^{-\frac{1}{4}}\langle x|H_0, A_0; E_i, -1\rangle^{-}.$$

Let us write

$$(7.15)\quad b(k) = \exp[-i2k\alpha]g(k)$$

where $g(k)\to O(k^{-1})$ as $|k|\to\infty$.

The integral of Eq. (7.14) becomes

$$(7.16)\quad \frac{1}{2\pi}\int_{-\infty}^{\infty}g(k)\exp[-ik(x+2\alpha)]\,\mathrm{d}k\,.$$

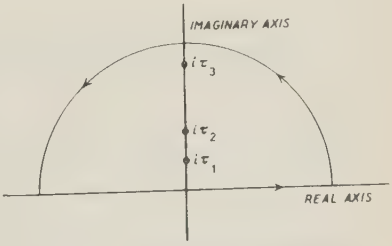

Fig. 2. Complex k-Plane.

When $x < -2\alpha$, one can close the contour by the infinite semi-circle in the upper half of the k-plane, since the integral over this semi-circle will contribute nothing.

The integral (7.16) is equal to the sum of the residues of the integrand, namely,

$$(7.17)\quad \frac{1}{2\pi}\int_{-\infty}^{\infty}g(k)\exp[-ik(x+2\alpha)]\,\mathrm{d}k = i\sum_j r_j\exp[2ik_j\alpha]\exp[-ik_jx]\,,$$

where r_j are the residues of $g(k)$ at the poles k_j. Since the integral must be real for all x, it is clear that the poles k_j must lie on the positive imaginary axis. We shall write $k_j = i\tau_j$ where τ_j are positive real numbers see (Fig. 2). Likewise, ir_j must be real.

Finally, then, we can write for $x < -2\alpha$.

$$(7.18)\quad \varepsilon\langle x|\,\Omega_-\,0\rangle = 2\sqrt{\pi}\exp[i\pi/4]i\sum_j r_j \exp[2\tau_j\alpha](-E_j)^{\frac{1}{4}}\langle x|\,H_0, A_0; E_j, -1\rangle^+ +$$

$$+\frac{1}{2\sqrt{\pi}}\exp[i\pi/4]\sum_i [C(E_i)]^{-1}|\,A(E_i)^2\,(-E_i)^{-\frac{1}{4}}\langle x|\,H_0, A_0; E_i, -1\rangle^+ ,$$

where in the first sum $E_j = k_j^2 = -\tau_j^2$ (see Fig. 1).

Since $\langle x|\,\Omega\,|0\rangle$ is to vanish for $x < -2\alpha$ it is clear that it is sufficient to require that the poles k_j of $g(k)$ be equal to $i\sqrt{-E_j}$, where E_j are the point eigenvalues of H, and that

$$(7.19)\qquad [C(E_i)]^{-1}|\,A(E_i)\,|^2 = -4\pi i\tau_i r_i \exp[2\tau_i\alpha] .$$

From (7.19) it is seen that r_i must be a positive imaginary number in order that $C(E_i)$ be positive.

On using (7.19) in (7.14) we obtain

$$(7.14a)\quad \varepsilon\langle x\,|\,\Omega\,|\,0\rangle = \frac{1}{2\pi}\int_{-\infty}^{\infty} dk\, b(k)\exp[-ikx] - i\sum_j r_j \exp[\tau_j(x+2\alpha)] .$$

One then obtains the results in terms of the notation of the introduction by writing

$$x|\,H, A; E, a\rangle = \frac{1}{2\sqrt{\pi}}E^{-\frac{1}{4}}\Psi_k(x) ,$$

where $k = a\sqrt{E}$.

We have given sufficient conditions for the reproduction of the reflection coefficient $\langle -1|\,S(E)\,|+1\rangle$, in particular, the condition that $V(x) = 0$ for $x < -\alpha$. However, we are not as yet able to obtain conditions to guarantee the vanishing of $V(x)$ for x sufficiently large. This vanishing is a necessary condition for the full scattering operator to exist. It is, in fact, possible to give examples where the prescribed reflection coefficient exists, but where the full scattering operator does not exist.

Incidentally, the use of a triangular operator $\langle x|K|x'\rangle$ which vanishes when $x < -\alpha$ has the consequence that $\langle x|H, A; E, a\rangle = \langle x|U|H_0, A_0; E, a\rangle$ is an analytic function of E in the complex E-plane. Furthermore, the bound states $\langle x|H, E_i\rangle$ can be obtained from the analytic continuation of $\langle x|H, A; E, -1\rangle$. In fact

$$\langle x|H, A; E_i, -1\rangle^+ = \langle x|U|H_0, A_0; E_i, -1\rangle^+ = [A(E_i)]^{-1}\langle x|H, E_i\rangle . \tag{7.20}$$

Usually one chooses the arbitrary function $A(E_i)$ to be unity, to simplify the relation (7.20). However, to obtain the results in terms of the notation of the introduction, we write

$$A(E_i) = 2\sqrt{\pi}\exp[i\pi/4](-E_i)^{\frac{1}{2}} .$$

8. – Examples.

We shall now discuss three examples. In what follows we shall take $\varepsilon = 1$ for simplicity.

8·1. *The repulsive δ-function potential.* – Let us consider the case where

$$\langle -1|S(E)|+1\rangle = \frac{-(iA)\exp[-2i\sqrt{E}\alpha]}{2E^{\frac{1}{2}} + iA}, \qquad (A > 0). \tag{8.1}$$

or equivalently

$$b(k) = \frac{-i(A/2)\exp[-2ik\alpha]}{k + (iA/2)} . \tag{8.2}$$

We see that $b(-k) = b^*(k)$ (for real k) as required. Furthermore, $b(k) = O(k^{-1})$ for $|k|\to\infty$. Since $b(k)$ has no poles on the positive imaginary axis, there will be no bound states.

From (1.8) we have

$$\langle x|\Omega|x'\rangle = \langle x + x'|\Omega|0\rangle = \tag{8.3}$$

$$= \frac{1}{2\pi}\int_{-\infty}^{+\infty} dk\, b(k)\exp[-ik(x + x')] = \frac{-iA}{4\pi}\int_{-\infty}^{+\infty}\frac{dk}{k + (iA/2)}\exp[-ik(x + x' + 2\alpha)] =$$

$$- \frac{A}{2}\eta(x + x' + 2\alpha)\exp\left[-\frac{A}{2}(x + x' + 2\alpha)\right] .$$

The Gelfand-Levitan equation (1.7) is

$$\langle x|K|x'\rangle = \frac{A}{2}\eta(x+x'+2\alpha)\exp\left[-\frac{A}{2}(x+x'+2\alpha)\right]+\frac{A}{2}\eta(x+x'+2\alpha)\cdot \tag{8.4}$$

$$\cdot\int_{-(2\alpha+x')}^{x}\langle x|K|x''\rangle\eta(x''+x'+2\alpha)\exp\left[-\frac{A}{2}(x''+x'+2\alpha)\right]\mathrm{d}x''\,.$$

It is easily verified that the solution of (8.4) is

$$\langle x|K|x'\rangle = \frac{A}{2}\eta(x+x'+2\alpha)\,. \qquad x'<x. \tag{8.5}$$

Hence on using the potential $V(x)$ is

$$V(x) = 2\frac{\mathrm{d}}{\mathrm{d}x}\frac{A}{2}\eta(2x+2\alpha) = A\delta(x+\alpha)\,. \tag{8.6}$$

It is clear that $V(x)=0$ and $\langle x|K|x'\rangle = 0$ when $x<-\alpha$ as required.

The eigenfunctions of $H=-\mathrm{d}^2/\mathrm{d}x^2+A\,\delta(x+\alpha)$ are given by

$$\langle x|H,A;E,a\rangle = \langle x|H_0,A_0;E,a\rangle + \frac{A}{2}\int_{-\infty}^{\infty}\eta(x+x'+2\alpha)\langle x'|H_0,A_0;E,a\rangle\,\mathrm{d}x' = \tag{8.7}$$

$$= \langle x|H_0,A_0;E,a\rangle + \frac{A}{2}\eta(x+\alpha)\int_{-(x+2\alpha)}^{x}\langle x'|H_0,A_0;E,a\rangle\,\mathrm{d}x' =$$

$$= \langle x|H_0,A_0;E,a\rangle - \frac{iAa}{2}\eta(x+\alpha)E^{-\frac{1}{2}}\cdot$$

$$\cdot[\langle x|H_0,A_0;E,a\rangle - \langle x+2\alpha|H_0,A_0;E,-a\rangle]\,.$$

We shall now calculate the scattering operator for the problem. Toward this end we shall use

$$S = M_-M_-^{-1}\,. \tag{8.8}$$

(Cf. [6], Part I, Eq. (5.8)) or equivalently

$$\langle a|S(E)|b\rangle = \sum_c \langle a|\mu_+(E)|c\rangle\langle c|\mu_-^{-1}(E)|b\rangle\,. \tag{8.9}$$

Hence we shall have to evaluate $\langle a|M_+|b\rangle$ and $\langle a|M_-^{-1}(E)|b\rangle$.

From ([6]), Part I, Eq. (5.1) we have

$$M_{\pm} = U - \int \gamma_{\pm}(E - H_0) V U \delta(E - H_0)\, \mathrm{d}E \,. \tag{8.10}$$

If there were bound states, the above equation would have to be replaced by

$$M_{\pm}\eta(H_0) = U\eta(H_0) - \int \gamma_{\pm}(E - H_0) V U \eta(H_0)\, \delta(E - H_0)\, \mathrm{d}E \,. \tag{8.11}$$

Equation (8.10) is equivalent to

$$\sum_{a'} \langle x | H_0, A_0; E, a' \rangle \langle a' | \mu_{\pm}(E) | a \rangle =$$

$$= \langle x | H, A; E, a \rangle \mp \frac{i}{2} (E)^{-\frac{1}{2}} \int_{-\infty}^{\infty} \exp\left[\mp i\sqrt{E}|x - x'|\right] V(x') \langle x' | H, A; E, a \rangle \, \mathrm{d}x' \,. \tag{8.12}$$

In obtaining (8.12) from (8.10) we used Eqs. (3.10) and (2.7a).

On using (8.6) and (8.7) we have for $x < -\alpha$

$$\sum_{a'} \langle x | H_0, A_0; E, a' \rangle \langle a' | \mu_{\pm}(E) | a \rangle =$$

$$= \langle x | H_0, A_0; E, a \rangle \mp \frac{Ai}{2} (E)^{-\frac{1}{2}} \exp\left[\pm i\sqrt{E}(x + \alpha)\right] \langle -\alpha | H_0, A_0; E, a \rangle \,, \tag{8.13}$$

or

$$\sum_{a'} \langle x | H_0, A_0; E, a' \rangle \langle a' | \mu_{\pm}(E) | a \rangle =$$

$$= \langle x | H_0, A_0; E, a \rangle \mp \frac{Ai}{2} E^{-\frac{1}{2}} \exp\left[-i\alpha(a \mp 1)\sqrt{E}\right] \langle x | H_0, A_0; E, \pm 1 \rangle \,. \tag{8.14}$$

Since $\langle a | \mu_{\pm}(E) | a' \rangle$ must be independent of x, we have

$$\langle a | \mu_{-}(E) | a' \rangle = \begin{pmatrix} 1 & 0 \\ \dfrac{AiE^{-}}{2} \exp\left[-2i\alpha\sqrt{E}\right] & 1 + \dfrac{AiE^{-\frac{1}{2}}}{2} \end{pmatrix}, \tag{8.15}$$

$$\langle a | \mu_{+}(E) | a' \rangle = \begin{pmatrix} 1 - \dfrac{AiE^{-\frac{1}{2}}}{2} & -\dfrac{AiE^{-\frac{1}{2}}}{2} \exp\left[2i\alpha\sqrt{E}\right] \\ 0 & 1 \end{pmatrix}. \tag{8.16}$$

Since the matrix $\langle a\ \mu_{-}^{-1}(E) | a' \rangle$ is just the reciprocal of $\langle a\ \mu_{-}(E) | a' \rangle$ we see that

$$\langle a|\mu^{-1}(E)|a'\rangle = \begin{pmatrix} 1 & 0 \\ \dfrac{-Ai\exp[-2i\alpha\sqrt{E}]}{2\sqrt{E}+iA} & \dfrac{2\sqrt{E}}{2\sqrt{E}+iA} \end{pmatrix}. \tag{8.17}$$

Finally on using (8.9)

$$\langle a|S(E)|a'\rangle = \begin{pmatrix} \dfrac{2\sqrt{E}}{2\sqrt{E}+iA} & \dfrac{-Ai\exp[2i\alpha\sqrt{E}]}{2\sqrt{E}+iA} \\ \dfrac{-iA\exp[-2i\alpha\sqrt{E}]}{2\sqrt{E}+iA} & \dfrac{2\sqrt{E}}{2\sqrt{E}+iA} \end{pmatrix}. \tag{8.18}$$

The reflection coefficient

$$-1|S(E)|+1\rangle = \frac{-Ai\exp[-2i\alpha\sqrt{E}]}{2\sqrt{E}+iA}$$

is just the one we started with.

8·2. *The attractive δ-function potential.* – Let us now consider the reflection coefficient

$$\langle -1|S(E)|+1\rangle = \frac{iB\exp[-2i\alpha\sqrt{E}]}{2\sqrt{E}-iB}, \qquad B>0, \tag{8.19}$$

or

$$b(k) = \frac{i(B/2)\exp[-2i\alpha k]}{k-(iB/2)}. \tag{8.20}$$

In this case there is a bound state, since $b(k)$ has a singularity on the positive imaginary axis. In fact we have

$$\begin{cases} \tau_1 = \dfrac{B}{2} \\ r_1 = \dfrac{iB}{2}, \end{cases} \tag{8.21}$$

and the bound state E_1 is given by

$$E_1 = -\tau_1^2 = \frac{B^2}{4}. \tag{8.22}$$

We have

$$(8.23)\quad \langle x|\Omega|x'\rangle = \frac{1}{2\pi}\int_{-\infty}^{+\infty} b(k)\exp[-ik(x+x')]\,dk - ir_1\exp[\tau_1(x+x'+2\alpha)] =$$

$$= \frac{iB}{4\pi}\int_{-\infty}^{+\infty}\frac{\exp[-ik(x+x'+2\alpha)]}{k-(iB/2)}\,dk + \frac{B}{2}\exp\left|\frac{B}{2}(x+x'+2\alpha)\right| =$$

$$= -\frac{B}{2}\eta(-x-x'-2\alpha)\exp\left|\frac{B}{2}(x+x'+2\alpha)\right| + \frac{B}{2}\exp\left|\frac{B}{2}(x+x'+2\alpha)\right| =$$

$$= \frac{B}{2}\eta(x+x'+2\alpha)\exp\left|\frac{B}{2}(x+x'+2\alpha)\right|.$$

The solution of the Gelfand-Levitan equation is

$$(8.24)\quad \langle x|K|x'\rangle = -\frac{B}{2}\eta(x+x'+2\alpha),$$

and the potential $V(x)$ is

$$(8.25)\quad V(x) = 2\frac{d}{dx}\langle x|K|x\rangle = -B\delta(x-\alpha).$$

The eigenfunctions of the continuous spectrum are

$$(8.26)\quad \langle x|H, A; E, a\rangle = \langle x|H_0, A_0; E, a\rangle + \frac{iBa}{2}\eta(x+\alpha)(E)^{-\frac{1}{2}}\cdot$$
$$\cdot[\langle x|H_0, A_0; E, a\rangle - \langle x+2\alpha|H_0, A_0; E, -a\rangle],$$

while the proper eigenfunction corresponding to the eigenvalue $E_1 = -B^2/4$ is on using (7.20) and (5.5)

$$(8.27)\quad \langle x|H, E_1\rangle = A(E_1)\langle x|H, A; E_1, -1\rangle^+ =$$
$$= \frac{A(E_1)}{2\sqrt{\pi}}\exp\left[-\frac{i\pi}{4}-\frac{B}{2}\alpha\right]\exp\left[-\left|\frac{B}{2}(x+\alpha)\right|\right],$$

where, in accordance with (7.19) and (8.21)

$$(8.28)\quad [C(E_1)]^{-1}|A(E_1)|^2 = \frac{4\pi B^2}{4}\exp[B\alpha].$$

We can choose either $A(E_1)$, in which case the normalization $C(E_1)$ is determined or $C(E_1)$ in which case $A(E_1)$ is determined to within a phase factor.

It can also be shown that

$$\langle a|\mu_-(E)|a'\rangle = \begin{pmatrix} 1 & 0 \\ \dfrac{-BiE^{-\frac{1}{2}}\exp\left[-2i\alpha\sqrt{E}\right]}{2} & 1-\dfrac{BiE^{-\frac{1}{2}}}{2} \end{pmatrix}, \tag{8.29}$$

$$\langle a|\mu_+(E)|a'\rangle = \begin{pmatrix} 1+\dfrac{BiE^{-\frac{1}{2}}}{2} & \dfrac{B}{2}iE^{-\frac{1}{2}}\exp\left[2i\alpha\sqrt{E}\right] \\ 0 & 1 \end{pmatrix}, \tag{8.30}$$

$$\langle a|\mu_-^{-1}(E)|a'\rangle = \begin{pmatrix} 1 & 0 \\ \dfrac{Bi\exp\left[-2i\alpha\sqrt{E}\right]}{2\sqrt{E}-iB} & \dfrac{2\sqrt{E}}{2\sqrt{E}-iB} \end{pmatrix}, \tag{8.31}$$

$$\langle a|S(E)|a'\rangle = \begin{pmatrix} \dfrac{2\sqrt{E}}{2\sqrt{E}-iB} & \dfrac{Bi\exp\left[2i\alpha\sqrt{E}\right]}{2\sqrt{E}-iB} \\ \dfrac{Bi\exp\left[-2i\alpha\sqrt{E}\right]}{2\sqrt{E}-iB} & \dfrac{2\sqrt{E}}{2\sqrt{E}-iB} \end{pmatrix}. \tag{8.32}$$

8·3. *A more complicated example.* – We shall now summarize the results of a more complicated example discussed in more detail in (7).

Let us find the potential whose reflection coefficient is given by

$$\langle -1|S(E)|+1\rangle = -\exp\left[-2i\alpha\sqrt{E}\right]\frac{1}{E+1}\,. \tag{8.33}$$

or

$$b(k) = -\exp\left[-i2\alpha k\right]\frac{1}{(k+i)(k-i)}\,. \tag{8.34}$$

There is only one pole in the upper k-plane, namely $k_1 = i$, and hence we can calculate the quantities associated with the bound states:

$$\begin{cases} \tau_1 = 1\,, \\ r_1 = \dfrac{i}{2}\,, \\ E_1 = -1\,, \\ C^{-1}(E_1)|A(E_1)|^2 = 2\pi\exp\left[2\alpha\right]. \end{cases} \tag{8.35}$$

Also

$$\langle x'|\Omega|x'\rangle = \eta(x+x'+2\alpha)\sinh\left(x+x'+2\alpha\right). \tag{8.36}$$

Then it can be shown that the solution of the Gelfand-Levitan equation is

$$\langle x|K|x'\rangle = -\frac{1}{\sqrt{2}}\eta(x+x'+2\alpha)\frac{\sinh\sqrt{2}(x+\alpha)+\sinh\sqrt{2}(x'+\alpha)}{\cosh\sqrt{2}(x+\alpha)}. \tag{8.37}$$

The potential $V(x)$ is

$$V(x) = 2\frac{\mathrm{d}}{\mathrm{d}x}\langle x|K|x\rangle = -4\eta(x+\alpha)\operatorname{sech}^2\sqrt{2}\,(x+\alpha). \tag{8.38}$$

The eigenfunctions of the continuous spectrum are given by

$$\langle x|H, A; E, a\rangle = \frac{(E)^{-\frac{1}{2}}}{2\sqrt{\pi}}\exp[i\alpha\sqrt{E}x] \quad \frac{\eta(x+\alpha)}{\sqrt{2\pi}}\frac{(E)^{-\frac{3}{2}}}{(E+2)}\exp[-ia\sqrt{E}\alpha]\cdot \tag{8.39}$$

$$\cdot\{\operatorname{tgh}\sqrt{2}(x+\alpha)[a(E+2)\sin a\sqrt{E}(x+\alpha) - iaE\cos a\sqrt{E}(x+\alpha)] + \\ + \sqrt{2}i\sqrt{E}\sin a\sqrt{E}(x+\alpha)\}.$$

The single eigenstate corresponding to a point eigenvalue is given by

$$\langle x|H, E_1\rangle = A(E_1)\exp[-i\pi/4]\cdot \tag{8.40}$$

$$\cdot\left\{\frac{\exp[x]}{2\sqrt{\pi}} + \frac{\eta(x+\alpha)}{\sqrt{2\pi}}\exp[-\alpha][\operatorname{tgh}\sqrt{2}(x+\alpha)\exp[-(x+\alpha)] - \sqrt{2}\sinh(x+\alpha)]\right\}.$$

It is readily verified that $\lim_{x\to\pm\infty}\langle x|H, E_1\rangle = 0$.

We also derive using the methods of Part A

$$\langle a|\mu_-(E)|a'\rangle = \begin{pmatrix} 1 & 0 \\ \dfrac{\exp[-2i\sqrt{E}\alpha]}{\sqrt{E}(\sqrt{E}+i\sqrt{2})} & \dfrac{E+1}{\sqrt{E}(\sqrt{E}+i\sqrt{2})} \end{pmatrix}, \tag{8.41}$$

$$\langle a|\mu_-^{-1}(E)|a'\rangle = \begin{pmatrix} 1 & 0 \\ -\dfrac{\exp[-2i\sqrt{E}\alpha]}{(E+1)} & \dfrac{\sqrt{E}(\sqrt{E}+i\sqrt{2})}{(E+1)} \end{pmatrix}. \tag{8.42}$$

$$\langle a|\mu_+(E)|a'\rangle = \begin{pmatrix} \dfrac{(E+1)(\sqrt{E}+i\sqrt{2})}{\sqrt{E}(E+2)} & \dfrac{\exp[2i\alpha\sqrt{E}](\sqrt{E}+i\sqrt{2})}{\sqrt{E}(E+2)} \\ 0 & 1 \end{pmatrix}. \tag{8.43}$$

$$(8.44)\qquad \langle a \mid S(E) \mid a' \rangle = \begin{pmatrix} \dfrac{\sqrt{E}(\sqrt{E}+i\sqrt{2})}{(E+1)} & \dfrac{\exp[2i\alpha\sqrt{E}](\sqrt{E}+i\sqrt{2})^2}{(E+2)(E+1)} \\ \dfrac{\exp[-2i\alpha\sqrt{E}]}{(E+1)} & \dfrac{\sqrt{E}(\sqrt{E}+i\sqrt{2})}{(E+1)} \end{pmatrix}.$$

In (7) it is shown how one may solve the Gelfand-Levitan equation when one is given any reflection coefficient which is a rational function of $\sqrt{E}$. In such a case, the Gelfand-Levitan equation reduces to a system of algebraic equations for which a procedure for solving them can be found. The method is analogous to that used by V. BARGMANN for the radial equation.

RIASSUNTO (*)

Il procedimento per il calcolo dei potenziali di scattering dalle funzioni spettrali di misura dell'Hamiltoniana perturbata discusse in precedenti lavori, è stato adattato al problema di ottenere il potenziale di scattering dall'operatore di scattering per l'equazione di Schrödinger unidimensionale ($-\infty < x < \infty$). Si dànno esempi dell'uso del procedimento.

(*) *Traduzione a cura della Redazione.*

Cloud Chamber Study of Cosmic Ray Electronic Showers Under Dense Materials (II).

G. Di Caporiacco and M. Giovannozzi

Istituto di Fisica dell'Università - Firenze

(ricevuto il 28 Novembre 1955)

Summary. — Pictures have been taken by means of a counter controlled cloud chamber on electronic showers produced in lead plates 1, 3 and 4 cm thick. The angular distribution of tracks has been compared with the calculations of Roberg and Nordheim and of Franchetti and Giovannozzi. The distribution of showers as a function of the number of electrons has been used to check the results given by Jánossy and Messel and by Arley.

1. – Introduction.

This paper discusses further measurements on electronic showers performed with the same procedure and experimental set up as in a previous article by S. Franchetti (1) (hencefort referred to as I).

The present measurements refer to thicknesses of 1, 3, 4 cm Pb.

We shall sum up briefly the criteria followed in the collection and selection of the data. Other details can be found in the previous article.

Only those showers whose axes formed a projected angle of less than 15° with the vertical were considered. In addition some other events (less than 1% of the total number) were discarded which showed tracks of heavy particles attributable to the presence of nuclear explosions.

The direction of the shower axis, when the primary was not visible, was determined approximately by the second method described in I, 3.

Showers were classified in three categories: electron-initiated showers when having a visible primary; photon-initiated showers when falling in the central

(1) S. Franchetti: *Nuovo Cimento*, **10**, 551 (1953).

portion of the chamber and not showing a visible primary: uncertain showers when falling in the lateral portions of the chamber where primaries were not visible.

The stereoscopic reconstruction of the exit points of the tracks from the lead plate was carried out graphically and allowed to estimate the intersection of the axis to certainly better than 1 cm.

The spatial distribution of these intersections showed indeed that the showers with a visible primary were mainly contained in a central strip about 4 cm wide.

Recording probabilities were also taken into account following the method described in I, with minor modifications which will be dealt with in 3, when they are more important.

Table I summarizes the raw results of the experiment.

TABLE I.

Thickness of Pb (cm)	Number of Showers		
	electron-initiated	photon-initiated	uncertain
1	66	87	41
3	16	37	11
4	16	36	41

2. – Angular distribution of showers.

For each shower the root mean square of the angles of the single tracks with the shower axis was evaluated. This mean angle is plotted against the number of electrons in the shower in Figs. 1, 2, 3: each full small circle represents an electron-initiated shower while each empty circle represents a photon-initiated shower; the triangles represent uncertain showers.

By inspection of the distribution of the points a correlation of the mean angle with the number of electrons in the shower is apparent. This fact is brought out more clearly if we group the events in classes according to the number of shower particles and take the general average of the angles for each class. This is done in Figs. 1, 2, 3. The rectangles are centered on the value of this average and have an height equal to the standard statistical error and a basis equal to the width of the class. In Fig. 1 full-line rectangles refer to electron-initiated showers and dotted line rectangles to photon-initiated showers. In Figs. 2 and 3 no distinction is made between electron and photon-initiated showers; in the calculation of the average « uncertain » showers are also included because no appreciable difference was found among the various categories.

The general trend of the distribution is clearly similar to that reported in I for two cm Pb. Likewise a curve of equation $a + b/N$ was fitted to the experimental points and drawn in each graph (values of the parameters shown in the caption).

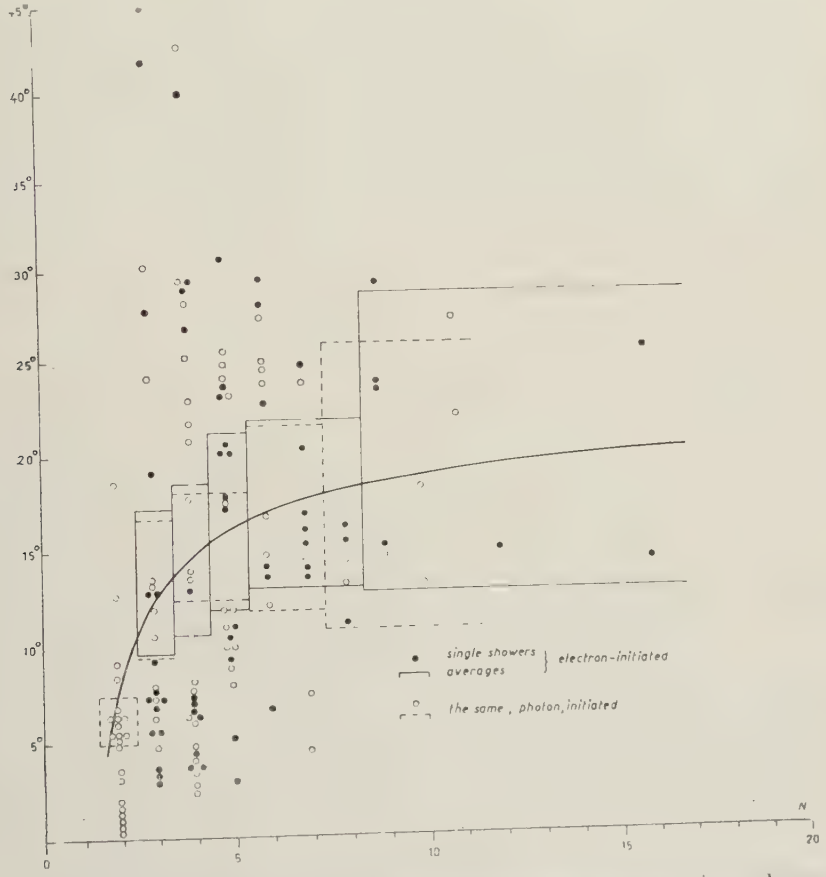

Fig. 1. – The root mean square (projected) angle of the electrons in a shower under 1 cm Pb as a function of the number of electrons: $a = 21°$, $b = 25°$.

The mean apertures of the showers show a similar trend. The results of these calculations which take into account the mean weights are shown in Table II.

In Table III some data are reported about the angular distribution of the tracks for showers with at least 5 and at least 10 electrons.

The values contained in the second column are the mean frequencies of showers with at least 4 electrons under 1 cm Pb obtained giving to each track the weight of the shower to which it belongs. The values of the columns 3, 4

TABLE II.

Number of electrons	1 cm Pb		3 cm Pb		4 cm Pb	
	mean weight	projected angle	mean weight	projected angle	mean weight	projected angle
2	45	15°	41	14.5°	44	15°
3 – 4	14.7	16°	17.7	17°	17.5	16.5°
5 – 6	8.2	17.5°	8.7	17.5°	7.7	18°
7 – 9	5.3	18.5°	5	18°	4.8	18°
10 – 12	3.5	19°	2.6	17°	3.5	19°
13 – 15	2.7	19.5°	2	17°	2.9	20°
16 – 20	2	20.5°	1.5	16.5°	2	20.5°

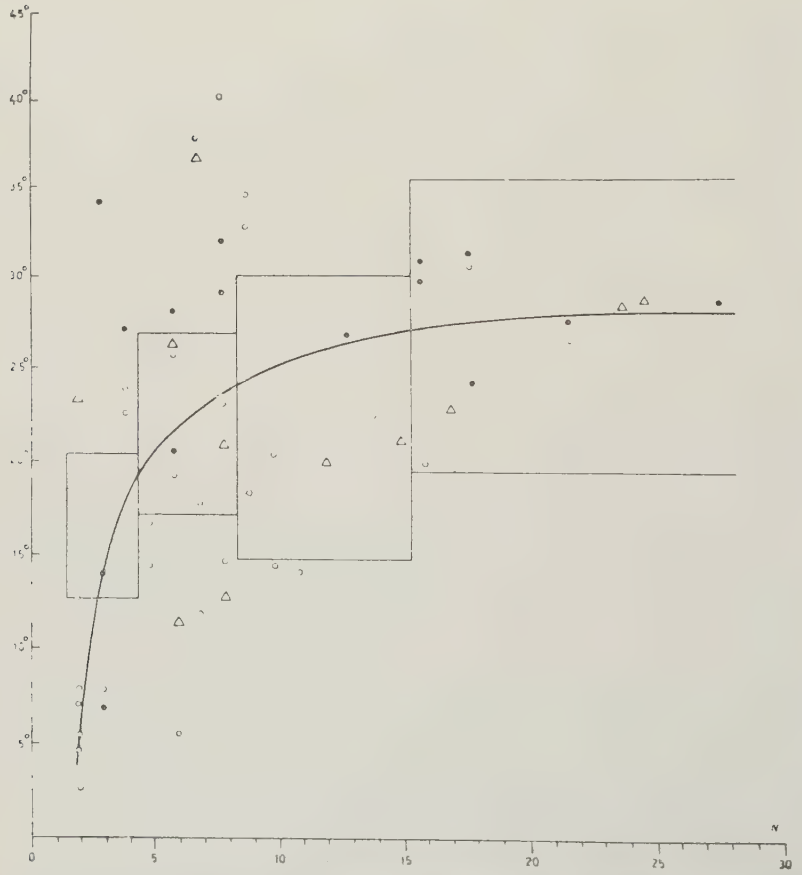

Fig. 2. The root mean square (projected) angle of the electrons in a shower under 3 cm Pb as a function of the number of electrons: $a = 30°$; $b = 49°$.

TABLE III.

Angular Class	Number of Electronic tracks per 10^o					
	1 cm Pb $N \geqslant 4$	2 cm Pb $N \geqslant 5$ (1)	3 cm Pb $N \geqslant 5$	4 cm Pb $N \geqslant 5$	all thickn. $N \geqslant 5$	all thickn. $N \geqslant 10$
$0^o - 5^o$	100.0 ± 6.2	100.0 ± 6.2	100.0 ± 5.6	100.0 ± 8.7	100.0 ± 3.3	100.0 ± 5.3
$5^o - 15^o$	48.7 ± 3.2	63.0 ± 3.3	79.0 ± 6.1	68.9 ± 4.5	63.9 ± 2.0	67.2 ± 3.3
$15^o - 30^o$	25.8 ± 2.5	27.6 ± 1.9	29.8 ± 2.8	42.4 ± 3.2	30.9 ± 1.2	33.0 ± 1.9
$30^o - 50^o$	7.6 ± 0.1	13.5 ± 1.2	14.9 ± 1.7	14.0 ± 1.2	12.3 ± 0.6	18.9 ± 1.3
$50^o - 70^o$	1.5 ± 0.3	5.0 ± 0.8	8.8 ± 1.8	6.5 ± 0.9	5.2 ± 0.4	7.2 ± 0.8
$70^o - 90^o$	1.8 ± 0.1	0.8 ± 0.3	1.7 ± 0.5	1.0 ± 0.3	1.0 ± 0.3	1.2 ± 0.2

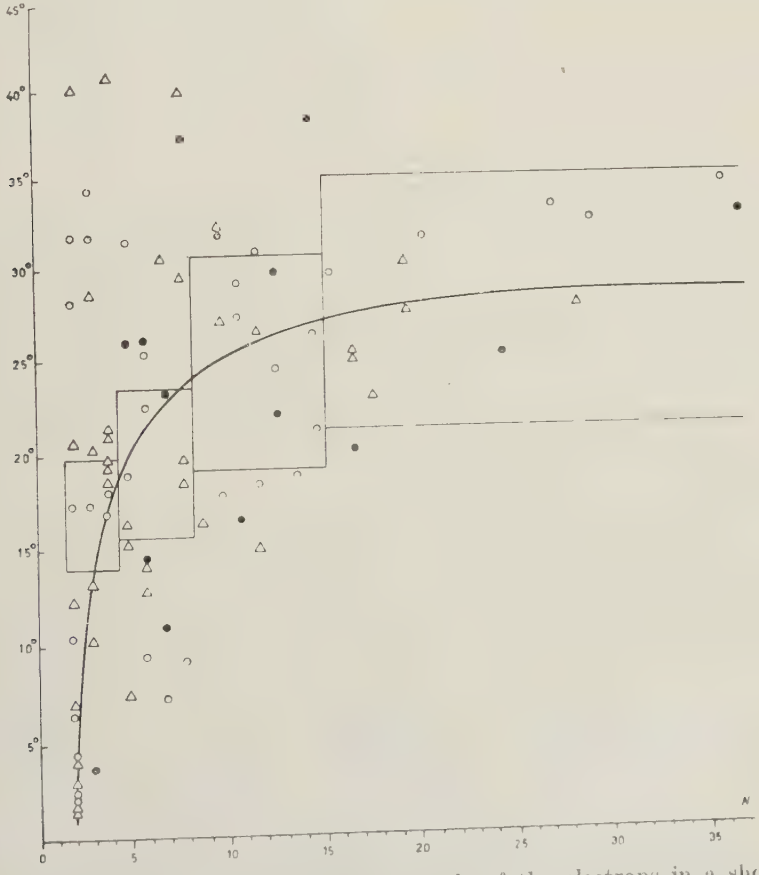

Fig. 3. – The root mean square (projected) angle of the electrons in a shower under 4 cm Pb as a function of the number of electrons: a = 30°; b = 50°.

and 5 are obtained for showers with at least 5 electrons under 2, 3 and 4 cm Pb (values for 2 cm Pb referred from I). The values of column 6 are obtained

taking the averages of the values obtained for different thicknesses of Pb. (no significant difference is apparent from inspection between the various thicknesses). The values of the last column are obtained in a similar manner taking into account only the showers with at least 10 electrons. The frequencies are all normalized at the angle of 2.5°. The errors are standard deviations. No distinction was made between electron-initiated and photon-initiated showers as much as no appreciable differences were found between the two classes.

In order to facilitate the comparison of the experimental results with the calculations of ROBERG and NORDHEIM (2) and of FRANCHETTI and GIOVANNOZZI (3) Fig. 4 has been drawn. The dotted curves gives the results of R. and N.; the full line those of F. and G. The full small circles give the experimental results for showers with at least 5 electrons. The values are obtained averaging the results obtained for different thicknesses of Pb. The empty circles are the values obtained in a similar manner for showers with at least 10 electrons.

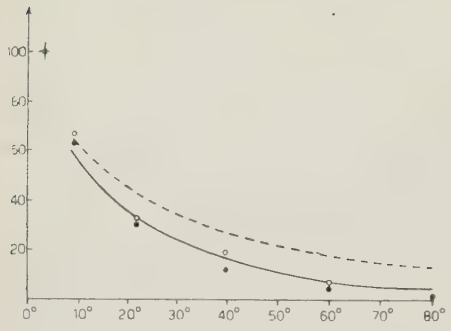

Fig. 4. – Angular distribution for showers of either origin. Broken line: curve calculated by ROBERG and NORDHEIM; full line: curve calculated by FRANCHETTI and GIOVANNOZZI. Full circles: experimental results for showers with at least 5 electrons; empty circles: showers with at least 10 electrons (Averages of the values obtained for 1, 2, 3 and 4 cm Pb).

3. Distribution of showers as a function of the number of particles.

The data collected with the lead plates of 1 and 2 cm thickness have also been used to check the results given by JÁNOSSY and MESSEL (4) and by ARLEY (5) for the mean number of shower electrons and also for the fluctuation problem.

This latter problem is generally discussed seeking for the probability $P(\varepsilon, N, t)$ that under a thickness of t cascade units (6) a shower emerges con-

(2) J. ROBERG and L. W. NORDHEIM: *Phys. Rev.*, **75**, 444 (1949).

(3) S. FRANCHETTI and M. GIOVANNOZZI: *Nuovo Cimento*, **8**, 312 (1951).

(4) L. JÁNOSSY and H. MESSEL: *Proc. Phys. Soc.*, **63**, 1101 (1950); **64**, 1 (1951); *Proc. Ir. Ac.*, **54** A, 217 (1951); H. MESSEL: *Proc. Phys. Soc.*, **74**, 807 (1951).

(5) N. ARLEY: *Stochastic Processes and Cosmic Radiation* (New York, 1948).

(6) A cascade unit being defined as $\Delta t = [(4NZ/137)\ r_0 \log_e (183Z^{-\frac{1}{3}})]$, according to JÁNOSSY: *Cosmic Rays* (Oxford, 1948), p. 204.

aining *exactly* N electrons with energy larger than εE_0, E_0 being the energy of the primary.

For $\varepsilon = 10^{-2}$ and for electron-initiated showers this function has been calculated by MESSEL according to the statistical models of Polya and Poisson.

For other values of ε and for both models, MESSEL gives the elements which allow us to calculate this probability, both in the case of electron and photon-initiated showers.

For the comparison with experimental results, however, it is necessary to derive from $P(\varepsilon, N, t)$ the probability $\pi(N, t)$ of recording a shower of exactly N particles under the thickness t, given the energy cut introduced by the experimental set up and given the energy spectrum of the primary radiation.

Such a probability is obviously:

$$\pi(N, t) = \int_{E_0}^{\infty} P(\varepsilon, N, t)\, F(E_0)\, \mathrm{d}E_0 , \tag{1}$$

where $\varepsilon = E_t/E_0$, E_t is the energy cut, $F(E_0)$ is the energy spectrum of the primary radiation and E_c is the critical energy for the material employed.

We have given E_t a value of 0.8 MeV, corresponding to the fact that an electron of approximately this energy suffers such a large scattering that in the selection of the data it would be discarded because its direction could not be traced back with reasonable accuracy.

For the energy spectrum we have used the form given by ARLEY [7]: namely, for primary electrons:

$$F_{el}(E_0)\, \mathrm{d}E_0 = \begin{cases} \alpha C \dfrac{\mathrm{d}E_0}{E^*} & \text{for } 0 \leqslant E_0 < E^* \\ C \left(\dfrac{E^*}{E_0}\right)^{1+\gamma} \dfrac{\mathrm{d}E_0}{E^*} & \text{for } E_0 \geqslant E^* \end{cases} \tag{2}$$

where $E^* = 2 \cdot 10^8$ eV, $\gamma = 1.5$, $\alpha = 10$ and C is a normalization constant; and for primary photons:

$$F_{ph}(E_0)\, \mathrm{d}E_0 = \begin{cases} C' \dfrac{\mathrm{d}E_0}{E_0} & \text{for } E' \leqslant E_0 < E'' \\ C' \left(\dfrac{E''}{E_0}\right)^{\gamma} \dfrac{\mathrm{d}E_0}{E_0} & \text{for } E_0 \geqslant E'' , \end{cases} \tag{3}$$

where $E' = 10^7$ eV, $E'' = 1.5 \cdot 10^8$ eV, $\gamma = 1.5$ and C' is the normalization constant.

---

[7] N. ARLEY: loc. cit., pp. 165-170.

The evaluation of integral (1) has been carried out graphically.

In Fig. 6 curve I gives the distribution of electron-initiated showers as a function of the number of particles, i.e. the probability $\pi(N, t)$ plotted against N, for $t = 1$ cm Pb, calculated using the solutions of the diffusion equations obtained by MESSEL in approximation A.

Curve II has instead been calculated from MESSEL's data applying the correction required for approximation B according to the method of BHABHA and CHAKRABARTY (8).

We have evaluated separately the normalized distributions for the electron and photon-initiated showers (see Fig. 5). Since in our experiment the showers

Fig. 5. - Theoretical distributions of showers under 1 cm Pb as a function of the number of electrons, from MESSEL's data in approximation B. -·-·- electron-initiated showers; – – – photon initiated; ——— mean values.

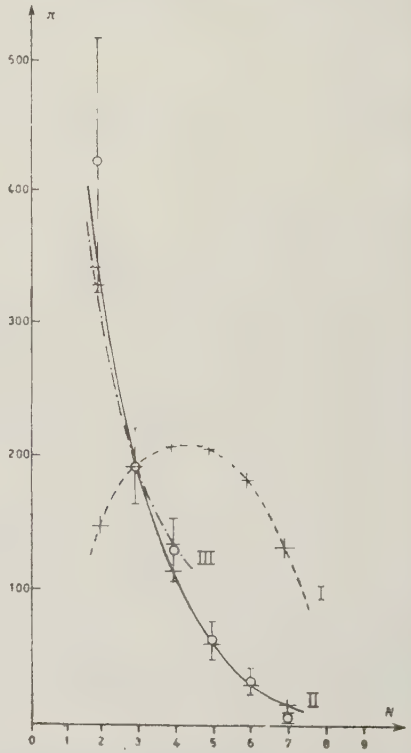

Fig. 6. – Distribution of showers under 1 cm Pb as a function of the number of electrons. Curves are theoretical distributions: I, MESSEL's calculations, approximation A (only electron initiated showers); II, MESSEL's calculations, approximation B (all showers); III, ARLEY's calculations (all showers).

(8) BHABHA and CHAKRABARTY: *Proc. Roy. Soc.*, **181**, 267 (1943); *Phys. Rev.*, **74**, 1352 (1948).

of both classes were equally numerous, the arithmetical mean of the two distributions was taken (curve II Fig. 6).

Curve III gives the distribution of the showers (which is again the average of the two classes) obtained directly by ARLEY's results.

The small circles give the experimental results (sum of weights of the showers) with their statistical errors.

Figs. 7 and 8 show the results obtained in the same manner, for two cm Pb. All these results are reported also in Tables IV and V.

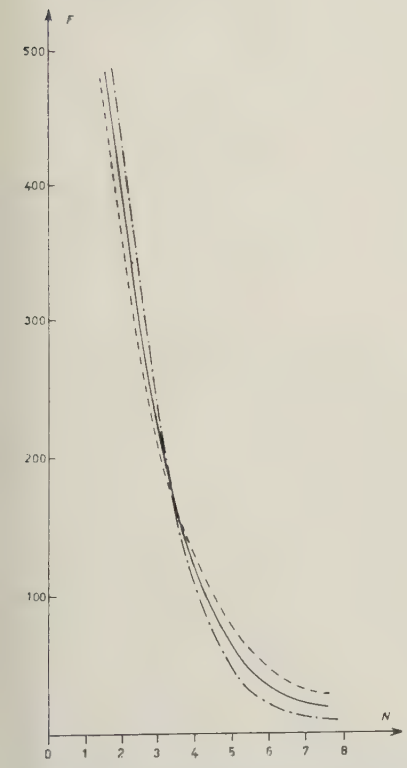

Fig. 7. – Theoretical distribution of showers under 2 cm Pb as a function of the number of electron, from MESSEL's data in approximation B. –·–·– electron-initiated showers; – – – – photon-initiated showers; ——— mean values.

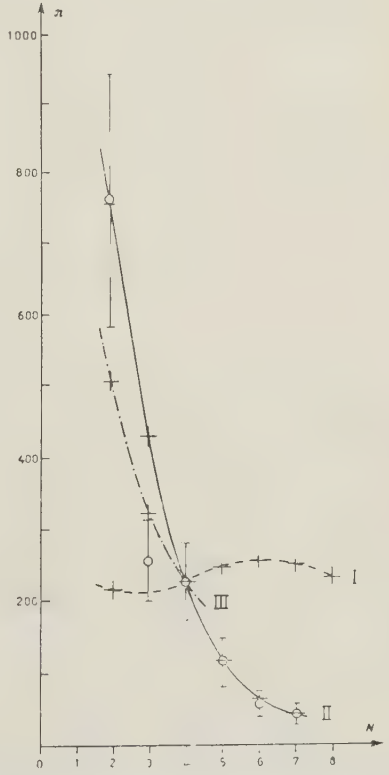

Fig. 8. – Distribution of showers under 2 cm Pb as a function of the number of electrons. Curves are theoretical distributions: I, MESSEL's calculations, approximation A (only electron-initiated showers); II, MESSEL's calculation, approximation B (all showers); III, ARLEY's calculations (all showers).

It is to be noted that the weights of the showers obtained with the method described in I have been corrected to take into account the fact that several showers cannot give the fourfold coincidence which triggered the chamber.

In these conditions the pictures have to be ascribed to accidental or extraneous coincidences. To make this correction, particularly important for showers of two particles, those showers have been selected whose particles crossed the counters, by determining the probable incidence point of the tracks on the plane of the lower counters.

TABLE IV.

N	ARLEY's calculations	MESSEL's calc. approx. A electron-in. showers	MESSEL's calculation, approximation B			Experimental results (1 cm Pb)
			electron-in. showers	photon-in. showers	mean values	
2	715	334	485.6	747	747	530 ±209
3	425.3	425.3	445.7	405	425.3	425.3± 58.7
4	301	444	298.2	223.5	210.8	291 ± 49.4
5	—	473	178	98	138	145 ± 30.9
6	—	408	90.8	49.3	70.5	80.3± 21.6
7	—	294.5	46.8	20.2	33.5	20 ± 7.8

TABLE V.

N	ARLEY's calculations	MESSEL's calc. approx. A electron-in. showers	MESSEL's calculations, approximation B			Experimental results (2 cm Pb)
			electron-in. showers	photon-in. showers	mean values	
2	270	117.8	454.16	398	426.1	408 ±94.5
3	171	114.8	247.14	217	232.1	138.2±29.7
4	121.4	121.4	112.15	130.7	121.4	121.4±29
5	—	134.9	50.9	80	65.4	62.8±17.9
6	—	143	21.7	45.2	33.4	31.8± 9.6
7	—	136.7	14	31.9	22.9	24.8± 8.9

The showers which could not have triggered the counters by themselves have been rejected; this procedure eliminated up to about 50% of the showers of two particles.

A number of pictures have also been taken, with a glass plate 3.5 g/cm² thick, beneath the lead plate (1 cm thick) and 5 cm far from it.

Taking into account the uncertainty of glass composition and of the direction of the trajectory, the energy loss suffered by an electron in crossing the glass was estimated to be 7 MeV to about 10% (9). This is therefore the

(9) This value comes out from a mean between the energy losses suffered by an electron in mass equivalent Al and Cu as quoted by HEISEMBERG: *Cosmische Strahlung* (Berlin, 1953), p. 493.

order of magnitude of the energetic cut which is introduced, if we include in the statistics only those particles which cross the glass, as, in fact, we did.

In the course of the examination of the series of pictures one has to take into account, besides the origin point of the shower and the axis inclination, also the incidence points of each track on the glass. In fact to decide surely if an electron has stopped or not in the glass plate one has to be sure that the electron could not possibly be scattered out of the illuminated region of the chamber.

This determination was carried out with a graphical method.

Fig. 9. – Theoretical distribution of showers under 1 cm Pb as a function of the number of electrons with energy over 7 MeV, from MESSEL's data in approximation A. –·–·– electron -initiated showers; – – – – photon-initiated showers; ——— mean values.

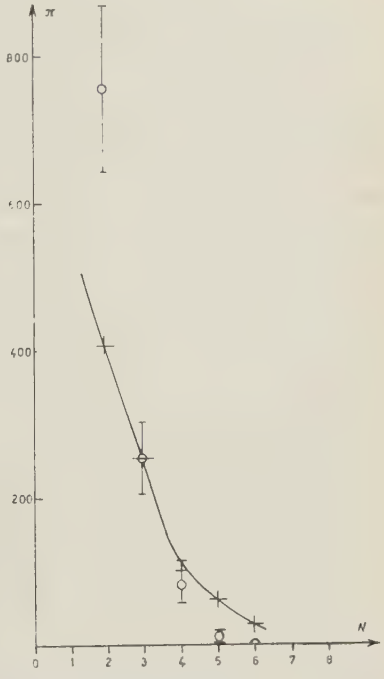

Fig. 10. – Distribution of showers under 1 cm Pb as a function of the number of electrons which cross 3.5 g/cm of glass. The curve is calculated from MESSEL's data in approximation B.

The results of these measurements have been plotted in Fig. 10 together with the theoretical curve calculated from MESSEL's data in approximation A, taking into account a cut of 7 MeV.

In this case too the curve has been obtained from the average of the two curves for electron and photon-initiated showers, which are drawn separately in Fig. 9.

4. – Conclusions.

From the examination of Figs. 1, 2, 3 we can see that the distribution of mean angles according to the number of electrons obtained for the various thicknesses of lead have a shape quite similar to that found in I for 2 cm of lead. We can only observe that when the thickness increases the mean angle for large values of N, increases also, and seems to approach a saturation value of about 30°.

No significant difference can be found among the results obtained for various thicknesses of lead in plotting the number of tracks versus the angle (formed with the axis). Taking this fact into account we have reported in Fig. 4 the total number of tracks obtained for all the thicknesses (results reported in I included). These numbers show a substantial agreement with the calculations of F. and G. The agreement is better for showers with a large number of electrons ($N \geqslant 10$), as was to be expected, because with larger numbers of electrons the hypotheses and conditions of the F. and G. calculations are better fulfilled.

The calculations of curves I, II, III, of Figs. 6 and 8 have been made according to Polya's statistical model. It has to be pointed out, however, that with the thicknesses used by us, such a model gives results which do not differ appreciably from those of Poisson's model (they are practically identical for two cm Pb).

It is therefore pointless to seek for a proof for one or the other model from our data.

From the comparison of the various curves with experimental points we can instead appraise the reliability of the various solutions of the diffusion equations.

TABLE VI.

N	Electron-initiated showers	Photon-initiated showers	Mean values	Experimental results
2	124.2	155.5	134.5	221.3 ± 34.1
3	86.77	74.3	80.53	80.53 ± 13.4
4	41.96	34.8	38.38	23.8 ± 6.35
5	34.19	16.67	24.93	0.4 ± 0.19
6	10.42	7.4	8.91	0.06

Arley's calculations, do not seem to fit closely the experimental points. Instead the solutions obtained by MESSEL with the saddle point method show a very good agreement with the experimental data, *provided approximation* B *is used.*

Approximation A solutions are obviously inconsistent with experimental results.

From examination of Fig. 10 one notices that in passing from a cut of 0.8 MeV to one of 7 MeV, the disagreement among results of approximation A and experimental points is greatly reduced and the theoretical calculation already gives a qualitative idea of the shape of the true distribution. The disagreement is however still noticeable especially for small values of N.

* * *

We wish to thank Prof. S. FRANCHETTI who suggested this work, for helpful advice and large encourament during its execution, and Prof. MANDÒ for useful discussions.

We thank also Dr. M. C. AMERIGHI and Dr. M. G. DAGLIANA for their kind help in the calculations and Mr. G. TORTORICI for careful drawing of the graphs.

RIASSUNTO

Sono state effettuate fotografie con camera di Wilson controllata da contatori su sciami elettronici generati al livello del mare in lastre di 1, 3, 4 cm di Pb. La distribuzione angolare delle tracce elettroniche è stata confrontata con i calcoli di ROBERG e NORDHEIM e di FRANCHETTI e GIOVANNOZZI. La distribuzione degli sciami in funzione del numero di elettroni è stata utilizzata per verificare i risultati dati da JÁNOSSY e MESSEL e da ARLEY.

IL NUOVO CIMENTO Vol. III, N. 2 1° Febbraio 1956

Charge Properties of the Weak Decay Interactions of the New Particles.

R. Gatto

Istituto di Fisica dell'Università - Roma
Istituto Nazionale di Fisica Nucleare - Sezione di Roma

(ricevuto il 28 Novembre 1955)

Summary. — Relations and inequalities are given—which can be verified by experiment—between the transition probabilities of different decay modes of new particles and light hyperfragments. In particular restrictions are found for the relative probabilities of the different decay modes of charged Σ-particles, for the relative probability of the τ and of the τ'-decays, and for the different mesonic decay modes of the lightest Λ^0-nuclei. These restrictions follow from the hypothesis that the weak decay interactions transform in charge space as the component, which satisfies charge conservation, of a spherical tensor of rank $\frac{1}{2}$.

Introduction.

In the present work we give relations and inequalities between the transition probabilities of different decay modes of the new particles and of the light hyperfragments. These relations can be verified experimentally. In particular:

— If we call Y the ratio between the mean life of Σ^+ and that of Σ^-, and X the ratio between the frequency of $\Sigma^+ \to p + \pi^0$ and that of $\Sigma^+ \to n + \pi^+$, the representative point $P = (Y, X)$ in the $Y - X$ plane should lie inside the permitted region in Fig. 1.

— The ratio between the frequency of $\tau^+ \to 2\pi^0 + \pi^+$ and that of $\tau^+ \to 2\pi^+ + \pi^-$ shloud be between $\frac{1}{4}$ and 1 (for a spin 0 τ^+-meson we expect

a value closer to $\frac{1}{4}$, and for a spin 1 τ^+-meson a value closer to 1—however, final state interaction may alter this results)—which is the same result obtained by DALITZ (1) under the different assumption of charge independence.

— The transition probabilities of the different mesonic decay modes of the lightest Λ^0-nuclei should satisfy the relations and inequalities which are reported in Table I (mesonic decay modes of $^3H_\Lambda$ for which we postulate isotopic spin $I = 0$), in Table II (mesonic decay modes of $^4He_\Lambda$ and $^4H_\Lambda$ for which we postulate $I = \frac{1}{2}$) and in Table III (mesonic decay modes of $^5He_\Lambda$ for which we postulate $I = 0$).

These restrictions follow from the hypothesis that the decay interaction transforms in charge space as the component of a spherical tensor of rank $\frac{1}{2}$ which satisfies charge conservation. (2).

In section **1** we discuss the role of isotopic spin in the phenomenology of the new particles. In section **2** the discussion is limited to the transformation properties in charge space of the weak decay interactions. In section **3** we discuss the decay modes of Σ^+ and Σ^-, in section **4** the decay modes of Ξ^-, Ξ^0 and of Λ^0, and in section **5** the decay modes τ^+ and τ'^+. Section **6** contains the discussion of the decay modes of the light hyperfragments. A digression on the problem of the hyperfragments with higher Q-values can be found in footnote (11). Section **7** contains a general discussion and some particular remarks.

1. – Isotopic spin and new particles.

Present experimental evidence suggests that isotopic spin plays a relevant role in the phenomenology of the new particles. The available data are however too poor for a definitive conclusion. In the following we shall try to illustrate this point in more detail.

One might ask if the new particles (hyperons and heavy mesons) possess isotopic spin – this demands that they can be classified into charge multiplets, and that some of their interactions depend on the assigned isotopic spins. Present experimental data are consistent with this assumption. We shall list

---

(1) R. H. DALITZ: *Proc. Phys. Soc.*, **66**, 710 (1953); see also M. GELL-MANN: *Proceedings of the Pisa Conference* 1955, discussion following the relation of Prof. E. AMALDI.

(2) M. GELL-MANN: *Phys. Rev.*, **92**, 833 (1953); M. GELL-MANN and A. PAIS: *Proceedings of the Glasgow Conference* 1954; A. PAIS: *Proceedings of the Rochester Conference* 1955. A similar model has been developed gy T. NAKANO and K. NISHIJIMA: *Prog. Theor. Phys.*, **10**, 581 (1953). A more general discussion is given in a paper by R. G. SACHS (in the press). A more specific model is due to M. GOLDHABER (in the press).

here the main points with regard to this evidence—anyhow, they should form part of a well definite program in order to reach a conclusion on this question.

(i) The possibility of classifying the new particles into charge multiplets – as Gell-Mann has pointed out (2), these are « displaced charge multiplets ».

(ii) The supermultiplet structure of the levels of the light Λ^0-nuclei – this feature has been pointed out by DALITZ (3) and is now supported by growing experimental evidence.

(iii) From the assignment of isotopic spins and from the postulate of charge independence for strong interactions one can derive relations and inequalities between the transition probabilities of different fast reactions. Fast reactions which can be used for such a verification are: (*a*) reactions starting from ordinary particles (production processes); (*b*) interactions of new particles with ordinary particles (reactions following the capture of Y^- and K^- (4), interactions in flight). Present data are still too poor for detailed conclusion – there is a good evidence that some fast reactions which would contrast with $\boldsymbol{I}$ conservation in fact do not occur; however, only $I^{(3)}$ conservation is required to forbid such reactions.

Let us now discuss the decay reactions. To be definite, let us consider, for instance, the case of the Λ^0.

We first discuss in more detail the isotopic spin assignment to the Λ^0. No charged counterpart has been found so far of the Λ^0. Charged hyperons have been found but their mass is considerably larger (the mass difference between the $\Sigma^{\pm}$ and the Λ^0 is of the order of 75 MeV, a value larger than one would expect as due to charge dependent interactions; moreover there are indications (5) of the existence of a rapidly decaying neutral counterpart of the $\Sigma^{\pm}$). If we like to assign an isotopic spin to the Λ^0 its value should then preferably be $I_\Lambda = 0$ —with other assignments we would expect to find charged counterparts, which should be produced with comparable abundances, if charge independence is assumed at production (6). The proposed supermultiplet structure of the levels of the light Λ^0-nuclei is also in accordance with the assignment $I_\Lambda = 0$.

If we assume that the Λ^0 has isotopic spin zero, then it follows that both I^2

---

(3) R. H. DALITZ (in the press).

(4) T. D. LEE: *Phys. Rev.*, **99**, 337 (1955).

(5) W. B. FOWLER, R. P. SHUTT A. M. TORNDIKE and W. L. WHITTMORE: *Phys. Rev.*, **98**, 121 (1955).

(6) This question was discussed in two papers: R. GATTO: *Nuovo Cimento*, **11**, 448 (1954); **12**, 160 (1954).

and $I^{(3)}$ cannot be conserved for the observed decay mode into $p+\pi^-$. Following GELL-MANN (2) we may further assume: (i) that strong interactions are charge independent; (ii) that photons interact with other particles only by the conventional coupling with charge and currents. It follows that the Λ^0 cannot decay into a nucleon via strong or electromagnetic interactions. In that case a weak interaction which does not conserve I^2 nor $I^{(3)}$ will be responsible for the observed decay.

The result that, due to the failure of isotopic spin conservation and of conservation of the third component of isotopic spin, strong and/or electromagnetic interactions cannot produce the decay of the new particles provides a simple explanation for the observed long lifetimes. Such an explanation was the starting point of Gell-Mann's theory (2).

2. – Transformation properties of the weak decay interactions.

Let us consider a decay mode of a new particle which leads to final particles which are baryons or mesons. The initial state is a pure state of the total isotopic spin I and of the third component $I^{(3)}$, with eigenvalues I' and $I^{(3)\prime}$ — I' and $I^{(3)\prime}$ are those assigned to the particle. The final state will be a pure state of $I^{(3)}$—for it possesses a definite charge—but it will in general be a superposition of pure states of total isotopic spin, which may pertain to different eigenvalues. Let us call $I^{(3)\prime\prime}$ the eigenvalue of $I^{(3)}$ in the final state; $I^{(3)\prime\prime}$ will be different from $I^{(3)\prime}$, for it is assumed that the weak decay interaction does not conserve $I^{(3)}$.

It has been noted by GELL-MANN and PAIS (2) that the difference $\Delta I^{(3)} = I^{(3)\prime\prime} - I^{(3)\prime}$ takes only the values $\pm \frac{1}{2}$ for all observed decays. The rule $\Delta I^{(3)} = \pm \frac{1}{2}$ is assumed to be a general property of the weak decay interactions. If an isotopic spin $\frac{1}{2}$ is assigned to the Ξ^-, this rule provides a simpler explanation for the presumed absence of the decay mode of the Ξ^- into $n+\pi^-$. The Ξ^- is observed to decay into $\Lambda^0+\pi^-$—for this decay one has $\Delta I^{(3)} = -\frac{1}{2}$. However, one would expect the decay into $n+\pi^-$ to be preferred due to the larger energy release—for this decay one has $\Delta I^{(3)} = -1$. This latter decay mode can be excluded if the rule $\Delta I^{(3)} = \pm \frac{1}{2}$ is assumed.

In this paper we shall consider a very specific hypothesis for the weak decay interactions, namely that they transform as components of spherical tensors of rank $\frac{1}{2}$ for rotation in charge space. We do not give any argument in favour of such hypothesis. We would like to remark that:

(i) This hypothesis seems to be a very simple one, from a group-theoretical viewpoint, with regard to the transformation properties of the weak decay interactions, in the framework of Gell-Mann's model, therefore it will

anyhow be of interest to derive its physical consequences. All the observed decays are in accordance with the hypothesis, which offers a simpler explanation for the apparent forbiddness of the decay mode $\Xi^- \to n + \pi^-$—however, the weaker hypothesis $\Delta I^{(3)} = \pm \frac{1}{2}$ also accounts for these facts.

(ii) In the following we shall derive a number of physical consequences of the hypothesis, which must be verified by the experimental data. These physical consequences are in the form of relations or inequalities between the decay probabilities of the different decay modes—the experimental verification only requires a sufficient statistics and corrections for the possible experimental bias.

In some experiments in order to derive values for the cross-sections one has sometimes to postulate the branching ratios between different decay modes, some of which remain completely unobserved, as, for instance, the decay mode $\Lambda^0 \to n + \pi^0$. For these ratios we would suggest to assume the values derived here under the hypothesis that the weak decay interactions transform as components of tensors of order $\frac{1}{2}$.

3. – The decay of Σ^+ and of Σ^-.

We first discuss the decay modes of Σ^+ and of Σ^-. According to Gell-Mann's model Σ^-, Σ^0, Σ^+ form and isotopic spin triplet, what implies: (i) isotopic spin $I_\Sigma = 1$, and (ii), the relation, charge $= I_\Sigma^{(3)}$. The Σ^0 can however rapidly decay into $\Lambda^0 + \gamma$. Therefore we only consider the possible decay modes of Σ^+ and Σ^- into a nucleon and a pion:

(1) $$\Sigma^+ \to p + \pi^0$$

(1′) $$\Sigma^+ \to n + \pi^+$$

(2) $$\Sigma^- \to n + \pi^- .$$

In each case the initial state has isotopic spin 1, while the final state will be a superposition of isotopic spin states $\frac{1}{2}$ and $\frac{3}{2}$. Assuming the transition matrix to transform as the component of a tensor of rank $\frac{1}{2}$ (we note that perturbation theory should be valid for these weak decay interactions: it is sufficient that the required property only holds at the first non-vanishing order of perturbation theory), two independent reduced matrix elements [7] intervene, that leading to the final isotopic spin state $\frac{1}{2}$, which we call $\mathcal{A}$, and

---

[7] E. P. WIGNER: *Gruppentheorie* (Braunschweig, 1931).

that leading to the final isotopic spin state $\frac{1}{2}$, which we call $\mathcal{B}$. Three unknown real quantities are contained in the expression of the transition probabilities for (1), (1′) and (2), namely the moduli of $\mathcal{A}$ and $\mathcal{B}$ and the relative phase, which we call φ—it is not possible to determine their values without more detailed hypotheses on the transition matrix.

The transition probabilities of (1), (1′) and (2) can be related to the lifetimes of Σ^+ and Σ^- if we assume that no other disintegration channels essentially contribute to the total decay rate. This seems to be suggested by present experimental evidence. Other decay modes can be imagined to occur, however they should be rather infrequent.

We call Y the ratio

$$Y = \frac{w(\Sigma^- | \mathrm{n}\pi^-)}{w(\Sigma^+ | \mathrm{p}\pi^0) + w(\Sigma^+ | \mathrm{n}\pi^+)}$$

where $w((i|f)$ is the transition probability for $i \to f$. If we assume that the other possible modes of decay of the $\Sigma^\pm$ occur very rarely, so that they do not contribute appreciably to the total decay rate, we can take for Y the ratio between the mean life of Σ^+ and that of Σ^-

$$Y = \frac{\tau_+}{\tau_-}$$

We next introduce the ratio

$$X = \frac{w(\Sigma^+ | \mathrm{p}\pi^0)}{w(\Sigma^+ | \mathrm{n}\pi^+)}$$

between the frequency of Σ^+ decays into $\mathrm{p}+\pi^0$ and that of Σ^+ decays into $\mathrm{n}+\pi^+$.

It can be shown that the reality condition for φ leads to the inequality

$$f_Y(X) = (Y-2)^2X^2 + \\ + 2(Y^2-3Y-2)X + (Y-1)^2 \leqslant 0\,,$$

which can be regarded as a condition on X, depending on the parameter Y. For varying Y, $f_Y(X)$ generates a family of parabolae whose concavity is oriented upwardly, and the condition to be fulfilled for any Y is that

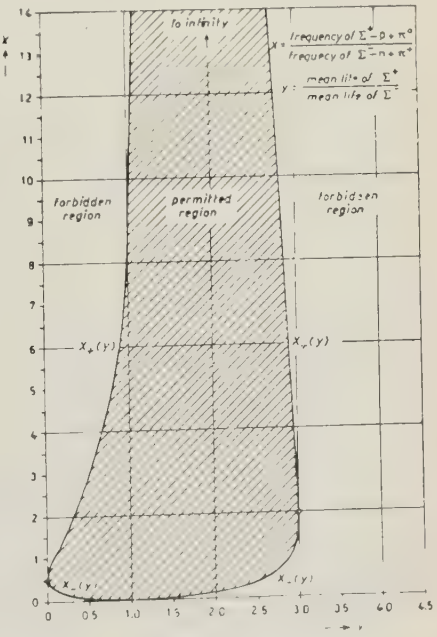

Fig. 1

$$X_-(Y) \leqslant X(Y) \leqslant X_+(Y)\,,$$

where $X_-(Y)$ and $X_+(Y)$ are the two roots of the equation $f_Y(X) = 0$. In the Y–X plane we therefore will have a forbidden region and a permitted region (see Fig. 1).

We conclude that, if the transition matrix for the decays $\Sigma \to$ nucleon + pion transforms in charge space as the component required by charge conservation of a spherical tensor of order $\frac{1}{2}$, the two measurable parameters of the decay, Y–the ratio between the mean life of Σ^+ and that of Σ^-—and X–the ratio between the frequency of decays of Σ^+ into $p+\pi^0$ and the frequency of decays into $n+\pi^+$ must be such that the point $P=(Y, X)$ in the Y–X plane lies in the permitted region of Fig. 1.

Mean life measurements for Σ particles have been carried out recently [8] and the most recent value is $3.5^{+1.5}_{-1.1}\cdot 10^{-11}$ s. To compare the present theory with experiment we need the values of the two ratios X and Y. No measurements of these numbers have been published so far—we would like to suggest such measurements to the experimentalists working in the field.

4. – Other Hyperons.

According to the Gell-Mann model Ξ^- and Ξ^0 form an isotopic spin doublet, what implies: (i) isotopic spin $I_\Xi = \frac{1}{2}$, and, (ii) the relation charge $= I_\Xi^{(3)} - \frac{1}{2}$. No evidence has been reported so far of the Ξ^0 which would decay into $\Lambda^0+\pi^0$. For the transition probabilities we are led to the relation

$$w(\Xi^-|\Lambda^0\pi^-) = 2w(\Xi^0|\Lambda^0\pi^0)\,.$$

For the Λ^0, which is assumed to form an isotopic spin singlet — (i) isotopic spin $I_\Lambda = 0$, and (ii), the relation, charge $= I_\Lambda^{(3)}$ — the transition probabilities of the two possible decay modes into a nucleon and a pion would satisfy the relation

$$w(\Lambda^0|p\pi^-) = 2w(\Lambda^0|n\pi^0)\,.$$

The relations derived here for the Ξ and Λ^0 decays are not easy to be experimentally verified—however, they should be of some use in situations where

---

[8] E. Amaldi, C. Castagnoli, G. Cortini and C. Franzinetti: *Nuovo Cimento*, **12**, 668 (1954); J. H. Davies, D. Evans, P. H. Fowler, P. R. Francois, M. W. Friedlander, R. Hiller, P. Iredale, D. Keefe, M. G. K. Menon, P. H. Perkins and C. F. Powell: *Proceedings of the Pisa Conference* (1955).

an estimate is needed of the probable number of events involving neutral particles for a given number of charged events.

5. – The decay of τ-meson.

Many modes of decay of heavy mesons have been discovered: six different K^+-decay modes ([9]) namely, τ^+, τ'^+, $K^+_{\pi 2}$, $K^+_{\mu 2}$, $K^+_{\mu 3}$, K^+_{e3}—two different K^0-decay modes—the established θ^0 and the suggested τ^0—and at least two different K^--decay modes – τ^- and $K^-_{\pi 2}$. On the other hand the recent analysis of DALITZ ([10]) suggests that the decay modes $\tau^\pm$ (and $\tau'^\pm$) and $K^\pm_{\pi 2}$ are due to different particles. One could assume the viewpoint that different particles correspond to the different decay modes. However, it seems a preferable viewpoint that a few different particles, possibly only the θ-mesons and the τ-mesons are responsible for the great variety of different decay modes. Then one is faced with a situation in which a same particle has competing disintegration channels. In such case the transition probabilities of the modes on which we are especially interested—i.e., that leading to final particles which are only pions—are not directly related to the mean life.

A possibility for comparison with experiment is, however, offered by the two possible decay modes of the τ^+ into three pions. The two possible decay modes are

$$\tau^+ \to \pi^+ + \pi^- + \pi^+ ,$$

$$\tau^+ \to \pi^+ + \pi^0 + \pi^0 .$$

Three pions with total charge unity may be in states with total isotopic spin 1, 2 and 3. According to Gell-Mann's model τ^+ and τ^0 are assumed to form one isotopic spin doublet, what implies: (i) isotopic spin $I_\tau = \frac{1}{2}$, and, (ii) the relation, charge $= I^{(3)}_\tau + \frac{1}{2}$. From the assumption that the transition matrix behaves as the component of a spherical tensor of rank $\frac{1}{2}$ for rotation in charge space, we conclude that the final state of the three escaping pions has total isotopic spin $I = 1$. Three independent states of three pions with total charge unity may be formed having isotopic spin $I = 1$. For the ratio between the frequency of decay into two neutral and one charged and the frequency of decay into three charged pions one again obtains Dalitz's condition that it must be comprised between $\frac{1}{4}$ and 1 ([1]). This result was obtained by

---

([9]) See, for instance, a recent work by D. M. RITSON, A. PEVSNER, S. C. FUNG, M. WIDGOFF, G. T. ZORN, G. GOLDHABER and S. GOLDHABER (to be published).

([10]) R. H. DALITZ: *Proceedings of the Rochester Conference* (1955).

DALITZ on the assumption of isotopic spin $I_\tau = 1$ for the τ^+-meson and on the assumption that the transition matrix for the decay behaves as a scalar for rotation in charge space (charge independence). The same result follows here from the assumption of isotopic spin $I_\tau = \frac{1}{2}$ for the τ^+-meson and from the assumption that the transition matrix for the decay behaves as the component of a spherical tensor of rank $\frac{1}{2}$ for rotation in charge space.

We note that the branching ratio is $\frac{1}{2}$ if the final state is totally symmetric in the spacial coordinates of the three pions. For a spin zero τ-meson we expect the final state to be predominantly symmetric in the spacial coordinates of the three emitted pions. The branching ratio is 1 if the final state has an orbital symmetry corresponding to the 2-dimensional representation of the permutation group S_3. For a spin 1 τ-meson we expect the final state to have predominantly an orbital symmetry corresponding to the 2-dimensional representation of the permutation group S_3.

6. – The decay of light hyperfragments.

The hypothesis that the transition matrix behaves as the component—required from charge conservation—of a spherical tensor of rank $\frac{1}{2}$ gives restrictions on the relative probabilities of the different decay modes of light hyperfragments. In the following we shall limit our discussion to the mesonic decay modes of light Λ^0-nuclei, a similar discussion can be given for the non-mesonic decay modes, and it could be extended to possible K-fragments if they exist ([11]).

([11]) W. F. FRY and M. S. SWAMI: *Phys. Rev.*, **96**, 809 (1954); A. PAIS and R. SERBER (in the press).

A case of an hyperfragment with an anomalous Q-value ($\gtrsim 340$ MeV) has been reported recently by C. CASTAGNOLI, G. CORTINI and C. FRANZINETTI (*Nuovo Cimento*, **2**, 560 (1955)). The interpretation of the hyperfragment as a possible example of K-nucleus fits the data. The hyperfragment is produced together with a K-particle which decays at rest, therefore it is highly probable that this K-particle is positive (a τ^+ or a θ^+). According to Gell-Mann's model τ^+, τ^0, θ^+ and θ^0—but not their charge conjugate—can form metastable hyperfragments (lifetimes $\sim 10^{-10}$ s) if a sufficient attractive force with nucleons exists. For the reported event, the simplest production scheme fitting the interpretation and consistent with Gell-Mann's model would be the associated production of a K^+, another K^+ or K^0 (that bound to the fragment) and a Ξ-hyperons (a Ξ^0, or a Ξ^-). The Ξ-particle, if neutral, would have escaped detection, if charged it could be one of the few tracks, emerging from the parent star, which were difficult to identify due to the large experimental errors. We would like to remark that, if similar events were found in the future, a proper identification of the possible other new particles emitted from the parent star may greatly illuminate on the nature of these suggested anomalous hyperfragments. If the interpretation as possible K-fragments were correct, then we would expect these higher Q-hyperfragments to be produced

Our discussion refers to the possible non-mesonic decay modes of the Λ^0-nucleus from its ground state directly to the final state considered.

---

either in association with a Λ^0 or a Σ, or in association with a K^- or a $\overline{K}^0$, or in association with another K^+ or K^0 and a Ξ, or by more complicated production schemes which would involve at least four new particles. Of course the most frequent case for not too high energies should be the association with a Λ^0 or a Σ.

For completness we also discuss other possible bound systems which can be metastable according to Gell-Mann's theory, provided of course that they effectively exist as bound states. With a Ξ and a nucleon we can form siglet isotopic spin states ($I = 0$) and triplet isotopic spin states ($I = 1$, $I^{(3)} = -1, 0, 1$). The lowest state with $I = 1$, $I^{(3)} = -1$ (formed by $\Xi^- + n$) and the lowest state with $I = 1$, $I^{(3)} = +1$ (formed by $\Xi^0 + p$), if bound, will correspond to metastable hyperfragments which presumably would disintegrate according to

$$(\Xi^-,\ n) \to \Lambda^0 + \pi^- + n$$

$$(\Xi^0,\ p) \to \Lambda^0 + \pi^0 + p \qquad \text{or} \qquad \to \Lambda^0 + \pi^+ + n$$

with a $Q = 63 \pm 4$ MeV $- \varepsilon$, where ε is the binding energy. The force between a Ξ and a nucleon could well be mediated (at least in part) by π-mesons and therefore have a range of the order of $1/m_\pi$. Similarly, with a Ξ and two nucleons we can form states with $I = \frac{1}{2}$ and states with $I = \frac{3}{2}$. The lowest state with $I = \frac{3}{2}$, $I^{(3)} = -\frac{3}{2}$ ($\Xi^- + n + n$), and the lowest state with $I = \frac{3}{2}$, $I^{(3)} = +\frac{3}{2}$ ($\Xi^0 + p + p$), if bound, will correspond to metastable hyperfragments which presumably disintegrate into a Λ^0, a pion, and a nucleon. With more nucleons we have again a corresponding situation. It must, however, be noted that the isotopic spin of such possible metastable systems is alway sthe largest permitted (we know from ordinary nuclear physics that the lowest lying state usually has isotopic spin 0 or $\frac{1}{2}$). No examples of such systems has never been reported. With a Σ and a nucleon we can form states with $I = \frac{1}{2}$ and states with $I = \frac{3}{2}$. The lowest state with $I = \frac{3}{2}$, $I^{(3)} = -\frac{3}{2}(\Sigma^- + n)$ and the lowest with $I = \frac{3}{2}$ $I^{(3)} = \frac{3}{2}$ $(I^+ + p)$, if bound, will behave as metastable hyperfragments which presumably disintegrate according to

$$(\Sigma^-,\ n) \to \pi^- + n + n$$

$$(\Sigma^+,\ p) \to \pi^+ + p + n \qquad \text{or} \qquad \to \pi^0 + p + p\,,$$

with a $Q = 108 \pm 4$ MeV $- \varepsilon$, ε being the binding energy. The binding force may have a range of $1/m_\pi$, differently to the Λ^0-nucleon force which should have a smaller range and therefore be less efficient. Similarly with a Σ and two nucleons we can have $I = 0$, 1 and 2. Only the lowest $I = 2$, $I^{(3)} = -2$ state ($\Sigma^- + n + n$) and the lowest $I = 2$, $I^{(3)} = 2$ state ($\Sigma^+ + p + p$), if bound, can form metastable hyperfragments which presumably disintegrate into a pion and three nucleons—and a corresponding situation again occurs with more nucleons. Again we note that the isotopic spins of the possible metastable systems are the largest permitted -what makes one rather dubious of their existence as bound systems. We remark that bound systems as (Σ^-, n) and (Σ^+, p) would be easily observable, but there are no examples so far. Finally we may add that systems formed by nucleons and two bound Λ^0's could also be metastable (see M. W. Friedlander, Y. Fujimoto, D. Keefe and M. G. K. Menon: *Nuovo Cimento*, **1**, 90 (1955)): their production seems rather improbable, however one can imagine that a Ξ is captured and it produces two Λ^0 which remain bound inside the nucleus. No examples have been reported so far.

No direct experimental evidence exists as to the values of the isotopic spin of the ground states of the Λ^0-nuclei. In a recent paper DALITZ ([3]) has called attention to the possible supermultiplet structure of the levels of the Λ^0-nuclei and has given specific predictions without invoking particular assumptions.

The present discussion is based on a specific assignment of isotopic spin values to the ground states of the lightest Λ^0-nuclei. Λ^0-nuclei with $B = 2$ (we call B the number of baryons of the Λ^0-nucleus—we think of the Λ^0-nucleus as formed by A nucleons and a Λ^0, so that $B = A + 1$) presumably do not exist, and will not be considered here. The levels of the Λ^0-nuclei with $B = 3$ ($A = 2$) may have $I = 0$, or 1. We assume that the lowest state has $I = 0$, to be identified with the ground state of the observed ${}^3H_\Lambda$. It seems improbable that the lowest state with $I = 1$ is also bound, in this case ${}^3n_\Lambda$ would exist an possibly also ${}^3He_\Lambda$, but no examples have been reported. The levels of the Λ^0-nuclei with $B = 4$ ($A = 3$) may have $I = \frac{1}{2}$ or $\frac{3}{2}$. We assume that the lowest state has $I = \frac{1}{2}$ and its two substates are the ground states of the observed ${}^4He_\Lambda$ and ${}^4H_\Lambda$. If the lowest $I = \frac{3}{2}$ state is bound—a very improbable case—${}^4n_\Lambda$ and possibly also ${}^4Li_\Lambda$ would exist, but no examples are known. The levels of the Λ^0-nuclei with $B = 5$ ($A = 4$) may have $I = 0, 1, 2$. We assume that the lowest state has $I = 0$ and it is the ground state of ${}^5He_\Lambda$. The first $I = 1$ state is expected to lie lower than the $I = 2$ states, but it could be unbound—if it is a bound state, then ${}^5H_\Lambda$ and possibly also ${}^5Li_\Lambda$ would exist, but no examples have been reported.

The relations and inequalities among the various possible mesonic decay modes of the lightest hyperfragments which follow from the isotopic spin assignment just discussed and from the assumed hypothesis on the transition matrix are reported in Tables I, II and III. The relations and inequalities

TABLE I. – *Mesonic decay modes of* ${}^3H_\Lambda$ ($B=3$, *isotopic spin* $I=0$).

${}^3H_\Lambda \to \pi^+ nnn$ $\to \pi^0 pnn$ $\to \pi^- ppn$	
${}^3H_\Lambda \to \pi^0 nd$ $\to \pi^- pd$	$w({}^3H_\Lambda \mid \pi^- pd) = 2w({}^3H_\Lambda \mid \pi^0 nd)$
${}^3H_\Lambda \to \pi^0 {}^3H$ $\to \pi^- {}^3He$	$w({}^3H_\Lambda \mid \pi^- {}^3He) = 2w({}^3H_\Lambda \mid \pi^0 {}^3H)$

reported in the tables refer to the total transition probabilities (and not to the differential transition probabilities).

TABLE II. – *Mesonic decay modes of* $^4He_\Lambda$ *and* $^4H_\Lambda$ ($B=4$, *isotopic spin* $I=\frac{1}{2}$).

$^4He_\Lambda \to \pi^+ pnnn$ $\to \pi^0 ppnn$ $\to \pi^- pppn$	
$^4He_\Lambda \to \pi^+ nnd$ $\to \pi^0 pnd$ $\to \pi^- ppd$	$[w(^4He_\Lambda \mid \pi^+ nnd) - w(^4He_\Lambda \mid \pi^- ppd)]^2 \leqslant$ $\leqslant 8w(^4He_\Lambda \mid \pi^0 pnd)[w(^4He_\Lambda \mid \pi^+ nnd) + w(^4He_\Lambda \mid \pi^- ppd)]$
$^4He_\Lambda \to \pi^0 dd$	
$^4He_\Lambda \to \pi^+ n^3H$ $\to \pi^0 p^3H$ $\to \pi^0 n^3He$ $\to \pi^- p^3He$	$[w(^4He_\Lambda \mid \pi^+ n^3H) - w(^4He_\Lambda \mid \pi^- p^3He)]^2 \leqslant$ $\leqslant 2[w(^4He_\Lambda \mid \pi^+ n^3H) + w(^4He_\Lambda \mid \pi^- p^3He)] \cdot$ $\cdot [w(^4He_\Lambda \mid \pi^0 p^3H) + w(^4He_\Lambda \mid \pi^0 n^3He)]$ $[w(^4He_\Lambda \mid \pi^0 p^3H) - w(^4He_\Lambda \mid \pi^0 n^3He)] \leqslant$ $\leqslant 2[w(^4He_\Lambda \mid \pi^+ n^3H) + w(^4He_\Lambda \mid \pi^- p^3He)] \cdot$ $\cdot [w(^4He^\Lambda \mid \pi^0 p^3H) + w(^4He_\Lambda \mid \pi^0 n^3He)]$
$^4He_\Lambda \to \pi^0\ ^4He$	
$^4H_\Lambda \to \pi^+ nnnn$ $\to \pi^0 pnnn$ $\to \pi^+ ppnn$	
$^4H_\Lambda \to \pi^0 nnd$ $\to \pi^- pnd$	$w(^4H_\Lambda \mid \pi^- pnd) \geqslant w(^4H_\Lambda \mid \pi^0 nnd)$
$^4H_\Lambda \to \pi^- dd$	
$^4H_\Lambda \to \pi^0 n^3H$ $\to \pi^- p^3H$ $\to \pi^- n^3He$	$[w(^4H_\Lambda \mid \pi^- p^3H) + w(^4H_\Lambda \mid \pi^- n^3He)] \geqslant w(^4H_\Lambda \mid \pi^0 n^3H)$ $[2w(^4H_\Lambda \mid \pi^0 n^3H)]^2 + [w(^4H_\Lambda \mid \pi^- p^3H)]^2 + [w(^4H_\Lambda \mid \pi^- n^3He)]^2 \leqslant$ $\leqslant \frac{1}{2}[2w(^4H_\Lambda \mid \pi^0 n^3H) + w(^4H_\Lambda \mid \pi^- p^3H) + w(^4H_\Lambda \mid \pi^- n^3He)]^2$
$^4H_\Lambda \to \pi^-\ ^4He$	

Some cases, for which the number of independent matrix elements which intervene in the expression of the transition probabilities is very large are not discussed—in this case no stringent limitations are expected for the transition probabilities. We note that one would roughly expect the most probable disintegration modes to be those associated with the largest energy release. The energy release is larger when some of the final particles are emitted as bound and in fact in this cases a smaller number of independent matrix elements intervene.

TABLE III. – *Mesonic decay modes of* $^5He_\Lambda$ ($B=5$, *isotopic spin* $I=0$).

$^5He_\Lambda \to \pi^+ pnnnn$ $\to \pi^0 ppnnn$ $\to \pi^- pppnn$	
$^5He_\Lambda \to \pi^+ nnnd$ $\to \pi^0 pnnd$ $\to \pi^- ppnd$	
$^5He_\Lambda \to \pi^0 ndd$ $\to \pi^- pdd$	$w(^5He_\Lambda \mid \pi^- pdd) = 2w(^5He_\Lambda \mid \pi^0 ndd)$
$^5He_\Lambda \to \pi^+ nn\,^3H$ $\to \pi^0 pn\,^3H$ $\to \pi^- pp\,^3H$ $\to \pi^0 nn\,^3He$ $\to \pi^- pn\,^3He$	$w(^5He_\Lambda \mid \pi^- pn\,^3He) \geqslant w(^5He_\Lambda \mid \pi^0 nn\,^3He)$ $w(^5He_\Lambda \mid \pi^+ nn\,^3H) + w(^5He_\Lambda \mid \pi^0 nn\,^3He) \geqslant \frac{1}{3} w(^5He_\Lambda \mid \pi^- pp\,^3H)$ $[w(^5He_\Lambda \mid \pi^+ nn\,^3H)]^2 + [w(^5He_\Lambda \mid \pi^- pp\,^3H)]^2 + [2w(^5He_\Lambda \mid \pi^0 nn\,^3He)]^2 \leqslant$ $\leqslant \frac{1}{2}[w(^5He_\Lambda \mid \pi^+ nn\,^3H) + w(^5He\Lambda \mid \pi^- pp\,^3H) + 2w(^5He\Lambda \mid \pi^0 nn\,^3He)]^2$ $w(^5He\Lambda \mid \pi^+ nn\,^3H) - 2w(^5He_\Lambda \mid \pi^0 pn\,^3H) + w(^5He\Lambda \mid \pi^- pp\,^3H) -$ $- 2w(^5He\Lambda \mid \pi^0 nn\,^3He) + w(^5He\Lambda \mid \pi^- pn\,^3He) = 0$
$^5He_\Lambda \to \pi^0 d\,^3H$ $\to \pi^- d\,^3He$	$w(^5He\Lambda \mid \pi^- d\,^3He) = 2w(^5He\Lambda \mid \pi^0 d\,^3H)$
$^5He_\Lambda \to \pi^0 n\,^4He$ $\to \pi^- p\,^4He$	$w(^5He\Lambda \mid \pi^- p\,^4He) = 2w(^5He\Lambda \mid \pi^0 n\,^4He)$

Other effects as coulomb forces and neutron proton mass differences may alter in some cases the relations and inequalities reported in the tables. These effects will not be discussed here, but they are expected to be small but for exceptional cases.

7. – Final Remarks and Discussion.

We have derived relations and inequalities between the transition probabilities of different decay modes of new particles and light hyperfragments, which follow from the hypothesis that the decay matrix transforms in charge space as a component of a spherical tensor of rank $\frac{1}{2}$. We have remarked that no theoretical arguments can be given in favour of this hypothesis. If this hypothesis is assumed, the selection rule $\Delta S = \pm 1$ (S = strangeness), which seems to be satisfied by the weak decay interactions, directly follows as a less restrictive consequence. (We may perhaps remark that the rule

$\Delta S = \pm 1$ would not hold if the τ^+-meson were assigned strangeness $+2$). In the case of strong interactions the rule $\Delta S = 0$ is presumably linked to the rotation invariance of the interaction hamiltonian in charge space. In the case of electromagnetic interactions the same rule, $\Delta S = 0$, is presumably linked to the invariance of the electromagnetic interaction under rotations about the third axis of charge space. In the case of weak interactions, is the rule $\Delta S = \pm 1$ linked to a peculiar transformation property of the decay matrix under the complete rotation group in charge space? The experimental verification of the restrictions found in the present work will provide a direct answer to the question.

Some work has been recently devoted to understand all the weak interactions on the assumption of universal forms: universal Fermi interaction ([12,13]) and possibly also an universal boson-fermion interaction ([14]). From such a viewpoint one has not general arguments to exclude a mixture of terms in the decay matrix which transform as components of tensors of rank $\frac{3}{2}$.

Some preliminary indications have been reported suggesting that the lifetime of Σ^- can be longer than that of the Σ^+ ([15]). As Fig. 1 shows, the hypothesis that the transition matrix transforms as the component of a tensor of rank $\frac{1}{2}$ imposes rather stringent conditions in this case—if these conditions are not satisfied, this would imply an admixture of terms transforming as components of higher order tensors. If we take the transition matrix to transform as the component of a spherical tensor of rank $\frac{3}{2}$ we find that the representative point $P = (Y, X)$ in the Y-X plane again lies in the permitted region of Fig. 1, provided we now take for Y the ratio between the Σ^+- and the Σ^--lifetime multiplied by 4 while X retains its old definition. However, for a superposition with unknown coefficients of terms transforming as components of $\frac{1}{2}$- and $\frac{3}{2}$-rank tensors no effective limitation subsists.

For the Ξ hyperons a pure $\frac{1}{2}$-term has given a decay rate of Ξ^- double than that of Ξ^0 with a pure $\frac{3}{2}$-term the decay rate of Ξ^- would be one half that of Ξ^0. For the Λ^0 a pure $\frac{1}{2}$-term has given a decay rate into a proton double than that into a neutron with a pure $\frac{3}{2}$-term the decay rate into a proton would be one half than that into a neutron. For the τ^+ a pure $\frac{1}{2}$-term has given the restriction that the ratio between the frequency of τ'-decays and that of τ-decays should lie between $\frac{1}{4}$ and 1. If the τ has spin zero the ratio should be nearly $\frac{1}{4}$. This result is not changed if an admixture of terms

---

([12]) M. Gell-Mann: *Proceedings of the Pisa Congress*, 1955.

([13]) N. Dallaporta: *Nuovo Cimento*, **1**, 962 (1955).

([14]) S. Ogawa, H. Okonoji and S. Oneda: *Prog. Theor. Phys.*, **11**, 330 (1954); K. Iwaka, S. Ogawa, O. Okonoji, B. Sakita and S. Oneda: *Progr. Theor. Phys.*, **13**, 19 (1955). See also R. Gatto: *Nuovo Cimento*, **1**, 372 (1955).

([15]) W. F. Fry, J. Schneps, G. A. Snow and M. S. Swami: preprint.

transforming as components of $\frac{3}{2}$-rank tensors is present. In fact, if the final state is predominantly symmetric in the space coordinates, the isotopic spin can only have values 1 and 3, and only 1 is permitted. If the τ has spin 1 the ratio should be nearly 1. This result would hovewer be lost if an admixture of $\frac{3}{2}$-terms were present—assuming an orbital symmetry corresponding to the 2-dimensional representation of the permutation group, the isotopic spin can have values 1 and 2, and both would be permitted.

7·1. *The problem of the lifetime of the charged* θ*-mesons.* – The hypothesis that the transition matrix transforms in charge space as component of a spherical tensor of rank $\frac{1}{2}$ gives restrictions on the relative probabilities of the decay modes of the θ-mesons into two pions.

We limit our discussion to the θ^+ and θ^0; corresponding results hold for the charge-conjugates θ^- and $\bar{\theta}^0$. According to GELL-MANN and PAIS ([16]), the θ^0 is a mixture of θ_1^0 and a θ_2^0 exhibiting two different lifetimes, but the lifetime of the θ_2^0 is expected to be much longer. Rigorously, the transition probabilities considered here should be referred to the average decay of the θ_1^0 and of the θ_2^0

We distinguish two cases:

(i) θ^+ and θ^0 have even spin (and therefore also even parity). In this case it follows from the hypothesis considered for the transition matrix

$$w(\theta^+|+0) = 0\,, \qquad w(\theta^0|00) = \tfrac{1}{2}\, w(\theta^0|+-)\,.$$

(ii) θ^+ and θ^0 have odd spin (and therefore also odd parity)

$$w(\theta^+|+0) = 2w(\theta^0|+-)\,, \qquad w(\theta^0|00) = 0$$

(the latter result holds in any case if the θ^0 has odd spin).

These transition probabilities are the total transition probabilities for decay into the final state considered. The θ-mesons presumably have also other competing disintegration channels. Therefore the transition probabilities for decay into two pions are not directly related to the mean lives.

Recent experimental results ([17]) give a relative frequency of $15 \approx 30\,\%$ for the decay mode $\chi \to \pi + \pi^0$ of charged K-mesons. For the following consideration it will be assumed that the decay modes of the θ-mesons into two pions have a significant frequency, not much smaller than the frequencies of possible other dominant decay modes.

Examples of well-identified θ^+-mesons which live a time $\sim 10^{-8}$ have been

([16]) M. GELL-MANN and A. PAIS: *Phys. Rev.*, **97**, 1387 (1955).
([17]) G-STACK COLLABORATION: *Nuovo Cimento*, **2**, 1063 (1955).

reported ([18]). The mean life of neutral θ-mesons on the other hand is known to be $\sim 10^{-10}$ s. From the preceding results, which follow from the hypothesis on the transition matrix which is under examination, we see that:

(i) in the case of even spin for the θ-mesons the two-pion decay of the θ^+ is forbidden. If the experiments are to be interpreted as indicating a lifetime of θ^+ about 100 times longer than that of θ^0, this result is in the right direction qualitatively — although — quantitatively, it could be very difficult to account for the observed decay of the θ^+ into two pions (a smaller component transforming in charge space as a spherical tensor of order $\frac{3}{2}$ should be invoked).

(ii) In the case of odd spin for the θ-mesons the total probabilities for decay into two pions of the θ^+ and of the θ^0 are of comparable magnitude and therefore it would be very difficult to account for a lifetime of the θ^+ about 100 times longer than that of θ^0.

Quite different experimental results for the lifetime of the θ^+ have been obtained by ARNOLD, BALLAM and REYNOLDS ([19]). Their results indicate a lifetime of the charged θ-mesons of the order of $3 \div 8.5 \cdot 10^{-10}$ s, not very different from that of the θ^0.

From the preceding results on the transition probabilities, under the hypothesis on the transition matrix which we are considering, we see that one could account for this experimental result in the case of odd spin for the θ-mesons — we have already remarked that presumably other decay channels intervene to determine the ratio of the two lifetimes.

The apparent experimental paradox of a θ^+ which exhibits two different lifetimes would be resolved by assuming that it has a natural lifetime of the order of $10^{-9} \div 10^{-10}$ s (as the experiment of ARNOLD, BALLAM and REYNOLDS indicates) but it also sometimes results from the decay of another heavy meson (presumably the τ-meson) having a longer lifetime, of the order of 10^{-8} s ([20]).

Assuming that the parent particle is the τ^+-meson, supposed to have a slightly larger mass than the θ^+, one has to consider two cases:

(i) The τ has the same strangeness as the θ (which is $S = +1$, from the existence of the θ^0). In this case, if they both have spin zero, the transition occurs via emission of two gammas and it is expected to occur in a long lifetime unless the two masses are very different. If at least one of the two has spin different from zero one should invoke a very small mass difference to avoid

---

([18]) See for instance: G. GOLDHABER, E. HELMY and J. E. LANNUTTI: *Proceedings of the Pisa Conference* (1955).

([19]) W. A. ARNOLD, J. BALLAM and G. I. REYNOLDS: *Phys. Rev.*, **100**, 295 (1955).

([20]) A similar model has been proposed by LEE and OREAR (private communication by Prof. N. KROLL).

rapid decay via emission of a single gamma (and/or a large difference in the values of the two spins).

(ii) The τ has not the same strangeness as the θ—to avoid introducing doubly charged particles it must have strangeness $+2$. In this case the decay occurs via weak interactions. However from this assignment of strangeness it would follow: the non-existence of the τ^0, the non-validity of the rule $\Delta S = \pm 1$ for the decay of the τ^+ into three pions, the τ would never be produced in association with a single Λ^0 or Σ-hyperon (if the only heavy mesons are the τ and the θ the heavy mesons produced in association with a single Λ^0 or Σ should always have a lifetime $\sim 10^{-9} \div 10^{-10}$).

From the preceding discussion we may conclude as follows. To reconcile the hypothesis on the decay matrix which we are considering with the experimental data:

— if the « natural » lifetime of the θ^+ is much longer (about 100 times) than that of the θ^0, one would assume even spin for the θ—in which case only a weaker component transforming as a $\frac{3}{2}$-rank tensor should produce the 2π-decay of the θ^+.

— if the « natural » lifetime of the θ^+ is comparable to that of the θ^0 one would assume that the θ has odd spin and that the τ, with strangeness $+1$, can decay into a θ and a gamma (very slowly, due, for instance, to a very small mass difference).

We would like to add that if the transition matrix transforms as a mixture with unknown coefficients of $\frac{1}{2}$- and $\frac{3}{2}$-terms:

1) in the case of even spin one still finds a limitation for the partial lifetimes for decay into two pions

$$\tau_{\theta^+} \geqslant \tfrac{2}{3}\, \tau_{\theta^0} \ ;$$

2) in the case of odd spin no limitation subsists.

7·2. *General restrictions upon the branching ratios.* – G. Takeda [21] has recently derived restrictions upon the branching ratios of the different decay modes of Σ^+, Λ^0 and θ^0 which follow from the invariance properties of the transition matrix. For completeness, we give here a simplified derivation of Takeda's results. To be definite, let us consider the decay of the Λ^0. We assume the existence of a unitary and symmetric transition matrix [22] which connects the three independent channels: channel 1 describing the Λ^0, channel 2 describing the final particles in the $I = \frac{3}{2}$ state, channel 3 describing the final

[21] G. Tadeka: *Phys. Rev.* (in the press).

[22] See: E. Fermi: *Suppl. Nuovo Cimento*, **2**, 60 (1955).

particles in the $I = \frac{1}{2}$ state. If the weak decay interaction is turned off the transition matrix reduces to diagonal form and its elements are: $S_{11} = 1$, $S_{22} = \exp[2i\alpha_3]$, $S_{33} = \exp[2i\alpha_1]$, where α_3 and α_1 are the pion-nucleon phase shifts. When the weak decay interaction is turned on, non-diagonal matrix elements appear, and it readily follows from the assumed unitarity and symmetry ([22]) that, in first approximation, our decay matrix elements are: $S_{12} = i\varrho_3 \exp[i\alpha_3]$, $S_{13} = i\varrho_1 \exp[i\alpha_1]$, where ϱ_3 and ϱ_1 are real numbers. It follows that the amplitude for the physical state (n, o) is given by $(\sqrt{2}z \exp[i\alpha_3] - \exp[i\alpha_1])$ and that for (p, o) by $(z \exp[i\alpha_3] + \sqrt{2} \exp[i\alpha_1])$, where $z = \varrho_3/\varrho_1$ — which is Takeda's results. As shown by Takeda these restrictions for the decay amplitudes do not limit very strongly the branching ratios — although they are of interest due to their generality.

* * *

I would like to express my gratitude to Prof. B. Ferretti for the interest he has shown in the present work.

I would like to thank Prof. M. Goldhaber and Prof. N. Kroll for discussions and fruitful conversations.

Particular thanks are due to Prof. M. Gell-Mann, who has contributed helpful remarks and suggestions.

RIASSUNTO

Vengono date delle relazioni e delle disuguaglianze tra le probabilità di transizione di differenti modi di decadimento di nuove particelle e di iperframmenti leggeri, che sono suscettibili di verifica sperimentale. In particolare: vengono trovate delle limitazioni per le probabilità relative dei diversi modi di decadimento dei Σ carichi, per le probabilità relative dei decadimenti τ e τ' e per i differenti modi di decadimento dei nuclei Λ^0 più leggeri. Queste limitazioni seguono dall'ipotesi che l'interazione debole di decadimento si trasformi come la componente, richiesta dalla conservazione della carica, di un tensore sferico di ordine $\frac{1}{2}$.

A Magnetic Differential Probe. Its Employment for the Determination of the Static Median Magnetic Surface in the Gap of a Synchrotron.

G. Diambrini Palazzi

Istituto Nazionale di Fisica Nucleare, Sezione Acceleratore - Roma

(ricevuto il 5 Dicembre 1955)

Summary. — A differential magnetic probe, developed for determining the median magnetic surface of the static field in a weak-focusing synchrotron gap, is described. The probe consists of two thin ferromagnetic wires subjected to equal and opposite alternating magnetic fields at 1000 Hz. The method of measurement consists in determining the position of the probe for which the components of the magnetic field along the two wires (parallel to the radius of the synchrotron and lying in a vertical plane) are equal and opposite. The arrangement described gives the localisation of the median magnetic surface within $\pm$ 1 mm in static fields between 20 and 500 gauss. The possibility is also mentioned of measuring the field index n by means of this probe with an accuracy of 5% in fields not exceeding 500 gauss. Finally the technique used for preparing the ferromagnetic wires is explained in some detail.

1. – Introduction.

Wires and strips of very permeable material are at present used for special measurements related to the magnetic field in the synchrotron gap [1]. In many cases, however, their real possibilities of employment present several doubts, and few detailed papers on this argument have so far been published. We think, therefore, that a detailed exposition of a new employment of ferromagnetic wires for the determination of the magnetic median surface (m.m.s.),

[1] J. M. Kelly: *Rev. Sci. Instr.*, **22**, 256 (1951); S. Giordano, G. K. Green and E. J. Rogers: *Rev. Sci. Instr.*, **24**, 848 (1953).

in a static field between 20 and 500 gauss in the synchrotron gap to an accuracy of ± 1 mm, may be useful. The differential probe constructed for this purpose is also employable for the determination of the field lines curvatures, i.e. for the measurements of the field index n (see 2·2) to a predictable accuracy of about 5%. The latter kind of measurement will not be taken into consideration in this paper. In the following we shall also explain the preparation technique of the ferromagnetic wires (see note II) and of the probe (see 3·2) as in our opinion it may be useful for some other kinds of measurement.

2. – Basic Principles of the Method and its Limitations.

2·1. – We shall now explain qualitatively the working principle of the device. Let two thin ferromagnetic wires of high permeability, supposed equal, parallel and straight, be subjected to an alternating sinusoidal magnetic field

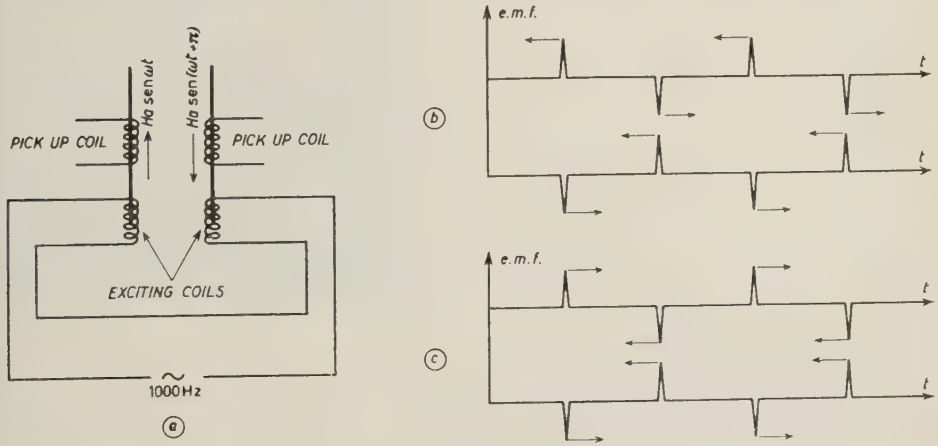

Fig. 1.

whose frequency is $r \cong 1000$ cycles and whose amplitude is such as to saturate the ferromagnetic material. Let the field always be equal and opposite in the two wires, and each of them be surrounded in its central region by a pick-up coil (Fig. 1*a*). Then a series of pulses of induced e.m.f., alternating in sign, may be obtained from each of the two coils. If we series-connect the two coils in the same direction, the picked-up e.m.f. will be zero (or a minimum), since we shall have, altogether, pairs of like pulses, opposed and simultaneous (or very nearly). Now, if we subject the wires thus excited to a steady magnetic field, the pulses will shift in time in the direction indicated by the arrows in Fig. 1*b*. The leading of a pulse of one coil will correspond to a delay of the corresponding pulse of the other one. Thus a pulse-difference (Fig. 2) whose

peak-to-peak amplitude is proportional, within certain limits, to the applied, steady magnetic field will arise at the output of the two series-connected coils. If, on the other hand, we subject one wire to a steady field, equal and opposite to that acting on the other, we shall again have a e.m.f. zero (or a minimum) at the output of the two series-connected coils and in the same direction, since the pulses will now be shifted as in Fig. 1*c*, and a pulse delay coming from one coil will correspond to an equal delay of the corresponding pulse from the other one; a similar situation will occur for the leadings.

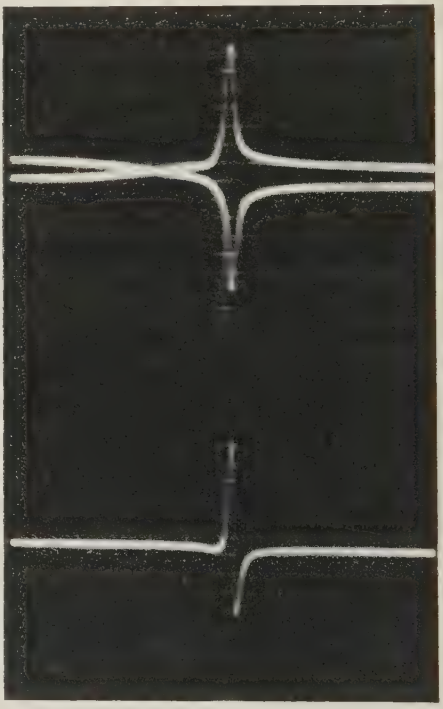

Fig. 2.

What we have said is valid in the case where the steady field is less than the alternating field-amplitude.

We thus conclude that this device may be a very sensitive detector of the function « algebraic sum » of the components along the wires of a magnetic field. If the alternating magnetic field had the same sense in the two wires at every instant the device would reveal variations of the function « algebraic difference » of the components.

As detector of the function « algebraic sum », it is employable in the determination of the m.m.s. in the gap of a magnet of sufficient size, particularly in the gap of a weak-focusing synchrotron. In fact the m.m.s. is defined as the locus of the points in which the radial component B_r of the field is zero.

In the case of a synchrotron, we may indicate the radial and vertical coordinates with origins at the centre of curvature of the circular sector of the synchrotron and on the m.m.s. respectively, by r and z. The latter represents the surface of symmetry for the field-lines; in this way one will have inside the gap:

$$B_r(r, z) = -B_r(r, -z) , \qquad B_r(r, 0) = 0 .$$

Now, if we put the wires parallel to each other, parallel to the vertical plane and to the radial direction, and displace them vertically so that this parallelism is maintained, the device will inform us when:

$$B_{1r}(r, z_1) + B_{2r}(r, z_2) = 0 ,$$

where z_1, z_2, B_{1r}, B_{2r} are coordinates of the centres of the two wires and the respective components.

Then also: $z_1 = -z_2$ and the altitude of the m.m.s. will be that of the midpoint between the centres of the two wires.

We propose to determine the position of the m.m.s. in the gap of a weak-focusing synchrotron (of radius $R = 360$ cm and with poles shaped for a field index $n = 0.6$) within ± 1 mm.

The characteristics of this synchrotron are about the same as those described in ref. (2), week-focusing solution.

2·2. – We want to show that the sensitivity of the method is broadly sufficient for this purpose and to explain the requirements which must be satisfied. Following the current symbolism in accelerator literature, we shall define, inside the gap: $n \simeq (R/B_z)\,\mathrm{d}B_z/\mathrm{d}R$, where R is the radius of the synchrotron and B_z is the z component of the field.

Since the azimuthal component of curl B is zero, and therefore:

$$\frac{\partial B_z}{\partial R} = \frac{\partial B_r}{\partial z}$$

we obtain immediately:

$$B_r = -\int_0^z \frac{n}{R} B_z \,\mathrm{d}z \cong -\frac{nB_z}{R} \cdot z \,,$$

B_r being the radial component of the field and the origin of the z-axis lying on the m.m.s.

Admitting a perfect mechanical precision in the alignment and movement of the device, to obtain a precision of Δz in the vertical localization of the m.m.s., a minimum detectable variation (of the algebraic sum of the field components) along the wires given by

$$\Delta B = \frac{2nB_z}{R} \Delta z = \frac{B_z}{3\,000} \Delta z \,,$$

is necessary, where Δz is the vertical displacement of the probe. For example, to obtain $\Delta z = 1$ mm, we may have $\Delta B = 0.03$ gauss if $B_r = 100$ gauss, etc.

Now we shall show that the device satisfies this requirement.

A convincing estimate may be made considering the concrete case of mu-metal wires, Φ 0.1 mm, length 4 cm, supplied with a 10^3 Hz alternating field of amplitude $B_a = 5$ gauss, surrounded for a length of 5 mm in their central

(2) G. Salvini: *Suppl. Nuovo Cimento*, **2**, 442 (1955).

zone by a small coil of 400 turns of wire, Φ 0.05 mm. Under these conditions the pulse obtained is of the order of 0.10 V.

Taking $\tau = 10$ μs as « base time » for this pulse, one will have the difference pulse shifting from zero (or a minimum) to 0.10 V, when the algebraic sum of the components along the two wires becomes $\Delta B \cong (\tau/2) B_a \omega \cong 0.15$ gauss (note I), which corresponds to a sensitivity for the detector of the order of 1 V/gauss. It is obvious that by using amplifiers and adequate differential electronic voltmeters, threshold sensitivities of 10^{-4} or 10^{-5} gauss may be reached, values like those obtained by us experimentally.

Considering an ideal electronic chain, the limit appears to be of the order of 10^{-7} gauss ([4]) and it is given by the discontinuity in the changes of induction caused by the rotation of ferromagnetic domains. Therefore the sensitivity of our device may be higher than is strictly necessary for our purpose. In fact, an oscilloscope check of the form of the difference-pulse may be sufficient.

2·3. – The determination of the m.m.s. within $\pm$ 1 mm is hindered, however, by the fact that, in addition to the component B_r, the ferromagnetic wires are also submitted to a perpendicular field B_z, so that $B_r/B_z \cong 1/3\,000$. This requires the following conditions to be satisfied:

a) The wires must be straight.
b) The wires must have a sufficiently large length diameter ratio.
c) The wires must form with the median geometrical plane (m.g.p.), (and with each other) an angle not greater than $2.5 \cdot 10^{-4}$ rad.

The condition indicated in *a*) is obvious. If the wire presents a finite radius of curvature in some zones, the component along the axis of the wire will not be homogeneous and in some points its value will be too high. The pulses to 1000 Hz will be « destroyed » to values lower of B_z.

For the condition indicated in *b*) we bear in mind that an infinitely long ferromagnetic wire of permeability μ, submitted to a perpendicular external field B_e, will have ([3]), internally, the induction:

$$B_i = \frac{2\mu}{\mu + \mu_0} B_e ,$$

for which the induction inside the wire is only twice that outside, even for an infinite permeability. A very long mumetal wire submitted to a field of $3 \div 4 \cdot 10^3$ gauss, normal to its axis, is already practically saturated transversally. Its permeability in the axial direction is practically zero.

([3]) E. WEBER: *Electromagnetic Fields* (New York) p. 242.
([4]) P. M. S. BLACKETT: *Phil. Trans. Roy. Soc. London*, A **245**, 309 (1952).

The pulses induced by axial excitation are practically « destroyed ». Our experimental results relating to the mumetal wires, length 4 cm, Φ 0.1 mm, show that this destruction occurs at about 500 gauss, even with wires carefully prepared. Using wires of these dimensions the m.m.s. cannot be determined above 500 gauss.

For the requirement indicated in *b*) it may easily be seen that if the wires, supposed parallel to each other, form an angle θ with the median geometrical plane (m.g.p.), the error made in the localization of the m.m.s. is given by:

$$\Delta z = \frac{R}{n} \operatorname{tg} \theta \, .$$

Since in our case $R/n \cong 6000$ mm it is therefore necessary, to obtain $\Delta z = \pm 1$ mm, that the alignment with the m.g.p. be maintained within an angle $\theta = \pm 2.5 \cdot 10^{-4}$ rad.

In the case of one wire aligned with the m.g.p. and the other forming an angle θ with it, the error Δz is about a half:

$$\Delta z = \frac{R}{n} \operatorname{tg} \frac{\theta}{2} ,$$

for which $\Delta z = \pm 1$ mm for $\theta = \pm 5 \cdot 10^{-4}$ rad.

If it were possible to make the axis of symmetry of the wires parallel to the m.g.p., the error Δz would be zero for obvious reasons of simmetry, and a large angle of divergence between the projections of the wires on the (z, r) plane would be tolerable up to the point in which the components of the field become large with respect to the amplitude of the exciting field.

The angle formed by the wires with the vertical radial (z, r)-plane is not critical. The same can be said for the angle between the latter and the plane defined by the two wires (supposed coplanar).

3. – Experimental realization.

3·1. – We shall now explain the details of the experimental realization of the mechanical part of the device and of the method of calibration used.

It must first be noted that the pulses produced by the two wires will generally never be symmetrical about the time-axis and that therefore the resultant signal will never be zero. They have been given a suitable shape, to obtain, in the simplest case (sufficient for our purpose), a difference pulse in the form of two adjacent peaks of like amplitude. This is useful as a sure oscilloscopic reference, and was obtained by differentiating one of the pulses. Otherwise a series of difference pulses alternately positive and negative

(see Fig. 4) can be obtained by the circuit of Fig. 3, which differentiates one pulse and fits the amplitude of the other. In this case, if the algebraic sum

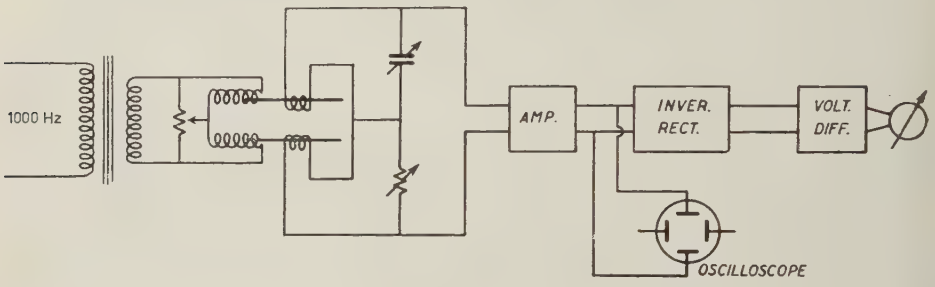

Fig. 3.

of the steady magnetic fields acting along the wires varies, the pulses in one part of the time-axis increase while the others decrease. It is known ([5]) that this arrangement permits high sensitivities to be reached by the use of an electronic device.

With both these methods, however, it is important to obtain experimentally an output reference signal (oscilloscopic or electronic) relative to a zero axial field. The device must therefore be calibrated. This reference will not alter if the two wires are submitted to equal opposite fields until these fields are small with respect to the amplitude of the exciting field.

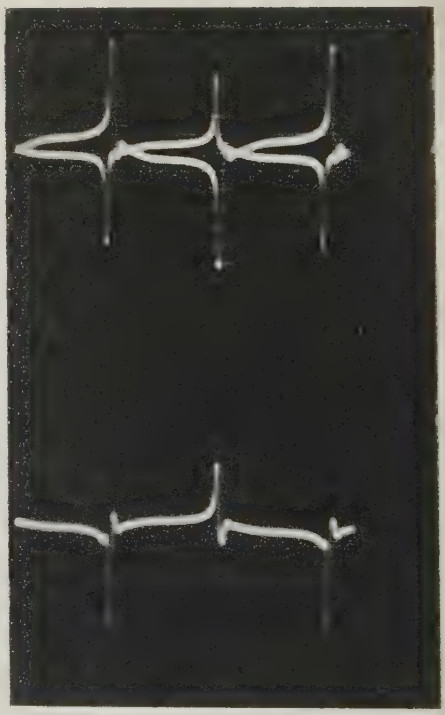

Fig. 4.

3·2. – One of the types of differential probe made according to the circuit of Fig. 3 is shown in Fig. 5. The two exciting toroidal coils are wrapped on a small lucite tube of rectangular form. In the type shown in Fig. 6 the frame of the toroidal coils is a sterling tube of ellipsoidal form. They are made of a single enamelled copper coil ∅ 0.15 mm. In the longer side of each toroidal coil and on the same side are threaded the peaking strips, in the form of a small glass tube containing a mumetal wire ∅ 0.1 mm, length 4 cm, main-

([5]) R. O. Wjchoff: *Geophysics*, **13**, 182 (1948).

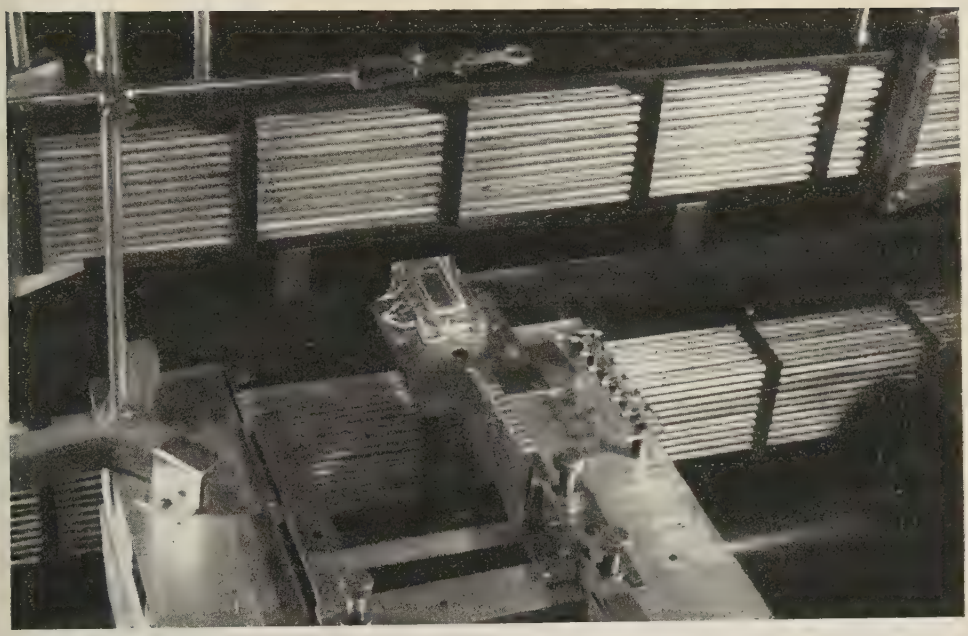

Fig. 5.

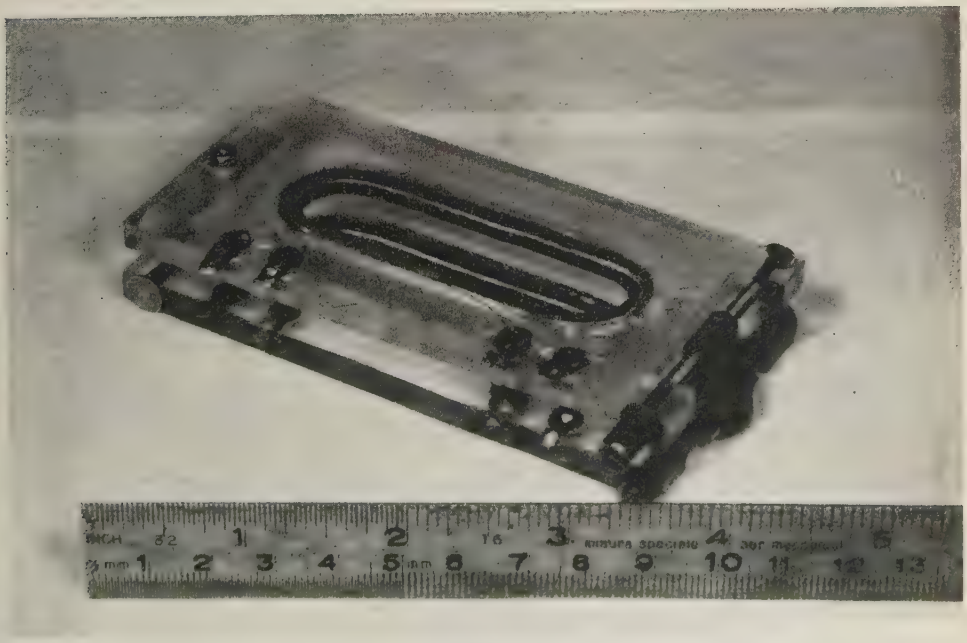

Fig. 6.

tained under tension with an araldite filling (see note II). In its central part it has a 400-turn coil length 5 mm, of wire ∅ 0.05 mm. Toroidal coils have been adopted both to obtain a greater uniformity of field with the same radial extension, and to minimize the dispersed flux, thus minimizing any eddy currents in the iron and inductive coupling between the coils. The two toroidal coils lie firmly stuck and clamped in two lucite planes, which have the two angular degrees of freedom necessary to make the wires parallel. They are series-connected and in opposition to the ends of the secondary circuit of the output transformer of a 1 Hz oscillator. The r.m.s. current that flows through them is normally 125 mA eff. corresponding to an amplitude B_a of the alternating field of about 10 gauss produced along the axis. The distance between the two wires, parallel and in a vertical plane, is 1.5 cm in the model shown in Fig. 6, and 1 cm in that shown in Fig. 5.

3·3. – We shall now explain the alignment and calibration method successfully experimented. The lucite frame is fixed on a brass plate supported by a brass bar (see Fig. 5), whose height and inclination may be regulated by three adjusting screws placed on the vertices of a right-angled triangle with a cathetus parallel to the peaking strips. The brass plate, supporting the probe, has three reference screws (see Fig. 5) electrically insulated from the plate itself, as a connection to the warning light, and placed on the vertices of a right-angled triangle with a cathetus parallel to the peaking strips. Procedure is as follows. The differential probe is introduced into the gap of a standard magnet, which guarantees a magnetic field perpendicular within $\pm 0.5'$ to the parallel surfaces of the poles, in such a way that the wires are coplanar in a plane nearly orthogonal to the above-mentioned surfaces. After demagnetization, the magnet is excited up to a field B of 100 or 200 gauss and only the pulses coming from the lower wire to the oscilloscope are observed. By inversion of the field, if the component B_l exists, it is reversed along the wire and so the pulses « shift » along the time-axis by an amount

$$\Delta\tau \cong \frac{2B_l}{B_a\omega} = \frac{B_l}{3\cdot 10^4}\,\mathrm{s} \qquad \text{for } B_l \ll B_a\,.$$

The angle of $1'$ between the normal to the wire and the field B therefore produces a pulse shift:

$$\Delta\tau \cong \frac{2B_l}{B_a\omega} = \frac{2B\cdot 2.5\cdot 10^{-4}}{B_a\omega} \cong 2\ \mu\mathrm{s}\,,$$

for $B = 200$ gauss which may be observed.

It is therefore necessary to correct the inclination of the wire by the adjusting screws outside the magnet at the end of the bar (see Fig. 5), until the

pulses remain unchanged after the inversion of the field. The same must be done with the upper wire, by manipulating the screws of the lucite hinge (see Fig. 6), on which the upper toroidal coil rotates. At the end of this lining up the wires will be perpendicular to the standard magnet field, certainly within 1′, and parallel to the surface of the poles within the same limit. Their projections on a plane normal to the polar surfaces will also be parallel within 1′, while there is no need to worry about the parallelism of their projections on the polar surfaces, since this need only be respected the within 1°.

At this point the output of two peakers placed in series and in the same direction is observed, and the capacities and resistances for obtaining the required electronic or oscilloscopic reference are arranged. Finally the reference screws are advanced until the lighting of three warning lights advise us that contact with the surface of the lower pole has taken place. At this point it may be said that the mumetal wires are also parallel to the plane defined by the extremities of the three reference screws. Now the probe is ready to be introduced into the synchrotron gap, in order to determine the m.m.s. If we consider the case in which the m.g.p. is not horizontal, the three screws must be pushed on in simultaneous contact with the lower pole; the probe will be rotated by $\frac{1}{2}\alpha$ (where α is the angle between the surfaces of the two poles) in such a direction that the wires are placed parallel to the m.g.p. (within $\pm 1'$). Then the probe is raised parallel to itself until the same oscilloscopic or electronic reference that there was in the magnet with the strips normal to the field, becomes visible at the output. In this position the components B_r will be equal and opposite on the two wires and the position of the midpoint between the two pick-up coils will coincide with the position of a point on the m.m.s.

The measurement was actually carried out in a magnet with $\frac{1}{2}\alpha = 14'$. An optical system allowed both the angle to be read and the raising of the probe to be controlled.

Of course, if the p.g.m. can be assumed horizontal, it becomes superfluous to measure the angle $\frac{1}{2}\alpha$. The optical control also becomes superfluous if an accurate enough mechanical raising device is available.

The electronic device (Fig. 3) consists in an amplifier with gain $\times 800$, whose output is connected to an inverter rectifier and to a differential voltmeter whose sensitivity in output current is 0.5 mA/V for difference in tension applied to the two input grids. With a full-scale milliameter of 1 mA the sensitivity obtained was $4 \cdot 10^{-4}$ gauss per division.

4. – Measurements and conclusions.

The measurements carried out with this first mechanical realisation have confirmed the expectations, allowing the expected measurement of the m.m.s.

The error in the relative distances between the various points of the m.m.s. is not usually greater than ± 0.25 mm, while their absolute distances from the m.g.p. require a careful calibration since they are determined to ± 1 mm. As an example we report a result obtained concerning the behaviour of the m.m.s. in the gap of a cast iron magnet (Fig. 5); the gap is 4 cm high and 12 cm deep. With a field of 230 gauss the three series of measurements were carried out in the following way: the first under normal conditions, the second threading a thin strip 0.35 mm thick in the 1 mm gap present between the upper surface of the upper pole and the surface of the C-shaped magnet, the third unscrewing completely the bolts which press the upper pole against the supporting columns. The presence of the thin 0.35 mm strip produces a rise of 3 mm of the m.m.s. in the centre of the gap. Unscrewing the bolts lowers the m.m.s. by 1 mm.

With this device the curvature of the lines can also be determined point by point and the field-index n can also be measured, bearing in mind the relation:

$$n = \frac{R}{z} \operatorname{tg} \theta$$

and by a relative error:

$$\frac{\Delta n}{n} \cong \frac{\Delta z}{z} + \frac{\Delta \theta}{\theta},$$

which may be estimated at 5%.

This error is essentially due to the measurement of the angle θ, which is measurable to within $3 \div 4\%$ with an optical device.

Of course, this measurement would also be limited to fields lower than 500 gauss, i.e. to the value for which transverse saturation of the wires used by us takes place.

* * *

The author wishes to thank Professor Giorgio Salvini, Director of the « Sezione Acceleratore », for the stimulating criticism shown in many discussions on this subject, and Professor Italo F. Quercia for projecting the electronic part of the device and for discussing in detail the basic ideas of this work.

The author also wishes to thank all his colleagues and particularly Dr. Giorgio Ghigo and Dr. Franco Corazza for valuable discussions.

The mechanical construction of the probes was carried out by Mr. V. Bettini and Mr. P. Bellagotti.

Note I

Let us suppose that the ferromagnetic wire has dimensions such as to allow the formation neither of induced currents nor of demagnetising field. Neglecting hysteresis, we approximate the magnetization cycle of the ferromagnetic material used by the function:

$$B = \frac{2}{\pi} B_s \operatorname{arc\,tg} \frac{H'(t)}{H_0},$$

where B_s is the saturation induction, H_0 is the value for which $B = \frac{1}{2}B_s$ when $H' = H_0$; $H'(t)$ is the instantaneous total field acting along the wire. We have

$$H'(t) = H_a \sin \omega t + H,$$

where H is the steady field. Thus H_0 and B_s determine the shape of the magnetization cycle. The induced e.m.f. picked up on a peaker will thus be given by:

$$V_i = -A \frac{dB}{dt} = -\frac{2AB_sH_a\omega}{H_0} \cdot \frac{\cos \omega t}{\left[1 + \frac{(H'(t))^2}{H_0^2}\right]},$$

where A = area-spire of peaker, ω and H_a are the pulsation and amplitude of the excitation field.

For $H = 0$ the maximum amplitude, which occurs with alternate signs, for $\omega t = n\pi$ $(n = 0.\,1.\,2, \ldots)$, takes the value:

$$V_{i\,\max} = \pm \frac{2AB_sH_a\omega}{H_0}.$$

Assuming, in our case, $A = 3.2 \cdot 10^{-2}$ cm^2, $B_s = 5 \cdot 10^{-3}$ gauss, $\omega = 6.3 \cdot 10^3$ s^{-1}, $H_0 = 0.1$ gauss, one obtains $V_{i\,\max} \simeq 0{,}3$ V, an order of magnitude in agreement with experimental results relating to very long mumetal wires. The peak value just estimated, which exists at time $t = 0$ when $H = 0$, will exist at a time t^* when $H \neq 0$. The function $t^*(H)$ is obviously obtainable from $\dot{V}_i = 0$. If we neglect the term in $\sin^3 \omega t$ in the latter equation, and consider the pulse in the region of $t = 0$, we get for the function $t^*(H)$:

$$t^* = -\frac{1}{\omega} \operatorname{arc\,sin} 2 \frac{H/H_a}{2 + (H_0/H_a)^2 + (H/H_a)^2}.$$

For $H_0^2 + H^2 \ll 2H_a^2$ this reduces to

$$t^* \cong \frac{H}{H_a\omega}.$$

Note II

Here we shall give some details of our technique for the preparation of peaking strips.

Our aim was to obtain perfectly straight mumetal wires (available for us with Φ 0.1 mm) 4 cm long. To obtain this by means of a permanent applied tension, the wire must be prevented from magnetically destructive torsion. The reversing of the magnetization of our wire takes place by a rotation of the domains mainly with a displacement of 180° of the walls and the consequent enucleation of adjacent domains with opposite magnetization ([6]). If

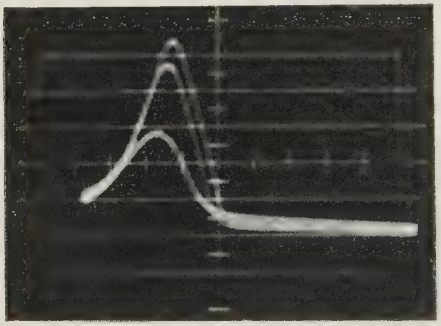

Fig. 7.

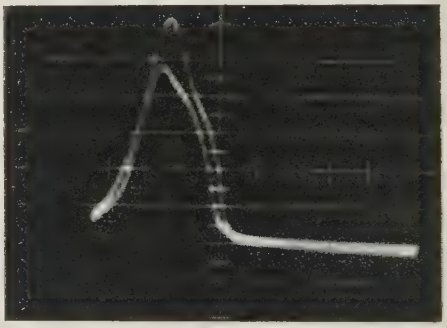

Fig. 8.

the wire is subjected to a torsion, the helical lines along which it acts constitute directions of easy magnetization, so that the final orientation forming the smallest angle with these lines will be preferred. The resultant macroscopic effect will thus be an inclination of the magnetization with respect to the axis of the wire, a variation of the permeability of and the pulses picked up with an axial coil.

The following device was therefore used. The mumetal wire held taut by a suitable weight and passing through a small glass tube covered by the 400 turns and through a larger exciting coil of 1000 Hz, can be controlled by the pulses it generates, which are observable on the oscilloscope. The tension and torsion of the wire are regulated freely until the pulses are satisfactory. Then we alide the exciting coil so as to uncover the small glass tube and fill it with a colt type *D* liquid araldit (CIBA) which enters by capillarity up to the opposite end. Once the araldit is well set, the wire at each end is cut, and the peaking strip is ready for use and to support a field of $5 \cdot 10^2$ gauss normal to the wire.

The results have been satisfactory. Fig. 7 shows the variations in the form of a pulse when the wire is subjected to a torsion of several rotations (lowest pulse) and when this torsion is removed (mean pulse). The highest pulse is obtained when the tension (8 kg/mm²) is removed as well.

Fig. 8 shows the case where the pulse amplitude increases with application of tension. The time scale is 0.05 gauss/cm and the ordinate scale is 0.03 V/cm.

([6]) *Journ. Appl. Phys.*, **26**, 8 (1955).

RIASSUNTO

Viene descritta una sonda differenziale magnetica realizzata con lo scopo di determinare la superficie magnetica mediana del campo statico nell'intraferro di un sincrotrone a focalizzazione debole. La sonda è costituita da due sottili fili ferromagnetici sottoposti a campi magnetici alternati a 1000 Hz uguali e opposti in ogni istante. Il metodo di misura consiste nel determinare la posizione della sonda per cui le componenti del campo magnetico lungo i due fili (paralleli al raggio del sincrotrone e giacenti in un piano verticale), sono uguali e opposte. Il dispositivo descritto permette la localizzazione della superficie magnetica mediana entro $\pm$ 1 mm in campi statici tra 20 e 500 gauss. Si accenna pure alla possibilità di misurare l'indice di campo n mediante questa stessa sonda con la precisione del 5 % in campi non maggiori di 500 gauss. Infine viene esposta con qualche dettaglio la tecnica usata per la preparazione dei fili ferromagnetici.

Diffusion Coefficient of N in α-Fe.

I. Barducci

Istituto Nazionale di Ultracustica « O. M. Corbino » - Roma

(ricevuto il 9 Dicembre 1955)

Summary. — The diffusion coefficient of N in α-Fe has been measured by many experimenters at different temperatures, but experimental values of the heat of activation and of the constant D_0 are not always in a good agreement. Some years ago Wert repeated the measurements in a more extended interval of temperatures, and observed that the agreement of actual experimental data with theoretical calculations is not so good as for some similar interstitial solid solutions. He suggested that further measurements in a more extended temperature range would probably lead to a better agreement with theory. Nevertheless an experimental investigation made by the Author with the cooperation of Dr. P. Gence, has confirmed the experimental data obtained by Wert for the heat of activation and for the constant D_0. In this paper the problem is theorically discussed and it is shown that the observed differences between theoretical and experimental results are within the limits of precision of present experimental techniques.

---

1. – It is well known [1] that interstitial solid solutions in b.b.c. lattices offer the possibility of a very accurate and extended study on the dependence of diffusion coefficient from temperature. This is so because the bulk diffusion measurements by standard metallurgical methods, in the high temperature range, can be extended to much lower temperatures by use of elastic relaxation phenomena, related to diffusion in an atomistic scale.

Measurements by this method were accomplished on different alloys, i.e.: N or C in Fe, and O, or N, or C in Ta, etc. Solid solutions in α-Fe, have received special attention and many experimental data have been published.

---

[1] C. A. Wert: *Journ. Appl. Phys.*, **21**, 1196 (1950).

The diffusion of C in α-Fe was recently the object of a very accurate and exhaustive analysis by WERT (2), who measured the diffusion coefficient by the low temperature relaxation methods and related his results with those obtained by STANLEY (3), in the high temperature range, by standard methods. The experimental information covers a very extended range of diffusion coefficient, i.e. 14 logarithmic units. The corresponding temperature range goes from — 35 °C to 700 °C.

All experimental data agree with the formula (*):

$$D = D_0 \exp[-H/RT]\,. \tag{1}$$

The heat of activation H, for the case of C in α-Fe, can so be measured with good precision.

Experimental results by WERT and STANLEY agree very well with the conclusions of a theoretical analysis developed by WERT and ZENER (4); it seems therefore reasonable to conclude that the experimental results are reliable.

In a further research, WERT did a similar study for diffusion of N in α-Fe (1). However in this case the experimental information covers a range of only 3 logarithmic units, that is a range much more restricted than for C in α-Fe. As the Author himself pointed out, further measurements at higher temperatures are needed for really accurate determination of the heat of activation and the constant D_0.

In this respect it must be observed that the agreement of experimental results with theoretical predictions does not seem so good as for diffusion of C in α-Fe and for some other interstitial solid solutions.

The measure of diffusion coefficient based on elastic relaxation phenomena, have been generally made at low frequencies and correspondingly low temperatures; however the extension to much higher temperatures and frequencies doesn't offer serious difficulties for modern electroacoustical technique.

By means of two apparatuses which have been in use for some years at the « Istituto di Ultracustica », in Rome (5,6) and a similar apparatus designed at the « Laboratoire d'Essais du Conservatoire National des Arts et Métiers » in Paris (7) and with the cooperation of Dr. P. GENGE, we could extend the experimental

---

(2) C. A. WERT: *Phys. Rev.*, **79**, 601 (1950).

(3) J. K. STANLEY: *Journ. Metals*, **1**, 752 (1949).

(*) It must be observed that all measurements were accomplished on very dilute solid solutions.

(4) C. A. WERT and C. ZENER: *Phys. Rev.*, **76**, 1169 (1949).

(5) I. BARDUCCI, G. PASQUALINI: *Nuovo Cimento*, **5**, 416 (1948).

(6) P. G. BORDONI: *Nuovo Cimento*, **4**, 177 (1947).

(7) R. CABARAT: *Rev. Metall.*, **46**, 617 (1949).

investigation on diffusion of N in α-Fe over a temperature range that goes from 90 °C to 200 °C; the corresponding frequency of vibration goes from nearly 3000 to 130000 Hz. These measurements, together with those made measurements, together with those made by WERTa nd others ([1,4,8-10]), cover a temperature range that goes from — 30 °C to 200 °C; the range for the diffusion coefficient is of 8 logarithmic units. This last interval of measurements, it not so large as for C in α-Fe, is more than twice the corresponding range considered by WERT.

Our values for the heat of activation and for the constant D_0 are the same, within experimental errors, as those given by WERT, i.e.: $H = 18200$ cal/mol and $D = 3 \cdot 10^{-3}$ cm²/s.

Therefore our measurements in a higher temperature range, when compared with those of WERT, confirms WERT's results; so the agreement with theory seems to remain much less satisfactory than for other interstitial solid solutions.

However it will be shown in this paper, by a critical discussion of this point, that the observed differences between theory and experimental results are within the limits of the experimental errors. If a more accurate check of the theory is sought, further improvement in the experimental techniques should first be obtained.

2. – We begin with a short summary of the results of the theoretical analysis according to WERT and ZENER ([4]); as it has been said before these results have been confirmed in the case of diffusion of C in α-Fe and for some other alloys.

The relation for diffusion coefficient in interstitial solid solutions in the b.c.c. lattices is:

$$D = \alpha a^2 / \tau \,. \tag{2}$$

Where a is the lattice parameter; α is a pure number depending on the crystal geometry, whose value is 1/24 for b.c.c. lattices; τ is the mean time-of-stay of a solute atom at a given interstitial position.

Comparing (2) with (1) we obtain

$$\tau = \tau_0 \exp[H/RT] \,. \tag{3}$$

([8]) C. BOULANGER: *Compt. Rend. Acad. Sci.*, **224**, 1286 (1947).

([9]) T. S. KÊ: *Amer. Inst. of Mining and Metallurgical Eng.*, Techn. pubbl. no. 2370 (1948).

([10]) L. GUILLET and B. HOCHEID: *Compt. Rend. Acad. Sci.*, **238**, 905 (1954).

Wert's experiences have confirmed that, at least for C in α-Fe, H is really a constant over a very large temperature range. WERT and ZENER found the following expression for the constant τ_0:

$$\tau_0^{-1} = n\nu \exp[\Delta S/R] . \tag{4}$$

Here n is the number of nearest neighbor interstitial positions ($n = 4$ for b.c.c. lattices); ν is the frequency of small oscillations of a solute atom in its interstitial position and ΔS is the *entropy of activation.*

Comparing (2), (3) and (4) with (1) we obtain for D_0 the following expression:

$$D_0 = n\alpha a^2 \nu \exp[\Delta S/R] . \tag{5}$$

With elastic relaxation methods what is measured directly is the time of relaxation τ_r, or the corresponding frequency of vibration f that leads to maximum internal friction at a given temperature; f is related to τ_r by the expression

$$2\pi f \tau_r = 1 . \tag{6}$$

WERT and ZENER have shown that:

$$\tau = \tfrac{3}{2}\tau_r . \tag{7}$$

Therefore one obtains for the diffusion coefficient:

$$D = \frac{4}{3}\pi\alpha a^2 f = \frac{\pi}{18} a^2 f . \tag{8}$$

3. – As we said before, the validity of (8) has been checked by WERT for diffusion of C in α-Fe.

From the measured values of D at different temperatures one can immediately obtain the heat of activation H, which is proportional to the slope of $\log D$ considered as a function of $1/T$. The constant D_0 can then be calculated from (1).

The measurement of the diffusion coefficient D is obtained with a satisfactory precision, because it consists essentially in a frequency measurement, whose experimental error can easily be reduced to $1‰$. However it must be observed that the principal cause of errors in the determination of D (and consequently of H) as a function of temperature is probably the uncertainty in evaluating the temperature of maximum internal friction. Because of the shape of the maximum, it is almost impossible to reduce such uncertainty to

less than ± 2 or ± 3 °C (Fig. 1), even if the temperature is measured with a higher precision. If the temperature range is sufficiently extended, H can however be determined with a satisfactory precision.

It is obvious, on the contrary, that the error in evaluating D_0 must be much larger, because of the exponential law (1); it can be easily seen that an error of 2% on the heat of activation leads to an error of nearly 70 or 80% on D_0, when H has a value of approximately 18000 cal/mol.

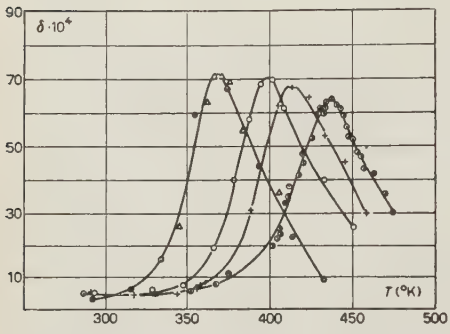

Fig. 1. – Internal friction in interstitial solid solution of N in α-Fe. The four curves have been determined on the same rod, at four different frequencies of vibration.

Folling Wert (1), the validity of theoretical results may be controlled by comparing the values of the entropy of activation obtained in two different ways. The first expression for the entropy of activation is a direct consequence of (5), that is:

$$\frac{\Delta S}{R} = \ln \frac{D_0}{n\alpha a^2 \nu} = \ln \frac{6 D_0}{a^2 \nu} . \tag{9}$$

In (9) all the parameters, but the frequency ν, can be obtained from experimental observations or from lattice geometry; ν must be evaluated from theoretical considerations. Wert and Zener calculated an approximate value of ν assuming that the potential energy varies in a sinusoidal manner when a solute atom moves from an interstitial position to a near one. One obtains, $\nu = 1.1 \cdot 10^{13}$ Hz.

The second way of calculating the entropy of activation is based upon the hypothesis that all the work done by diffusing atoms goes into straining the lattice. This leads to:

$$\Delta S = - H \, (d \ln \mu / \mathrm{d}T) . \tag{10}$$

Here $(d \ln \mu / \mathrm{d}T)$ is the temperature coefficient for the logarithm of the elastic modulus. With α-Fe, $(d \ln \mu / \mathrm{d}T) = -26 \cdot 10^{-5}$ in the case of shear modulus; the temperature coefficient is only a little different for other elastic moduli. With $H = 18200$ one obtains

$$\Delta S / R = 2.3 . \tag{11}$$

This value for $\Delta S/R$ is indeed an upper limit, as it may easily be seen from the assumption which has lead to (10).

Nevertheless, in the case of C in α-Fe the value of $\Delta S/R$ given by (9),

assuming for D_0 its experimental value, is in good agreement with (11); the same is for some other cases as it is seen in Fig. 2, which has been taken from WERT's paper.

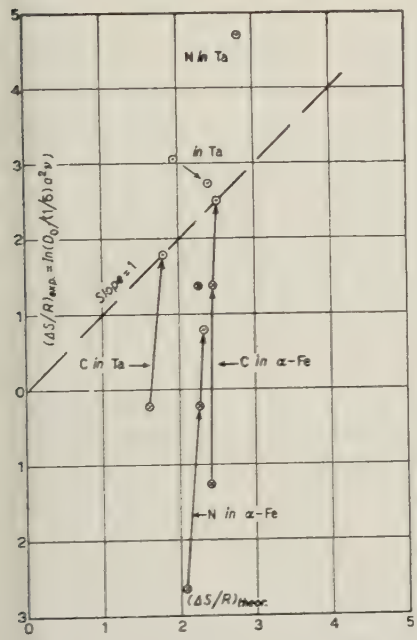

Fig. 2. – $(\Delta S/R)$ as computed from Eq. (9) *vs.* $(\Delta S/R)$ as computed from Eq. (10). For each material successive points are taken from different Authors (see C. A. WERT [1]).

When the experimental errors are reduced, Fig. 2 shows a better agreement with the theoretical value calculated by use of (10). From this WERT concludes that, most probably, the agreement between the values of $\Delta S/R$ deduced from (9) and (10) would be equally good for N in α-Fe as for other cases, if the precision of measurements were sufficiently high.

However we have yet observed that our measurements in an extended temperature range confirm Wert's results. This is shown in Fig. 3, where $\log D$ is given as a function of $1/T$. It is seen that our experimental points are placed on the same straight line obtained by WERT and others. It is obvious, therefore, from the same figure, that the great differences in experimental values of the heat of activation given from different authors (see Table I) are largely a consequence of the fact that the explored temperature range was, in general, too small for calculating the slope of the experimental straight line with a reasonable precision.

As Wert's values for H and D_0 have been confirmed by extending the temperature range towards higher temperatures, it must be concluded that the disagreement in the values of ΔS deduced by the two different ways has not been eliminated from our measurements.

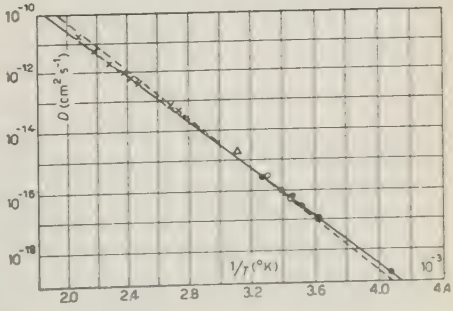

Fig. 3. – Diffusion coefficient D for N in α-Fe, *vs.* T^{-1}. The different points are taken from: ● C. A. WERT [1]; ○ T. S. KÊ [9]; ▲ C. BOULANGER [4]; x P. GENCE and the Author (to be published). The dotted line holds for the calculated value of the heat of activation: $H = 19\,000$ cal/mol.

Nevertheless it will be shown that, if the comparison between theoretical and experimental results is done in a somewhat different way, the agreement seems perhaps to be more satisfactory than it would appear by taking as a basis for comparison the two values of ΔS given by (9) and (10).

Firstly one can observe that the values of ΔS determined from (9) doesn't seem to be really an experimental one. Indeed such a value is a function of the frequency ν that, as remarked, can not be measured, but must be theorically evaluated, and it is obvious that the assumptions made for this calculation can give only a rough approximation. Secondly it has been observed that the determination of D_0 from experimental data leads easily to very large errors, even if the precision for H is satisfactory. It can be easily deduced that this leads to a very large error also for $\Delta S/R$, in spite of the fact that, in (9), $\Delta S/R$ depends on the logarithm of D_0.

On account of this fact, we have thought it convenient to compare theoretical and experimental results in a somewhat different way. We assume, as done by WERT, that the value (11) for $\Delta S/R$ is correct, as it appears to be confirmed by the results obtained for C in α-Fe. The value of D_0 which would agree with $\Delta S/R$ so calculated, in the hypothesis that all other parameters are free of error, can then be deduced from (9). Such value of D_0 is found to be 5 times larger than the experimental value 0.003.

We assume besides that the experimental value of the diffusion coefficient is correct for a given temperature, chosen in the central part of the experimentally explored range. We can then deduce, from (1), the value of H that would agree with the calculated D_0 at the assumed temperature. One so obtains $H = 19200$ cal/mol. This value is only 5% larger than the experimental one, i.e.: 18200.

As the errors on H are probably ± 300 or ± 400 cal/mol, it is seen that the difference between $H_{\text{theor.}}$ and $H_{\text{exp.}}$ is only 2 or 3 times the supposed experimental errors.

TABLE I. – *Heat of activation for diffusion of* N *in* α-Fe.

Experimenter	H (cal/mol)	$\pm \Delta H$ (cal/mol)
SNOEK [11-12]	16400	—
KÊ [9]	20000	$\pm$ 2000
WERT and ZENER [4] . .	17700	$\pm$ 400
WERT [1]	18200	—
GUILLET and HOCHEID [10]	18600	—
BARDUCCI and GENCE . .	18200	$\pm$ 300

[12] J. L. SNOEK: *New Development in Ferromagnetic Materials* (New York and Amsterdam, 1947).

[11] J. L. SNOEK: *Physica*, 8, 711 (1941).

The latter result becomes more significant if one compares the said difference ($H_{\text{theor.}} - H_{\text{exp.}}$) with the maximum and minimum experimental values of H, according to Table I.

This is done in Fig. 4, giving the dependence of H from D_0, calculated from (11), (9) and (1) as said before.

It is seen that the calculated point falls in the central part of the experimental range for H, so that the difference ($H_{\text{theor.}} - H_{\text{exp.}}$) is very much smaller than the similar difference between the maximum and minimum experimental values. In our calculations we have accounted only for the errors made on D_0; if the experimental errors on other parameters, and the precision in evaluating the frequency ν are also considered, the agreement with theory may, perhaps, be obtained for a value of H that is closer to the experimental one.

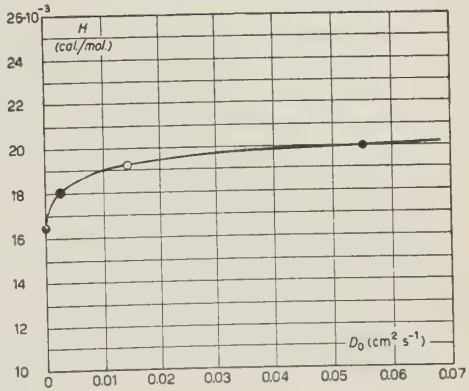

Fig. 4. – Heat of activation H *vs.* constant D_0; according to Eqs. (11), (9) and (1); ● limits of experimental values (from Table I); ⊙ experimental point according to C. A. WERT and to P. GENCE and the Author; ○ calculated point.

Finally it must be observed that, in theoretical calculations no attempt is made of accounting for the effect of impurities on the diffusion coefficient and its dependence from temperature. The exact chemical analysis of samples is not always given by the different Authors; in our experiments (which, as said before, agree with those of WERT and others), the impurity content, (and particularly that of C) was not at all negligible, as compared to the percentage of N.

The diffusion of N could be studied equally well, because, as L. GUILLET and B. HOCHEID pointed out ([10]), the relaxation effects of N and C are easily separated by a suitable heat treatment. Nevertheless it is evident that this does not mean that any influence of C on diffusion of N in α-Fe lattice has surely been eliminated.

4. – In conclusion, we hope to have shown that the disagreement of experimental data with theoretical results in case of solid solution of N in α-Fe, according to Wert and Zener's theory, is perhaps not so large as it would appear assuming as a basis for comparison the entropy of activation.

It is true that for other alloys the situation appears to be much more satisfactory; but we think it would not be easy to obtain, from actual experimental procedures, a precision sufficient to allow a more strict control of the theoretical conclusions.

RIASSUNTO

La misura della costante di diffusione dell'N nel Fe-α è stata oggetto di numerose ricerche, le quali hanno dato valori talora notevolmente discordanti per il calore di attivazione H e per la costante D_0: Alcuni anni or sono WERT, ripetendo le misure su un intervallo di temperature abbastanza esteso, ha trovato come valori più probabili: $H = 18200$ cal/mole e $D_0 = 3 \cdot 10^{-3}$ cm^2/s. Egli ha però osservato che, confrontando i dati sperimentali da lui ottenuti con quelli calcolati in base a considerazioni teoriche, si ottiene un accordo meno soddisfacente che per il caso del Fe-α contenente C e per altre soluzioni solide interstiziali in reticoli cubici a c.c. WERT conclude da ciò che, probabilmente, si otterrebbe un accordo migliore se si eseguissero misure su un intervallo di temperature più esteso, e quindi notevolmente più precise. Una ricerca sperimentale eseguita a tale scopo dall'Autore in collaborazione con il dr. P. GENCE, ha invece confermato perfettamente i valori sperimentali ottenuti da WERT. Un accurato esame della questione ha, tuttavia, consentito di concludere che il disaccordo fra dati teorici e sperimentali è contenuto nei limiti che si possono prevedere ammettendo una ragionevole precisione di misura.

IL NUOVO CIMENTO Vol. III, N. 2 1° Febbraio 1956

Notes on the Design of Distributed Amplifiers.

G. Fidecaro (*) and A. M. Wetherell

Nuclear Physics Research Laboratory - University of Liverpool

(ricevuto il 9 Dicembre 1955)

Summary. — A study of distributed amplifiers is made, taking into account the self capacity of the coils and the effect of using anode and grid lines with different propagation speeds. The latter effect can be useful in avoiding the large increase in gain of the *m*-derived filter type amplifier at the upper end of the band. A possible procedure for a practical design is suggested, as well as an experimental method for the determination of the characteristics of the two lumped lines.

1. – Introduction.

The theory of distributed amplifiers, which is based on an idea of Percival [1], was developed primarily by Ginzton *et al.* [2]. Later, other workers published designs [3], but a more detailed description has never been presented.

This paper is limited to pointing out some details of design which may be useful in constructing amplifiers fast enough for general use in nuclear physics. For a more general description, and for points which are not treated here, the original paper by Ginzton *et al.* should be consulted.

A method for the measurement of the characteristics of the lumped lines which form the grid and anode circuits will be described briefly. The measu-

(*) CERN (European Organization for Nuclear Research, Theoretical Study Division). On leave of absence from the University of Rome.

(1) W. S. Percival: *British Patent Specification* No. 460, 562.

(2) E. L. Ginzton, W. R. Hewlett, J. H. Jasberg and J. D. Noe: *P.I.R.E.*, 36, 956 (1948).

(3) For a description of the theory and a list of references see I. A. D. Lewis and F. H. Wells: *Millimicrosecond Pulse Techniques* (London, 1954).

rement of the properties of entire lines provides more information than can be obtained from measurements of single components.

2. – Analysis of an Amplifier Section.

M-derived low pass filters are commonly used in distributed amplifiers because of their well known advantages over constant K filters [4].

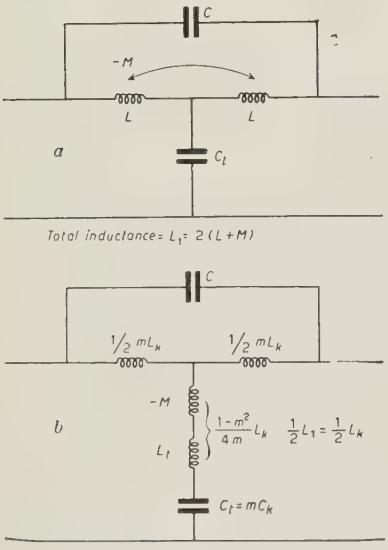

Fig. 1.

For a more complete analysis the distributed capacity of the coil should be taken into account, because the filter characteristics can be greatly changed in the high frequency region. The element to be studied in this case is shown in Fig. 1*a*.

More accurately, the self capacity of the half coil should be taken into account, but this may be neglected unless the frequencies considered approach the half coil resonance.

The filter is equivalent to the element shown in Fig. 1*b*, where the stray inductance L_t is shown in the shunt arm. In the following, we suppose the parasitic inductance included in the term $((1-m^2)/4m)L_k$, where m is a design parameter.

C is the self capacity of the coil, C_t the appropriate tube capacity, including parasitic capacities.

The characteristic impedance of the element (1*a*) is:

$$Z = \sqrt{\frac{L_k}{C_k}} \cdot \sqrt{\frac{1-(\omega/\omega_c)^2}{1-(\omega/\omega_r)^2}} = R_0 \sqrt{\frac{1-(\omega/\omega_c)^2}{1-(\omega/\omega_r)^2}} . \tag{1}$$

$$R_0 = \sqrt{\frac{L_k}{C_k}} ; \tag{1a}$$

where

$$\omega_c = 2\pi f_c = \frac{2}{\sqrt{L_k C_k}} \tag{1b}$$

is the cut-off frequency,

$$\omega_r = 2\pi f_r = \frac{1}{\sqrt{L_1 C}} \tag{1c}$$

is the resonance frequency of the whole coil.

---

[4] H. E. KALLMANN: *P.I.R.E.*, **34**, 646 (1946).

Fig. 2 shows the behaviour of Z for several values of ω_r/ω_c: For simplicity we put $n = \omega_r/\omega_c$ and we consider only cases such that $n \geqslant 1$. Z is real for ω varying in the intervals $0 - \omega_c$ and $\omega_r - \infty$. For $\omega_c \leqslant \omega \leqslant \omega_r$ Z is imaginary and the frequencies in this interval are attenuated. The characteristic impedance tends to the constant value $\sqrt{L_k/C_k}$ when n approaches 1. Thus it is possible to obtain good termination of a line without employing terminal half sections. For $n = \infty$ we have the case of the M-derived filter; for $n = 1$ the case of the bridged T filter suggested by GINZTON *et al.*

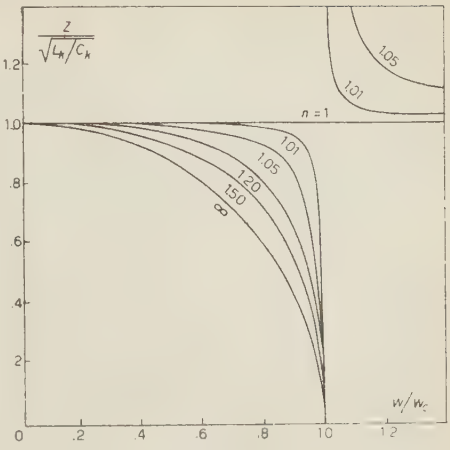

Fig. 2.

The expression for the phase is:

$$\theta = 2 \operatorname{arctg} \left\{ m \frac{\omega}{\omega_c} [1 - (\omega/\omega_c)^2]^{-\frac{1}{2}} [1 - (\omega/\omega_r)^2]^{-\frac{1}{2}} \right\}. \tag{2}$$

Fig. 3 shows θ for various values of m and n. The usual value $m = 1.27$ is close to the value 1.3 which we have calculated. The best linearity is ob-

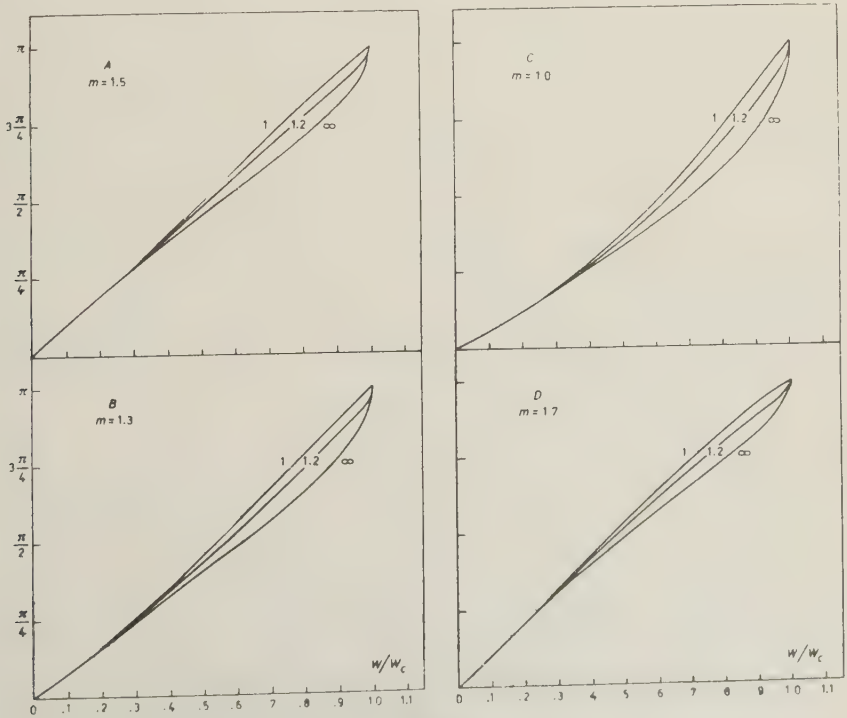

Fig. 3.

tained, in this case, when $n = \infty$, i.e. when the capacity of the coil is entirely neglected. However, this linearity is not as good as that for $m = 1.5$, $n = 1.2$. It should be noted that the bridging capacity, for the case $m = 1$, cannot be considered as a self capacity.

The delay, as a function of frequency, is given by the slope of the phase curve. For $\omega = 0$, one finds that:

$$\tau_0 = \left(\frac{\mathrm{d}\theta}{\mathrm{d}\omega}\right)_{\omega=0} = 2\,\frac{m}{\omega_c}\,. \tag{3}$$

This formula is useful, as it allows a determination of the parameter m experimentally, from a measurement of the phase curve.

The gain of an amplifier section, when the grid and anode lines are identical is given by:

$$-g_m\,\frac{R_0}{2}\,\sqrt{\frac{1-(\omega/\omega_r)^2}{1-(\omega/\omega_c)^2}}\,\frac{\exp\left[-j\theta\right]}{\{1-(\omega/\omega_r)^2\}\{1-(\omega/\omega_c)^2\}+(m(\omega/\omega_c))^2}\,, \tag{4}$$

where g_m is the mutual conductance of the tube.

If the lines are different, the gain becomes:

$$-g_m\,\frac{R_{01}R_{02}}{2Z_1}\,\frac{\sin(\theta_1/2)}{m_1(\omega/\omega_{c1})}\,\frac{\sin(\theta_2/2)}{m_2(\omega/\omega_{c2})}\,\exp\left[-j\,\frac{\theta_1+\theta_2}{2}\right], \tag{5}$$

where the suffix 1 refers to the grid line and 2 to the anode line.

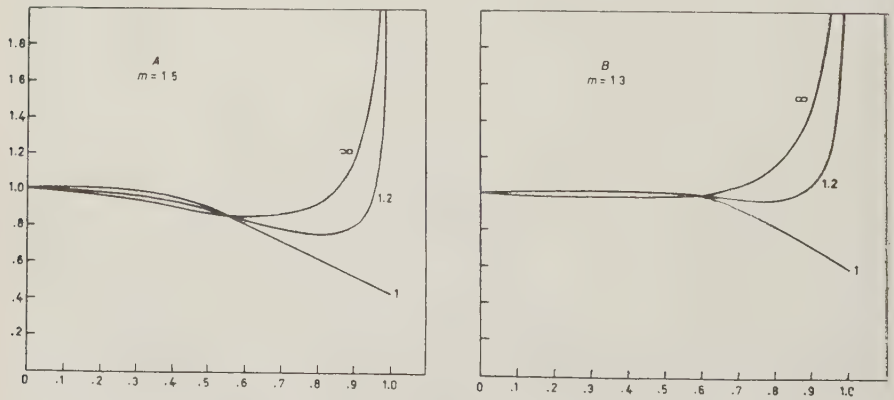

Fig. 4.

Fig. 4 shows the expression (5) for different values of m and n, including the extreme values $n = 1$ and $n = \infty$.

In the above the effects of grid damping and mistermination of the lines have been neglected, as both have been treated by GINZTON *et al.*

3. – Grid and anode lines with different propagation speeds.

It is shown in Fig. 4 that if the case $n = 1$ is excluded the gain of a section goes to infinity at $\omega = \omega_c$. To avoid the increase in the gain produced by the K constant section GINZTON *et al.* proposed the use of the M-derived or bridged T with $n = 1$ filters.

However the only advantage gained by employing the m derived and also bridge T with $n \neq 1$, over the K constant, is a more uniform gain and a more linear phase shift over a wider frequency band. The case $n = 1$, which is the only case where the gain does not rise to a peak, is not easy to realize practically, as it involves the tuning of two circuits to the same frequency. This is difficult, as the adjustment must be carried out for each section of the amplifier, with the additional complication that ω_c (grid) is a sensitive function of the anode current.

It has bee found possible to control the shape of the frequency response curve, to a certain extent, by properly adjusting the speeds of anode and grid lines; for example the peaking of the gain at the upper end of the band may be avoided.

The gain of a single section (5) may be written:

$$A(\omega) \exp\left| -j\left(\frac{\theta_1 + \theta_2}{2} - \pi\right)\right|, \tag{6}$$

where

$$A(\omega) = \frac{g_m}{2} \frac{R_{01}R_{02}}{Z_1} \frac{\sin(\theta_1/2)}{m_1(\omega/\omega_{c1})} \frac{\sin(\theta_2/2)}{m_2(\omega/\omega_{c2})} . \tag{7}$$

The maximum of $A(\omega)$, which in practice is limited by the losses, occurs at $\omega = \omega_{c1}$.

If the amplifier is composed of s sections the contribution of the q-th section is given by:

$$A(\omega) \exp\left|-j\left\{\frac{\theta_1 + \theta_2}{2} - \pi + (q-1)\theta_1 + (s-q)\theta_2\right\}\right| \tag{8}$$

and the total gain by:

$$A(\omega) \frac{\sin(s(\theta_1 - \theta_2)/2)}{\sin((\theta_1 - \theta_2)/2)} \exp\left| -j\left(s\frac{\theta_1 + \theta_2}{2} - \pi\right)\right|. \tag{9}$$

It is seen from (9) that if $\omega_{c1} < \omega_{c2}$ the maximum in $A(\omega)$ is annulled if

$$s\{\pi - \theta_2(\omega_{c1})\} = 2\pi . \tag{10}$$

For $\omega_{c1} \quad \omega_{c2}$ the attenuation introduced by the fact that θ_2 is imaginary at $\omega = \omega_{c1}$ merely diminishes the maximum. This attenuation can be controlled by varying ω_{c2}.

The formula (10) shows that when the number of tubes s is increased the relation remains satisfied for a smaller phase difference.

If the propagation speeds are altered, only just sufficiently to compensate for the peak in the gain, the frequency response in the working band is not very much affected, as may be seen from (9). Fig. 5 shows the experimental response of a compensated amplifier, in which the lines were empirically adjusted to give a good frequency response. The continuous curve in the figure is obtained from (9) using phase shifts as described in section 4. This curve was normalized to the experimental gain at low frequencies. The rise time corresponds to 2.5 mμs.

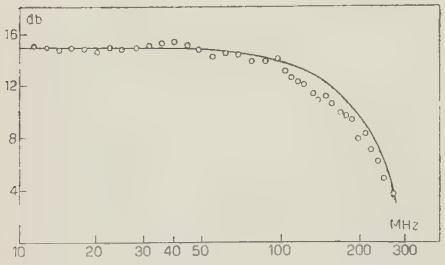

Fig. 5.

It is possible to examine the transient response in a little more detail, For simplicity we examine the case

$$A(\omega) = 1\ ; \qquad \theta_1 = \frac{\pi}{\omega_c}\omega = \omega\tau_1; \qquad \theta_2 = \frac{\pi}{\omega_c(s/(s-2))}\omega = \omega\tau_2\ .$$

The response of the amplifier to a unit step function is given by an integral of the form.

$$(11) \qquad V(t) = \frac{1}{2\pi}\int \frac{\exp\{+j[\omega t - s((\theta_1+\theta_2)/2) + \pi]\}}{j\omega} \frac{\sin(s(\theta_1 - \theta_2)/2)}{\sin((\theta_1-\theta_2)/2)}\,d\omega\ ,$$

which corresponds to a signal of the form shown in Fig. 6, delayed in time by $s(\tau_1+\tau_2)/2$. The expression $(s-1)|\tau_1-\tau_2|$ corresponds to the rise time.

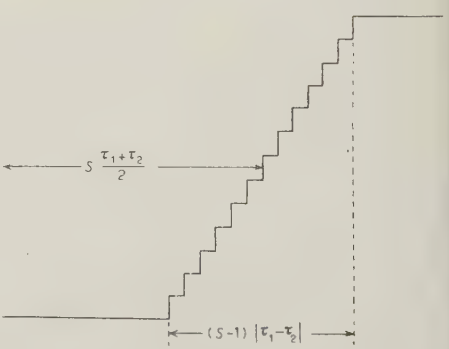

Fig. 6.

In a practical case, in which $A(\omega)$, θ_1 and θ_2 are functions of ω corresponding to actual line characteristics, it is inconvenient to calculate the integral (11). It is clear that the response will still be composed of s steps, each having now a finite rise time. The sharp corners shown in Fig. 6 will be smoothed out if $|\tau_1 - \tau_2|$ is much smaller than the rise time of a section. This result is obvious, as an actual amplifier will

not pass the high frequency components belonging to the sharp corners. Of course, the total effective rise time of an entire amplifier is not much larger than $(s-1)|\tau_1-\tau_2|$.

In practical cases the transient response may be calculated, instead, by approximate methods, once the response and phase shift curves have been determined experimentally.

It should be noticed that as the phase function of a complete amplifier depends on $(\theta_1+\theta_2)/2$ it is possible to adjust the characteristics of the grid and anode lines to compensate for non linearities introduced by the lines separately.

Obviously a peak in a response curve is associated with the possibility of oscillations. Instability has been observed at the upper extreme of the frequency band of a 12 tube amplifier, but a reduction of gain at these high frequencies, by the method suggested, has resulted in complete stability.

4. The determination of the characteristics of lines.

For the determination of the phase characteristics of lines the arrangement shown in Fig. 7, with the line short circuited, has been used. Here, (1) and (2) are high frequency voltmeters, and the procedure was to keep the output of the signal generator, as measured by (1), constant and note the reading of (2) at different frequencies. The resonance frequencies were detected as minima in the reading of (2). If $\theta(\omega)$ is the phase shift per section, and the line is composed of s sections, the resonance condition is:

$$s\theta = k\pi \qquad (1 \leqslant k \leqslant s). \tag{12}$$

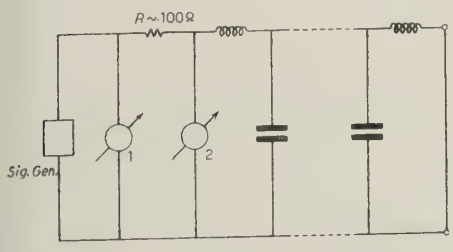

Fig. 7.

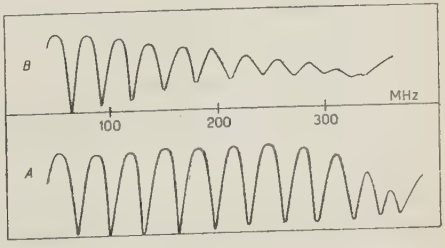

Fig. 8.

There are thus s resonances, excluding $\omega = 0$. From (12) we have that a frequency ω_r corresponds to a phase shift $\pi r/s$. When $r = s$, the corresponding frequency is the cut-off frequency.

In Fig. 8 a series of measurements made with the arrangement of Fig. 7

is shown. The two curves refer to the grid line of a 12 section amplifier using 6AK5 tubes. The curve (*a*) was taken with cold tubes and (*b*) with the tubes under operating conditions. The change in capacity and the increase in the losses at high frequencies can be seen in *b*).

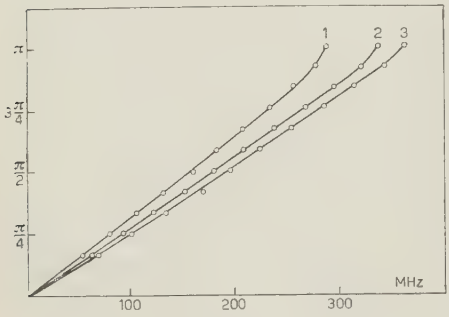

Fig. 9.

The curve (2) in Fig. 9 has been calculated to fit the resonances of Fig. 8-*b*) using formula (2). Of the three necessary parameters, ω_r and ω_c were measured directly, and m was determined from the initial slope of the experimental phase shift curve according to formula (3). The curves (3) and (1) of Fig. 9 refer to anode line resonances before and after loading with condensers to reduce the propagation speed. As an example, we present the parameters of the three curves in the following table:

	m	f_c	f_r
1	1.44	292 MHz	425 MHz
2	1.46	342	445
3	1.43	368	425

The experimental points are shown in Fig. 9 for comparison with the calculated curves. It was also found by direct measurement that the lines transmitted again above the frequency ω_r in agreement with formula (1).

From curves (1) and (2) the response curve shown in Fig. 5 has been calculated.

The same arrangement (Fig. 7) can be used to measure the characteristic impedance, if the phase curve is known. The input impedance of a short-circuited line and condenser in series is:

$$Z_{tot} = \frac{1}{j\omega c} + jZ \operatorname{tg} \Xi(\omega) , \tag{13}$$

where

$$\Xi(\omega) = s \cdot \theta(\omega)$$

is the phase shift of the complete line. At resonance, since Z_{tot} is zero, it is sufficient to know C to determine Z at that frequency.

5. – The practical design.

The first step in a practical design is to select the parameters m, ω_c, ω_r for the two lines. Figs. 2, 3 and 4 will help in the choice of m and n, from the points of view of good frequency response and phase linearity.

However, the final values of m and n, as well as the values of ω_{c1} and ω_{c2}, will depend on a compromise between a number of points, some of which are listed briefly in the following.

The choice of the characteristic impedance Z_2 of the anode line, determines not only the gain, but also ω_{c2}. This is due to the fact that, for a given tube and given m, ω_c and Z are not independent, as they are related, in the working band, by the formula:

$$f_c Z \cong f_c R_0 = \frac{m}{\pi c_t}, \tag{14}$$

where R_0 is the low frequency impedance (1*a*) defined in section 2. ω_{c1} is of the same order of magnitude as ω_{c2}, even if the lines have different speeds, so that once ω_{c2} is decided, the grid line impedance is no longer completely arbitrary. In general, it will be smaller than the anode line impedance, as the input capacity of a tube is larger than the output capacity. The reduction of gain in cascading stages when $Z_1 < Z_2$, and the impedance of connecting cables, both place a lower limit on the practical size of the grid impedance.

In choosing the number of tubes and number of stages the rule that each stage should have a gain of about $e = 2.7$ is not of much practical importance, since other things should be taken into account. For example, the number of tubes in an output stage depends on the maximum signal amplitude desired; the number of stages is even or odd, according to the polarity of the pulses.

A method of changing the speed of the lines, without altering the coils, is to place small fixed condensers in parallel with the tube capacity. When the optimum value of the padding condensers has been found experimentally, it is possible to design new coils, so that the same phase curve is obtained, but with higher characteristic impedance.

It should be noted that the grid line phase curve is quite sensitive to changes in the anode current of the tube.

Having selected the three parameters m, ω_c and ω_r for both lines, the sizes of the coils must be calculated.

From (1*a*), (1*b*) and Fig. 1 of section 2 the total inductance is:

$$L_1 = m L_k = \frac{R_0 m}{\pi f_c}. \tag{15}$$

The inductance of a half coil is:

$$L = \left(\frac{1 + m^2}{4m}\right) \cdot L_k + L_t \,, \tag{16}$$

and the numerical value of the mutual inductance

$$M = \left(\frac{m^2 - 1}{4m}\right) \cdot L_k + L_t \,, \tag{17}$$

where L_t is the parasitic inductance. Thus the total inductance $L_1 = 2(L+M)$ does not depend on L_t. However the presence of L_t should be taken into account in deciding the correct amount of coupling between the two half coils.

It can be shown that when the Nagaoka formula ([5]) for coils, is valid, the quantity

$$\frac{L+M}{L} = \frac{mL_k/2}{((1+m^2)/4m) \cdot L_k - L_t} = F\left(\frac{D}{l}\right), \tag{18}$$

where

$$\frac{D}{l} = \frac{\text{Diameter of the coil}}{\text{Length of the coil}} \,.$$

This function can be computed from a table of the numerical factors entering into the Nagaoka formula.

A plot of the relation (18) has been presented by KELLEY ([6]).

When D/l is known, for the required total inductance L_1, one obtains from the Nagaoka formula: $D \cdot (\text{total number of turns})^2$. The number of turns and D can be adjusted within this product, to obtain a coil of reasonable dimensions.

This procedure, for the determination of the size of the coils, is only a rough approximation, if the number of turns is very small.

The next step should be to measure the total inductance of the coil, for example with a Q meter, and alter the size to obtain the correct inductance. Following this, to adjust the phase curve, and therefore m, one should make a model amplifier with a reasonable number of tubes and use the method described in section **4**.

By proceeding in this way it is not necessary to know in advance, with great accuracy the stray capacity and inductance of the tube, so that rough values of C_t and L_t can be used for the provisional design. From the experi-

---

([5]) F. E. TERMAN: *Radio Engineers' Handbook* (New York, 1943), pp. 53 to 55.
([6]) G. G. KELLY: *Rev. Scient. Instr.*, **21**, 75 (1950).

nentally determined ω_c and m, together with the experimental value of R_0 or the value of the total inductance L_1 determined by Q-meter) it is possible to get C_t. On the contrary, no information is obtained by this method for L_t. We have obtained for a 6AK5 tube C_t grid = 7.1 pF and C_t anode = 4.3 pF. These values of course refer to our own arrangement of tubes and coils, but can be taken as a guide for other designs. The grid capacity corresponds to an anode current of about 10 mA.

The distributed capacity of the coil depends on the diameter of the wire, the dielectric constant of the former and the depth of the groove in which the wire lies, if the coil is not close wound.

A paper by PALERMO (7) gives very rough information on the distributed capacity of a coil. However a direct measurement of the resonance frequency is much more reliable as it gives ω_r. It is thus possible to adjust the size of the wire, or the other two variables, to get the desired ω_r.

In conclusion of this section we would like to remark that direct measurement of the characteristics of the lumped lines is useful as it gives the information which is required for understanding the behaviour of an amplifier, including the variation of the components with frequency, the effect of the half coil distributed capacity, and other possible effects, which cannot be calculated conveniently.

* * *

The progress of our work was aided by using a set of coils suggested by Professor W. L. KRAUSHAAR of M.I.T. We would like to thank Dr. B. COLLINGE for helpful comments. One of us (G.F.) would like to thank Professor H. W. B. SKINNER for his kind hospitality.

APPENDIX

On completion of the present paper, an article by G. D. SARMA, in *Proc. Inst. Elc. Eng.*, part B, September, 1955, was brought to our notice by Dr. B. COLLINGE, of this laboratory.

This article is concerned with the effects of « staggering » the anode and grid lines, treated here in Section 3.

In the present paper, « staggering » was suggested mainly to avoid the peak in the gain at the upper end of the band, without affecting very much the working band, as can be seen on consideration of the explicit sine terms in (9).

---

(7) A. J. PALERMO: *P.I.R.E.*, **22**, 897 (1934).

In our discussion suitable adjustment of the parameters m, ω_c, ω_r, for each line, leads to a flat response curve and a more linear phase shift characteristic. The Figs. 2, 3 and 4, may be used as a guide in judging the correct direction for variation of these parameters.

In SARMA's paper all the cases treated have an anode line cut-off at a frequency lower than grid line cut-off. If this is so, the vectors sum on the anode line in phase at $\omega = \omega_{c1}$, so that the peak in gain which occurs just at $\omega = \omega_{c1}$, is not removed, although, of course, the attenuation in the anode line decreases it.

The experimental response curve, in Fig. 16 of SARMA's paper, should have a peak just above the working band, but unfortunately no experimental data is presented for this region.

By increasing the grid line m, the peak, finite in height because of the losses, moves towards higher frequencies and decreases in size. In Sarma's amplifier the grid losses should be small, as the frequency does not go much above 1 MHz; it is thus the Q's of the line sections which play the main role.

The improvement in damping of the after pulse oscillations, shown in Fig. 15 of SARMA's paper, may be interpreted as being due more to a decrease in the peak, than to an improvement in the shape of the frequency response curve.

RIASSUNTO

Viene presentata un'analisi del comportamento di un amplificatore distribuito, tenendo conto della capacità propria delle bobine, e l'effetto della differente velocità di propagazione dei segnali nelle due linee, di placca e di griglia. Quest'ultimo effetto può essere utilizzato per evitare il forte aumento di guadagno che si verifica all'estremo superiore della banda di un amplificatore con sezioni del tipo M-derivato. Si suggerisce un possibile metodo per il progetto pratico di un amplificatore ed una disposizione sperimentale per la determinazione delle caratteristiche delle due linee di trasmissione.

On the Causes Affecting the Phase Grating Permanence, at the Stopping of the Ultrasounds.

F. Porreca

Istituto di Fisica Sperimentale dell'Università - Napoli

(ricevuto il 9 Dicembre 1955)

Summary. (*) — Some experimental facts are related which allow to ascribe to electrostatic causes an important role in the formation of the phase grating which builds up in the suspensions traversed by ultrasonics and persists at the stopping of these. One may indeed observe that the effect manifests itself in suspensions of polar liquids and is absent in the apolar ones. Moreover, in the suspensions of mixtures of liquids, which singly produce the effect, it fails in the concentration range in which there is motive to retain that the maximum number of molecular associations builds up. Finally the first results are given on the permanence time of the diffracted lines at the stopping of ultrasonics, in suspensions of starch in electrolytic solutions, which show a diminution of the effect with increasing concentration of the ions in suspension. In agreement with these experimental results we retain it as consequent to affirm that the permanence effect manifests itself when the suspended particles are surrounded by free dipoles of the liquid so as to present around them a zone whose refringence index is different from the one proper of the liquid. In this way the particles which are ordered by the stationary ultrasonic waves in planes equidistant by 5/2, build up an own phase grating with the same periodicity.

(*) *Editor's Translation.*

When a liquid suspension is subjected to ultrasonic stationary waves of a wavelength λ, the suspended particles gather in uniformly spaced parallel planes at distance from each others of $\lambda/2$ [1], just as it is the case in a Kundt's pipe.

The persistance of this arrangement of the particles after the stopping of

(1) A. Carrelli and F. Porreca: *Nuovo Cimento*, **10**, 885 (1953).

the ultrasonic waves, allows the observation of some optical effects already described in preceding works ([2-5]).

If n is the number of suspended particles for each cm^3 of the suspension before the generation of the ultrasonic waves, this number varies when the ultrasonic waves are generated, and one obtains a distribution represented by

$$n_z = n + \Delta n_0 \cos \alpha z = n + \Delta n_0 \exp [i\alpha z], \tag{1}$$

where $\alpha = 2\pi/\lambda$, n is the statistical mean in these new conditions and z is the coordinate of the considered plane in the propagation direction of the waves.

To a denser gathering of the particles in the nodal planes corresponds a greater value of Δn and, after the stopping of the ultrasounds, a longer time of permanence of the diffracted lines.

At the ceasing of the action of the ultrasonic perturbation, Δn grows less and lesser, and the same happens to the observed optical effects. Equation

$$\Delta n = \Delta n(t) \tag{2}$$

is a function decreasing in time with $\mathrm{d}\Delta n/\mathrm{d}t < 0$.

Among the dinamical causes acting on the particles from the instant of the stopping of the ultrasonic perturbation, one must remember in the first place the osmotic phenomena. One has in effect to postulate also in our suspensions, as in general in solutions and colloids, the existence of an osmotic pression which contributes to the diffusion of the particles from the places of greater concentration to those of lesser concentration, until uniformity is reached everywhere in the liquid.

The sizes of the grains in our suspensions being bigger ($\sim 10^{-4}$ cm) than the dimension of the colloidal particles, the diffusion velocity becomes lesser than in colloidal solutions.

Moreover it must be remembered that up to this point we have always thought these particles to be electrically neutral. On the contrary it has been experimentally proved ([6]) that they are always charged. Most of them are negatively charged when the dispersing medium is water ([7]). If this is assumed, it is clear that the particles accumulated in the nodal planes by the elastic

([2]) A. Carrelli and F. Porreca: *Nuovo Cimento*, **10**, 1406 (1953).
([3]) A. Carrelli and F. Porreca: *Nuovo Cimento*, **1**, 527 (1955).
([4]) F. Fanti and F. Porreca: *Nuovo Cimento*, **1**, 532 (1955).
([5]) F. Porreca: *Nuovo Cimento*, **2**, 904 (1955).
([6]) W. C. Lewis: *Traitè de Chimie Physique* (Paris, 1920).
([7]) Linder and Picton: *Trans. Chem. Soc.*, p. 160 (1892).

waves repel one another and tend therefore to expand uniformly in the liquid medium at the stopping of the ultrasounds.

Starting from these observations we want now to see if it is possible to explain, at least qualitatively, the following experimental facts.

1) It was already observed, by us ([4]) and by others (*) also, that the grating permanence effect takes place in the case of water or alcohol as dispersing medium (polyatomic liquids which produce molecular associations ([8])) and fails in the case of C_6H_6 or CH_4 as dispersing medium (polyatomic liquids which do not produce molecular associations ([8])). Now the structural distinction between both liquid categories consists in the fact that only the first one contains free electric dipoles and therefore the grating permanence effect can take place only in this case, because the suspended particles are surrounded by free dipoles and consequently in their whereabouts the refractive index becomes different from the one of the pure liquid.

On the basis of this assumption, the particles gathered by the ultrasounds in parallel planes distant $\lambda/2$ from each other, at the stopping of the ultrasonic waves produce *a phase grating* of the same periodicity, until thermal and mechanical causes do not equalize everywhere in the liquid the particles' concentration and consequently the refractive index.

Such an interpretation fails if one does not assume the particles as electrically charged and therefore the presence of the effect in these conditions proves that the particles in suspension must be electrically charged.

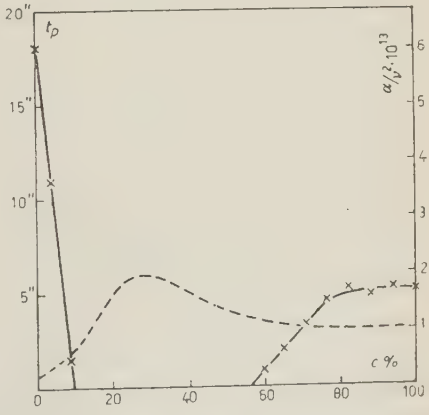

Fig. 1.

2) Continuing the subject further, we are led to investigate the diffracted lines permanence effect in a binary liquid mixture, each of whose constituents produces that effect, as for instance water and an alcohol. In effect, there are some reasons of assuming that such mixtures contain molecular associations ([9]), expecially at some characteristic concentrations. In other words this fact means that the dipoles of the mixture constituents can associate and consequently the permanence effect in this condition must decrease.

The results of the effect in a starch suspension of a water-ethyl alcohol

(*) Particularly by the Dr. F. S. GAETA.

([8]) J. M. M. PINKERTON: *Proc. Phys. Soc.*, B **62**, 129 (1949).

mixture are shown in Fig. 1, which gives the duration of the diffracted lines t_p, from the stopping of the ultrasonic waves, against the concentration c of the mixture expressed in percent weigth fraction. The starch concentration is 0.1 g/l, the ultrasounds duration 5 s and the power such as to observe, with the ultrasonic waves, the sixth diffracted line order.

The t_p decreases if the concentration of either constituent increases and the effect fails between $10\% \pm 2.5\%$ and $55\% \pm 5\%$ of c.

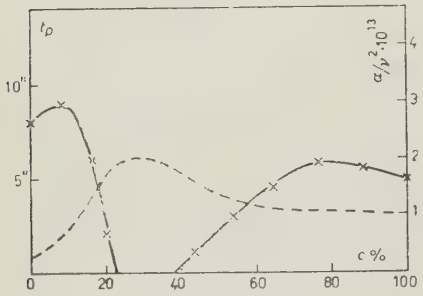

Fig. 2 *a*).

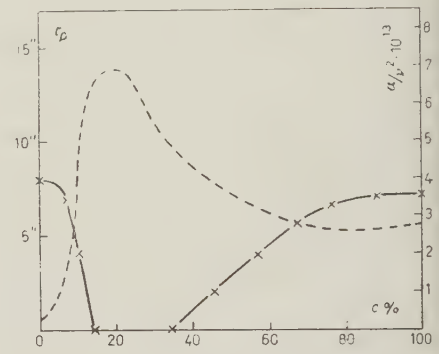

Fig. 2 *b*).

The experimental curves of Fig. 2 have the same interest, showing the t_p variation with c, in the lycopodium suspension of water-ethyl alcohol and water-isopropyl alcohol. In the first (Fig. 2*a*) the effect fails between $22.5\% \pm 2.5\%$ and $38\% \pm 4\%$ of the ethyl alcohol concentration in water. In the second suspension (Fig. 2*b*)) the range of c without effect is $15\% \pm 2.5\%$ and $35\% \pm 5\%$.

Now, it is well known that such water-alcohol suspensions, miscible in all the c values, have the property of a maximal value of the ultrasonic absorption coefficient for a concentration characteristic of the liquid constituents of the mixture ([9-11]).

The concentration value corresponding to the maximal absorption decreases in going from the simplest to the superior alcohols. Moreover, these binary liquid mixtures reach at the same concentration a maximum of the viscosity coefficient η and of the mixing heat ([12]).

The explanation of this behaviour interested many researchers, suggesting the assumption that in those mixtures molecular associations are present, whose equilibrium depends strongly upon the temperature changes of the

([9]) L. R. O. Storey: *Proc. Phys. Soc.*, B **65**, 943 (1952).
([10]) C. J. Burton: *J.A.S.A.*, **20**, 186 (1948).
([11]) D. Sette: *Nuovo Cimento*, **1**, 800 (1955).

ultrasonic waves. Moreover, it seems plausible to establish that the maximum of the absorption coefficient is reached at the concentration of the maximal number of molecular associations ([9-13,14]).

Now, in our researches it is important to observe, from Fig. 1 and 2, that the values of the concentration corresponding to the maximums fall exactly in the concentration range where no diffracted line permanence effect is observed. Therefore, the dotted lines of Fig. 1 and 2*a*) show the behaviour of the ultrasonic absorption coefficient in water-ethyl alcohol, with the maximum at about $c = 30\,\%$ and the dotted line of Fig. 2*b*) shows the ultrasonic absorption coefficient in water-isopropyl alcohol, with the maximum at about $c = 20\,\%$.

It seems also clear that the assumption accepted for explaining the existence of the maximum allows us to justifie the disappearance of the diffracted line permanence effect: in fact, as around this concentration the maximum molecular association is reached, the liquid becomes practically apolar, i.e. deprived of free dipoles, from whence the formation of the phase grating around the suspended particles, gathered in the nodal planes by the ultrasounds, is not possible.

3) In order to the previous assumptions, it is also to be foreseen that the duration t_p of the grating permanence effect depends upon the presence of ions in the suspension under examination: these, in fact, can block up some dipoles of the liquid and consequently cause a decrease of the effect.

In this aim, we are studying the effect in a suspension of particles in electrolytic solutions and at present the first results with starch in the aqueous solutions of NaCl, KCl and $HgCl_2$ are shown. Fig. 3 shows the experimental curves of the duration t_p of the diffracted lines against the concentration of the electrolytic solutions, until saturation. The starch concentration is 0.075 g/l.

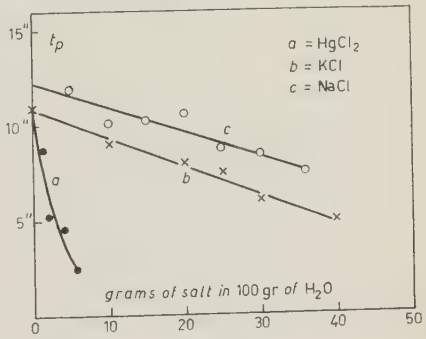

Fig. 3.

These curves show, as was foreseen, a decrease of t_p with the increase of the salt concentration and, hence, with the increase of the number of the ions in solution, giving the most direct proof that the studied effect depends upon the electric charges present in the suspensions.

([12]) *International Critical Tables*, vol. V, p. 22 (1928).
([13]) P. Pashad: *Ind. Journ. Phys.*, **15**, 323 (1941); *J.A.S.A.*, **20**, 66 (1948).
([14]) J. R. Parkington: *Advanced Treatise on Physical Chemistry*, **2**, 115 (1951).

The decreasing behaviour of t_p with the increasing of c is explained with the fact that the number of the free dipoles disposable for the starch particles becomes less with the presence of the ions. These also, in effect, attract some free dipoles and cause a decrease in the number of those which, around the particles in suspension, give the phase grating with the ultrasounds.

The work is progressing with the aim of a quantitative examination of the contents of this paper.

* * *

We wish to express many thanks to the Prof. Antonio Carrelli for his precious suggestions and material help.

RIASSUNTO

Si mettono in evidenza alcuni fatti sperimentali che permettono di attribuire a cause di natura elettrostatica un ruolo importante nella formazione del reticolo di fase, che si forma nelle sospensioni attraversate dagli ultrasuoni e che persiste al cessare di questi. Si osserva, infatti, che l'effetto si ha nelle sospensioni di liquidi polari e manca in quelli apolari. Inoltre nelle sospensioni di miscele di liquidi, che da soli presentano l'effetto, questo viene a mancare nel range di concentrazione in cui si ha motivo sufficiente di ritenere che si formi il massimo numero di associazioni molecolari. Infine si dànno i primi risultati del tempo di permanenza delle righe diffratte, al cessare degli ultrasuoni, in sospensioni di amido in soluzioni elettrolitiche, che mostrano una diminuzione dell'effetto al crescere della concentrazione degli ioni in soluzione. In accordo con questi fatti sperimentali, ci sembra conseguente affermare che si ha l'effetto di permanenza quando le particelle in sospensione possono circondarsi di dipoli liberi del liquido, in modo da presentare nel proprio intorno una zona ad indice rifrangente diverso da quello proprio del liquido. In questo modo le particelle, ordinate dal regime di onde stazionarie ultrasonore in piani equidistanti di $\lambda/2$, generano un proprio reticolo di fase, della stessa periodicità.

Investigations on the β-Decay of $^{208}_{81}$Tl(ThC″).

F. Demichelis, R. A. Ricci and G. Trivero

Istituto di Fisica Sperimentale del Politecnico - Torino

(ricevuto il 12 Dicembre 1955)

Summary. — The β-spectrum of $^{208}_{81}$Tl has been investigated by the following experimental methods: the absorption method, the β-γ coincidence technique and the grey wedge oscillographic method. The experimental results show the existence of a new β-transition with maximum energy 2.37 MeV from the ground state of $^{208}_{81}$Tl to the first excited state of $^{208}_{82}$Pb. Its relative intensity (branching ratio) is ≈ 1.5 % of the disintegrations of $^{208}_{81}$Tl. The 2.37 MeV β-transition is followed by a 2.62 MeV γ-ray. Moreover our research finds the already known β-transition of maximum energy 1.79 MeV and detects β-transitions of maximum energy 1.28 MeV; 1.52 MeV which were supposed by other authors, but hitherto not yet experimentally verified. At the same time, we notice the existence of a β-branch of maximum energy (2.15 ± 0.11) MeV; it must be assigned to $^{212}_{83}$Bi (value already known: 2.25 MeV) which is present with $^{208}_{81}$Tl in our radioactive source ($^{228}_{90}$RdTh in equilibrium with its decay products). In conclusion the degree of forbiddeness of the higher energy components (2.37 MeV; 2.25 MeV; 1.79 MeV) is discussed.

1. – Introduction.

This paper contains a further report on the experimental set of researches dealing with the decay schemes of some heavy naturally radioactive nuclei. In these pages we consider the β-decay of $^{208}_{81}$Tl.

Several authors (1) have already investigated the β-disintegrations of $^{228}_{90}$RdTh decay products. However the experimental results are not numerous.

(1) J. A. Chalmers: *Proc. Camb. Phil. Soc.*, **25**, 331 (1929); W. J. Henderson: *Proc. Roy. Soc.*, A **147**, 572 (1934); R. Arnoult: *Ann. de Phys.*, **11**, 12, 241 (1939); K. Siegbahn and A. Johansson: *Ark. Mat. Ast. Fys.*, **34** A, 10 (1946); D. G. E. Martin.

Among the $^{228}_{90}$RdTh decay products, $^{212}_{83}$Bi(ThC) decays either by emitting β-particles to form $^{212}_{84}$Po(ThC′) (66%) or by emitting α-particles to form $^{208}_{81}$Tl(ThC″) (34%).

$^{208}_{81}$Tl (half-life $t_{\frac{1}{2}} = 3.1$ min) decays by emitting β-particles to form $^{208}_{82}$Pb(ThD) in several excited states.

The latter reaches the stable ground state by emitting γ-rays.

We are aware of the following experimental data about the decay of $^{208}_{81}$Tl:

1) a β-branch with an upper energy limit (maximum energy) ranging between 1.72 and 1.82 MeV, according to the various authors ([1,2]); the value assumed up to date is 1.79 MeV. $^{208}_{81}$Tl by this β transition gives $^{208}_{82}$Pb in the second excited state;

2) a 2.62 MeV γ-ray from the first excited state to the ground state of $^{208}_{82}$Pb with 100% relative intensity (number of quanta per β-disintegration of $^{208}_{81}$Tl) ([3,4]);

3) a γ-γ cascade (0.58 MeV − 2.62 MeV) from the 3.2 MeV excited state to the ground state of $^{208}_{82}$Pb ([4]);

4) other γ-rays emitted in such a manner that the decay scheme should assume the form of Fig. 1 ([5]).

It follows from this and similar proposed decay schemes that, besides the β-transition 1), other ones are present from the $^{208}_{81}$Tl ground state to the several excited states of $^{208}_{82}$Pb.

From Fig. 1, which includes the results of various authors ([3-5]) we must deduce that the β-transitions to the excited levels having an energy higher than 3.2 MeV, are certainly existent, though not experimentally verified. These transitions are represented in Fig. 1 by dashed straight lines.

Moreover, β-transitions to the levels having an energy lower than 3.2 MeV,

---

H. O. W. Richardson and Y. K. Hsü »: *Proc. Phys. Soc.*, **60**, 466 (1948); H. O. W. Richardson: *Nature*, **161**, 516 (1948); D. G. E. Martin and H. O. W. Richardson: *Proc. Roy. Soc.*, A **195**, 287 (1948); N. Feather, J. Kyles, and R. W. Pringle: *Proc. Phys. Soc.*, **61**, 466 (1948); L. G. Elliott, L. G. Graham, R. L. Walker and J. L. Wolfson: *Phys. Rev.*, **93**, 356 (1954).

([2]) J. Surugue: *Journ. de Phys. et le Rad.*, (8), **7**, 146 (1946).

([3]) G. D. Latishev: *Rev. Mod. Phys.*, **19**, 132 (1947); D. G. E. Martin and H. O. W. Richardson: *Proc. Phys. Soc.*, **62**, 223 (1950).

([4]) H. O. W. Richardson: *Nature*, **161**, 516 (1948); H. E. Petch and N. W. Johns: *Phys. Rev.*, **80**, 478 (1950); L. G. Elliott, L. G. Graham, R. L. Walker and J. L. Wolfson: *Phys. Rev.*, **93**, 356 (1954).

([5]) *Nuclear Data National Bureau Standards*; J. W. Weale: *Proc. Phys. Soc.*, **68**, 35 (1955).

if existent, should not have a relative intensity (branching ratio) higher than 2% according to MARTIN, RICHARDSON and HSÜ [1].

According to WEALE [5] (private communication by J. WALKER), ELLIOTT and WOLFSON should have detected a weak β-transition to the 2.62 MeV level of $^{208}_{82}$Pb.

This transition is represented in Fig. 1 by a dotted and dashed straight line.

The aim of our research is the experimental investigation of the $^{208}_{81}$Tl β-spectrum in order to verify the existence and to determine, if possible, the relative intensitj of the β-transitions from the ground state of $^{208}_{81}$Tl to the excited states of $^{208}_{82}$Pb.

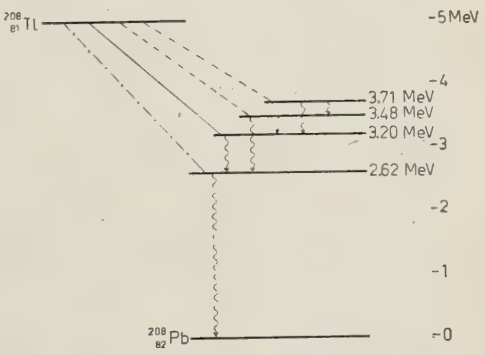

Fig. 1. – Decay scheme of $^{208}_{81}$Tl. The continuous straight line indicates the β-transition already experimentally verified. Dashed lines indicate β-transitions supposed by the existence of the associated γ-levels. Dashed and dotted line indicates the β-transition, whose existence was uncertain. This transition, as well as the other β-transitions indicated in the scheme, have been experimentally determined as described in this paper.

2. – Experimental methods.

We have used a $^{228}_{90}$RdTh source (about 10 microcurie) in equilibrium with all of the decay products.

The very thin layer of radioactive deposit was enclosed between two lucite discs (0.1 mm thick).

Our experiments were designed to investigate the β-spectrum and the β-γ coincidences of the decay products of $^{228}_{90}$RdTh.

2·1. *β-spectrum.* – Two experimental methods have been used in order to determine the endpoint energy of the entire β-spectrum: the absorption and the grey wedge oscillographic methods.

2·1.1. Absorption method. – First of all, we have measured the entire β-absorption curve by placing aluminium absorbers of various thicknesses, between the source and the β detector.

As β detector we used a stilbene crystal (thickness ≈ 3 mm, diameter ≈ 13 mm) and a 6291 DuMont photomultiplier. The output pulses, conveniently amplified and thereafter shaped, are counted by a suitable scaler

We took particular care to achieve those geometrical arrangements in order to minimize scattering and other secondary effects ([6]).

We have also measured, as necessary, the background absorption curve with the source covered by 9 mm beryllium corresponding to 1.63 g/cm² (all the β-particles are absorbed) in order to identify with sufficient accuracy the absorption endpoint. Also the weak absorption of the γ-rays in beryllium was taken into account.

The random fluctuations of the threshold of the pulse shaper do not appreciably influence the experimental results, because the output pulses, as indicated above, are conveniently amplified. The usual procedure has been used to get normalized experimental data.

2·1.2. Grey-wedge method. – The maximum energy of the entire β-spectrum has been also determined by the grey wedge method.

As β-detector we used a stilbene crystal (thickness $\approx$ 13 mm, diameter $\approx$ 13 mm) and a 6291 DuMont photomultiplier. This detector is sketched in Fig. 2 and acts as a proportional β counter ([7]).

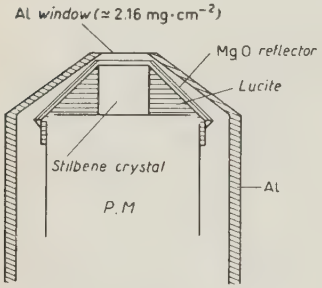

Fig. 2.

The pulses from the photomultiplier are linearly amplified and lengthened, so that the pulse flat top lasts for $\approx$ 5 μs, and then are fed to the vertical deflection plates of a wide band oscillograph.

The oscillographic screen is normally dark and the grid that drives the intensity of the cathode ray beam is triggered above the cut-off by an external pulse, that corresponds to each recorded β-particle.

On the oscillographic screen every pulse gives rise to a horizontal straight line as a spectral line whose height (distance from the straight line to the horizontal time axis) is proportional to β energy.

A grey wedge (optical density 0.7 ÷ 3) is placed on the screen in such a way that the isodensity lines are perpendicular to the spectral lines.

The differential spectrum obtained is photographed for a time corresponding to a photographic action of $\approx$ 100000 pulses.

This technique is substantially similar to that already used for γ spectroscopy ([8]).

([6]) P. E. Cavanagh: *Progress in Nuclear Physics*, Editor Frisch, I, 140 (London, 1950); L. Katz and A. S. Penfold: *Rev. Mod. Phys.*, **24**, 28 (1952).

([7]) D. Maeder and P. Staehelin: *Helv. Phys. Acta*, **28**, 193 (1955).

([8]) F. Demichelis and R. Malvano: *Nuovo Cimento*, **12**, 358 (1954); B. Chinaglia and F. Demichelis: *Nuovo Cimento*, **5**, 51 (1956).

We have used a hard emulsion (Duplo Pan); the γ pulses (background of the β detector) were not recorded by the film.

The determination of the endpoint energy of the $^{228}_{90}$RdTh spectrum is made possible by comparing this spectrum with those obtained from $^{60}_{27}$Co ($E_0 = 0.32$ MeV), $^{204}_{81}$Tl ($E_0 = 0.765$ MeV), $^{226}_{88}$Ra, in equilibrium with its decay products ($E_0 = 3.17$ MeV), in the identical conditions of time exposure and number of pulses.

2·2. β-γ *coincidences.* – In order to identify the maximum energy of the β transitions followed by γ-rays, we used the β-γ coincidence technique. The experimental apparatus is similar to that used in previous experiments [9].

2·2.1. Absorption method. – First we measured the β-γ coincidence absorption curve (the background coincidence curve is obtained by covering the source with the beryllium absorber).

As β detector we used the above indicated non proportional detector. As γ detector we used a NaI(Tl) crystal (thickness ≈ 20 mm; diameter ≈ 20 mm) and a 6292 DuMont photomultiplier.

The resolving time of the coincidence circuit was: $\tau = 3.25 \cdot 10^{-7}$ s.

2·2.2. Grey wedge method. – Second, the grey wedge method was used with the proportional detector in order to photograph the coincidence differential β-spectrum. The β pulses from the photomultiplier are fed to the oscillograph in the same manner as described above. The grid that drives the intensity of the cathode ray beam is triggered, in this case, by the pulses from the coincidence circuit.

3. – Experimental results.

Fig. 3. shows the β absorption curve. The number n_β of recorded pulses is represented against the absorber thicknesses (mm of aluminium). The continuous line represents the total number of pulses; the dashed line represents the background obtained as above stated. The margin of errors in the experiment is less than 2%.

It can be seen that the absorption endpoint (intersection of the total curve with the background curve) is between 3.9 and 4.3 mm of aluminium corresponding to a maximum energy between 2.25 MeV and 2.40 MeV according to the Flammersfeld relationship [10].

---

[9] R. A. Ricci and G. Trivero: *Nuovo Cimento*, **2**, 745 (1955).
[10] A. Flammersfeld: *Zeits. f. Naturforsch.*, **24**, 370 (1947).

A better determination of the end point energy has been obtained making use of the KATZ-PENFOLD method (6).

Fig. 4 shows $(y/f)^{1/n}$ against the β energies for the two most energetic β-branches; y is the fractional transmission and f a correction factor.

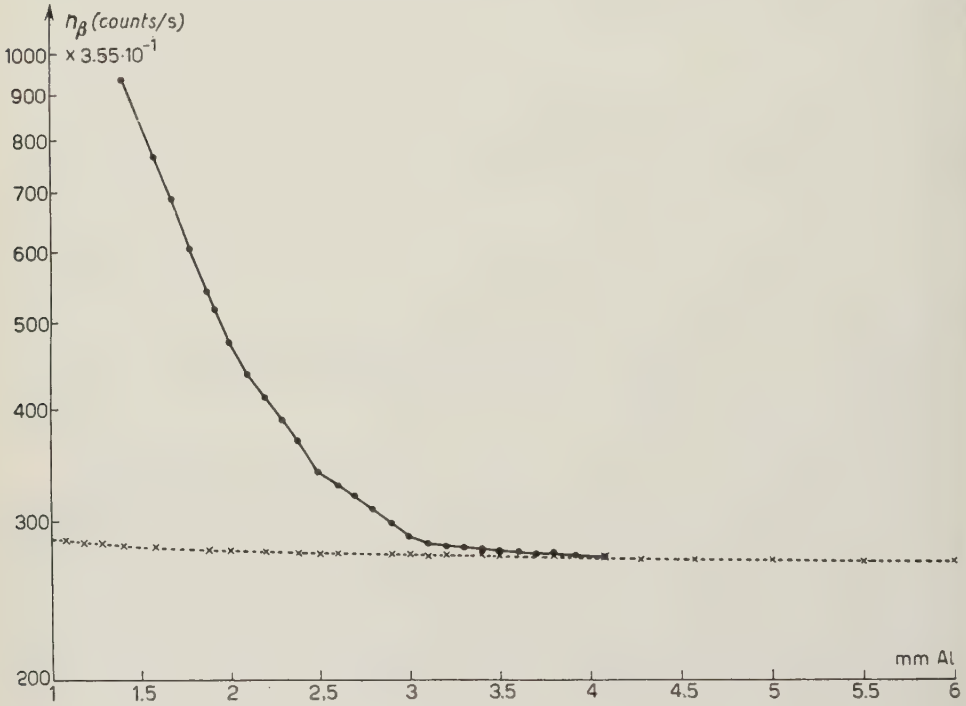

Fig. 3.

For the highest energy component we have obtained as maximum energy the value (2.38 ± 0.08) MeV; while the second component would have an energy (2.15 ± 0.11) MeV.

Fig. 5 shows the spectrograms obtained by means of the grey wedge method; these spectrograms represent the differential spectra of the β pulses against the energy.

In Fig. 5 *a*) *b*) *c*) respectively, are shown: the β-spectrum of $^{204}_{81}$Tl ($E_0 = 0.765$ MeV); the β-spectrum of $^{226}_{88}$Ra in equilibrium with its decay products ($E_0 = 3.17$ MeV); and the β-spectrum of the $^{228}_{90}$RdTh in equilibrium with its decay products.

Comparing this spectrum with those of $^{204}_{81}$Tl and of $^{226}_{88}$Ra, and assuming the linearity on the energy axis it can be seen that it should have an endpoint energy $(2.38 \pm .011)$ MeV in agreement with the value found by the absorption method.

Therefore, we may assume that the upper energy limit of the β transitions relative to the decay products of $^{228}_{90}$RdTh has a value ≈ 2.38 MeV.

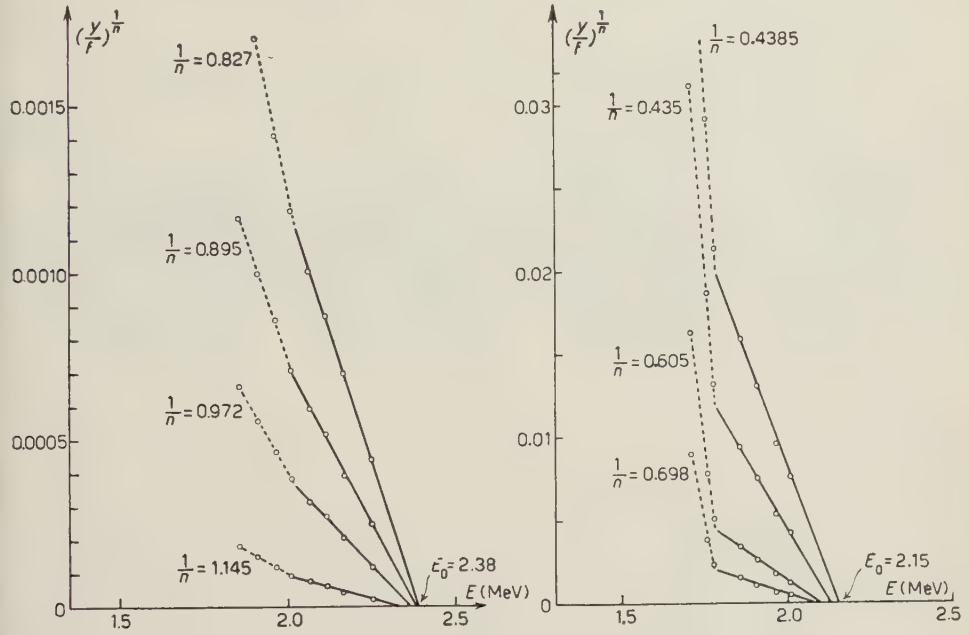

Fig. 4.

The $^{228}_{90}$RdTh decay products, which disintegrate by emitting β-particles are:

$^{212}_{82}$Pb for which the maximum β energy, corresponding to the ground to ground transition, has a value 0.582 MeV (1);

$^{212}_{83}$Bi (66%) with a maximum β-energy 2.25 MeV (transition from the ground state of $^{212}_{83}$Bi to the ground state of $^{212}_{84}$Po) (1);

and $^{208}_{81}$Tl.

The β-transition with energy ≈ 2.38 MeV must, therefore, be present in

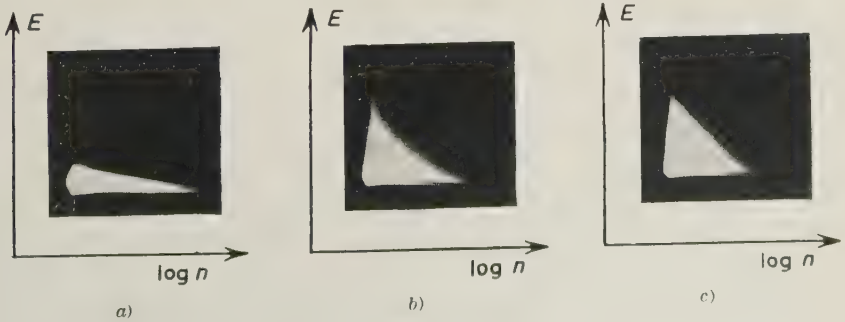

Fig. 5.

the decay of the latter, and it is reasonable to assume that it corresponds to the transition from the ground state of $^{208}_{81}$Tl to the first excited state of $^{208}_{82}$Pb.

A support of this assumption is the existence of β-γ coincidences between a 2.38 MeV β-branch and a 2.62 MeV γ-ray.

This has been experimentally verified, as described below.

From the decay scheme of Fig. 1 we can deduce that the 1.79 MeV β-transition is followed by γ-rays and consequently β-γ coincidences exist associated with this β-transition.

Since the β-transitions, having an energy higher than 1.79 MeV, are only the 2.25 MeV β-transition of $^{212}_{83}$Bi (not followed by γ-rays) and the 2.38 MeV β-transition of $^{208}_{81}$Tl, the determination of the β-γ coincidence endpoint via the absorption method, is sufficient to verify that the 2.38 MeV β-transition is followed by the 2.62 MeV γ-ray.

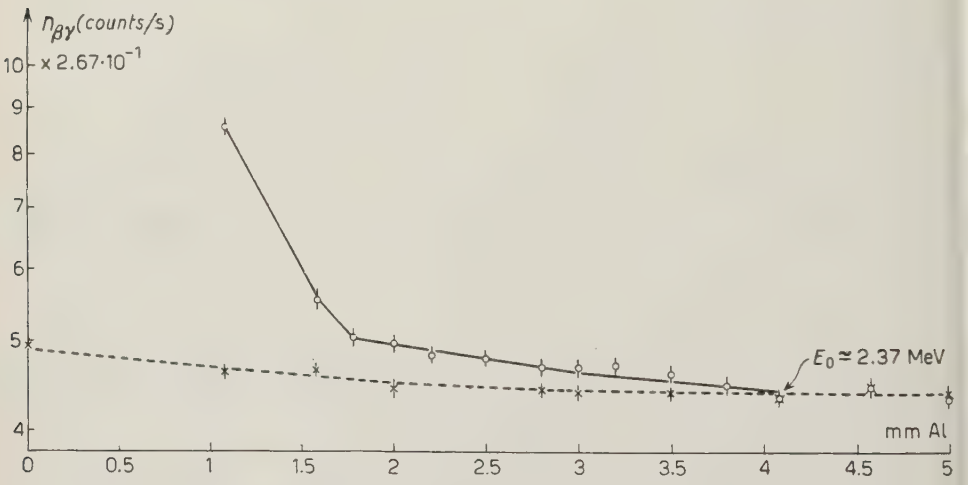

Fig. 6.

In Fig. 6 is plotted the β-γ coincidence absorption curve; the number $n_{\beta\gamma}$ of the effective coincidence pulses is represented against the absorber thicknesses (mm of aluminium).

In this diagram the experimental points are indicated with their probable errors.

The continuous line represents the total absorption curve, dashed line represents the background curve.

From Fig. 3 and Fig. 6 it can be seen that the coincidence endpoint is, within the margins of errors indicated, the same endpoint of the β absorption curve.

The value found for the β-γ coincidence upper energy limit is (2.37 ±0.16) MeV

Assuming that the total disintegration energy ($^{208}_{81}$Tl → $^{208}_{82}$Pb) is 4.99 MeV

(see Fig. 1) and since the energy value of the γ-ray from the first excited state to the ground state of $^{208}_{82}$Pb has been definitively determined (2.62 MeV), we can deduce that the acceptable energy value of the identified β-transition is 2.37 MeV.

The grey wedge method described in § 2.2 has also been used.

Fig. 7 shows:

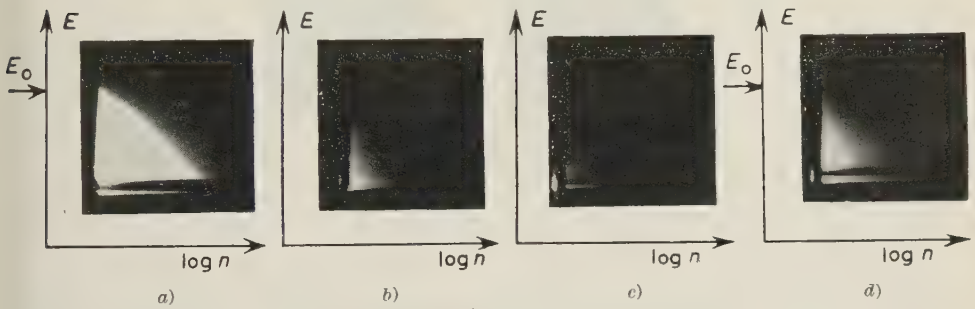

a) *b*) *c*) *d*)

Fig. 7.

a) the differential β-spectrum of $^{228}_{90}$RdTh, which has been obtained in a similar manner as the spectrograms of Fig. 5 (single spectrum);

b) the same β-spectrum, when the grid which drives the cathode ray beam is triggered by the total coincidence pulses (total coincidence spectrum);

c) the same spectrum obtained as in *b*) by adding the beryllium absorber on the source (background coincidence spectrum); we can immediately observe that the effect of the background coincidences is negligible;

d) the β-spectrum obtained when the grid is triggered by the accidental coincidence pulses (accidental coincidence spectrum).

The accidental coincidences are obtained by using two independent sources, one placed above each of the two detectors, conveniently separated from one another. The number of the pulses detected by each counter was the same as in the case of Fig. 7 *b*).

All of the spectrograms of Fig. 7 are obtained with the identical degree of brightness of the oscillographic patterns, using the same photographic diaphragm, and with the same exposure time corresponding to ≈ 160000 pulses from the the coincidence circuit.

Comparing Fig. 7-*a* and Fig. 7-*b* we can deduce that the total coincidence spectrum has the same endpoint energy (≈ 2.38 MeV) as the single β-spectrum.

We can observe in Fig. 8-*a* the total coincidence spectrum, when a suitable aluminium thickness, which stops all the β-particles having an energy lower than 1.8 MeV, is placed between the source and the β detector.

Fig. 8-*b* shows the same spectrum as in Fig. 8-*a* when the source is covered with the beryllium absorber.

In both cases the accidental coincidence pulses did not darken the film.

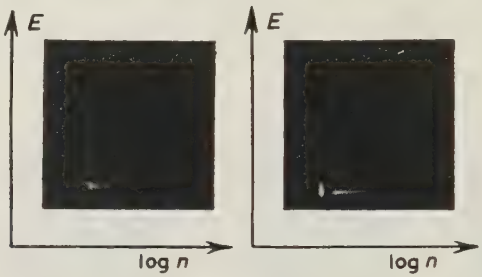

a) *b*)

Fig. 8.

Fig. 8-*a* and 8-*b*, although the films are only slightly darkened, confirm again the existence of β-γ coincidences relative to β-transitions having energy higher than 1.8 MeV.

4. – Discussion.

From the experimental results of § 3, we may deduce that:

1) either no transition or a very weak β-transition ($< 1\%$) from the ground state of $^{208}_{81}$Tl to the $^{208}_{82}$Pb ground state is present;

2) a 2.37 MeV β-transition to the first excited state of $^{208}_{82}$Pb certainly exists. This β-transition is followed by a 2.62 MeV γ-ray.

With a more complete analysis of the β absorption curve by the $f - n$-th power method it is possible to identify other β-branches and to determine the relative intensities (branching ratios) of the higher energy components.

This analysis is reproduced in Fig. 9. The plot of $(y/f)^{1/n}$ against the energy is obtained from the β absorption curve (the background curve was subtracted from the total absorption curve of Fig. 3) and from the fourth approximation used to determine the endpoint energy of the $^{228}_{90}$RdTh β-spectrum.

The relative intensity of the 2.37 MeV β-transition should be $\approx 1.50\%$ of the $^{208}_{81}$Tl β-disintegrations.

The (2.15 ± 0.11) MeV β-branch, corresponding with reasonable certainty to the 2.25 MeV β-transition from the ground state of $^{212}_{83}$Bi to $^{212}_{84}$Po ground state, should have, according to our analysis, a relative intensity $\approx 2.6\%$ (this intensity is referred to the $^{212}_{83}$Bi β-disintegrations).

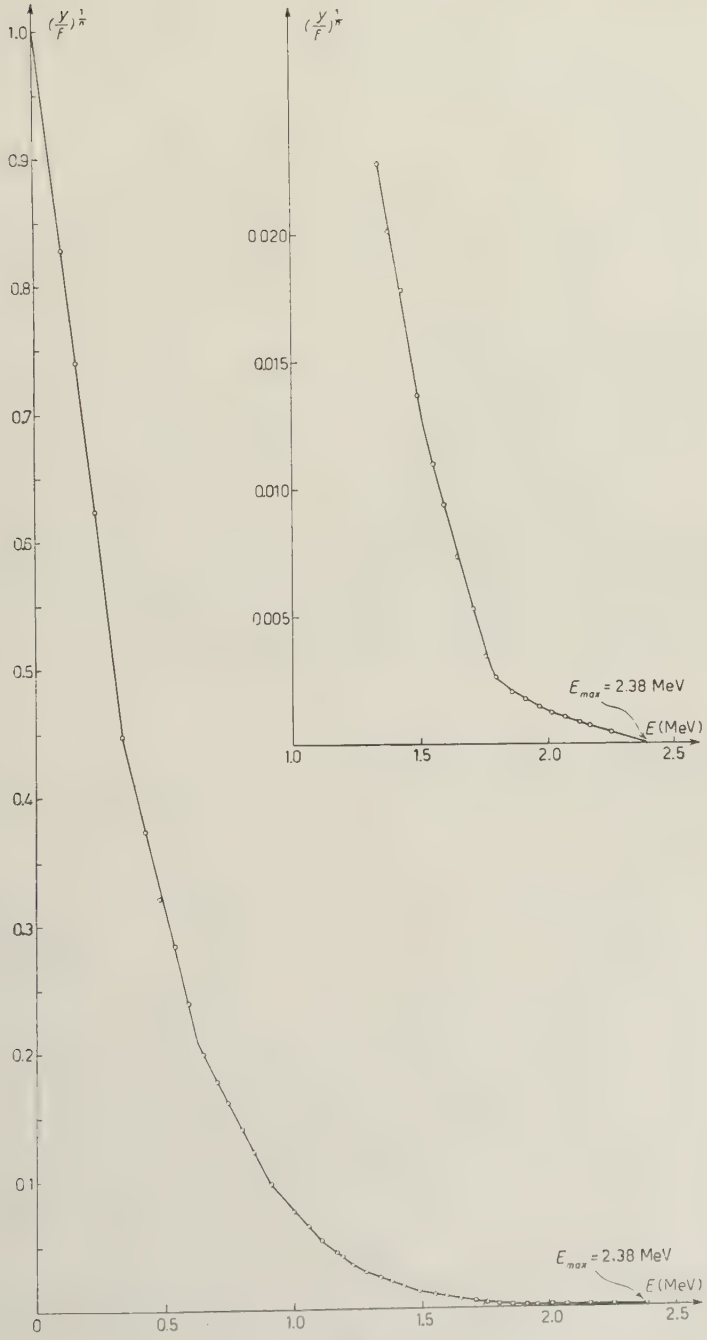
$(\frac{Y}{F})^{\frac{1}{\pi}}$
1.0
0.9
0.8
0.7
0.6
0.5
0.4
0.3
0.2
0.1
0
0.5
1.0
1.5
2.0
2.5
E_{max} = 2.38 MeV
E (MeV)
$(\frac{Y}{F})^{\frac{1}{\pi}}$
0.020
0.015
0.010
0.005
1.0
1.5
2.0
2.5
E_{max} = 2.38 MeV
E (MeV)

Fig. 9.

The 1.79 MeV β-branch of $^{208}_{81}$Tl, suggested by the shape of the curve of Fig. 9, should have a relative intensity $\approx 22\%$ of the $^{208}_{81}$Tl β-disintegrations.

The breaks in the $(y/f)^{1/n}$ plot indicate the presence of other β-branches having the following energies: 1.52 MeV; 1.25 MeV; 1.12 MeV; 0.91 MeV; 0.63 MeV; 0.34 MeV.

These β-branches correspond to β-transitions of the nuclides $^{212}_{82}$Pb, $^{212}_{83}$Bi, $^{208}_{81}$Tl.

More specifically the β-branches 1.52 MeV, 1.25 MeV, 0.63 MeV, 0.34 MeV agree with the values of the β-transition energies, already known from the existence of the γ-levels ([1]).

These β-transitions are:

1.53 MeV ($^{212}_{83}$Bi); 1.51 MeV ($^{208}_{81}$Tl);

1.28 MeV ($^{208}_{81}$Tl); 0.64 MeV ($^{212}_{83}$Bi);

0.344 MeV ($^{212}_{82}$Pb).

In conclusion if we take into account the values of the relative intensities, as indicated above, of the 2.37 MeV and 1.79 MeV transitions of $^{208}_{81}$Tl, and 2.25 MeV of $^{212}_{83}$Bi, we can deduce, according to Moszowski's method ([11]), the values of $\log ft$ and of $\log (W_0^2 - 1)ft$.

The results are summarized in Table I.

TABLE I.

Transition Energy	Relative Intensity	Nuclide	$\log ft$	$\log (W_0^2 - 1)ft$	J	Parity Change	Type
2.37 MeV	1.5 %	$^{208}_{81}$Tl	7.72	9.1	0 or 1 or 2	yes	First forbidden or unique first forb.
1.79 MeV	22 %	$^{208}_{81}$Tl	5.9	—	0 or 1	yes	First forbidden
2.25 MeV	2.6 %	$^{212}_{83}$Bi	8.63	9.9	2	yes	Unique first forbidden

* * *

We should like to express our thanks to Prof. E. PERUCCA for his helpful interest.

([11]) S. A. MOSZOWSKI: *Phys. Rev.*, **82**, 35 (1951).

This research, as well as its previous developments, were made possible by the financial support of Consiglio Nazionale delle Ricerche. This valued aid enables us to make use in our researches of a first class oscilloscope. For this the authors wish to express their gratitude and appreciation.

RIASSUNTO

Lo spettro del $^{208}_{81}$Tl è stato studiato con il metodo dell'assorbimento, con la tecnica delle coincidenze β-γ, e con l'esame di spettrogrammi ottenuti all'oscillografo, facendo uso di un cuneo neutro. La sorgente radioattiva usata era $^{228}_{90}$RdTh, in equilibrio con i suoi prodotti di decadimento. I risultati ottenuti mostrano l'esistenza di una transizione β di energia 2.37 MeV dallo stato fondamentale del $^{208}_{81}$Tl al primo stato eccitato del $^{208}_{82}$Pb; questa transizione avrebbe una intensità (branching ratio) di $\approx$ 1.5 %, ed è seguita dal raggio γ di 2.62 MeV. Si è confermata inoltre l'esistenza della transizione 1.79 MeV (intensità $\approx$ 22 %) e delle due transizioni 1.51 MeV, 1.28 MeV, queste ultime note dall'esistenza dei livelli γ associati. Si è determinata una transizione β (2.15±0.11) MeV da ascriversi al decadimento del $^{212}_{83}$Bi, di intensità pari al 2.6 % delle disintegrazioni del $^{212}_{83}$Bi. Il valore dell'energia trovato è in accordo con il valore 2.25 MeV determinato da altri autori. Si discute infine il tipo delle transizioni 1.79 MeV e 2.37 MeV del $^{208}_{81}$Tl e della transizione 2.25 MeV del $^{212}_{83}$Bi.

A Simple Non-Local Quantum Electrodynamics.

P. Sen (*)

Dehra Dun, India

(ricevuto il 12 Dicembre 1955)

Summary. — The Dirac-Maxwell equations are modified, according to Wataghin, by displacing the fields at the point of their interaction by introducing displacement parameters. When these parameters, which are taken to be small, tend to zero the original Dirac-Maxwell equations are obtained. The original charge renormalization program, the theory of Feynman « cut-off » and Yukawa's non-local theory of particles with internal structure and the consequent convergent quantum electrodynamics can be considered as special cases of these modified Dirac-Maxwell equations. By combining the methods of these processes a convergent quantum electrodynamics, in which the original Feynman graph integrals are modified by the multiplication of a simple modifying factor, is obtained. This is illustrated by the calculations of second order Feynman graphs. It is then suggested that these equations can be considered to be free from the need of charge renormalization and the actual charge renormalization is due to the use of the Born approximation.

1. – Introduction.

The divergences of the Dirac-Maxwell equations have been eliminated in several independent ways. The most successful treatment which has given quantitative confirmation is that of mass and charge renormalization and has been extensively developed by Schwinger (1), Feynman (2) and Dyson (3). Here all the divergences of the Dirac-Maxwell equations are shown to be contained in physically insignificant terms which can be unambiguously re-

(*) Now at Istituto di Fisica dell'Università, Torino.

(1) J. Schwinger: *Phys. Rev.*, **74**, 1439 (1948); **75**, 651 (1949); **76**, 790 (1949). *Proc. Nat. Acad. Sci.*, **37**, 452, 455 (1951).

(2) R. P. Feynman: *Phys. Rev.*, **76**, 749, 769 (1949).

(3) F. J. Dyson: *Phys. Rev.*, **75**, 486, 1736 (1949).

moved and the remainder is found to be a finite physically significant contribution. However these seperations by means of mass and charge renormalization are complicated processes and there is always a wish to modify the Dirac-Maxwell equations so that the renormalization terms are removed in the beginning or the end and not at intermediate steps of the calculation. To do this FEYNMAN ([2,4]) proposed a « cut off » theory, which was generalized by PAULI and VILLARS ([5]). Here there are no divergences higher than the logarithmic, but the necessity for mass and charge renormalization remains. The finite physically significant contributions are found to be independent of the actual cut off and to have the same values as obtained by the first method. But the modified equations are very different from the original Dirac-Maxwell equations and these alterations do not appear to be justified due to their non physical and purely formal nature and when there is a lack of certainty in the method of approach, as in the meson theory, the original method of renormalization of Schwinger, Feynman and Dyson seems to be preferred. Then YUKAWA ([6]) has suggested that a non-local theory, in which an elementary particle has an internal structure, leads to a non divergent quantum electrodynamics.

To obtain a convergent quantum electrodynamics, WATAGHIN ([7]) has suggested the use of modified Dirac-Maxwell equations obtained by displacing the fields at their point of interaction. Now let us consider such a set of Dirac-Maxwell equations, each of which are modified from the original one by the introduction of a vector parameter. When these parameters are put equal to zero, the original Dirac-Maxwell equations are obtained. Let these additional parameters introduce modifying factors which eliminate all the divergences of quantum electrodynamics. The nature of the parameters is unspecified. They may be chosen within the coordinate field of the original Dirac-Maxwell equations and then they will correspond to a « cut off », or they may be considered to be vectors in an independent set of coordinates and then, in accordance with YUKAWA, they can be taken to represent the internal structure of the electron and the photon. Furthermore let the contributions of the finite physically significant parts be independent of the vector parameters. Thus we obtain for them the values obtained by SCHWINGER, FEYNMAN and DYSON.

Such a hypothesis is stated in § **3** and is illustrated with second order calculations in § **4**. This procedure has the advantage that, due to the unspecified

---

([4]) R. P. FEYNMAN: *Phys. Rev.*, **74**, 1430 (1948).

([5]) W. PAULI and F. VILLARS: *Rev. Mod. Phys.*, **21**, 434 (1949).

([6]) H. YUKAWA: *Phys. Rev.*, **77**, 219 (1950); **80**, 1047 (1950); D. R. YENNIE: *Phys. Rev.*, **80**, 1053 (1950).

([7]) G. WATAGHIN: *Nuovo Cimento*, 8, 592 (1951); *Zeits. f. Phys.*, **88**, 92 (1934).

nature of the parameters, we can follow either of the three methods as a guide and check to our calculations and can combine the advtanages of all of them into a single development. Thus if we put the parameters equal to zero we find ourselves dealing wtih the original Dirac-Maxwell equations and, for the second order Feynman graphs, with the calculations of KARPLUS and KROLL [8]. But with small finite values of the vector parameters all the terms become finite and the renormalization can be deferred to the end of the calculations. By means of this we find that the infrared divergences of the KARPLUS and KROLL calculations are due to the necessity of an early separation of the divergent terms and can easily be avoided. Then when working analogously to the « cut off » theory [4,5] we can adopt the auxiliary Yukawa conditions without referring to the internal coordinates and use them instead of the PAULI and VILLARS regularization scheme to obtain conservation of charge and gauge invariance. Thus the physical significance of these parameters remains undecided and this problem has been discussed by WATAGHIN [9].

Of course in an ideal theory of the electromagnetic field there should be no use of the renormalization program. We will find that it is possible to take a step towards this because the absolute value of the vector parameters remains quite arbitrary in the statement of § **4**. Then we can choose these absolute values so that the second order vacuum charge renormalization and the charge renormalization due to the second order electron self energy Feynman graph are zero. Then there is only vertex charge renormalization for the second order graphs. Of course this is only implicit since the second order electron self energy and vacuum polarization charge renormalization expressions are actually found and then those values of the arbitrary parameters are chosen which make these expressions zero. Now we may choose those values for these constants which make the sum total of charge renormalization for all orders of electron self energy and vacuum polarization zero. Then utilizing Dyson's conjecture [3,10], that the total charge renormalizations for the electron self energy and vertex graphs are Z_2 and $1/Z_2$ respectively, the modified Dirac-Maxwell equations can be considered to be free of charge renormalization and the actual charge renormalization in the second order calculations can be considered to be due to the use of the Born approximation in them.

2. – The General Propagation Operators.

In this section we shall introduce the notation and state the results of FEYNMAN [2] and SCHWINGER [1], which will show how the Dirac-Maxwell

---

[8] R. KARPLUS and N. M. KROLL: *Phys. Rev.*, **77**, 536 (1950).
[9] G. WATAGHIN: *Nuovo Cimento*, **10**, 1618 (1953); **12**, 103 (1954).
[10] J. C. WARD: *Phys. Rev.*, **78**, 182 (1950).

equations have been modified in the next section, and make more obvious the results obtained from them. Let

$$(1)\quad \begin{cases} H'(x_\mu) = \gamma_\mu \dfrac{\partial}{\partial x_\mu} - i\lambda a'(x_\mu) + \varkappa\,, & \overline{H}'(x_\mu) = \gamma_\mu \dfrac{\partial}{\partial x_\mu} + i\lambda a'(x_\mu) - \varkappa\,, \\ H'^c(x_\mu) = \gamma_\mu \dfrac{\partial}{\partial x_\mu} + i\lambda a'(x_\mu) + \varkappa\,, & \overline{H}'^c(x_\mu) = \gamma_\mu \dfrac{\partial}{\partial x_\mu} - i\lambda a'(x_\mu) - \varkappa\,, \\ H(x_\mu) = \gamma_\mu \dfrac{\partial}{\partial x_\mu} + \varkappa\,, & \overline{H}(x_\mu) = \gamma_\mu \dfrac{\partial}{\partial x_\mu} - \varkappa\,, \\ \lambda = \dfrac{e}{\hbar c}\,, \quad \varkappa = \dfrac{mc}{\hbar}\,, & a'(x_\mu) = \gamma_\alpha A'_\alpha(x_\mu)\,. \end{cases}$$

The barred operators $\overline{H}(x_\mu)$, $\overline{H}'(x_\mu)$ and $\overline{H}'^c(x_\mu)$ are arranged to operate towards the left. Whenever there is no ambiguity the notation (1) for the space time point $x_\mu(1) = (r, ict)$ (1) and (12) for the vector $x_\mu(1) - x_\mu(2)$ is used. The real time coordinate $x_0 = x_4/i = ct$ is also used. Then the Dirac-Maxwell equations are

$$(2)\quad \begin{cases} H'(1)\psi'(1) = 0\,, & \overline{\psi}'(1)\overline{H}'(1) = 0 \\ H'^c(1)\psi'^c(1) = 0\,, & \overline{\psi}'^c(1)\overline{H}'^c(1) = 0 \\ H(1)\psi(1) = 0\,, & \overline{\psi}(1)\overline{H}(1) = 0 \\ \Box^2(1)A'_\mu(1) = -\dfrac{1}{c}\left(j'_\mu(1) + J_\mu(1)\right), & \Box^2 A_\mu(1) = 0\,, \\ \dfrac{\partial}{\partial 1_\mu} A'_\mu(1)\Psi' = 0\,, & \dfrac{\partial}{\partial 1_\mu} A_\mu(1)\Psi = 0 \end{cases}$$

and the Feynman Schwinger propagation operators are defined by

$$(3)\quad \begin{cases} H'(1)K'(1,2) = i\delta(12)\,, & H(1)K(12) = i\delta(12) \\ K'(1,2)\overline{H}'(2) = -i\delta(12)\,, & K(12)H(2) = -i\delta(12) \\ H'^c(1)\overset{c}{K}'(1,2) = -i\delta(12)\,, & H(1)\overset{c}{K}(12) = -i\delta(12) \\ \overset{c}{K}'(1,2)\overline{H}'^c(2) = i\delta(12)\,, & \overset{c}{K}(12)H(2) = i\delta(12) \end{cases}$$

and

$$(4)\quad \begin{cases} L'_{\mu\nu}(1,2) = L'_{\nu\mu}(1,2) \\ \Box^2(1)L'_{\mu\nu}(1,2) = i\hbar c\,\delta_{\mu\nu}(12) + i\hbar c\lambda^2 \int \Pi_{\mu\alpha}(1,3)\,L'_{\alpha\nu}(3,2)\,\mathrm{d}3, \\ \Box^2(2)L'_{\mu\nu}(1,2) = i\hbar c\,\delta_{\mu\nu}(12) + i\hbar c\lambda^2 \int L'_{\mu\alpha}(1,3)\,\Pi_{\alpha\nu}(3,2)\,\mathrm{d}3, \\ \Box^2(1)L_{\mu\nu}(12) = i\hbar c\,\delta_{\mu\nu}(12) = \Box^2(2)L_{\mu\nu}(12)\,, \end{cases}$$

where

$$\Pi_{\mu\nu}(1,2) \quad \mathrm{Tr}\,\gamma_\mu \overset{c}{K}'(1,2)\gamma_\nu K'(2,1) \tag{5}$$

and the integrations in (4) are over the whole $x(3)$ space.

Then the corresponding integral equations are

$$K'(1,2) = K(12) + \lambda\int K(13)a'(3)\,K'(3,2)\,\mathrm{d}3\,, \tag{6}$$

$$\overset{c}{K}'(1,2) = \overset{c}{K}(12) + \lambda\int \overset{c}{K}(13)\,a'(3)\,\overset{c}{K}'(3,2)\,\mathrm{d}3\,, \tag{7}$$

$$L'_{\mu\nu}(1,2) = L_{\mu\nu}(12) + \lambda^2\iint L_{\mu\alpha}(13)\Pi_{\alpha\beta}(3,4)\,L'_{\beta\nu}(4,2)\,\mathrm{d}3\,\mathrm{d}4\,, \tag{8}$$

$$j'_\mu(1) = -\frac{iec}{2}\,\mathrm{Tr}\left\{\gamma_\mu\left(\overset{c}{K}'(2,1) + K'(1,2)\right)\right\}\Big|_{2\to 1} = \tag{9}$$

$$= ice\lambda\int A'_\nu(2)\Pi_{\nu\mu}(2,1)\,\mathrm{d}2 = iec\lambda\int \Pi_{\mu\nu}(1,2)\,A'_\nu(2)\,\mathrm{d}2\,.$$

These Green's operator functions are related to the electron and photon fields by the relations

$$\left.\begin{aligned}
K'_{\alpha\beta}(1,2) &= \begin{cases} \psi'_\alpha(1)\bar{\psi}'_\beta(2) & \text{for} \quad x_0(1) > x_0(2) \\ -\bar{\psi}'_\beta(2)\psi'_\alpha(1) & \text{for} \quad x_0(1) < x_0(2) \end{cases} \\
\overset{c}{K}'_{\alpha\beta}(1,2) &= \begin{cases} \bar{\psi}'^{c}_\beta(2)\psi'^{c}_\alpha(1) & \text{for} \quad x_0(1) > x_0(2) \\ \psi'^{c}_\alpha(1)\bar{\psi}'^{c}_\beta(2) & \text{for} \quad x_0(1) < x_0(2) \end{cases} \\
L'_{\mu\nu}(1,2) &= \begin{cases} A'_\mu(1)A'_\nu(2) & \text{for} \quad x_0(1) > x_0(2) \\ A'_\nu(2)A'_\mu(1) & \text{for} \quad x_0(1) < x_0(2)\,. \end{cases}
\end{aligned}\right\} \tag{10}$$

Then it is known that the expectation values of $K(12)$ and $L_{\mu\nu}(12)$ for the vacuum state Ψ_0 of the free electron and photon fields are

$$(\Psi_0,\, K(12),\, \Psi_0) = \tfrac{1}{2}S_F(12) = -\,(\Psi_0,\, \overset{c}{K}(12),\, \Psi_0) \tag{11}$$

$$(\Psi_0,\, L_{\mu\nu}(12),\, \Psi_0) = \frac{hc}{2}\,\delta_{\mu\nu}D_F(12)\,. \tag{12}$$

Furthermore the transforms in momentum representation of the propagation functions $K(x)$ and $L_{\mu\nu}(x)$ are defined by the relations

$$K(x) = \frac{i}{(2\pi)^4}\int K(p)\,\exp\left[-\,ip\cdot x\right]\mathrm{d}^4x\,, \tag{13}$$

$$L_{\mu\nu}(x) = -\frac{i\hbar^2}{(2\pi)^4}\delta_{\mu\nu}\int L(p)\exp[-ip\cdot x]\,\mathrm{d}^4x \tag{14}$$

and when the expectation value for the vacuum state Ψ_0 of the free electron and photon fields is taken

$$K(p) = \frac{1}{i\gamma p + x}\,, \tag{15}$$

$$L(p) = \frac{1}{p^2}\,. \tag{16}$$

3. – The modified Feynman Propagation Operators.

We shall begin the modifications of the Dirac-Maxwell equations by replacing $A'_\mu(1)$ in the Dirac equation by $A''_\mu(1 - b_e) + A''_\mu(1 + b_e)$. The photon field in the interaction term is displaced by means of a four vector $b_{e,\mu}$ which is assumed to be small. Then in the limit $b_{e,\mu} \to 0$ we obtain the original Dirac equation by letting $A'_\mu(1) = 2A''_\mu(1)$. The modified Dirac equations are:

$$\left\{\begin{aligned}
&H(1)K''(1,2) - i\lambda(a''(1-b_e) + a''(1+b_e))K''(1,2) = i\delta(12)\\
&K''(1,2)\overline{H}(2) + i\lambda K''(1,2)(a''(2-b_e) + a''(2+b_e)) = -i\delta(12)\\
&H(1)\overset{\circ}{K}{}'(1,2) + i\lambda(a''(1-b_e) + a''(1+b_e))\overset{\circ}{K}{}''(1,2) = -i\delta(12)\\
&\overset{\circ}{K}{}''(1,2)\overline{H}(2) - i\lambda\overset{\circ}{K}{}''(1,2)(a''(2-b_e) + a''(2+b_e)) = i\delta(12)
\end{aligned}\right. \tag{17}$$

The modified electron propagation operators are represented by $K''(1,2)$ and replace $K'(1,2)$. Thus the integral equations corresponding to (6) and (7) are:

$$K''(1,2) = K(12) + \lambda\int K(13)(a''(3-b_e) + a''(3+b_e))K''(3,2)\,\mathrm{d}3\,, \tag{18}$$

$$\overset{\circ}{K}{}''(1,2) = \overset{\circ}{K}(12) + \lambda\int \overset{\circ}{K}(13)(a''(3-b_e) + a''(3+b_e))\overset{\circ}{K}{}''(3,2)\,\mathrm{d}3 \tag{19}$$

and when $b_{e,\mu}$ is put equal to zero, they reduce to the original Feynman integral equations.

In order to show the part that the displacements $b_{e,\mu}$ play here, we obtain from (18), as for the Feynman integral equation:

$$\begin{aligned}
K''(1,2) = K(12) &+ \lambda\int K(13)(a''(3-b_e) + a''(3+b_e))K(32)\,\mathrm{d}3 +\\
&+ \lambda^2\iint K(13)(a''(3-b_e) +\\
&+ a''(3+b_e))K(34)(a''(4-b_e) + a''(4+b_e))K(42)\,\mathrm{d}3\,\mathrm{d}4 + \dots
\end{aligned} \tag{20}$$

Here we are interested in the internal electron and photon lines only and wish to obtain such an expression for them, that the divergences of quantum electrodynamics are eliminated without altering the physically significant results. Indeed those $K(x)$ in (6), which represent external lines, have to be replaced by $\bar{\psi}(x)$ or $\psi(x)$. In Feynman's calculations the product $A'_\mu(1)A'(2)$ is replaced by the general propagation operator $L'_{\mu\nu}(1, 2)$. This operator obtains its propagation character through simultaneous absorption and emission at $x_0(1) = x_0(2)$. Now we shall replace this by the hypothesis that the absorption and emission at $x_0(1) = x_0(2)$ actually occur at $x_\mu(1) - b_{e,\mu}$, $x_\mu(2) - b_{e,\mu}$ and $x_\mu(1) + b_{e,\mu}$, $x_\mu(2) + b_{e,\mu}$ respectively. Thus the product $(A''_\mu(1 - b_e) + A''_\mu(1 + b_e)) \cdot (A''_\nu(1 - b_e) + A''_\nu(1 + b_e))$ leads to the propagation operator $L''_{\mu\nu}(1 - b_e\ 2 + b_e) + L''_{\mu\nu}(1 + b_e, 2 - b_e)$ and this replaces the Feynman-Schwinger function $L'_{\mu\nu}(1, 2)$ in our work. We note that when $b_{e,\mu}$ is put equal to zero, $L'_{\mu\nu}(1, 2) = 2L''_{\mu\nu}(1, 2)$.

We first displaced the photon field by means of a four vector $b_{e,\mu}$ and have then stated that when the electron and photon fields interact at the space-time point $x_\mu(1)$ the consequent absorption of the photon is in advance of $x_0(1)$ or the emission is retarded from $x_0(1)$. While this suggests that the electron has an internal structure whose extension is given by the four vector $b_{e,\mu}$ it is not incompatible with a point electron where $b_{e,\mu}$ is a function of the momentum of the electron. We shall show that $b_{e,\mu}$ does not appear in the physical observables and its significance remains undecided here.

Although we have stated our conclusions in the Feynman notation, perhaps a simpler and more direct statement can be given by following the procedure of Dyson [3] and constructing the S-operator from the interaction term

$$(21)\quad H^I(1) = -\frac{1}{2c}\int \bar{\psi}''(1)(a''(1-b_e) + a''(1+b_e))\psi''(1) + \bar{\psi}''^c(1)(a''(1-b_e) + a''(1+b_e))\psi''$$

The two terms in (21) are equivalent and we need to consider twice the first term only. Then the S operator is:

$$(22)\quad S(\infty) = \sum_{n=1}^{\infty}\left(-\frac{i}{\hbar c}\right)^n \frac{1}{n!}\int\ldots\int P(\bar{\psi}(1))a^0(1 - b_e) + a^0(1 + b_e))\psi(1), \ldots$$

$$\ldots, \bar{\psi}(n)(a^0(n - b_e) + a^0(n + b_e))\psi(n))\,\mathrm{d}1 \ldots \mathrm{d}n,$$

where $A^0_\mu(1)$ is the representation of $A''_\mu(1)$ in the interaction representation and we note that $A_\mu(1) = 2A^0_\mu(1)$. We also note that the time ordering in the P product is not influenced by the displacement $b_{e,\mu}$ since it is considered to be a function of coordinates which are independent of the space configuration coordinates. Now we use the hypothesis that in the internal lines $\langle P(A^0_\mu(1 - b_e) + A^0_\mu(1 + b_e), A^0_\nu(2 - b_e) + A^0_\nu(2 + b_e))\rangle_0$ which consists of absorptions and emissions, the absorptions take place at $x_\mu(1) - b_{e,\mu}$ or $x_\mu(2) - b_{e,\mu}$

and the emissions at $x_\mu(1)+b_{e,\mu}$ or $x_\mu(2)+b_{e,\mu}$. Then following the Dyson procedure we obtain the same results as obtained above in the Feynman formulation.

We note that the interaction term (21) does not modify the internal electron lines and the results for closed electron loops will remain unaltered. To modify these also we shall introduce the other displacement parameter $b_{p,\mu}$ to modify the current operator $j'_\mu(1)$. Consider the vector

$$j''_\mu(1, b_p) = -\frac{iec}{4}\operatorname{Tr}\gamma_\mu(K''(1+b_p, 1-b_p) + \overset{o}{K}''(1+b_p, 1-b_p)) , \tag{23}$$

where $b_{p,\mu}$ is the second vector parameter of our theory. Now

$$\operatorname{Tr}\gamma_\mu \frac{\partial}{\partial 1_\mu} K''(1+b_p, 1-b_p) = \operatorname{Tr}\,(a''(1+b_p-b_e) + a''(1+b_p+b_e) - a''(1-b_p-b_e) - a''(1-b_p+b_e))K''(1+b_p, 1-b_p) \tag{24}$$

and in order that the induced current vector be conserved we define it as

$$j''_\mu(1) = j''_\mu(1+b_p) + j''_\mu(1-b_p) . \tag{25}$$

Then we obtain

$$\frac{\partial}{\partial x_\mu} j''_\mu(x_\alpha)\Big|_4 = 0 . \tag{26}$$

When the approximate values of $j_\mu(1)$ are calculated, then in order to maintain the conservation of the current vector it will be necessary to postulate, in the momentum representation, the auxiliary condition

$$b_p \cdot A^0(p) = 0, \qquad b_p \cdot pA^0(p) = 0 . \tag{27}$$

Then we have the Lorentz condition

$$p \cdot A''(p) = 0 . \tag{28}$$

Analogously we can postulate the auxiliary condition

$$(b_e \cdot p)\Psi_0 = 0 . \tag{29}$$

for the electron field.

Such auxiliary conditions are included in Yukawa's non local theory [6] and

replace the regularization conditions of PAULI and VILLARS ([5]) in the « cut off » theory. In the limit of $b_{e,\mu}$, $b_{p,\mu} \to 0$ they vanish and we note that no auxiliary conditions are used by SCHWINGER, FEYNMAN and DYSON. We have determined the conditions (27) to obtain charge conservation and gauge invariance. We note the agreement with Ward's relation ([10])

$$\sum_{V^i} \Lambda_\mu(V^i, p, p) = -\frac{1}{2\pi} \frac{\partial}{\partial p_\mu} \sum (W, p) . \tag{30}$$

Here $\sum (W, p)$ is the contribution of a proper self energy graph W and $\Lambda_\mu(V^i, p, p)$ is the contribution of a vertex graph V^i obtained by inserting a photon line of zero energy and momentum in any of the electron lines. $\Lambda_\mu(V^i, p, p)$ is summed over all V^i. It is shown in the next section that the auxiliary conditions satisfy these requirements for the second order Feynman graphs. However the relation suggested by KARPLUS and KROLL between the second order electron self energy charge renormalization and vertex charge renormalization is found not to hold.

Now

$$\begin{aligned} j''_\mu(1, b_p) &= -\frac{iec}{4} \operatorname{Tr} \gamma_\mu (K''(1+b_p, 1-b_p) + \overset{c}{K}{}''(1+b_p, 1-b_p)) = \\ &= \frac{iec\lambda}{2} \operatorname{Tr} \gamma_\mu \int K''(1+b_p, 4)(a''(4-b_e) + a''(4+b_e)) \overset{c}{K}{}''(4, 1-b_p)\, d4 = \\ &= \frac{iec\lambda}{4} \operatorname{Tr} \int \{ \overset{c}{K}{}''(4+b_p, 1-b_p)\gamma_\mu K''(1+b_p, 4+b_p)(a''(4+b_p-b_e) + \\ &+ a''(4+b_p+b_e)) + \overset{c}{K}{}''(4-b_p, 1-b_p)\gamma_\mu K''(1+b_p, 4-b_p)(a''(4-b_p-b_e) + \\ &+ a''(4-b_p+b_e)) \}\, d4 \end{aligned} \tag{31}$$

or

$$j''_\mu(1, b_p) = \frac{iec\lambda}{2} \int \Pi_{\mu\nu}(1, 4, b_p)(A''_\nu(4-b_e) + A''_\nu(4+b_e))\, d4 , \tag{32}$$

where

$$\begin{aligned} \Pi_{\mu\nu}(1, 4, b_p) = \operatorname{Tr} \{ &\overset{c}{K}{}'(4+b_p, 1-b_p)\gamma_\mu K'(1+b_p, 4+b_p) \cdot \\ &\cdot \overset{c}{K}{}'(4-b_p, 1-b_p)\gamma_\mu K'(1-b_p, 4-b_p) \} \gamma_\nu \end{aligned} \tag{33}$$

on account of (26). This leads us to postulate

$$\Box^2(1)(A''_\mu(1-b_e) + A''_\mu(1+b_e)) = -\frac{1}{c} j''_\mu(1) \tag{34}$$

and

$$(35)\quad \begin{cases} \Box^2(1)2L''_{\mu\nu}(1,2) = i\hbar c\,\delta_{\mu\nu}\delta(12) + i\hbar c\lambda^2 \int \Pi''_{\mu\alpha}(1,4)2L''_{\alpha\nu}(4,2)\,\mathrm{d}4\,, \\ \Box^2(2)2L''_{\mu\nu}(1,2) = i\hbar c\,\delta_{\mu\nu}\delta(12) + i\hbar c\lambda^2 \int 2L''_{\mu\alpha}(1,4)\Pi''_{\alpha\nu}(4,2)\,\mathrm{d}4\,, \end{cases}$$

where $\Pi''_{\mu\alpha}(1,4) = \Pi_{\mu\alpha}(1,4,b_p) + \Pi_{\mu\alpha}(1,4,-b_p)$. The factor 2 appears in these equations as each of the two constituents of $A(1'_\mu)$, $A''_\mu(1\quad b_e)$ and $A''_\mu(1\quad -b_e)$ can combine with $A''_\nu(2+b_\rho)$ and $A''_\nu(2\quad -b_\rho)$ of $A'_\nu(2)$ respectively to form a $L'_{\mu\nu}(1,2)$ in the limit when $b_{e,\mu}$ tends to zero. The modified $L''_{\mu\nu}(1,2)$ is defined as one half of the photon propagation operator of § 2. Then

$$(36)\qquad L''_{\mu\nu}(1,2) = \frac{1}{2}L_{\mu\nu}(12) + \lambda^2 \int\int L_{\mu\alpha}(13)\Pi''_{\alpha\beta}(3,4,b_p)L''_{\beta\nu}(4,2)\,\mathrm{d}3\,\mathrm{d}4\,.$$

The integral equations (18), (19) and (36) for the modified general propagation operators are our final results and replace the Feynman-Schwinger integral equations (6), (7) and (8). The overlapping of singularities which introduces the ultraviolet divergences has now been removed by means of displacing them through a distance $b_{e,\mu}$ or $b_{p,\mu}$ and this is the only alteration that has been made in the modified Dirac-Maxwell equations (17) and (34) or in the modified Feynman-Schwinger equations (18) and (36). Indeed they revert back to the original equations when b_μ's are put equal to zero. This provides a constant check with the results of FEYNMAN, SCHWINGER and KARPLUS and KROLL. When these integrals are evaluated, as is usual, in the momentum space the modifying factor introduced by means of the displacements b_μ appears as a Fourier rearrangement factor for the energy and momentum of the internal lines. The high energy oscillations, which are the cause of the ultraviolet divergences when the calculations are performed in the momentum space, no longer have their contributions added up, and their signs get so arranged that these contributions cancel each other. But the finite low energy parts are not affected and remain the same as before. We shall illustrate these remarks by repeating the second order calculations of KARPLUS and KROLL, but we shall obtain some results which are significantly different from theirs, apart from the convergence of the integrals.

4. – The Second Order Functions.

We shall now evaluate the values of $K'(1,2)$, $L'_{\mu\nu}(1,2)$ and the vertex operator $\Lambda_\mu(1,2)$ up to the second power in λ. Some of the integrals that occur have been solved in the Appendix. These second order calculations have

been done repeatedly and we can follow the old procedures very closely and obtain the usual results. However these results will be a little different since the auxiliary conditions lead to different boundary conditions. But it is simpler to make the evaluations directly as all the integrals are convergent now. This permits a later separation of the renormalization terms and we shall find that this procedure eliminates the infrared divergences which appear to have been caused due to manipulation of infinite integrals. Of course the values of the physically significant contributions remain unaltered and it is seen that these values are independent of the value of b_μ as long as $b\varkappa$ is taken to be $\ll 1$. In this section the steps of KARPLUS and KROLL ([8]) are closely followed.

The expression for $K'(1, 2)$ up to the second power of λ, when no external electromagnetic fields are present, is

$$(37)\qquad K^{(0)}(1,2)+K^{(2)}(1,2)=$$

$$=K(12)+\frac{\lambda^2}{2}\int\!\!\int K(13)\gamma_\mu K(34)\gamma_\mu K(42)(L_{\mu\nu}(3\ \ -2b_e\ \ -4)+L_{\mu\nu}(3\ +2b_e\ \ -4))\,\mathrm{d}3\,\mathrm{d}4$$

and in the momentum representation it becomes

$$-\frac{i}{(2\pi)^4}\int \mathrm{d}^4p\,\frac{i\gamma\cdot p-\varkappa}{p^2+\varkappa^2}\exp[-ip\cdot(12)]+\frac{\alpha}{4\pi^3}\,\frac{1}{(2\pi)^4}\int\!\!\int \mathrm{d}^4p\,\mathrm{d}^4k\exp[-ip\cdot(12)]\cdot$$

$$\cdot\frac{i\gamma\cdot p-\varkappa}{p^2+\varkappa^2}\left\{\gamma_\mu\frac{i\gamma\cdot(p-k)-\varkappa}{(p-k)^2+\varkappa^2}\gamma_\mu\frac{\cos 2b_e\cdot k}{k^2}\right\}\frac{i\gamma\cdot p-\varkappa}{p^2+\varkappa^2}.$$

We note that

$$(38)\qquad \int \mathrm{d}^4k\gamma_\mu\frac{i\gamma\cdot(p-k)-\varkappa}{(p-k)^2+\varkappa^2}\gamma_\mu\frac{\cos 2b_e\cdot k}{k^2}=$$

$$-2\int \mathrm{d}^4k\int_0^1\mathrm{d}u\,\frac{(i\gamma\cdot p+\varkappa)(1-u)-i\gamma\cdot k+\varkappa(1+u)}{(k^2+\Lambda_e^2)^2}\cos 2b_e\cdot(k+pu)$$

$$=-2\int \mathrm{d}u\,((i\gamma p+\varkappa)(1-u)+\varkappa(1+u))i2\pi^2K_0(2b_e\Lambda_e),$$

where

$$(39)\qquad \Lambda_e^2=\varkappa^2u^2+(p^2+\varkappa^2)u(1-u).$$

Here the integrals over k_μ have been evaluated in the Appendix. The surface integral that appears when the variables of integration are changed is zero. Here we have used (29) and (A. 8). Let us now assume that $b_e\varkappa\ll 1$. Then using the relation (A.5) the u integration can be easily done and we

obtain

$$(40)\qquad K^{(2)}(1,2) = \frac{i\alpha}{2\pi}\cdot\frac{1}{(2\pi)^4}\int \mathrm{d}^4p\,\exp\left[-ip\cdot(12)\right]\frac{i\gamma p-\varkappa}{p^2+\varkappa^2}\cdot$$

$$\cdot\Big|\varkappa\Big\{\Big(-2+2\ln\gamma b_e\varkappa+\frac{p^2+\varkappa^2}{p^2}\ln\frac{p^2+\varkappa^2}{\varkappa^2}\Big)$$

$$-\Big(-\frac{1}{2}+\ln\gamma b_e\varkappa+\frac{p^2+\varkappa^2}{2(\varkappa^2-(p^2+\varkappa^2))}+\frac{p^2+\varkappa^2}{2p^4}\ln\frac{p^2+\varkappa^2}{\varkappa^2}\Big)\Big\}$$

$$+(i\gamma\cdot p+\varkappa)\Big\{\Big(-2+2\ln\gamma b_e\varkappa+\frac{p^2+\varkappa^2}{p^2}\ln\frac{p^2+\varkappa^2}{\varkappa^2}\Big)$$

$$\Big(-\frac{1}{2}+\ln\gamma b_e\varkappa+\frac{p^2+\varkappa^2}{2(\varkappa^2-(p^2+\varkappa^2))}+\frac{p^2+\varkappa^2}{2p^4}\ln\frac{p^2+\varkappa^2}{\varkappa^2}\Big)\Big\}\Big|\frac{i\gamma p-\varkappa}{p^2+\varkappa^2}\,.$$

Then the mass renormalization term is

$$(41)\qquad \delta_e^{(2)}(m) = -\frac{\alpha}{2\pi}\varkappa\Big(3\ln\gamma b_e\varkappa-\frac{5}{2}\Big)$$

and the charge renormalization term is

$$(42)\qquad \delta_e^{(2)}(Z) = \frac{\alpha}{2\pi}\Big(\ln\gamma b_e\varkappa-\frac{1}{2}\Big).$$

To make the charge renormalization zero we must take

$$(43)\qquad b_e = .93\,\frac{h}{mc}\,.$$

The remaining part of $K^{(2)}(12)$, which only is physically significant, is seen to be independent of $b_{e,\mu}$ as long as $b_e\varkappa$ is taken to be much smaller than 1. This feature of the theory is repeated in the other second order calculations and is similar to the results obtained by the use of the « cut off » procedures, for there also the physically significant quantities are found to be independent of the actual cut off.

Next, the expressions for $L'_{\mu\nu}(1,2)$ up to the second power of λ, when no external electron lines are present, is

$$(44)\qquad L_{\mu\nu}(12)+\frac{\lambda^2}{4}\int\!\!\int L_{\mu\varkappa}(13)\,\mathrm{Tr}\,(\mathring{K}(4-2b_p-3)\gamma_\varkappa K(34)\gamma_\beta\cdot\cdots$$

$$\cdots+\mathring{K}(43)\gamma_\varkappa K(3+2b_p-4)\gamma_\beta)\,L_{\beta\nu}(42)\,\mathrm{d}3\,\mathrm{d}4$$

and in the momentum representation it becomes

$$(45)\quad -\frac{i\hbar c}{(2\pi)^4}\,\delta_{\mu\nu}\int \mathrm{d}^4p\,\frac{\exp[-ip\cdot(12)]}{p^2}+\frac{1}{2}\,\frac{e^2}{\hbar^2c^2}\left(\frac{-i\hbar c}{(2\pi)^4}\right)^2\cdot$$
$$\cdot\iint \mathrm{d}^4p\,\mathrm{d}^4k\,\frac{\exp[-ip\cdot(12)]}{p^4}\,\mathrm{Tr}\left(\frac{i\gamma\cdot p-\varkappa}{k^2+\varkappa^2}\,\gamma_\mu\,\frac{i\gamma\cdot(p+k)+\varkappa}{(p+k)^2+\varkappa^2}\,\gamma_\nu\exp[2ib_\nu\cdot k]+\right.$$
$$\left.+\,\frac{-i\gamma\cdot(p+k)-\varkappa}{(p+k)^2+\varkappa^2}\,\gamma_\mu\,\frac{-i\gamma\cdot k-\varkappa}{k^2+\varkappa^2}\,\gamma_\nu\exp[-2ib_\nu\cdot k]\right).$$

Now

$$(46)\quad \mathrm{Tr}\,(i\gamma\cdot k-\varkappa)\gamma_\mu(i\gamma\cdot(p+k)-\varkappa)\gamma_\nu=$$
$$=\mathrm{Tr}\,(-i\gamma\cdot(p+k)-\varkappa)\gamma_\mu(-i\gamma k-\varkappa)\gamma_\nu=$$
$$=-4(2k_\mu k_\nu+k_\mu p_\nu+k_\nu p_\mu-\delta_{\mu\nu}(k^2+k\cdot p+\varkappa^2))$$

and the second term of the expression (45) is equal to

$$(47)\quad \frac{\alpha\hbar c}{\pi^3(2\pi)^4}\iint \mathrm{d}^4p\,\mathrm{d}^4k\,\frac{\exp[-ip\cdot(12)]}{p^4}\cdot$$
$$\cdot\frac{2k_\mu k_\nu+k_\mu p_\nu+k_\nu p_\mu-\delta_{\mu\nu}(k^2+k\cdot p+\varkappa^2)}{(k^2+\varkappa^2)((p+k)^2+\varkappa^2)}\cos 2b_\nu\cdot k=$$
$$=\frac{\alpha\hbar c}{\pi^3(2\pi)^4}\iint \mathrm{d}^4p\,\mathrm{d}^4k\int_0^1\mathrm{d}u\,\frac{\exp[-ip\cdot(12)]}{p^4}\cdot$$
$$\cdot\frac{2k_\mu k_\nu+k_\mu p_\nu+k_\nu p_\mu-\delta_{\mu\nu}(k^2+k\cdot p+\varkappa^2)}{((k+pu)^2+\Lambda_p^2)^2}\cos 2b_\nu\cdot k=$$
$$=\frac{\alpha\hbar c}{\pi^3(2\pi)^4}\iint \mathrm{d}^4p\,\mathrm{d}^4k\int_0^1\mathrm{d}u\,\frac{\exp[-ip\cdot(12)]}{p^4}\,\frac{\cos 2b_\nu\cdot k}{(k^2+\Lambda_p^2)^2}\{2(k_\mu-p_\mu u)(k_\nu-p_\nu u)+$$
$$+\,(k_\mu-p_\mu u)p_\nu+(k_\nu-p_\nu u)p_\mu-\delta_{\mu\nu}((k-pu)^2-(k-pu)\cdot p+\varkappa^2)\}=$$
$$=\frac{4i\alpha\hbar c}{\pi(2\pi)^4}\int \mathrm{d}^4p\int_0^1\mathrm{d}u\,\frac{\exp[-ip\cdot(12)]}{p^4}\,(p_\mu p_\nu-\delta_{\mu\nu}p^2)u(u-1)K_0(2b_\nu\Lambda_\nu),$$

where

$$(48)\quad \Lambda_p^2=\varkappa^2+p^2u(1-u).$$

We note that on account of the Yukawa auxiliary relation (27), $L_{\mu\nu}^{(2)}(12)$ is gauge invariant, and the photon self energy becomes zero. Indeed the Yukawa auxiliary conditions were determined by these requirements.

To evaluate the vacuum polarization term, we find that for $b_p \varkappa \ll 1$

$$(49)\qquad 8\int_0^1 \mathrm{d}u\, u(u-)\, K_0(2b_p \Lambda_p) =$$

$$= \left(\frac{p+(4\varkappa^2+p^2)^{\frac{1}{2}}}{p} + \frac{p^3+(4\varkappa^2+p^2)^{\frac{3}{2}}}{p^3}\right) \ln \frac{\gamma b_p}{2}\,(p - (4\varkappa^2 - p^2)^{\frac{1}{2}}) -$$

$$- \left(\frac{p-(4\varkappa^2+p^2)^{\frac{1}{2}}}{p} + \frac{p^3-(4\varkappa^2+p^2)^{\frac{3}{2}}}{p^3}\right) \ln \frac{\gamma b_p}{2}\,(-p + (4\varkappa^2+p^2)^{\frac{1}{2}}) + \frac{8\varkappa^2}{3p^3} - \frac{10}{9}\,.$$

Then the charge renormalization due to the second order vacuum polarization term is

$$(50)\qquad \delta_p^{(2)}(Z) = \frac{\alpha}{2\pi}\,\frac{1}{2}\left(\frac{4}{3}\ln \frac{\gamma b_p \varkappa}{2} - \frac{10}{9}\right)$$

and to make it zero we must put

$$(51)\qquad b_p = 1{\cdot}66\,\frac{\hbar}{mc}\,.$$

Finally the zero and second order contributions of the vertex operator

$$(52)\qquad \Lambda_\mu(1,2) = \int K'(1,3)\gamma_\mu K(3,2)\,\mathrm{d}3\,,$$

which describes the scattering of an electron by an external potential are

$$(53)\qquad \Lambda_\mu^{(0)}(1,2) + \Lambda_\mu^{(2)}(1,2) = \int K(13)\gamma_\mu K(32)\,\mathrm{d}3 +$$

$$+ \lambda^2 \int\int\int K(14)(a^0(4-b_e) + a^0(4+b_e))\,K(43)\gamma_\mu K(35)(a^0(5-b_e) + a^0(5+b_e))\cdot$$

$$\cdot K(52)\,\mathrm{d}3\,\mathrm{d}4\,\mathrm{d}5\,.$$

In the momentum representation we obtain

$$(54)\qquad \Lambda_\mu^{(0)}(1,2) + \Lambda_\mu^{(2)}(1,2) =$$

$$-\frac{1}{(2\pi)^4}\int\int \mathrm{d}^4p'\,\mathrm{d}^4p''\,\exp[-ip'\cdot(1) - ip''(2)]\cdot$$

$$\cdot \frac{i\gamma\cdot p' - \varkappa}{p'^2+\varkappa^2}\,(\gamma_\mu + L_\mu(p',p''))\,\frac{i\gamma\cdot p'' - \varkappa}{p''^2+\varkappa^2}\,,$$

where

$$(55)\qquad L_\mu(p', p'') = \frac{i\alpha}{2\pi^3}\int u\,du\int dv\int d^4k\,\cos 2b_e\cdot(k + u(p'v + p''(1-v)))\cdot \gamma_\mu(-k^2 + 4\varkappa^2(1-u-(u^2/2))) + 2K_\mu(p', p'', u, v)\over (k^2 + \Delta_v^2)^3$$

and

$$(56)\qquad \Delta_v^2 = u^2(\varkappa^2 + (p'-p'')^2\,v(1-v)) + u(1-u)((p'^2+\varkappa^2)v + (p''^2+\varkappa^2)(1-v))$$

and $K_\mu(p', p'', u, v)$ is the same as defined by SCHWINGER [1], KARPLUS and KROLL [8].

From (54) we obtain Schwinger's value for the anomalous magnetic moment of the electron and the calculations of BETHE [11] and FEYNMAN [2] of the Lamb-Retherford shift remain unaltered. So among the second order calculations only the charge renormalization due to the vertex $\Lambda_\mu^{(2)}(1, 2)$ still remains to be calculated. As before we can avoid the infrared divergence of the Karplus and Kroll calculations by carrying out, in the relevant integrals, the integration with respect to u first, and then separating the normalization terms. All the normalization terms of $\Lambda_\mu^{(2)}(1, 2)$ are contained in the integral

$$(57)\qquad I = \frac{i\alpha}{2\pi^3}\int_0^1 u\,du\int_0^1 dv\int d^4k\,\left[-2k^2\gamma_\mu + 4k_\mu\gamma\cdot k + 4\varkappa^2(1-u-(u^2/2))\gamma_\mu\right]\cos 2b_e\cdot k =$$

$$= \frac{-\alpha}{2\pi}\int_0^1 u\,du\int_0^1 dv\,\gamma_\mu\left(-2K_0(2b_e\Delta_v) + \frac{b}{2\Delta_v}\left(\Delta_v^2 + 4\varkappa^2(1-u-(u^2/2))K_1(2b_e\Delta_v)\right)\right) =$$

$$= -\frac{\alpha}{2\pi}\int_0^1 dv\,\gamma_\mu\left(\ln\gamma b_e\varkappa + \frac{B}{2(A-B)} + \frac{(A-B)^2 - B^2}{2(A-B)^2}\ln A - \frac{B^2}{2(A-B)^2}\ln B\right),$$

where

$$(58)\qquad \begin{cases} A = 1 + \dfrac{(p'-p'')^2}{\varkappa^2}\,v(1-v)\,, \\ B = \dfrac{p'^2+\varkappa^2}{\varkappa^2}\,v + \dfrac{p''^2+\varkappa^2}{\varkappa^2}\,(1-v)\,, \\ A - B = -\dfrac{1}{\varkappa^2}\,(p'v + p''(1-v))^2\,. \end{cases}$$

[11] H. A. BETHE: *Phys. Rev.*, **72**, 339 (1947). See also M. BARANGER, H. A. BETHE and R. P. FEYNMAN: *Phys. Rev.*, **92**, 482 (1953).

Thus the charge renormalization term is

$$\delta_v^{(2)}(Z) = -\frac{\alpha}{2\pi}\left(\ln \gamma b_e \varkappa - \frac{5}{2}\right). \tag{59}$$

It differs from the second order charge renormalization due to the self energy Feynman graph (42). This difference is accounted for by considering the term

$$\varkappa \frac{p^2+\varkappa^2}{\varkappa^2} \ln \frac{p^2+\varkappa^2}{\varkappa^2} = \frac{1}{\varkappa}\left((i\gamma\cdot p+\varkappa)^2 - 2\varkappa(i\gamma\cdot p+\varkappa)\right) \ln \frac{p^2+\varkappa^2}{\varkappa^2}, \tag{60}$$

from the contribution to the electron self energy graph. We note that it does not contribute to charge renormalization. Now differentiating it with respect to p_μ we obtain

$$i\frac{\partial}{\partial p_\mu}\frac{p^2+\varkappa^2}{\varkappa^2}\ln\frac{p^2+\varkappa^2}{\varkappa^2} = \frac{1}{\varkappa}\left((i\gamma\cdot p+\varkappa)\gamma_\mu + \gamma_\mu(i\gamma p+\varkappa) - 2\varkappa\gamma_\mu\right)\left(1+\ln\frac{p^2+\varkappa^2}{\varkappa^2}\right) \tag{61}$$

and we obtain a vertex charge renormalization which is just equal to the difference between the electron self energy and the vertex charge renormalization.

5. – Conclusion.

We have been able to show that from the modified Dirac-Maxwell equations (17) and (34) we obtain a finite quantum electrodynamics. The Feynman graphs of the original Dirac-Maxwell equations are altered by multiplying the internal photon line or one of the electron lines in a closed loop by a modifying factor. The modifying factor, by displacing the over-lapping divergences in the coordinate space and rearranging the high energy oscillations in the momentum space, leads to finite results for all processes. The second order physically significant results obtained from them are the same as those obtained from the original Dirac-Maxwell equations. They are obtained more directly and the infrared divergences of the latter equations are explicitly avoided. Furthermore the arbitrary parameters $b_{e,\mu}$ and $b_{p,\mu}$ can be so chosen that second order charge renormalizations due to electron self energy graph and the vacuum polarization are zero.

The Feynman «cut off» theory can be considered to be a generalization of the original Dirac-Maxwell equations and in the limit of no cut off it reverts back to them. Yukawa non-local theory in which the elementary particles

have an internal structure can be considered to be a generalization of the « cut off » theory where the cut off vector of the usual coordinate system is replaced by a vector of an independent set of coordinates. This generalization permits us to introduce the auxiliary Yukawa conditions in a simple manner. A synthesis of these three approaches has been attempted here so that with suitable limiting processes we can use either of the three methods. But as the work has progressed we have moved towards the more general basis in order to account for larger data, so that finally it has become necessary to choose the most general theory. In another paper it is shown that we can obtain a reasonable spectrum of the masses of the elementary particles from the internal structure of the elementary particles and thus we have obtained additional evidence in favour of Yukawa's theory.

The electron and photon structure factors $b_{e,\mu}$ and $b_{p,\mu}$ appear only in the non-significant quantities and we are unable to obtain a physical picture of their structures. Only when it is postulated that charge renormalization does not occur for the modified Dirac-Maxwell equations, we obtain a partial physical magnitude for them. While charge renormalization can be eliminated from the second order Feynman electron self energy and vacuum polarization graphs, it is not possible to do so simultaneously for the second order vertex graph also. However the charge renormalization term for it is independent of the structure factors and, as suggested in § **1**, it is possible that the use of Born approximation is responsible for the actual charge renormalization. The simplest physical magnitude for a particle is the radius of a sphere and from the second order calculations we obtain a reasonable value for b_e, which is $\approx \hbar/mc$, but the corresponding value of b_p, which is also $\approx \hbar/mc$, does not appear to have a physical significance.

* * *

The author is grateful to Professor G. Wataghin for kind hospitality at the Istituto di Fisica dell'Università and for helpful discussions.

Appendix

Some integrals that appear in the text are evaluated here. Utilizing the results [12]

$$\frac{b_0^{\nu}\Gamma(\frac{1}{2})K_{\nu}(b_0 z)}{\Gamma(\nu+\frac{1}{2})(2z)^{\nu}} = \int_0^{\infty} \mathrm{d}k_0 \frac{\cos b_0 k_0}{(k_0^2+z^2)^{\nu+\frac{1}{2}}} \tag{A.1}$$

[12] G. N. Watson: *Theory of Bessel Functions* (Cambridge, 1952).

nd

$$\text{A.2)} \qquad \frac{b^\mu}{a^\nu}\left(\frac{\sqrt{a^2+b^2}}{z}\right)^{\nu-\mu-1} K_{\nu-\mu-1}(z\sqrt{a^2+b^2}) = \int_0^\infty J_\mu(bt)t^{\mu+1}\frac{K_\nu(a\sqrt{t^2+z^2})}{(t^2+z^2)^{\nu/2}}\,\mathrm{d}t$$

ve obtain

$$\text{A.3)} \qquad \int \mathrm{d}^4k\,\frac{\cos b\cdot k}{(k^2+\Lambda^2)^\nu} = \frac{i\pi^2}{\Gamma(\nu)2^{\nu-3}}\,\frac{b^{\nu-2}}{\Lambda^{\nu-2}}\,K_{\nu-2}(b\Lambda)\,.$$

Here $b\cdot k = -b_0k_0 + b_1k_1 + b_2k_2 + b_3k_3$. We note that the integrand is symmetric in k_μ and all the terms in the expansion of its numerator which have a $\sin b_\nu k_\nu$ factor become zero. We can check that in the limit $b_\nu \to 0$, we obtain

$$\text{(A.4)} \qquad \int d^4k\,\frac{1}{(k^2+\Lambda^2)^3} = \frac{i\pi^2}{2\Lambda^2}$$

since for $0 < y \ll 1$

$$\text{(A.5)} \qquad K_0(y) \approx \ln\frac{2}{\gamma y}\,,$$

$$\text{(A.6)} \qquad K_\nu(y) \approx \frac{\pi}{4}\,\Gamma(\nu)\left(\frac{2}{y}\right)^\nu, \qquad \nu = 0,$$

where $\gamma = 1.781$. This is in agreement with Feynman's result and we note that for small b_ν it is independent of b_ν. We obtain from (A.3)

$$\text{(A.7)} \qquad \int \mathrm{d}^4k\,\frac{\cos b\cdot k}{(k^2+\Lambda^2)^2} = i2\pi^2 K_0(b\Lambda)$$

and the integral is seen to be finite and has the expected logarithmic divergence in the limit $b_\nu \to 0$.

Furthermore

$$\text{(A.8)} \qquad \int \mathrm{d}^4k\,k_\nu\,\frac{\cos b\cdot k}{(k^2+\Lambda^2)^\nu} = 0$$

due to the oddness of the integrand. Utilizing the results

$$\text{(A.9)} \qquad \begin{cases} \dfrac{\partial}{\partial b_\alpha}K_1(b\Lambda) = -\dfrac{b_\alpha\Lambda}{b}K_0(b\Lambda) - \dfrac{b_\alpha}{b^2}K_1(b\Lambda)\,, \\ \dfrac{\partial}{\partial b_\alpha}K_0(b\Lambda) = -\dfrac{b_\alpha\Lambda}{b}K_1(b\Lambda) \end{cases}$$

we also obtain

$$\text{(A.10)} \qquad \int \mathrm{d}^4k\,k_\alpha k_\beta\,\frac{\cos b\cdot k}{(k^2+\Lambda^2)^3} = \frac{i\pi^2}{2}\left(\delta_{\alpha\beta}K_0(b\Lambda) - \frac{b_\alpha b_\beta}{b}\Lambda K_1(b\Lambda)\right).$$

$$\text{(A.11)} \qquad \int d^4k\, k_\alpha k_\beta \frac{\cos b\cdot k}{(k^2+\Lambda^2)^2} =$$

$$= i2\pi^2 \left(\delta_{\alpha\beta} \frac{\Lambda}{b} K_1(b\Lambda) - 2 \frac{b_\alpha b_\beta}{b^3} \Lambda K_1(b\Lambda) - \frac{b_\alpha b_\beta}{b^2} \Lambda^2 K_0(b\Lambda) \right).$$

RIASSUNTO (*)

Si modificano, secondo Wataghin, le equazioni di Dirac-Maxwell spostando i campi nel punto della loro interazione per mezzo dell'introduzione di parametri di spostamento. Quando tali parametri, che debbono risultare piccoli, tendono a zero, si ottengono le equazioni originali di Dirac-Maxwell. Il programma originale di rinormalizzazione della carica, la teoria del « taglio » di Feynman e la teoria non locale di Yukawa delle particelle a struttura interna e l'elettrodinamica quantistica convergente che ne consegue possono considerarsi come casi speciali di queste equazioni di Dirac-Maxwell modificate. Combinando i metodi di questi procedimenti si ottiene una elettrodinamica quantistica convergente in cui i grafici di Feynman originali sono modificati per la moltiplicazione con un semplice fattore di modificazione. Di ciò si dà un'illustrazione calcolando alcuni grafici di Feynman del secondo ordine. Si argomenta poi che si può considerare che queste equazioni non richiedano la rinormalizzazione della carica e che la rinormalizzazione della carica che si esegue sia dovuta esclusivamente all'impiego dell'approssimazione di Born.

(*) *Traduzione a cura della Redazione.*

Some Comments on K^- Interactions at Rest.

J. M. Blatt and S. T. Butler

The F. B. S. Falkiner Nuclear Research and Adolph Basser Computing Laboratories, School of Physics (*), *The University of Sydney - Sydney, N.S.W.*

(ricevuto il 13 Dicembre 1955)

Summary. — The main conclusions of this paper are: (1) The energy spectrum of the charged π-mesons emerging from K^- captures at rest indicates, together with other evidence, that K^- capture occurs only well within nuclear matter, not at the nuclear surface. A very tentative hypothesis is suggested as an explanation, which can be tested by studying interactions in flight of K^--mesons passing through hydrogen. (2) A low energy ($\lesssim 20$ MeV) Λ^0 has a long mean free path in nuclear matter, at least of the order of the radius of one of the heavy nuclei in nuclear emulsions. This excludes strong Λ^0-nucleon forces of any kind, be they attractive or repulsive. (3) If a hyper-deuteron exists, it cannot be interpreted as a compound of a Λ^0 and a proton; if it emerges from a K^- capture at rest, it can also not be a compound of a K-particle and a nucleon. The only remaining reasonable interpretation, a compound of a Σ and a nucleon, violates conservation of strangeness. We therefore urge experimentalists to measure up carefully any event suspected to be of this type. (4) Measurement of the K^+/K^- ratio in neutron bombardment of nuclei would provide a direct test of the strangeness selection rule, as distinguished from the less specific «law of associated production».

1. – Introduction.

The purpose of this paper is to give some theoretical observations in connection with the experimental findings on stopped K^--particles by the Sydney

(*) Also supported by the Nuclear Research Foundation within the University of Sydney.

group (1) and by WEBB *et al.* in Berkeley (2). At the time of writing, the Berkeley data are more extensive (132 events compared to the 52 events from Sydney) but we have only preliminary information about them. We shall therefore concern ourselves primarily with the Sydney data, using the Berkeley data whenever more statistics are required for the conclusion.

The most interesting feature of these observations, in our opinion, is the energy spectrum of the emergent π-mesons. In reference (1) it was shown that the data are consistent with the following fundamental reaction for K^--capture:

$$K^- + \text{nucleon} = \text{hyperon} + \pi \tag{1.1}$$

provided other nucleons share some of the available energy and momentum from this reaction. The complete absence of emergent π-mesons of energies above 120 MeV indicates that such sharing of energy and momentum must occur in *every* capture event, and we shall see that this aspect of the capture mechanism is very hard to understand, and indicates that the K^--nucleon interaction has peculiar features. In section 2 we discuss the slowing down of K^--mesons and their cascading down from higher into lower Bohr orbits around the nucleus, by emission of electromagnetic radiation. Section 3 is devoted to the nuclear capture process itself. In section 4 we show that the mean free path of a low energy Λ^0 hyperon in nuclear matter must be at least comparable with the nuclear radius. This indicates a weak Λ^0-nucleon force. It is already known from hyper-fragment evidence that any attractive Λ^0-nucleon force must be weak, but the present evidence also rules out a very strong *repulsive* Λ^0-nucleon force.

Another aspect of the experimental observations on which we present some comments is the possible existence of a hyper-deuteron, i.e., an unstable fragment of mass 2. Unfortunately it has proved impossible to remove all doubt from this interpretation of the event, from the experimental point of view. However, we hope that the discussion of the consequences of the existence of hyper-deuterons, given in section 5, will stimulate experimentalists to carry out detailed measurements on any event which might fall into this class.

Finally, section 6 is devoted to a suggested experiment for testing the strangeness selection rule which has been suggested recently (3). The experiment would discriminate between mere « associated production » of strange particles and the more detailed « strangeness selection rule ».

---

(1) E. P. GEORGE, A. J. HERZ, J. H. NOON and N. SOLNTSEFF: *Nuovo Cimento* **3**, 94 (1956).

(2) WEBB, W. W. CHUPP, G. GOLDHABER and S. GOLDHABER: Private communication. We are very grateful to these authors for sending us preliminary information about their observations before publication.

(3) K. NISHIJIMA: *Prog. Theor. Phys.*, **13**, 285 (1955); M. GELL-MANN: *Report of the Pisa Conference* (to be published).

2. – Slowing down of K⁻ particles and capture into Bohr orbits.

The slowing down of the K⁻ is very similar to the correspinding process for π⁻-mesons, which has been discussed in the literature (⁴). π⁻-mesons eventually are captured into Bohr orbits around the nuclei of the material. Experimentally, it has been found that roughly 45 percent of the π⁻-mesons come to rest near one of the light nuclei in photographic emulsion (C, N, O), the remaining 55 percent near one of the heavy nuclei (Ag, Br). The slowing down and capture into outer Bohr orbits occurs through the interaction of the meson with the electrons in the medium, not with the atomic nuclei. Since the mass of the meson is much larger than the mass of an electron, the precise mass ratio is of little importance, and we can therefore take over the experimental results for π⁻-mesons in the discussion of K⁻-captures. We shall see that the conclusions of interest to us are not strongly dependent on the precise proportion of capture in light and heavy nuclei, provided at least half of the captures occur in the heavy nuclei.

We shall now show that, if the cascading down process occurs predominantly via the emission of electromagnetic radiation, and if the nuclear capture of the K⁻ is a «strong» interaction in the sense of GELL-MANN (³), then nuclear capture occurs from one of the Bohr orbits lying predominantly outside the nuclear volume. Bohr orbits lying predominantly inside the nuclear volume are never reached under these conditions.

Once a K⁻ is captured into one of the outlying Bohr orbits, it cascades down to lower-lying orbits with emission of electromagnetic radiation. The transition probability per unit time is given by (⁵)

$$A_{nn'} = \frac{64\pi^4}{3}\frac{e^2\nu^3}{hc^3}\,|\boldsymbol{r}_{nn'}|^2 \tag{2.1}$$

where $\boldsymbol{r}_{nn'}$ is the matrix element of the vector operator $\boldsymbol{r}$ between the states n and n'. In order to discuss this formula qualitatively, we rewrite it in the form

$$A_{nn'} = \frac{4}{3}\frac{e^2}{\hbar c}\left(\frac{E_{nn'}}{h}\right)^3\frac{|\boldsymbol{r}_{nn'}|^2}{c^2} \tag{2.2}$$

where $E_{nn'}$ is the energy available in the transition from n to n'. For order-of-magnitude estimates, it is sufficient to replace the matrix element $\boldsymbol{r}_{nn'}$ by the radius of the lower one of the two orbits involved.

(⁴) E. FERMI and E. TELLER: *Phys. Rev.*, **72**, 399 (1947); H. MUIRHEAD and O. ROCHAT: *Phil. Mag.*, **41**, 583 (1950).

(⁵) H. BETHE: *Handbuch der Physik*, vol. **24**, no. 1, chapter 3.

We consider K^--mesons in orbits around heavy nuclei in the emulsion. If one computes the radius of the $1s$ orbit on the basis of a point charge Coulomb potential, the radius turns out to be $1.3 \cdot 10^{-13}$ cm, well inside the nucleus itself. But inside the nucleus the effective Coulomb force acting on the K^- is proportional to the distance from the centre of the nucleus, not to the inverse square of that distance. Hence inside the nucleus we have a harmonic oscillator potential. Computing on this basis, the $1s$ wave function has a maximum ar $r = 3.9 \cdot 10^{-13}$ cm, which is still appreciably less than the nuclear radius, $R = 5.5 \cdot 10^{-13}$ cm. Hence the correction to the wave function due to the different potential outside the nucleus is small. If we assume no specifically nuclear attraction of the K^-, the binding energy of the $1s$ state is of the order of 8 MeV; a specifically nuclear interaction would contribute an approximately constant «optical model» potential, which would add to the binding energy if the interaction is attractive. Since the orbit is already inside the nucleus, the radius of the orbit would not be affected appreciably.

The next higher Bohr orbits, $2s$ and $2p$, are already outside the nucleus, predominantly, although an appreciable probability remains of finding the K^- inside the nucleus. We can ignore the $2s$ orbit in a rough consideration, since any state which can decay to the $2s$ orbit can also decay to the $1s$ orbit; the factor $(E_{nn'})^3$ in (2.2) easily outweighs the adverse change in the radius, so that most transitions would occur to the $1s$ rather than the $2s$ orbits.

In the case of π^--mesons stopped near heavy nuclei, it has been found experimentally [6] that nuclear absorption of the π^- takes place from one of the outer orbits ($2p$ or $3d$) before the mesons has time to cascade down into the $1s$ orbit. Indeed, the data show that already in iron, $Z = 26$, there is very appreciable competition between nuclear capture from the $3d$ state and electromagnetic transition $3d \to 2p$; in silver or bromine, most of the captures would occur from the $3d$ or higher orbits.

In the absence of certain knowledge about the nuclear interactions of K^--mesons, it is not clear whether these π^--meson results can be applied to K^--mesons as well. Indeed, we shall see from the experimental data [1,2] that this is almost surely not possible. We shall interpret the competition between nuclear capture and electromagnetic transitions in terms of a hypothetical «lifetime of a K^--meson in nuclear matter», which we shall call T. This time is defined as follows: assume that a K^- is placed inside nuclear matter, in such a way that its wave function is zero outside the nucleus; then T is the time the K^- lives before it undergoes nuclear absorption. For example, if a K^-

---

[6] M. Camac, A. D. McGuire, J. B. Platt and H. J. Schulte: *Phys. Rev.*, **99**. 897 (1955).

should be able to reach the $1s$ orbit [7] inside a heavy nucleus, then T is the mean time before nuclear absorption takes place. If the nuclear absorption is a « strong » interaction in the sense of GELL-MANN [3] the time T is expected to be of the order of 10^{-22} s.

If the capture occurs from an orbit « n » not entirely within the nucleus, the mean time taken for nuclear absorption is longer. Let P_n be the probability of finding the K^- particle within the nuclear volume (i.e., the integral of the square of the wave function of the K^- taken over the nuclear volume). Then we estimate the transition probability for nuclear absorption to be of the order of

$$B_n \sim P_n/T \,. \tag{2.3}$$

This is the quantity which should be compared with (2.2) to determine whether direct nuclear capture or electromagnetic transitions to lower orbits are most effective in depleting the population of the orbit n.

Let us now estimate the electromagnetic transition probability for the transition $np \to 1s$, which is the last step of a cascade leading to the $1s$ orbit: n here is any principal quantum number consistent with a p-state, i.e., $n \geq 2$. Since our estimate of the matrix element $\boldsymbol{r}_{nn'}$ is determined by the radius of the lower orbit, the principal quantum number of the p-orbit does not enter except through the energy difference. For the latter we shall make an overestimate, so as to favour the electromagnetic transitions, namely, we shall assume that $E_{nn'}$ is equal to the binding energy of the $1s$ state, which we have estimated above. Using 8 MeV for this binding energy and $4 \cdot 10^{-13}$ cm for the value of $\boldsymbol{r}_{nn'}$, equation (2.2) gives the estimate

$$A_{nn'} \sim 4 \cdot 10^{18} \text{ s}^{-1} \qquad \text{for} \quad np \to 1s \,. \tag{2.4}$$

In order to compare this with (2.3), we must make some assumption about the probability P_n of finding the K^- inside the nuclear volume when the K^- occupies the np orbit. Most of the transitions are expected to take place from the $2p$ orbit, for the same reason that few transitions are expected to go to the $2s$ orbit if the $1s$ orbit is available. In the $2p$ state, the probability P_n is certainly more than 1/10, and we shall used this value to get a lower limit

---

[7] Of course, this orbit makes sense only if T is itself long compared to a « period of revolution », that is $T \gg h/E$, where E is the level spacing. This condition can also be stated as follows: the mean free path for nuclear absorption of the K^- in nuclear matter must be long compared to the radius of the orbit, at kinetic energies corresponding to the mean kinetic energy in the orbit. Since the concept of a mean free path in bound states is difficult to make quantitative, we prefer to state our estimates in terms of a « mean free time » T.

for (2.3). If T in (2.3) is taken as a typical « nuclear » time, of order 10^{-22} s, then we get $B_n \sim 10^{21}$ s^{-1}, very much larger than the electromagnetic transition probability (2.4). Thus, on such an estimate, direct capture from the $2p$ state is very much more likely than an electromagnetic transition to the $1s$ state, and a similar estimate for π^- rather than K^--mesons is of course in accordance with experimental facts about the π^- captures in heavy nuclei ([6]).

Conversely, if we have reason to suspect that the nuclear capture occurs only from the $1s$ orbit, the comparison of (2.3) and (2.4) gives a lower limit for the time T that a K^- can live inside nuclear matter, of order $T \gg 3 \cdot 10^{-20}$ s: the « much larger » sign here is to be taken literally, as indicating at least a factor 10, since all our estimates so far have been weighted in the opposite direction. A lifetime of this order would certainly indicate a « weak » nuclear interaction.

The estimate (2.4) of the electromagnetic transition probability is subject to some doubt because we have used the binding energy in the $1s$ state computed on the basis of the Coulomb force alone, with no nuclear attraction or repulsion between the K^- and nuclear matter. Let us now compute what the energy difference $E_{nn'}$ would have to be in order to make the electromagnetic transition $2p \rightarrow 1s$ compete with direct capture, assuming $T \sim 10^{-22}$ s. This turns out to be $E_{nn'} \gtrsim 50$ MeV, which is a thoroughly unreasonable figure: if the attraction of the K^- to nuclear matter really were that high, then the $2p$ orbit itself would be drawn into the nucleus; to see whether capture occurs primarily from an orbit inside the nuclear volume, the relevant transitions would be of type $3d \rightarrow 2p$, for which the energy difference would again be smaller than 50 MeV.

Thus, if the cascading down process occurs predominantly via emission of photons, and if the nuclear capture process is a « strong » interaction, our estimates show that nuclear capture occurs from one of the Bohr orbits lying predominantly outside the nuclear volume itself. Bohr orbits lying predominantly inside the nuclear volume are never reached, under these conditions.

3. – Nuclear Capture of the K^-.

In reference ([1]) it was shown that the experimental data are consistent with the basic capture process (1.1), provided other nucleons share some of the available energy and momentum from the capture process in *all* events. It was furthermore shown that most of the captures go via the reaction

$$K^- + \text{nucleon} = \Lambda^0 + \pi\,, \tag{3.1}$$

rather than the alternative reaction

$$K^- + \text{nucleon} = \Sigma + \pi\,, \tag{3.2}$$

the branching ratio between (3.1) and (3.2) being of order 10:1. Combining the Sydney ([1]) data (10 mesons) and the Berkeley ([2]) preliminary data (32 mesons), we have 42 charged mesons, presumably all π-mesons, not a single one of which has an energy in excess of 120 MeV, and only one with an energy in excess of 100 MeV. The maximum in the energy distribution is around 50 MeV. This must be compared with the energy the π-meson would receive if the capture process (3.1) occurred at rest with no other particles around to take up energy and momentum, namely about 150 MeV. We conclude that there are *always* other particles about to share the energy and momentum, whenever a capture process (3.1) takes place, i.e., in the vast majority of all capture events.

The crucial word here is « always ». It is easy enough to understand that other nucleons will occasionally share the available energy and momentum, even that they will frequently do so. But it is very hard to understand why they should *always* do so. To see the difficulty, we recall the result of the last section: nuclear capture is expected to occur from one of the Bohr orbits lying predominantly outside the nuclear volume. In that case, the capture should occur quite frequently by a « surface » nucleon, one which is in the exponential « tail » of the nuclear distribution, and hence has no other nucleons close by to take up energy and momentum. Roughly half of the time that the capture occurs with a surface nucleon, the π-meson direction points away from the nuclear volume, and hence the π-meson should emerge with the full 150 MeV kinetic energy acquired at the point of production. The relative motion between surface nucleon and captured K^- tends to spread out this sharp energy into a distribution of energies around 150 MeV, but has no appreciable effect on the mean of the distribution, since the effect is as likely to raise the energy of the π as to decrease it. The experimental data force us to the conclusion that capture by surface nucleons occurs extremely rarely, if at all, and yet our estimates regarding the cascading down from higher to lower Bohr orbits (as well as experimental data concerning this same process for π^- capture) would lead us to expect surface capture rather frequently.

Let us now investigate possible mechanisms which might explain this discrepancy. The first, and simplest, explanation would be that the time T in (2.3) is much longer than 10^{-22} s, of the order of 10^{-18} s at least; i.e., we assume that the K^- nuclear capture reaction (1.1) is much slower than a typical « strong » interaction. Then the cascading down process would proceed down to the 1*s* state; this latter state has the wave function of the K^--particle concentrated inside the nucleus, so that surface capture is excluded. However,

there are two objections against this explanation: (1) in light nuclei, which represent an appreciable fraction of the capture, the 1*s* orbit lies outside the nucleus, and (2) the mean free path of K^- mesons in flight ([8]) indicates a geometric cross-section, i.e., a « strong » interaction. The first objection is not too serious, since it is well known that there are strong momentum correlations in light nuclei (a partial α-particle structure), but the second objection excludes this explanation. The kinetic energies of the K^- in its Bohr orbit and of the K^- in the interactions in flight are different, but not so different as to make it at all likely that $T \sim 10^{-22}$ s for K^- particles in flight, but $T > 10^{-18}$ s for K^--particles in Bohr orbits.

A second explanation might be given along the following lines: there is a hyperon created in every capture event, according to our basic reaction (1.1): let us assume this hyperon has a long-range interaction with nuclear matter, the range being longer than that of ordinary nuclear forces. Then momentum can be transferred to other nucleons in the nucleus by means of the hyperon-nucleon interaction, even if the capture itself took place with a surface nucleon. However, this explanation is inconsistent with the data on the hyperon-nucleon interactions available from the study of hyper-fragments ([9]). The hyper-fragment data show that a hyperon, when bound to a light nucleus, decays almost as if it were a free particle, i.e., there is very little momentum transfer between the hyperon and the nucleus to which it has been bound. In addition, one would expect on general theoretical grounds ([9]) that the range of the hyperon-nucleon interaction is, if anything, less than the range of ordinary nuclear forces, not more.

A third conceivable explanation runs as follows: let us assume that there is a strong K^--nucleon interaction, but that this interaction preserves the K^-, i.e., leads to K^--nucleon scattering rather than absorption of the K^-. A conceivable reaction might be the exchange of a virtual π-meson between the K^- and the nucleon. The capture reaction (1.1) would still be possible, but be much less likely than the scattering. In this case, the scattering reaction will speed up the cascading down process enormously, the more so the higher the probability of finding the K^- in nuclear matter, i.e., the more so the lower the Bohr orbit. Thus our estimate of the transition probability for cascading down, (2.2), fails because another process takes over: the K^- is now able to reach the 1*s* orbit, and thence be captured somewhere well inside the nucleus. This explanation, however, also runs afoul of the experimental data: the interactions in flight ([8]) indicate frequent occurrence of capture of K^- in flight;

([8]) G. Goldhaber: Private communication; see also, *Proceedings of the Pisa Conference*, to be published.

([9]) R. Levi-Setti: *Suppl. Nuovo Cimento*, **1**, 263 (1955); R. H. Dalitz: *Phys. Rev.*, **99**, 1475 (1955), and literature quoted in those papers.

.e., the capture reaction (1.1) is itself « fast », and competes appreciably with nere scattering or charge exchange scattering of the K^-. Our proposed explanation has assumed that (1.1) is much slower than the scattering reaction, and fails if the two are of comparable speed.

We conclude that there must be something specific about the reaction (1.1) which favours its occurrence inside nuclear matter, but works against it when a K^- encounters an isolated (e.g., surface) nucleon. Such a specific effect discriminating between the nuclear volume and nuclear surface is not unknown: the photo-production of π-mesons in heavy nuclei occurs primarily on the nuclear surface ([10]). A γ-ray interacting inside the main nuclear volume apparently does not produce π-mesons, whereas γ-rays interacting near the nuclear surface do so. The reason for this difference is not well understood at present, but the fact is there.

At the moment, the following hypothesis seems most likely to us: when a K^--meson interacts with isolated, surface nucleons, events in which the K^- preserves its identity (scattering events) dominate strongly over absorption via a reaction such as (1.1); but when a K^- interacts inside the main nuclear volume, reaction (1.1) competes effectively with mere scattering. In that case the data on interactions of K^- in flight are consistent with the energy distribution of the π-mesons emerging from capture at rest. It must be realized, of course, that this hypothesis is very much ad hoc, and we know of no theoretical reason why a K^- should behave in such a way. However, the experience with (γ, π) reactions makes it slightly more plausible that such an ad hoc explanation may actually be correct.

There is an experimental way of testing this hypothesis: if K^- mesons interact *in flight* with isolated nucleons (i.e., in hydrogen gas or liquid), scattering ought to dominate over reactions in which the K^- is absorbed, to a much greater extent than for K^- interactions in flight with complex nuclei. Surface nucleons are similar to isolated nucleons in this sense. Of course, after the K^- has come to rest it will go into a Bohr orbit around some proton, and eventually disappear via a reaction (1.1). The energy of the emitted π-meson in that case is uniquely determined, and this fact provides a second test of the assumption of (1.1) as the basic capture reaction.

The main purpose of this section has been to show that there is appreciable difficulty in understanding the data on K^--captures at rest, and that the more obvious attempts at explanation run afoul of experimental facts about interactions of K^--mesons in flight. The final explanation suggested here is only one possibility which may turn out to be quite wrong, its main virtue being

([10]) S. T. Butler: *Phys. Rev.*, **87**, 1117 (1952); E. P. George: *Proc. Phys. Soc. (London)*, to be published.

that it allows a straightforward experimental test, which will be of interest whether or not it confirms our hypothesis.

4. The mean free path of Λ^0 hyperons in nuclear matter.

It has been shown (1) that most of the capture events have considerably less visible energy than the rest mass energy of the K^-. This can be understood qualitatively by assuming that either the hyperon or the π-meson from reaction (1.1), or both, escape from the nucleus as neutral particles.

Since we have seen that practically all the captures occur well inside the nuclear volume, and since most of them produce Λ^0-hyperons, we can conclude that the mean free path of a Λ^0-hyperon in nuclear matter must be at least comparable to the nuclear radius; otherwise the hyperon would frequently be retained inside the nucleus together with the π-meson, in which case the full rest mass energy of the K^- would show up as nuclear excitation, contrary to experiment.

This mean free path argument is essentially classical, whereas the low energy (around 20 MeV) hyperon created in the capture process should be treated wave mechanically. However, the wave mechanical effects in general tend to inhibit emission from the nucleus ([11]) so that our mean free path estimate is all right as a lower limit, which is all we intended to get.

Unlike nucleons, whose long mean free path in nuclear matter can be understood on the basis of the Pauli exclusion principle ([12]), a long mean free path for the Λ^0 indicates a weak Λ^0-nucleon force. This conclusion is of course in full agreement with the small binding energies of Λ^0 hyperons in hyperfragments ([9]), but it is a somewhat stronger conclusion, since we can also rule out strong *repulsive* Λ^0-nucleon forces, whereas the hyperfragment evidence allows us to rule out only strong attractive forces, and says nothing about repulsive forces.

It should be possible in principle to make similar inferences about Σ hyperons, but the Sydney data (1) is not extensive enough for this purpose, and we do not have the final Berkeley data available to us at this time.

5. – Hyper-deuterons and strangeness.

One of the events described in reference (1) is an unstable fragment of measured mass $(2.0 \pm 0.5) M_{\text{proton}}$ and charge -1. The only visible decay product is a proton of energy 26 MeV. From the experimental point of view,

([11]) J. M. BLATT and V. F. WEISSKOPF: *Theoretical Nuclear Physics* (New York, 1952).

([12]) H. FESHBACH, C. E. PORTER and V. F. WEISSKOPF: *Phys. Rev.*, **96**, 448 (1954).

this is most likely to be a fragment consisting of one nucleon and one hyperon, i.e., a « hyperdeuteron », but it could also be a Σ^+ hyperon decaying just before coming to rest (residual range < 50 μm). Another possible hyper-deuteron has been reported by ALEXANDER *et al.* [13] but this event could also be a hyper-triton (fragment of mass 3). A third event, reported by ANDERSON *et al.* [14], could also be a hyper-deuteron but is more likely to be a hyper-triton.

Although the experimental evidence is thus quite uncertain, we would like to make a few remarks about the interpretation of a hyper-deuteron, if it could be established experimentally with certainty. The main point is that we do not believe that such a particle could be interpreted as a compound of a Λ^0 and a proton. The binding energy of a Λ^0 to nuclear matter is known to be small [9], much smaller than the binding energy of the « last » nucleon in the corresponding ordinary nucleus. Ordinary nuclear forces are just barely strong enough to make the deuteron a stable system [11]. Hence, the much weaker, Λ^0-nucleon force cannot produce a stable hyper-deuteron.

Although this argument has been mentioned in the literature [9,15], it is usually dismissed rather quickly because « possible many-body effects and a possible strong spin dependence of the Λ^0-nucleon force would easily invalidate such conclusions ». We would like to point out here that it is rather difficult to construct a Λ^0-nucleon force law which would be in agreement with a stable hyper-deuteron and yet account for the weak binding of the Λ^0 to other light nuclei, unless the range of the Λ^0-nucleon force is assumed to be extremely large ($> 5 \cdot 10^{-13}$ cm).

A simple spin-dependence will not do; even if we assume that there is an infinitely strong repulsion between Λ^0 and nucleon in one spin state, this will not prevent a hyper-triton from having a large binding energy, contrary to observation [9,14]. The Λ^0 does not obey the Pauli principle with respect to nucleons, hence it can form the same spin state with the proton and the neutron in a hyper-triton. It will form the favourable (attractive) spin state, of course, and the infinite repulsion will not come into play at all.

Many-body forces are possible, of course, but again would have to be rather queer. In general, we expect many-body forces to have a shorter range than two-body forces; and the Λ^0-nucleon force is already expected to have a short range itself [9]. A very short-range many-body force, even if repulsive, will have little influence on the binding energy of a hyper-triton or a hyper-α-

---

[13] G. ALEXANDER, C. BALLARIO, R. BIZZARRI, B. BRUNELLI, A. DE MARCO, A. MICHELINI, G. C. MONETI, A. ZAVATTINI, A. ZICHICHI and J. P. ASTBURY: *Nuovo Cimento*, **2**, 365 (1955).

[14] F. ANDERSON, G. LAWLOR and T. E. NEVIN: *Nuovo Cimento*, **2**, 605 (1955). We thank Dr. NEVIN for some helpful communication regarding this event.

[15] R. GATTO: *Nuovo Cimento*, **2**, 373 (1955).

particle, since the nucleons themselves cannot come close together as a result of the Jastrow-Levy repulsive core ([16]).

Furthermore, the argument of section 4 has shown that a strongly repulsive Λ^0-nucleon force is excluded as much as a strongly attractive one. In other words, it is not possible to assume that the small binding energy of hyper-fragments is due to a cancellation between strong attractive and repulsive forces, the strong attractive force being then responsible for a stable hyper-deuteron.

We conclude that either the Λ^0-nucleon force law is very queer indeed or a hyper-deuteron cannot be a Λ^0-proton compound. In this connection it is of interest that there exist unstable fragments in which the observed energy release is larger than the energy available from Λ^0-decay ([17]). Thus not all fragments are Λ^0 fragments, and a hyper-deuteron, if it exists, need not be a Λ^0 fragment either.

In the literature these other fragments have been interpreted as bound states of a light nucleus and a K-meson. We point out that such an interpretation *cannot* be used for a fragment emerging from the capture of a K^- at rest, because there is not enough energy available. The only way the fragment can get the kinetic energy with which it is ejected (some 40 MeV if the Sydeny event is a hyper-deuteron) is through a difference in binding energy of the K-particle to the heavy nucleus and to the single nucleon, the binding being *stronger* to the single nucleon by an amount equal to this kinetic energy plus the original heavy-nucleus binding energy. This is clearly most unlikely and need not be considered as a serious possibility.

Thus the only remaining reasonable interpretation of the Sydney event, on the assumption that the mass is 2, is in terms of a bound state of a Σ and a nucleon, most likely a Σ^+ and a neutron rather than a Σ^0 and a proton. It is well known that the theory of Gell-Mann ([3]) is inconsistent with such an interpretation, and it is easy to see that there is no simple way in which strangeness quantum numbers can be reassigned so as to allow such a compound and yet preserve conservation of strangeness as a significant selection rule ([18]).

In view of the general success of the strangeness concept, it is tempting to conclude that the Sydney event is a Σ^+-decay in flight rather than a hyper-deuteron, in spite of the result of the mass measurement. The main purpose

---

([16]) R. JASTROW: *Phys. Rev.*, **81**, 165 (1951); M. M. LEVY: *Phys. Rev.*, **88**, 72, 725 (1952).

([17]) W. F. FRY, J. SCHNEPS and M. S. SWAMI: *Phys. Rev.*, **99**, 1561 (1955).

([18]) It is of course always possible to relax Gell-Mann's requirement of « compulsory strong interactions », but then the strangeness selection rule loses much of its usefulness.

of our discussion has been to convince experimentalists to make the, admittedly very tedious, measurements necessary to narrow down the error on the mass determination in any event suspected to be a hyper-deuteron.

6. – A Test of the Strangeness Conservation Law.

Although the evidence for « associated production » of strange particles is quite strong, the evidence for the more detailed « conservation of strangeness » is less conclusive. In the following we propose an experimental test of the latter.

When nuclei are bombarded by high energy protons, many more K^+-mesons are produced than K^- mesons ([19]), the branching ratio being of the order of 100:1. This is usually explained in terms of conservation of strangeness, by assigning different strangeness quantum numbers to the K^+ and the K^-. In that case, one would expect a very similar $K^+:K^-$ ratio in the bombardment of nuclei by high energy *neutrons*. On the other hand, if the $K^+:K^-$ ratio is due to some other cause, then neutron bombardment may be expected to give a very different $K^+:K^-$ ratio.

We now show that the $K^+:K^-$ ratio in proton bombardment can be understood on the basis of conservation of charge together with « associated production », without invoking the more specific conservation of strangeness. The associated production reaction is taken to be

$$\text{Nucleon} + \text{nucleon} = \text{nucleon} + \text{hyperon} + \text{K} . \tag{5.1}$$

We use the experimental indication ([20]) that many more Λ^0 hyperons are produced in these reactions than charged hyperons of any kind, the ratio being at least 10:1 and more likely around 100:1. Thus we can gain a first rough view of the situation by assuming that the hyperon in (5.1) is a Λ^0 hyperon.

In proton bombardment, the reactions of type (5.1) then are

$$\text{P} + \text{P} = \text{P} + \Lambda^0 + \text{K}^+ \tag{5.2}$$

$$\text{P} + \text{N} = \text{P} + \Lambda^0 + \text{K}^0 \tag{5.3}$$

$$\text{P} + \text{N} = \text{N} + \Lambda^0 + \text{K}^+ . \tag{5.4}$$

([19]) G. GOLDHABER: Private communication.

([20]) In cloud chamber observations on cosmic rays, the ratio of V^0: $V^\pm$ is of order 10:1 (G. D. JAMES and R. A. SALMERON: *Phil. Mag.*, **46**, 571 (1955)). Roughly half of the V^0 events are hyperons (J. A. NEWTH and G. D. JAMES: *Bagnères Conference Report*, 1953) whereas no hyperons have been found among the charged V's (J. S. BUCHANAN, W. A. LOPER, D. D. MILLAR and J. A. NEWTH: *Phil. Mag.*, **45**, 1025 (1954)). Since charged and neutral hyperons have very similar lifetimes (AMALDI *et al.*: *Nuovo Cimento*, **12**, 668 (1954)), the experimental number ratio is close to the branching ratio at production.

None of these leads to production of K^--mesons, and hence a high K^+/K^- ratio can be understood as a consequence of charge conservation plus associated production plus dominance of Λ^0 production, without invoking strangeness as such.

If we now consider neutron bombardment, reaction (5.2) is excluded, reactions (5.3) and (5.4) can occur, but we also have the additional reactions

$$N + N = N + \Lambda^0 + K^0 \tag{5.5}$$

$$N + N = P + \Lambda^0 + K^- . \tag{5.6}$$

Unless reaction (5.6) is forbidden by a special selection rule (such as conservation of strangeness), its presence should lead to copious production of K^--mesons in neutron bombardment. The precise branching ratio is hard to predict, because one of the neutrons in (5.6) has to become a proton during the reaction, and the probability of this « charge-exchange » process at these energies is not well known. However, charge-exchange is by no means an infrequent event, and it is at least extremely likely that the K^+/K^- ratio in neutron bombardment is no higher than 10:1 if reaction (5.6) is allowed.

These considerations lead us to suggest the measurement of the K^+/K^- ratio in neutron bombardment as a test of the strangeness selection rule.

7. – Conclusions.

The main conclusions of this paper are:

(1) The energy spectrum of the charged π-mesons emerging from K^- captures at rest indicates, together with other evidence, that K^- capture occurs only well within nuclear matter, not at the nuclear surface. A very tentative hypothesis is suggested as an explanation, which can be tested by studying interactions in flight of K^--mesons passing through hydrogen.

(2) A low energy (< 20 MeV) Λ^0 has a long mean free path in nuclear matter, at least of the order of the radius of one of the heavy nuclei in nuclear emulsions. This excludes strong Λ^0-nucleon forces of any kind, be they attractive or repulsive.

(3) If a hyper-deuteron exists, it cannot be interpreted as a compound of a Λ^0 and a proton; if it emerges from a K^- capture at rest, it can also not be a compound of a K-particle and a nucleon. The only remaining reasonable interpretation, a compound of a Σ and a nucleon, violates conservation of strangeness. We therefore urge experimentalists to measure up carefully any event suspected to be of this type.

(4) Measurement of the K^+/K^- ratio in neutron bombardment of nuclei would provide a direct test of the strangeness selection rule, as distinguished from the less specific « law of associated production ».

* * *

We are grateful to Drs. E. P. George, A. J. Herz, J. H. Noon, and Mr. N. Solntseff for making their data available to us prior to publication, and to all of them for valuable discussions. We thank Dr. G. Goldhaber for some extremely helpful correspondence including a very much appreciated preliminary summary of the Berkeley data. Dr. T. E. Nevin has responded immediately and in a most helpful manner to our request for information. Last but not least, we would like to record our appreciation for the many stimulating discussions we have had with Professor H. Messel, Dr. D. D. Millar, and Mr. D. A. Tidman.

RIASSUNTO (*)

Le principali conclusioni del presente lavoro sono: 1) Lo spettro d'energia dei mesoni π carichi emergenti dalle catture di K^- a riposo indica, assieme ad altre prove, che la cattura dei K^- avviene solo ad una certa profondità nell'interno della materia nucleare, non alla superficie dei nuclei. Per tentare di spiegare lo svolgimento del fenomeno si formula un'ipotesi che può essere saggiata studiando le interazioni in volo dei K^- che attraversino idrogeno. 2) Un Λ^0 di bassa energia ($\lesssim$ 20 MeV) ha un lungo cammino libero medio nella materia nucleare, almeno dell'ordine del diametro di uno dei nuclei pesanti delle emulsioni nucleari. Questo esclude intense forze nucleari di qualsiasi specie agenti sui Λ^0, sia attrattive che repulsive. 3) Se esiste un iperdeutone, questo non può essere interpretato come la combinazione di un Λ^0 con un protone: se emerge dalla cattura di un K^- a riposo, non può neanche essere la combinazione di un K con un nucleone. L'unica interpretazione ragionevole che resta, la combinazione di un Λ con un nucleone, viola la conservazione dell'estraneità. Invitiamo pertanto gli sperimentali a misurare accuratamente ogni evento che possa interpretarsi come appartenente a questa categoria. 4) La misurazione del rapporto K^+/K^- risultante dal bombardamento di nuclei per mezzo di neutroni fornirebbe una verifica diretta della regola di selezione dell'estraneità, in quanto distinta dalla meno specifica « legge della produzione associata ».

(*) *Traduzione a cura della Redazione.*

On Generalised Dispersion Relations.

A. Salam

St. John's College - Cambridge, England

(ricevuto il 15 Dicembre 1955)

Summary. — A relation is derived which connects the real part of the non forward meson-nucleon scattering amplitude, to its imaginary part.

1. – A number of investigations [1] have recently appeared in which relations have been obtained connecting essentially the real part of the forward scattering amplitude to its imaginary part. More recent investigations are those of Karplus and Ruderman [2] and Goldberger [3] who have shown the great utility of such relations for the problem of meson-nucleon scattering.

Attempts to obtain more general relations, connecting for example the real part of the scattering amplitude at an arbitrary angle in the centre of mass system, to its imaginary part at the same angle, have in general not succeeded. In this paper we shall show that relations of the required type do exist for the meson-nucleon system, though indeed they do not connect the real and the imaginary parts of the amplitude at precisely the same angle in the centre of mass system. For the proof we need the concept of micro-causality, as interpreted in ref. [1] viz: the commutator of the field operators at two points vanishes if these points have a space-like separation. Our main result is eq. (27) of this paper.

2. – Consider a field theory describing neutral mesons of mass μ, interacting with nucleons of mass $\varkappa$. The interaction Lagrangian is $j(x)\varphi(x)$, while

[1] Gell-Mann, Goldberger and Thirring: *Phys. Rev.*, **95**, 1612 (1954).
[2] R. Karplus and M. Ruderman: *Phys. Rev.*, **98**, 771 (1955).
[3] M. L. Goldberger: *Phys. Rev.*, **99**, 979 (1955).

he causality condition demands that (4)

1) $$[j(x), j(y)] = 0 \qquad \text{when} \quad (x-y)^2 < 0$$

Let k, k' be the initial and the final meson and p, p' (5) the corresponding nucleon 4-momenta. The Feynman matrix element for scattering is given by

2) $$M_F(k, k'; p, p') = i \int \mathrm{d}^4x\, \mathrm{d}^4y \exp[ik'x - iky](p'|[j(x)j(y)]_+|p);$$

GOLDBERGER (3) has shown that the retarded matrix element

3) $$M(k, k'; p, p') = i \int \mathrm{d}^4x\, \mathrm{d}^4y \exp[ik'x - iky]\theta(x-y)(p'|[j(x), j(y)]|p)$$

coincides with M_F for $k_0 > 0$ and contains precisely the same information. Define

4) $$M_R(k; p, p') = i \int \mathrm{d}^4x\, \theta(-x)(p'|[j(0), j(x)]|p) \exp[-ikx]$$

5) $$M_A(k; p, p') = i \int \mathrm{d}^4x\, \theta(+x)(p'|[j(0), j(x)]|p) \exp[-ikx]$$

6) $$D(k; p, p') = \tfrac{1}{2}(M_R - M_A)$$

7) $$A(k; p, p') = \frac{1}{2i}(M_R + M_A)\,.$$

f M_R, M_A, D and A are considered as functions of k, p and p', the energy hell specifies the following conditions on these three vectors:

8) (i) $$k^2 = \mu^2\, p^2 = p'^2 = \varkappa^2\,,$$

9) (ii) $$p_0,\ p_0' > 0\,; \qquad k_0,\ p_0 + k_0 - p_0' > 0\,.$$

10) (iii) $$k\cdot(p - p') = p\cdot p' - \varkappa^2\,.$$

We now note from the definitions, that

11) $$M^*_{R,A}(k; p, p') = M_{R,A}(-k; p', p)\,,$$

12) $$\delta^4(k + p - p' - k')\, M_R(k; p, p') = -\delta^4(k + p - p' - k')\, M_A(-k'; p, p')\,.$$

(4) We use the metric $x^2 = x_0^2 - \boldsymbol{x}^2$.

(5) In this paper we consider only the no spin-slip case, so that spin suffixes for he nucleons will be omitted.

The last relation holds since both sides equal $(2\pi)^{-4} M(k, k'; p, p')$ (6).

Further

$$k\cdot(p+p') = k'\cdot(p+p'), \quad \text{since} \quad p^2 = p'^2 = \varkappa^2 , \tag{13}$$

$$k\cdot(p-p') = k'\cdot(p'-p) , \quad \text{since} \quad k^2 = k'^2 = \mu^2 . \tag{14}$$

Write

$$M_{R,A} = \bar{u}(p')\{L'_{R,A} + i\gamma k M'_{R,A}\}u(p) ;$$

L' and M' depend invariantly only on $k\cdot(p+p')$, $k\cdot(p-p')$, $p\cdot p'$, γk. Thus

$$M'_{R,A}(k; p, p') = M'_{R,A}(k'; p', p) \text{ etc.} \tag{15}$$

Combining (11), (12) and (15),

$$\delta^4(k+p-k'-p')\left(M'_R(k; p, p') + M'_A(k; p, p')\right) = 0 \text{ etc.} \tag{16}$$

Write $D = u\{L'_D + i\gamma k M'_D\}u$. From (6), (15) and (16), L'_D and M'_D are real. In the next section we choose a frame, where $\bar{u}u$, $\bar{u}i\gamma k u$ are also real. So we prove the important result that both $D(k; p, p')$ and $A(k; p, p')$ are real (7) on the energy shell and are respectively the real and the imaginary parts of $M_R(k; p, p')$. It is crucial for the above proof that relations (13) and (14) should hold and this is only true if the same particles participate in the initial and the final states.

3. – The « natural » frame of reference appears to be the frame in which the nucleons are at rest. In this frame, without loss of generality, choose

$$p = (P^2 + \varkappa^2)^{\frac{1}{2}}, \quad 0, \quad 0, \quad P, \tag{17}$$

$$p' = (P^2 + \varkappa^2)^{\frac{1}{2}}, \quad 0, \quad 0, \quad -P . \tag{18}$$

Since $p\cdot p' - \varkappa^2 = 2P^2$, we obtain but one condition on the vector, k from the energy-shell relations; in fact

$$k = k_0 , \quad k_1 , \quad k_2 , \quad P . \tag{19}$$

(6) This is proved by using $j(x) = \exp[iPx]j(0)\exp[-iPx]$.

(7) The author is indebted to Mr. W. GILBERT who first pointed this result to him.

Also

$$uu = p_0/k, \qquad \bar{u}i\gamma ku = k_0 .$$

Thus M_R really depends only on k_0 and P.

Considering the integral expression for M_R (eq. (4)), it is also clear that its k_0 dependence arises quite trivially from the factor $\exp[-ikx]$. This is because $(p'|[j(0), j(x)]|p)$ depends only on P in our frame of reference, through the invariants $(p+p')x$, etc. If we hold P fixed (or invariantly $p\cdot p'$ [8] fixed) the mathematical problem reduces to the same as presents itself for the forward scattering case and precisely the same steps as GOLDBERGER [3], can be followed to obtain generalized dispersion relations.

Write

$$J_1(P, x) = (p|[j(0), j(x)]|p') - (p'|[j(0), j(x)]|p) \tag{20}$$

$$J_2(P, x) = i\{(p|[j(0), j(x)]|p') + (p'|[j(0), j(x)]|p)\} . \tag{21}$$

From $M'_R(k; p, p') = M'_R(k'; p', p)$ and the evenness of $\theta(x)$ $(p'|[j(0), j(x)]|p)$ in x_1 and x_2 in the new frame, $(x = x_0, x_1, x_2, x_3)$,

$$M_R(k_0, \boldsymbol{k}; p, p') = M_R(k_0, -\boldsymbol{k}; p', p) . \tag{22}$$

Thus

$$M_R = \tfrac{1}{2}[M_R(k_0, \boldsymbol{k}; p, p') + M_R(k_0, -\boldsymbol{k}; p, p')] = \tag{23}$$

$$= \tfrac{1}{2}\int \theta(x) \exp[-ik_0x_0]\{J_1(P, x) \sin \boldsymbol{kx} + J_2(P, x) \cos \boldsymbol{kx}\} \, \mathrm{d}^4x$$

$$D(k_0, P) = \tfrac{1}{2}\int \theta(x) \cos k_0x_0\{J_1(P, x) \sin Px_3 + J_2(P, x) \cos Px_3\} \cdot \tag{24}$$

$$\cdot \cos(k_1x_1 + k_2x_2) \, \mathrm{d}^4x$$

$$A(k_0, P) = -\tfrac{1}{2}\int \theta(x) \sin k_0x_0\{J_1(P, x) \sin Px_3 + J_2(P, x) \cos Px_3\} \cdot \tag{25}$$

$$\cdot \cos(k_1x_1 + k_1x_1) \, \mathrm{d}^4x .$$

Using (24) and (25) we now verify directly that

$$\frac{D(\alpha, P) - D(\beta, P)}{\alpha^2 - \beta^2} = +\frac{1}{\pi} P \int_{-\infty}^{\infty} \frac{k_0 A(k_0, P) \, \mathrm{d}k_0}{(k_0^2 - \alpha^2)(k_0^2 - \beta^2)} \tag{26}$$

[8] In the centre of mass system, $p\cdot p' - \varkappa^2 = 2a^2 \sin^2 \theta/2$ where a is the magnitude of the 3-momentum in the problem.

$$(27) \qquad \frac{D(\alpha, P)-D(\beta, P)}{\alpha^2-\beta^2} = +\frac{2}{\pi} P \int_0^\infty \frac{k_0 A(k_0, P)\,\mathrm{d}k_0}{(k_0^2-\alpha^2)(k_0^2-\beta^2)} .$$

The proof follows by interchanging the order of x and k_0 integrations and performing a simple contour integration in the k_0 plane. Here, for the first time, the causality relation (1) is used. This part of the work is subject to the same limitations as noted by GOLDBERGER [3].

To see significance of the relation (27), consider the case of scalar nucleons. Here the k_0 dependence of D and A arises only from $k\cdot(p+p')$. In the laboratory system $p = \varkappa, 0\,0\,0$, $k\cdot(p+p') = 2k_0 + \varkappa(p_0'-\varkappa)$ and $p\cdot p' = \varkappa p_0'$. A variation of $k\cdot(p+p')$ while $p\cdot p'$ is held fixed is the same as the variation of the incoming meson energy k_0, while p_0', the final nucleon energy is fixed. Thus in the laboratory system, for scalar nucleons,

$$(28) \qquad \frac{\mathrm{Re}\, M(k_0^1, p_0') - \mathrm{Re}\, M(k_0^2, p_0')}{(k_0^1-k_0^2)(k_0^1+k_0^2+p_0'-\varkappa)} = -\frac{P}{\pi}\int \frac{(2k_0'+p_0'-\varkappa)\,\mathrm{Im}\, M(k_0, p_0')\,\mathrm{d}k_0}{(k_0-k_0^1)(k_0-k_0^2)(k_0+k_0^1+p_0'-\varkappa)(k_0+k_0^2+p_0^1-\varkappa)} .$$

4. – Returning to eq. (27), the imaginary part of the amplitude can, in principle, be determined from experiment for $k_0 \geqslant (\mu^2+P^2)^{\frac{1}{2}}$. In order to use relation (27) we have to determine the correct analytic continuation of $A(k_0, P)$ in the (unphysical) range $0 \leqslant k_0 < (\mu^2+P^2)^{\frac{1}{2}}$. From eq. (7),

$$(29) \qquad A(k) = \tfrac{1}{2}\int (p'|[j(0), j(x)]|p)\,\exp[-ikx]\,\mathrm{d}^4x$$

$$(30) \qquad = \frac{(2\pi)^4}{2_i}\sum_n (p'|j(0)|n)(n|j(0)|p)\,\delta^4(n-p-k) - \frac{(2\pi)^4}{2}\sum_n (p'|j(0)|n)(n|j(0)|p)\,\delta^4(n-p'+k) .$$

In the second term in (30), $n = p'-k$, and therefore the masses of the (physical) intermediate state are given by $(\varkappa^2+\mu^2-2p'\cdot k)^{\frac{1}{2}}$. The only possible state which can contribute is the single nucleon state corresponding to $\mu^2 - 2p'\cdot k = 0$. Its contribution to $A(k_0, P)$ for the no spin-flip case, with renormalized g properly defined, is

$$(31) \qquad -\frac{g^2}{4\pi}(4\pi^2 k_0)\delta(2p_0k_0-\mu^2-2P^2) . \quad [9]$$

[9] Considerations on this and the spin-flip case will be given in a second paper.

Now consider the first term in eq. (30). This term does not contribute at all for the forward scattering case. In the present case, however, for k_0 in the range $(\varkappa\mu - P^2)/(P^2+\varkappa^2)^{\frac{1}{2}}$, $(\mu^2+P^2)^{\frac{1}{2}}$, we find $n^2 = (k+p)^2 \geqslant (\varkappa+\mu)^2$, and meson-nucleon states may make a contribution. Indeed this is the price one really pays for a generalized dispersion relation, and it has not been possible to find a satisfactory method for the evaluation of this contribution. It is of course possible to make a perturbation approximation to $A(k_0, P)$ just for this range.

A relation similar to eq. (27) has previously been derived by BETHE and ROHRLICH [10] and applied to the case of small angle scattering of light by Coulomb field. The quantity held fixed in their case is b, an impact parameter.

* * *

The author is indebted to Dr. F. SMITHIES, Mr. W. GILBERT, Professor H. A. BETHE, and Dr. P. MARTIN for discussions.

---

[10] H. A. BETHE and F. ROHRLICH: *Phys. Rev.*, **86**, 10 (1952).

RIASSUNTO (*)

Si deriva una relazione che connette la parte reale dell'ampiezza dello scattering mesone-nucleone non diretto in avanti alla sua parte immaginaria.

(*) *Traduzione a cura della Redazione.*

On the Inelastic Scattering of Electrons from ^{12}C.

G. Morpurgo

Scuola di Perfezionamento in Fisica Nucleare dell'Università - Roma
Istituto Nazionale di Fisica Nucleare - Sezione di Roma

(ricevuto il 16 Dicembre 1955)

Summary. The theoretical interpretation of Fregeau and Hofstadter's experiment on the elastic and inelastic scattering of high energy electrons from ^{12}C is discussed; the excitation of the 4.43 MeV level is particularly considered, and the increase of the ratio $d\sigma_{inelastic}/d\sigma_{elastic}$ with the energy is explained as well as the constancy of $d\sigma_{inelastic}$ in the interval $80 \div 187$ MeV. Calculations are performed with the use of an oscillator shell model both in *LS* and *JJ* coupling. The quantitative agreement is satisfactory and better (by a factor of three) with *LS* than with *JJ* coupling.

Fregeau and Hofstadter [1] have recently investigated the elastic and inelastic scattering of electrons by ^{12}C; their most complete set of results for the inelastic scattering refer to the excitation of the 4.43 MeV level, other less complete sets of data referring to the 7.68 and 9.61 MeV levels. In this note we shall only consider the 4.43 MeV level which is known [2] to have spin 2 and parity +.

Calling $d\sigma_{in}(\theta)$ the differential cross-section for excitation of such level and scattering into the angle θ, and $d\sigma_{el}(\theta)$ the differential cross-section for elastic scattering, there are two points, which on examining the experimental material, are rather striking, and deserve an explanation: the first is the enormous increase for a given angle θ of the ratio $d\sigma_{in}/d\sigma_{el}$ with the energy p_0 of the incident

---

[1] H. Fregeau and R. Hofstadter: *Phys. Rev.*, **99**, 1503 (1955). In this paper is mentioned a work by Dr. Ravenhall, to be published; we hope not to duplicate too much Dr. Ravenhall's analysis, as yet not entirely finished (private communication from Dr. Ravenhall).

[2] F. Ajzenberg and T. Lauritsen: *Rev. Mod. Phys.*, **27**, 76 (1955).

electron: at 90° the above ratio increases by a factor ~ 50 when p_0 is varied from 80 to 150 MeV and by a factor ~ 6 when p_0 is varied from 150 to 187 MeV, as shown in Fig. 1 and in the first line of Table I; the second fact is the independence of $d\sigma_{in}$ at 90° from the energy p_0 in the interval 80 to 187 MeV (Fig. 2).

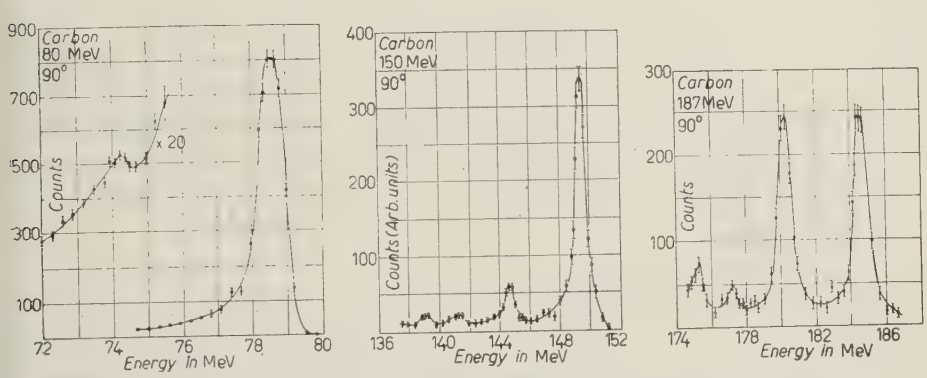

Fig. 1. – The elastic and inelastic peaks at 80, 150, 187 MeV and 90° (from ref. [1]).

TABLE I.

p_0 (MeV)	80	150	187
$(d\sigma_{in}/d\sigma_{el})^{exp}_{90^\circ}$	$2.5 \pm 2 \cdot 10^{-3}$	$1.4 \cdot 10^{-1}$	$9 \cdot 10^{-1}$
$(d\sigma_{in}/d\sigma_{el})^{LS}_{90^\circ}$	$3.6 \cdot 10^{-3}$	$0.9 \cdot 10^{-1}$	$3.6 \cdot 10^{-1}$
$(d\sigma_{in}/d\sigma_{el})^{JJ}_{90^\circ}$	$1.2 \cdot 10^{-3}$	$0.3 \cdot 10^{-1}$	$1.2 \cdot 10^{-1}$

We shall now give the results of a very simple calculation through which the above facts and the essential features of the inelastic scattering may be understood: use will be made of the Born approximation which in this Z region is a good one.

In the Born approximation the differential cross-section for elastic scattering of an electron from a nucleus, may be written, disregarding the recoil of the nucleus, in the extremely relativistic case:

$$d\sigma = \frac{4Z^2e^4p_0^2}{q^4}\cos^2\frac{\theta}{2}|F|^2 d\Omega\,, \tag{1}$$

where $\boldsymbol{q} = \boldsymbol{p}_0 - \boldsymbol{p}_f$ ($\boldsymbol{p}_f$ = final momentum of the electron), $q = 2p_0 \sin\theta/2$ and F is the nuclear form factor defined as:

$$F = F_{el} = \int \varrho_0(r) \exp[i\boldsymbol{q}\cdot\boldsymbol{r}]d\tau\,, \tag{2}$$

$\varrho_0(r)$ being the charge density of the nucleus in the ground state normalized to unity.

The same expression (1) is valid in the inelastic case provided that the excitation energy is small with respect to p_0, θ is not too near to 0° or 180° and F is replaced by:

$$F \equiv F_{\text{in}} = \int \varrho_{0f}(\boldsymbol{r}) \exp[i\boldsymbol{q}\cdot\boldsymbol{r}]\,\mathrm{d}\tau\,, \tag{3}$$

where $\varrho_{0f}(\boldsymbol{r})$ is the transition charge density; this last quantity is defined as:

$$\varrho_{0f}(\boldsymbol{r}) = Z^{-1} \sum_1^z{}_i \left[\int \psi_0^* \psi_{0f}\,\mathrm{d}\tau_1 \ldots \mathrm{d}\tau_{i-1}\,\mathrm{d}\tau_{i+1}\,\mathrm{d}\tau_A \right]_{r_i = r}\,, \tag{4}$$

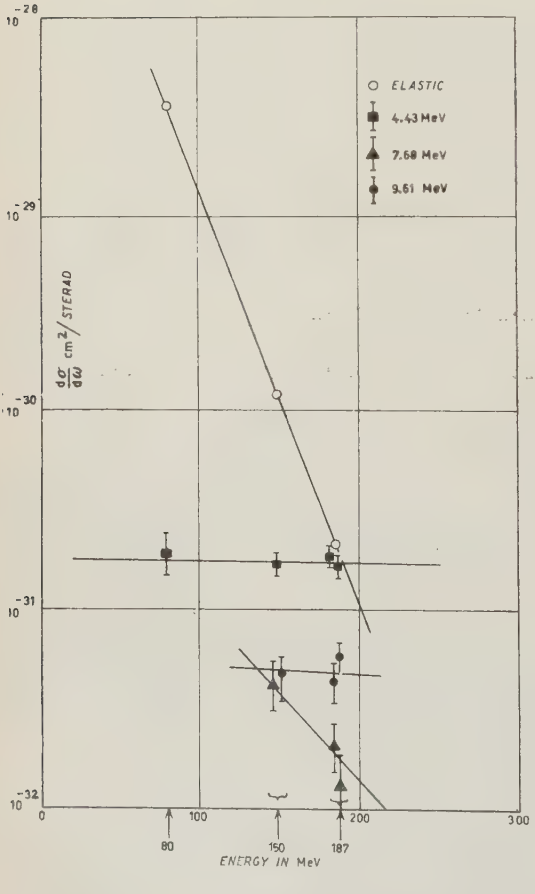

where the sum is extended to the protons, ψ_0 is the ground state wave function and ψ_f the wave function of the excited state under consideration. For $q \to 0$, $F_{\text{el}} \to 1$ and $F_{\text{in}} \to 0$.

We shall now assume an independent particle model for the nucleus; in the simplest case $\varrho_0(r)$ and $\varrho_{0f}(\boldsymbol{r})$ may then be written:

$$\varrho_0(r) = \frac{1}{Z} \sum_1^z{}_i |f_{n_i}(r)|^2\,, \tag{5}$$

$$\varrho_{0f}(\boldsymbol{r}) = \frac{1}{Z} f_{n_z}^*(\boldsymbol{r}) f_{n_z'}(\boldsymbol{r})\,. \tag{6}$$

Fig. 2. – The cross-sections for the elastic and inelastic peaks at 90° as a function of the energy (from ref. [1]); the two lowest curves refer to the excitation of levels not considered in this paper).

(3) The $J = 1$ state is energetically higher. (D. R. Inglis: *Rev. Mod. Phys.*, 25, 390 (1953)).

Here f_{n_z} are the individual wave functions for the protons and n_z is schematically the quantum number which is changed to n_z' in the excitation of the nucleus; we have written down explicitely the expressions (5) and (6) to remark that the ratio $|\varrho_{0f}/\varrho_0|$ looks as being of order Z^{-1}; apparently this would imply a ratio Z^{-2} between $d\sigma_{in}$ and $d\sigma_{el}$ contrary to the fact that at 90° and 187 MeV the ratio is about one. The above argument is however not correct because of interference effects; for sufficiently large values of q they will be shown to reduce considerably the value of F_{el} giving rise to a ratio $d\sigma_{in}/d\sigma_{el}$ in substantial agreement with the experiment.

To be more definite, and at the same time as simple as possible let's assume, oscillator functions for the nucleus; just one free parameter will thus appear in the formulas: it characterizes the radial part of the wave functions:

$$R_{1l} = N_{1l} \exp\left[-\frac{\nu}{2} r^2\right] r^{l+1}, \quad N_{1l}^2 = \frac{\sqrt{\nu}\nu^{l+1} 2^{l+2}}{\sqrt{\pi} 1 \cdot 3 \ldots (2l+1)}. \tag{7}$$

It will later be adjusted to give the best agreement with the elastic scattering.

We now proceed to perform the calculation of F_{el} and F_{in} both in jj and LS coupling.

In jj coupling the state ψ_0 belongs of course to the configuration $(1s_{\frac{1}{2}})^4(1p_{\frac{3}{2}})^8$; the state ψ_f, at 4.43 MeV, has clearly to be associated to the configuration $(1s_{\frac{1}{2}})^4(1p_{\frac{3}{2}})^7(1p_{\frac{1}{2}})$; more precisely it is the state with $J=2$, $T=0$ which may be formed from this configuration (3); in a concise notation the substate with $M_j = 2$ may be written:

$$\frac{1}{\sqrt{2}} (1\bar{p}^{(+)}_{\frac{3}{2},-\frac{3}{2}} 1p^{(+)}_{\frac{1}{2},\frac{1}{2}} + 1\bar{p}^{(-)}_{\frac{3}{2},-\frac{3}{2}} 1p^{(-)}_{\frac{1}{2},\frac{1}{2}}). \tag{8}$$

The first term of expression (8) means that a hole (as indicated by the upper dash) is created in the proton (+) state $J=\frac{3}{2}$, $m_j = -\frac{3}{2}$, and that the proton is transferred to the $J=\frac{1}{2}$, $m_j=\frac{1}{2}$ state, all the other nucleons retaining their places; the second term of expression (8) has the same meaning for the neutrons. It is easy to check that the wave function (8) belongs to a zero value of the isotopic spin (4).

In LS coupling the construction of the wave functions is slightly more complicated; from the paper of FEENBERG and PHILLIPS (5) we get that ψ_0 and ψ_f are respectively a ^1S and a ^1D state; to construct such wave functions it is of course convenient to use the fact that ^8Be and ^{12}C differ only through

(4) Only the values $T=0$, $T=1$ are present in the above configuration: the first corresponds to charge parity $+$, the second to charge parity $-$; the wave function (8) which clearly has charge parity $+$, must then have $T=0$.

(5) E. FEENBERG and M. PHILLIPS: *Phys. Rev.*, **51**, 597 (1937).

the change of holes and particles; we may therefore construct the wave functions for ^{8}Be and derive easily the results for ^{12}C. In writing down the wave functions we omit the s nucleon part and call 1, 2, 3, 4 the p nucleons; we shall also call p^+, p^0, p^- the three normalized components of a p state; moreover a, b, c, d, are symbols for αu, αv, βu, βv, where α and β are the spin functions, u and v the isotopic spin functions; $\underline{\underline{S}}$ will denote the operation of complete symmetrization, $\underline{\underline{A}}$ the operation of antisymmetrization; the normalized wave functions are then:

$$(9) \qquad {}^{11}S = \frac{1}{\sqrt{4!}}\underline{\underline{A}}a_1b_2c_3d_4\frac{1}{\sqrt{4!}}\frac{1}{\sqrt{120}}\underline{\underline{S}}(-4p_1^+p_2^-p_3^0p_4^0+4p_1^+p_2^+p_3^-p_4^-+p_1^0p_2^0p_3^0p_4^0)$$

$$(10) \qquad {}^{11}D_2 = \frac{1}{\sqrt{4!}}\underline{\underline{A}}a_1b_2c_3d_4\frac{1}{\sqrt{4!}}\frac{1}{\sqrt{28}}\underline{\underline{S}}(p_1^+p_2^+[2p_3^+p_4^- - p_3^0p_4^0])$$

where the $M=2$ component of the D state has been written; the nucleon coordinates are written as indices. That the wave functions (9) and (10) have the correct transformation character will be shown in an Appendix.

The calculation of ϱ_0, ϱ_{0f} is now straightforward; ϱ_0 is the same in jj and LS coupling, ϱ_{0f} differs in the two cases by a numerical factor:

$$(11) \qquad \varrho_0(r) = \frac{\nu\sqrt{\nu}}{3\pi\sqrt{\pi}}\exp[-\nu r^2]\left(1+\frac{4}{3}r^2\nu\right),$$

$$(12) \qquad {}^{(M_j=2)}\varrho_{0f}(\boldsymbol{r}) = -A\cdot\frac{1}{Z}\frac{\nu^2\sqrt{\nu}}{\pi\sqrt{\pi}}\sqrt{\frac{1}{3}}\exp[-\nu r^2](x+iy)^2,$$

where:

$$(13) \qquad A=1 \text{ for } jj \text{ coupling}; \qquad A=\sqrt{\frac{14\cdot 3}{15}}\cong\sqrt{3} \text{ for } LS \text{ coupling}.$$

Inserting in (2), (3) performing the integrations and squaring we get:

$$(14) \qquad |F_{\text{el}}|^2 = \left(1-\frac{q^2}{9\nu}\right)^2\exp\left[-\frac{q^2}{2\nu}\right],$$

$$(15) \qquad |{}^{(M_j=2)}F_{\text{in}}|^2 = \frac{A^2}{Z^2}\frac{1}{48}\frac{(q_x^2+q_y^2)^2}{\nu^2}\exp\left[-\frac{q^2}{2\nu}\right].$$

As the notation suggests (15) gives the square of the form factor for inelastic scattering to the $M_J=2$ substate; in order to obtain $|F_{\text{in}}|^2$ we have to calculate $|{}^MF_{\text{in}}|^2$ for each value of M and to sum over the five substates. This

can be done quite simply and the result is:

$$|F_{in}|^2 = \frac{1}{18}\frac{A^2}{Z^2}\left(\frac{q^2}{\nu}\right)^2 \exp\left[-\frac{q^2}{2\nu}\right]. \tag{16}$$

We are now in a position to calculate $d\sigma_{in}/d\sigma_{el}$. Making use of (16) and (14) we get:

$$\frac{d\sigma_{in}}{d\sigma_{el}} = \frac{9}{2}\frac{A^2}{Z^2}\left(\frac{q^2}{9\nu}\right)^2 \Big/ \left(1 - \frac{q^2}{9\nu}\right)^2 \tag{17}$$

with the usual meaning of A.

This expression explains qualitatively the fact illustrated in Table I: in fact, for small values of q ($q^2/9\nu \ll 1$) $d\sigma_{in}$ is very much less than $d\sigma_{el}$ both because the numerator is small with respect to one and because there is a big factor Z^2 ($= 36$ in this case) in the denominator; when $q^2/9\nu$ approaches one the ratio increases; it becomes one for $q^2/9\nu \simeq 0.6$ (in the case of LS coupling), and infinite (if the model has to be taken literally) for $q^2/9\nu = 1$; for $q^2/9\nu > 0.6$ the excitation cross-section is larger than the elastic one, though of course, both are small due to the exponential factor.

It is interesting at this point to examine how the agreement is quantitative; we must then determine the value of ν; this we do by comparing the theoretical elastic form factor with the experimental one, defined as $d\sigma_{el}(\theta)/d\sigma_{el}(\theta)_{\text{point charge}}$ and given at 187 MeV in the paper by FREGEAU and HOFSTADTER (compare their Fig. 11).

Putting for convenience $\nu = m^2/\gamma^2$, where $m = 150$ MeV is a convenient energy unit ($m^{-1} = 1.25 \cdot 10^{-13}$ cm), we determine γ^2 to be about 1.45 ([6]). Inserting this value in (17) we get for the ratio $d\sigma_{in}/d\sigma_{el}$ at 90° the values reported in the second line of Table I for LS coupling and in the third for jj coupling; such values clearly have the correct energy dependence showing the large increase with the energy, and, in the case of LS coupling are also sufficiently close, in absolute value, to the experimental values; there is agreement within a factor of 2.5, in the case of LS coupling, which is quite reasonable. Also the comparison of the theory with a larger set of experimental data (contained in the Table III and Fig. 9 of ([1])) confirms the above conclusions.

We now turn to the constancy of $d\sigma_{in}(90°)$ when the energy is varied from

---

([6]) With the charge density (11) this corresponds to a root mean square radius $(\int r^2 \varrho_0(r)\, d\tau)^{\frac{1}{2}} = ((13/6)(\gamma^2/m^2))^{\frac{1}{2}} = 2.23 \cdot 10^{13}$; in obtaining this value, as well as in all the previous calculations we have neglected all recoil effects, as for example the difference between the center of mass and laboratory scattering angle.

80 to 187 MeV. According to (1) and (13) the energy dependence of $d\sigma_{in}(90^\circ)$ is

$$(18) \qquad \sim p_0^2 \exp\left[-\frac{p_0^2}{m^2}\gamma^2\right].$$

From (18) the ratio between $d\sigma_{in}(90^\circ)$ at 80 and at 187 MeV turns out to be exactly one, due to the fact that the variation in the exponential factor is, by chance, compensated by the variation of p_0^2. We may conclude that this simple calculation explains in a satisfactory way the main features of the inelastic scattering in ^{12}C to the 4.43 MeV level. The angle and energy variation of $d\sigma_{in}(\theta)$ is given correctly (though the variation of $d\sigma_{el}$ with energy is somewhat too slow); in LS coupling, also the order of magnitude of $d\sigma_{in}(\theta)$ is completely reasonable, being too small by a factor 2.5, which, most probably (7), depends on the neglect of all kind of correlation implied by the shell model. It may be finally remarked that this calculation strongly favours an LS coupling for ^{12}C in agreement with other indications (8).

Appendix

It will now be shown that the wave functions (9) and (10) have the correct transformation character. As their space part is completely symmetrical it is first obvious that these functions are spin and isotopic spin singlets. We now show that they have also respectively $L = 0$ and $L = 2$. Putting

$$(\boldsymbol{p}_1 \cdot \boldsymbol{p}_2) = p_1^+ p_2^- + p_1^- p_2^+ + p_1^0 p_2^0$$

one has identically:

$$(A.1) \qquad \frac{1}{\sqrt{4!}}\frac{1}{\sqrt{120}}\hat{S}(-4p_1^+p_2^-p_3^0p_4^0 + 4p_1^+p_2^+p_3^-p_4^- + p_1^0p_2^0p_3^0p_4^0) =$$

$$= \frac{1}{\sqrt{45}}[(\boldsymbol{p}_1\cdot\boldsymbol{p}_2)(\boldsymbol{p}_3\cdot\boldsymbol{p}_4 + (\boldsymbol{p}_1\cdot\boldsymbol{p}_3)(\boldsymbol{p}_2\cdot\boldsymbol{p}_4) + (\boldsymbol{p}_1\cdot\boldsymbol{p}_4)(\boldsymbol{p}_2\cdot\boldsymbol{p}_3)]$$

and the right hand side is obviously rotation invariant. Similarly one

(7) Of course the choice of wave functions different from oscillator ones might improve the results; this topic (private communication from Dr. Ravenhall) will be discussed in Ravenhall's paper, but it appears that oscillator wave functions give the best fit among many others.

(8) D. R. Inglis: Ref. (3).

has:

$$(A.2)\qquad \frac{1}{\sqrt{4!}}\frac{1}{\sqrt{28}}\,\underline{S}[p_1^+p_2^+(2p_3^+p_4^- - p_3^0p_4^0)] = \frac{1}{\sqrt{42}}[p_1^+p_2^+(\boldsymbol{p}_3\cdot\boldsymbol{p}_4) +$$

$$- p_1^+p_4^+(\boldsymbol{p}_2\cdot\boldsymbol{p}_3) - p_1^+p_3^+(\boldsymbol{p}_2\cdot\boldsymbol{p}_4) - p_3^+p_4^-(\boldsymbol{p}_1\cdot\boldsymbol{p}_2) - p_2^+p_4^+(\boldsymbol{p}_1\cdot\boldsymbol{p}_3) - p_2^-p_3^-(\boldsymbol{p}_1\cdot\boldsymbol{p}_4)]$$

which transforms as a D_2 state.

It has been in fact by first writing the expressions on the right hand side of (A.1) (A.2) that the more convenient expressions (9) (10) in the text were written down.

RIASSUNTO

Vengono discusse le esperienze di Fregeau e Hofstadter sullo scattering elastico e inelastico di elettroni di alta energia dal ^{12}C, con particolare riferimento all'eccitazione del livello 2+ a 4.43 MeV e all'aumento del rapporto $d\sigma_{inelastico}/d\sigma_{elastico}$ con l'energia. Anche l'indipendenza dall'energia di $d\sigma_{inelastico}$ nell'intervallo 80—187 MeV viene spiegata. I calcoli sono eseguiti con un modello a shell sia nell'accoppiamento LS che nel JJ; l'accordo quantitativo è soddisfacente e migliore di un fattore tre nell'accoppiamento LS che nel JJ.

Covariant Canonical Equations for a Classical Field (I).

R. S. Liotta

Istituto di Fisica dell'Università - Roma
Istituto Nazionale di Fisica Nucleare - Sezione di Roma

(ricevuto il 21 Dicembre 1955)

Summary. — Hamilton's equations are written for a classical field by using the momenta conjugate to the field variables, with respect to all the directions of the time space frame of reference. The hamiltonian function becomes the spur of the canonical tensor and the equations become covariant ones. One can write Jacobi's equations in an invariant form and it can be shown that Jacobi's function is to be considered as the generator of a canonical transformation. With the introduction of convenient functionals one can study the evolution of the system when a certain space-like surface is made to vary.

Introduction.

The recent developments of electrodynamics are based on a covariant lagrangian formulation of quantum field theory. The lack of a corresponding classical method in a covariant hamiltonian form, makes one wonder whether such a type of theory could not be formulated, which could be useful in order to interpret field theory in terms of dynamical variables and their conjugate momenta.

In the present work we formulate in a covariant form the Hamilton equations and the Hamilton-Jacobi equation for a classical field. Our procedure is a generalization of the familiar methods which lead to the corresponding equations for a finite number of degrees of freedom.

In the above mentioned procedure the use of derivatives with respect to the time and space field coordinates leads automatically to functional derivatives of entities which are defined on certain space-like surfaces. In such a way one has the advantage of a covariant hamiltonian formulation which

involves dynamical quantities depending on a parameter (space-like surface) which allows one to follow the evolution of the system in «one» direction.

1. – Hamilton equations.

Let x_ν ($x_1, x_2, x_3, x_4 = ict$) denote a general point in a time-space frame of reference: let $A_{\mu^{(1)},\mu^{(2)},\ldots\mu^{(n)}}(x_\nu)$ ($\mu^{(1)}, \mu^{(2)}, \ldots, \mu^{(n)} = 1, \ldots, 4$) be a tensor of n-th order which is a regular function of x_α in a certain region.

Without reducing the generality of the argument we can suppose that the tensor be one of first order $A_\mu(x)$. In the following we shall suppress the symbol of summation according to the usual procedure.

The Lagrange equations for a system with an infinite number of degrees of freedom represented by a tensor $A_\mu(x)$, are given by

$$\frac{\partial}{\partial x_\nu}\frac{\partial L}{\partial(\partial A_\mu/\partial x_\nu)} - \frac{\partial L}{\partial A_\mu} = 0 \tag{1}$$

where the lagrangian differential function L is of the type

$$L = L\left(A_\mu, \frac{\partial A_\mu}{\partial x_\nu}\right) \tag{2}$$

and may also be dependent on the x explicitly. In general it is a quadratic form of A_μ and $\partial A_\mu/\partial x$ and is relativistically invariant.

Let

$$4\frac{\partial L}{\partial(\partial A_\mu/\partial x_\nu)} = P_{\mu\nu}. \tag{3}$$

It follows from (2) that

$$P_{\mu\nu} = P_{\mu\nu}\left(A_\mu, \frac{\partial A_\mu}{\partial x_\nu}\right),$$

which can be solved with respect to the $\partial A_\mu/\partial x_\nu$:

$$\frac{\partial A_\mu}{\partial x_\nu} = U_{\mu\nu}(A_\mu, P_{\mu\nu}). \tag{4}$$

The lagrangian function L will then be a function of A_μ and $P_{\mu\nu}$. Using (1) and (3) we can write

$$\frac{\partial P_{\mu\nu}}{\partial x_\nu} = 4\frac{\partial L(A_\mu, P_{\mu\nu})}{\partial A_\mu}. \tag{5}$$

Putting

$$H = P_{\mu\nu}\frac{\partial A_\mu}{\partial x_\nu} - \delta_{\mu\nu}L = P_{\mu\nu}\frac{\partial A_\mu}{\partial x_\nu} - 4L, \tag{6}$$

where δ indicates some arbitrary variations of A_μ and $P_{\mu\nu}$: keeping x constant, we get,

$$\delta H = \frac{\partial H}{\partial A_\mu}\,\delta A_\mu + \frac{\partial H}{\partial P_{\mu\nu}}\,\delta P_{\mu\nu} \tag{7}$$

and from (6) and (3)

$$\delta H = -4\,\frac{\partial L}{\partial A_\mu}\,\delta A_\mu + \frac{\partial A_\mu}{\partial x_\nu}\,\delta P_{\mu\nu}\,. \tag{8}$$

Subtracting (7) from (8), δA_μ and $\delta P_{\mu\nu}$ being arbitrary increments, we obtain considering also (5),

$$\begin{cases} \dfrac{\partial P_{\mu\nu}}{\partial x_\nu} = -\dfrac{\partial H}{\partial A_\mu} \\ \dfrac{\partial A_\mu}{\partial x_\nu} = \dfrac{\partial H}{\partial P_{\mu\nu}} \end{cases} \tag{9}$$

which are the generalization of the Hamilton equation for a system of an infinite number of degrees of freedom.

The simultaneous equations (9) have a higher number of dynamical variables, as compared with a normal canonical system; but this does not involve any inconvenience since the number of the equations is also higher. On the other hand, even if the conjugate momenta are four times as many as the field variables, in fact only a certain combination of them will appear in the equations which describe the dynamical evolution of the system.

We remark that the new hamiltonian function is not a positive defined one and that it is not to be interpreted as the energy of the system which in such case is given by the component T_{44} of the canonical tensor.

The canonical tensor is defined by

$$T_{\mu\nu} = P_{\alpha\mu}\frac{\partial A_\alpha}{\partial x_\nu} - \delta_{\mu\nu}L\,. \tag{10}$$

It follows that

$$H = T_{\nu\nu} = \text{Spur}\; T_{\mu\nu}\,,$$

H being relativistically invariant, and equations (9) are then covariant.

In the case of the electromagnetic field, putting

$$L = -\frac{1}{2}\,\frac{\partial A_\mu}{\partial x_\nu}\frac{\partial A_\mu}{\partial x_\nu}\,,$$

one obtains

$$H = -\frac{1}{8}\,P_{\mu\nu}P_{\mu\nu}\,, \qquad P_{\mu\nu} = -4\,\frac{\partial A_\mu}{\partial x_\nu}$$

and equations (9) become

$$\frac{\partial P_{\mu\nu}}{\partial x_\nu} = 0 \tag{11}$$

$$\frac{\partial A_\mu}{\partial x_\nu} = -\frac{1}{4} P_{\mu\nu} . \tag{12}$$

Introducing (12) into (11) we get

$$\Box A_\mu = 0 .$$

So that (12) can be considered as the equation which defines the momenta conjugate to the A_μ and (11) the equation of motion. With this choice of lagrangian the Lorentz condition is to be introduced separately.

For the real scalar meson field, putting

$$L = -\frac{1}{2}\left(\frac{\partial \varphi}{\partial x_\nu}\right)^2 - \frac{1}{2}\mu^2\varphi^2 ,$$

we get

$$P_\nu = -4\frac{\partial \varphi}{\partial x_\nu} , \quad H = -\frac{1}{8} P_\nu P_\nu + 2\mu^2\varphi^2$$

and the Hamilton equations can be written as follows:

$$\frac{\partial P_\nu}{\partial x_\nu} = -\frac{\partial \varphi}{\partial H} = -4\mu^2\varphi , \tag{13}$$

$$\frac{\partial \varphi}{\partial x_\nu} = \frac{\partial P_\nu}{\partial H} = -\frac{1}{4} P_\nu . \tag{14}$$

If one substitutes equation (14) which defines the momenta conjugate to the field variables φ, into (13), one gets the Klein-Gordon equation.

2. – On a different form of Hamilton's equations and their integration.

Jacobi's equation – In the left side of equations (9) the derivatives of the dynamical variables with respect to all the four coordinates x_α are involved. Usually in canonical equations only the derivatives with respect to time appear. That means that to study the evolution of a system one usually has to consider a family of surfaces $t = \text{const}$ of the time space reference (which is not covariant for a Lorentz transformation), and the derivatives with respect to time are the derivatives referred to the perpendicular to these surfaces.

In order to study the evolution of equations (10), maintaining the covariance of our representation, we introduce a family of space-like surfaces σ which covers entirely the chronotopus by varying only one parameter in such a way that given one point x_α it belongs to one and only one surface $\sigma(x)$. One can see then that the scheme considered in the present paper is formally analogous to the usual hamiltonian scheme. In the present case it is convenient to introduce some other dynamical variables, which are some functions of A_μ and $P_{\mu\nu}$, defined on a generic surface σ, and to consider their functional derivatives with respect to σ.

To this effect we define a differential quadrivector

$$\mathrm{d}\sigma_\mu \equiv (\mathrm{d}x_2\,\mathrm{d}x_2\,\mathrm{d}x_0,\ \mathrm{d}x_1\,\mathrm{d}x_3\,\mathrm{d}x_0,\ \mathrm{d}x_1\,\mathrm{d}x_2\,\mathrm{d}x_0,\ \mathrm{d}x_1\,\mathrm{d}x_2\,\mathrm{d}x_3/i)\ ,$$

$ix_0 = x_4$ and we assume it as defining the direction perpendicular to a surface σ. Then this vector is necessarily a time-like vector and its length is

$$\mathrm{d}\sigma_\mu^2 < 0\ .$$

Let

$$R_\mu(\sigma) = \int_\sigma P_{\mu\nu}(x')\,\mathrm{d}\sigma'_\nu\ , \tag{15}$$

$$S_{\mu\nu}(\sigma) = \int_\sigma A_\mu(x')\,\mathrm{d}\sigma'_\nu\ , \tag{16}$$

σ being an arbitrary portion of a surface containing the point x. It follows that

$$\frac{\partial P_{\mu\nu}}{\partial x_\nu} = \frac{\delta R_\mu(\sigma)}{\delta\sigma(x)}\ , \tag{17}$$

$$\frac{\partial A_\mu}{\partial x_\nu} = \frac{\delta S_{\mu\nu}(\sigma)}{\delta\sigma(x)}\ , \tag{18}$$

where the symbols δ indicate functional derivatives [1].

Remembering (17) and (18), the Hamilton equations (10) can be written

$$\begin{cases} \dfrac{\delta R_\mu(\sigma)}{\delta\sigma(x)} = -\dfrac{\partial H}{\partial A_\mu} \\ \dfrac{\delta S_{\mu\nu}(\sigma)}{\delta\sigma(x)} = \dfrac{\partial H}{\partial P_{\mu\nu}} \end{cases} \tag{19}$$

where the terms on the right hand sides are supposed to be expressed in terms

[1] See f. 1 Schwinger: *Phys. Rev.*, **74**, 1439 (1948).

of R_μ and $S_{\mu\nu}$. The solutions of equations (19) will be of the type

$$R_\mu = R_\mu(R^0_\mu, S^0_{\mu\nu}, \sigma) \tag{20}$$

$$S_{\mu\nu} = S_{\mu\nu}(R^0_\mu, S^0_{\mu\nu}, \sigma) \tag{21}$$

being

$$R^0_\mu \equiv R_\mu(\sigma^0)\,, \qquad S^0_{\mu\nu} \equiv S_{\mu\nu}(\sigma^0)\,, \tag{22}$$

assuming that σ^0 is the particular surface σ starting from which the motion of our system is being studied.

Because of (17) and (18) in close analogy with the usual procedure followed when canonical system are considered, we shall write the solutions of our system (10) making use of the functionals

$$A_\mu = A_\mu(A^0_\alpha, P^0_{\alpha\beta}, x_\lambda)\,, \tag{23}$$

$$P_{\mu\nu} = P_{\mu\nu}(A^0_\alpha, P^0_{\alpha\beta}, x_\lambda)\,, \tag{24}$$

A^0_α and $P^0_{\alpha\beta}$ being the values taken by the dynamical variables A_α and $P_{\lambda\beta}$ on the surface σ_0 while x_λ belong to an generic surface σ [2].

We shall consider next the functional

$$V_\mu = V_\mu(A_\nu(x), x)\,. \tag{25}$$

Putting

$$\frac{\partial V_\nu}{\partial A_\mu} = P_{\mu\nu}, \tag{26}$$

we write the Jacobi equation making use of V_ν:

$$\frac{\partial V_\nu}{\partial x_\nu} + H\left(A_\mu, \frac{\partial V_\nu}{\partial A_\mu}\right) = 0\,, \tag{27}$$

where the $\partial/\partial x_\nu$ are derivatives with respect to the x explicitly and the function H is the same which appears in the hamiltonian equations (9) when one takes into account (26).

We intend to show now that if an integral of (27) exists, which is of type

$$V_\nu = V_\nu(A_\mu, A^0_\mu, x), \tag{28}$$

[2] We would like to remark that, as seen above, $P_{\mu\nu}$ represents $\partial A_\mu/\partial x_\nu$ apart from a constant factor (the hamiltonian function is in fact quadratic in A_μ and $\partial A_\mu/\partial x_\nu$). Therefore, when on a given surface σ the A_μ are known, the derivatives of A_μ on the surface are automatically known, and the $P_{\mu\nu}$ are only used to indicate the behaviour of the derivatives of A_μ on the perpendicular to the σ.

we can then obtain the integral of equations (9) putting

$$\frac{\partial V_\nu}{\partial A_\mu} = P_{\mu\nu}(A_\mu, A^0_\mu, x)\,, \tag{29}$$

$$\frac{\partial V_\nu}{\partial A^0_\mu} = P^0_{\mu\nu}(A_\mu, A^0_\mu, x)\,. \tag{30}$$

Solving equations (30) with respect to A_μ we obtain,

$$A_\mu = A_\mu(A^0_\mu, P^0_{\mu\nu}, x) \tag{31}$$

and considering (29)

$$P_{\mu\nu} = P_{\mu\nu}(A^0_\nu, P^0_{\mu\nu}, x)\,, \tag{32}$$

i.e. (31) and (32) are formally similar to (23) and (24). We can easily show that they are also solutions of the equations of motion. Performing the derivatives of $P_{\mu\nu}$ with respect to x_ν keeping A^0_μ constant, and then summing with respect to x, we obtain, remembering the equations (9),

$$\frac{\partial}{\partial A_\mu}\left(\frac{\partial V_\nu}{\partial x_\nu} + H\right) = 0,$$

which is certainly verified since (28) is a solution of the Jacobi equation (27). In a similar way, calculating the derivatives of (30) with respect to the x_ν ($A^0_\mu = \text{cost}$) and summing with respect to ν, we get

$$\frac{\partial}{\partial A^0_\mu}\left(\frac{\partial V_\nu}{\partial x_\nu} + H\right) = 0\,,$$

an equation which is certainly verified for the same reasons as before.

Also equation (27) can be put in a form which is more suitable for physical interpretation. We only need to introduce the functional $V(\sigma)$ defined as follows

$$V(\sigma) = \int_\sigma V_\nu(x')\,\mathrm{d}\sigma'_\nu\,. \tag{33}$$

We get immediately

$$\frac{\delta V(\sigma)}{\delta\sigma(x)} = \frac{\partial V_\nu}{\partial x_\nu}$$

so that Jacobi's equation can be written

$$\frac{\delta V(\sigma)}{\delta\sigma(x)} + H\left(A_\mu, \frac{\partial V_\nu}{\partial x_\nu}\right) = 0\,. \tag{34}$$

3. – Canonical transformations.

The condition discussed above allows one to write the necessary conditions to ensure that a transformation be a canonical one. This will be done following, in close analogy, the procedure followed in analytical mechanics for systems having a finite number of degrees of freedom.

Clearly one defines as canonical a transformation of variables A_μ, $P_{\mu\nu}$, into some other variables a_μ, $p_{\mu\nu}$ which can be inverted and depends on the x_α and transforms the canonical equations (9) into

$$\text{(35)} \qquad \begin{cases} \dfrac{\partial p_{\mu\nu}}{\partial x_\nu} = -\dfrac{\partial \overline{H}}{\partial a_\mu} \\ \dfrac{\partial a_\mu}{\partial x_\nu} = \dfrac{\partial \overline{H}}{\partial p_{\mu\nu}} \end{cases}$$

where $\overline{H} = \overline{H}(a_\mu, p_{\mu\nu})$ is a new hamiltonian function which is not necessarily equal to the transform of H.

From equation (6) we have

$$\text{(36)} \qquad 4L = P_{\mu\nu}\frac{\partial A_\mu}{\partial x_\nu} - H$$

and from the new variable we can define a lagrangian function $\overline{L}$ such that

$$4\overline{L} = p_{\mu\nu}\frac{\partial a_\mu}{\partial x_\nu} - \overline{H}\,.$$

Since Lagrange equations can be deduced from the variational equation [3]

$$\delta\int_\Omega L\,\mathrm{d}w = 0,$$

it follows that

$$\delta\int_\Omega\left(p_{\mu\nu}\frac{\partial a_\mu}{\partial x_\nu} - \overline{H}\right)\mathrm{d}w = \delta\int_\Omega\left(p_{\mu\nu}\frac{\partial A_\mu}{\partial x_\nu} - H\right)\mathrm{d}w = 0,$$

where δ indicates some arbitrary infinitesimal variation of the dynamical variables at any point inside the volume Ω which however vanishes on the boundary surface of Ω.

Therefore, if V_μ is a function of the dynamical variables and in some cases

[3] G. WENTZEL: *Quantum Theory of Fields* (New York, 1949).

of the x, the variations δV_μ on the surface of Ω (x_α being constant) will vanish; remembering Gauss' theorem, from the preceding equation we get

$$P_{\mu\nu}\frac{\partial A_\mu}{\partial x_\nu} - H = p_{\mu\nu}\frac{\partial a_\mu}{\partial x_\nu} - \overline{H} + \frac{\mathrm{d}V_\nu}{\partial x_\nu}$$

and if we assume V_ν to be of the form

$$V_\nu = V_\nu(A_\mu, a_\mu, x),$$

we see that it must follow that

$$P_{\mu\nu} = \frac{\partial V_\nu}{\partial A_\mu}, \qquad p_{\mu\nu} = -\frac{\partial V_\nu}{\partial a_\mu},$$

$$H = \frac{\partial V_\nu}{\partial x_\nu} + H = \frac{\delta V(\sigma)}{\delta\sigma(x)} + H\,.$$

These equations show that Jacobi functions V_ν given by (28) can be considered as the generator of a canonical transform in which the transformed hamiltonian function is given by the left side of the Jacobi equation (27).

* * *

Further developments will be published later in a subsequent paper. I wish to express my gratitude to Prof. B. Ferretti for useful discussions and helpful advice.

RIASSUNTO (*)

Si scrivono le equazioni di Hamilton per un campo classico usando i momenti coniugati alle variabili di campo, rispetto a turte le direzioni del sistema di riferimento spazio-temporale. La funzione hamiltoniana diventa la traccia del tensore canonico e le equazioni diventano covarianti a vista. Si scrive l'equazione di Jacobi in forma invariante e si dimostra che la funzione di Jacobi si può considerare come la generatrice di una trasformazione canonica. Con l'introduzione di convenienti funzionali si può studiare l'evoluzione del sistema al variare una determinata superficie spaziale.

IL NUOVO CIMENTO Vol. III, N. 2 1° Febbraio 1956

On the Observation of an Antiproton Star in Emulsion Exposed at the Bevatron.

O. Chamberlain, W. W. Chupp, G. Goldhaber, E. Segrè and C. Wiegand

Radiation Laboratory, Department of Physics, University of California, Berkeley, California

E. Amaldi, G. Baroni, C. Castagnoli, C. Franzinetti and A. Manfredini

Istituto di Fisica dell'Università - Roma
Istituto Nazionale di Fisica Nucleare - Sezione di Roma

(ricevuto il 5 Gennaio 1956)

Summary. — In connection with the antiproton investigation at the Bevatron several stacks of nuclear emulsions have been exposed in a magnetically selected beam of negative particles. The selected particles were produced in a copper target, bombarded with protons of 6.3 GeV, and had a momentum of 1.09 GeV/c. The experiments were designed to observe the annihilation process undergone by an antiproton brought to rest inside the emulsion. The details of the investigation are given in Section 2. Section 3 contains an estimate of the number of expected annihilation stars as obtained from previous measurements with counter experiments reported by Chamberlain, Segrè, Wiegand and Ypsilantis. Section 4 contains the description of the only event found so far. The mass of the primary particle responsible for it, as obtained from a weighted average using several independent methods is $(1824 \pm 51)\, m_e$. The star produced by it, is associated with a minimun release of « visible » energy of ~ 826 MeV while the corresponding unbalanced « visible » momentum amounts to ~ 520 MeV/c.

1. – Introduction.

Among the major research plans for the Bevatron was the investigation of the possible production of antiprotons and their study. This problem has been attacked in several ways and the first success has been the identification

of particles of protonic mass and charge equal to that of the electron by CHAMBERLAIN, SEGRÈ, WIEGAND and YPSILANTIS [1]. Stability againts spontaneous decay and the excitation function for production were also investigated as much as possible.

Another aspect of the problem is the study of the terminal process of the antiproton, especially the demonstration of the large energy release upon annihilation. Some information on the energy released by the particles selected in the experiment of reference [1] was obtained by BRABANT, CORK, HORWITZ, MOYER, MURRAY, WALLACE and WENZEL [2].

A few months ago the authors of this paper started to collaborate in the search for stars produced by antiprotons that annihilated in nuclear emulsions exposed at the Bevatron. Several events in cosmic rays that could very possibly be interpreted as due to antiprotons had been found by HAYWARD [3], COWAN [4] and BRIDGE, COURANT, DESTAEBLER and ROSSI [5]. Most pertinent of these was the peculiar event found in a photographic emulsion exposed to the cosmic rays in the upper atmosphere by AMALDI, CASTAGNOLI, CORTINI, FRANZINETTI and MANFREDINI [6] consisting of two stars connected by a black track.

The probability that such an event [6] be due to an accidental coincidence in space, although not negligible, was sufficiently small to justify the consideration of an interpretation in terms of a physical process. From a detailed study of the two stars (energy released in the primary star greater than 5 GeV and greater than or equal to 1.5 GeV in the secondary star) it was concluded that the more plausible interpretation was that of an annihilation process of a heavy particle, possibly that of an antiproton. However, the short range of the connecting particle dit not allow a determination of its mass.

The search for other events of the same or of a similar type fitted in a natural way into the program in progress at the Radiation Laboratory and led to the combined effort by the present authors.

The experiments on which we report here were designed to observe the annihilation process undergone by an antiproton of given momentum brought to rest inside the emulsion.

---

[1] O. CHAMBERLAIN, E. SEGRÈ, C. WIEGAND and T. YPSILANTIS: *Phys. Rev.*, **100**, 947 (1955).

[2] J. M. BRABANT, B. CORK, N. HORWITZ, B. I. MOYER, J. J. MURRAY, R. WALLACE and W. A. WENZEL: *Phys. Rev.* (in press).

[3] E. HAYWARD: *Phys. Rev.*, **72**, 937 (1947).

[4] E. W. COWAN: *Phys. Rev.*, **94**, 161 (1954).

[5] H. S. BRIDGE, H. COURANT, H. DESTAEBLER and B. ROSSI: *Phys. Rev.*, **95**, 1101 (1954).

[6] E. AMALDI, C. CASTAGNOLI, G. CORTINI, C. FRANZINETTI and A. MANFREDINI: *Nuovo Cimento*, **1**, 492 (1955).

The energy released in the elementary process of annihilation of a pair of nucleons ($2M_pc^2 = 1876$ MeV) can be taken away by annihilation products such as two or more pions whose states (charge, parity, angular momentum) must satisfy the selection rules imposed by conservation theorems (7). The phenomenon is further complicated if the annihilation process takes place in a nucleus as we expect will normally be the case if it happens in nuclear emulsion.

Two types of exposures (called respectively plan A and plan B) have been made. They are described in Section 2. Section 3 describes the scanning methods employed and estimates the number of antiprotons stopped in the stacks. Section 4 gives the details of the first event found in the laboratory of Rome (8).

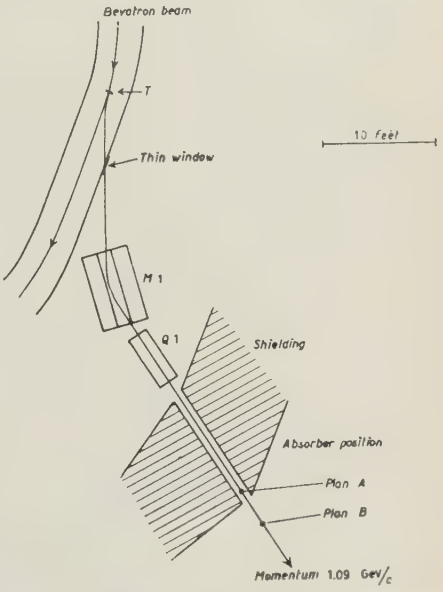

Fig. 1. – Plan view of the magnetic selection and focusing magnets.

2. – Experimental Procedure.

A schematic diagram of the experimental arrangement is shown in Fig. 1. The 6.3 GeV proton beam impinged on a 1-inch-thick copper target. Negative particles produced in the forward direction were deflected outward through a thin window of effective thickness equal to 1.8 g cm^{-2} Al. These particles were accepted by the bending magnet M_1 and deflected an additional 32° into a strong-focusing lens $Q1$. In the two experiments, to be called plan A and plan B, the lens $Q1$ focussed the particles at the points A and B respectively, just outside the Bevatron shielding wall.

A copper absorber located at either position A or B (Fig. 1) decreased the energy of antiprotons a sufficient amount to permit them to stop in emulsion stacks placed after the absorber.

All emulsion stacks used in these experiments were of a uniform size and shape. Each stack consisted of 60 pellicles 600 μm thick of Ilford G-5 emulsion 4×7 sqinch in area. The beam entered normal to the 4-inch dimension and the plane of the emulsion was horizontal.

(7) D. Amati and B. Vitale: *Nuovo Cimento*, **2**, 719 (1955).

(8) A preliminary report has been submitted for publication at the *Phys. Rev.* and has also been presented at the Accademia Nazionale dei Lincei on Decembre 10th, 1955.

The momentum dispersion of the magnetic focusing system, measured at the focus, was $\Delta p/p = 0.007$ per inch lateral displacement. The overall uncertainty in momentum at any point in the image plane was estimated to be $\Delta p/p = 0.02$.

In the choice of the momentum adopted in the actual experimental conditions ($p = 1.09$ GeV/c corresponding to protons of $T = 500$ MeV, K-particles of $T = 700$ MeV and pions of $T = 960$ MeV kinetic energy), we have been guided by considerations of feasibility and by the considerations presented in the Appendix where an estimate is given of the spectrum of the emitted antiprotons based only on statistical factors, Lorentz transformations, and the movement of the nucleons in the target.

The first detection method, called plan A, involved putting the emulsion stack directly in the momentum analyzed beam, behind a copper absorber. Two exposures were carried out using this plan.

In the first exposure, we placed two emulsion stacks (63 and 64) directly behind the copper absorber which was located at the position A indicated in Fig. 1. This absorber was wedge-shaped (Fig. 2) and oriented in such a way as to

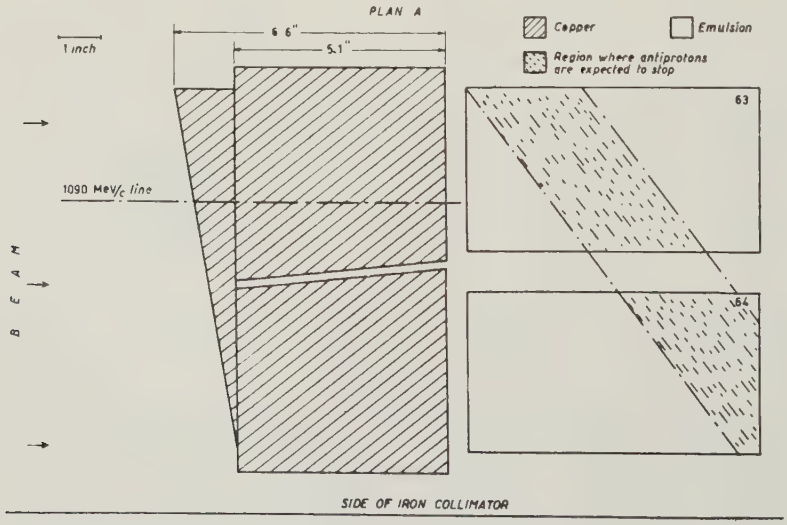

Fig. 2. – Arrangement of absorbers and emulsions in plan A.

double the momentum dispersion. The purpose of increasing the dispersion was to diminish the danger that a slight misalignment might cause the end point of the antiprotons to fall completely out of the stack. This arrangement gave an expected region for antiprotons stopping as shown in Fig. 2. The total width of the band in which antiprotons were expected to stop was about 7 cm. This width was determined from the combined effects of range straggling,

momentum dispersion and multiple scattering. Stacks 63 and 64 were exposed to the flux of particles produced by $1.7 \cdot 10^{13}$ and $3 \cdot 10^{13}$ protons on the target, respectively. A π-meson count gave a flux of $5.3 \cdot 10^4$ and $1.3 \cdot 10^5$ pions per cm^2, respectively, at the entrance of the stack. The wedge absorber used in the way described above makes acceptable a momentum uncertainty corresponding to a variation in total range of ± 30 g cm^{-2} Cu equivalent.

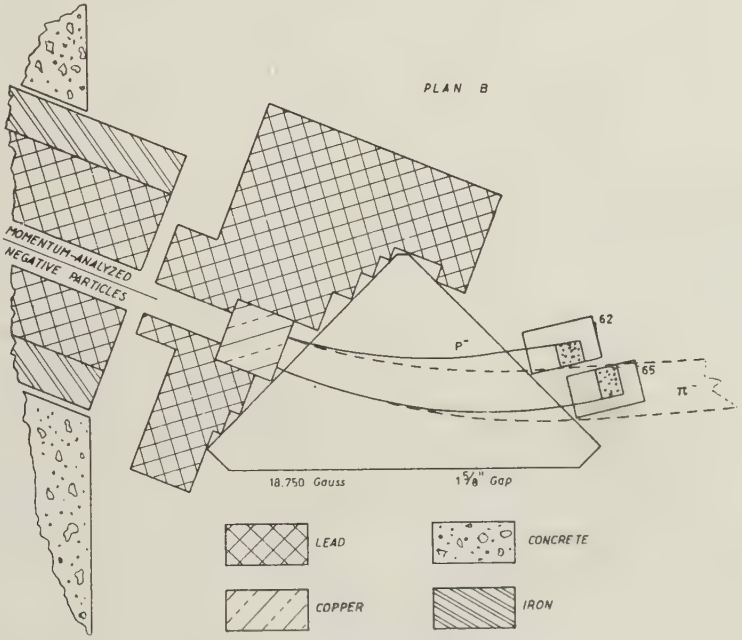

Fig. 3. – Arrangement of plan B.

Later we became more confident of the absolute value of the momentum of the beam, so the second exposure (stack 66) was carried out with the wedge reversed. The wedge in this case cancelled the momentum dispersion, so that the average energy of antiprotons entering the emulsion was the same over the whole face of the stack, and the volume of the emulsion to be scanned was reduced. The antiprotons were expected to stop in a band parallel to the short dimension of the plates and 3.5 cm wide. In this exposure the stack received a particle flux resulting from $1 \cdot 10^{13}$ protons on the bevatron target. A π-meson count gave a flux of $3.3 \cdot 10^4$ pions per cm^2 entering the stack. An overall check of this arrangement was made using protons.

In the second detection method, called plan B, the copper absorber (surface density $= 132$ g cm^{-2}) was located at position B, indicated in Fig. 1. Note that antiprotons and pions entering the copper absorber with the same momentum emerge with different momenta. A deflecting magnet was placed

immediately behind the absorber to provide a further deflection of particles transmitted by the absorber as shown in Fig. 3. Because antiprotons and pions now have a different momentum a partial separation is obtained. The magnet pole tips were cut in the shape of a 90° wedge focusing sector. The gap was $1\frac{5}{8}$ inches and the field intensity was 18750 gauss. At the exit boundary of the field, two stacks (62 and 65) of emulsion were placed.

Ahead of the copper absorber, the beam was defined to a width of 3 inches by a lead collimating slot. This defined a momentum channel centered at 1.09 GeV/c and varying from 1.08 to 1.10 GeV/c. At the point of exit from the absorber the mean momentum of pions was 867 MeV/c and the mean momentum of expected antiprotons was 652 MeV/c. A horizontal separation of 2 inches between the central pion and antiproton momenta was achieved at the stack position. Antiprotons of 652 MeV/c were expected to have a range of 10.4 cm in the stacks. The magnetic wedge sector, besides increasing the relative abundance of antiprotons in the beam, also had other favorable effects: namely it provided a clearing field for positive particles produced by pion interactions in the absorber thereby reducing the number of spurious tracks in the emulsion and facilitating the scanning; and it also resulted in the restriction of the angles of incidence of antiprotons to a narrow angular range slightly different from that of the pions.

The angular restrictions which were thus placed on particles entering the emulsion, together with a grain density criterion, have been adopted as necessary conditions that an antiproton must satisfy. These conditions make the possibility of a chance coincidence between the end point of a selected stopped particle and a neutron star negligibly small.

Stacks 62 and 65 were exposed in this experimental arrangement with a total flux of $4.7 \cdot 10^{13}$ protons on the target.

3. – Yield Estimates and Scanning Methods.

The ratio $p^-/\pi^- = 1/44000$ obtained in the counter experiments ([1]) was measured at a momentum of 1.19 GeV/c and at a distance of 80 feet from the target. In the emulsion experiments, the stacks were approximately 40 feet distant from the target and the momentum was 1.09 GeV/c. The ratio p^-/π^- in the beam incident at the absorber position in these experiments becomes $p^-/\pi^- = 1/52000$ if we correct for the pion decay in flight and assume that the production ratio is not affected by the change in momentum.

The calculation of the number of antiprotons expected in plan *A* exposures is straightforward except for the fact that the absorption cross-section in copper for antiprotons is unknown. In the planning of the present experiments we assumed that the attenuation of antiprotons in the absorber would

be about the same as that for pions. Recently, DUERR and TELLER (9) have proposed a model which predicts that the cross-section of antiprotons may be as large as twice geometric in a medium weight element such as copper. We have therefore calculated upper and lower limits for the expected number of antiprotons in the stacks based on the assumption of $\sigma_{p^-} = \sigma_{\pi^-} \sim \sigma$ (geometric) for the upper limit and $\sigma_{p^-} = 2\sigma_{\pi^-}$ for the lower limit.

The expected number of antiprotons in the exposure of plan *B* can be estimated as follows: we use the measured value of the total pion flux incident on stacks 62 and 65. This number is 10^6 pions. The effect of multiple scattering in the copper absorber is different for the pions and antiprotons, and this produces an impoverishment of antiprotons in the beam by a factor 0.7. The usable front edges of the stacks receive 75 percent of the antiproton flux. Therefore we expect $10^6 \cdot 0.7 \cdot 0.75/52\,000 = 10$ antiprotons if the antiprotons and pions have the same attenuation. It the antiprotons have a nuclear cross-section twice the pion cross-section, their number is reduced to 4.

In scanning the emulsions three general methods were adopted.

a) *Area Scanning.* – Area scanning was carried out principally on stack 64, in the region where negative protons were expected to end (Fig. 2). The flux, which is $1.3 \cdot 10^5\ \pi/\text{cm}^2$ at the leading edge of stack 64, is reduced, due to the additional attenuation in passing through 15 cm of emulsion, to $8.4 \cdot 10^4\ \pi/\text{cm}^2$ at the scanning position. As the width of the region in which the negative protons are expected to end is 7 cm, the scanning of 1 cm² (600 μm emulsion) corresponds to $7.6 \cdot 10^2$ π-mesons. If we use $\sigma_{p^-} = \sigma_{\pi^-}$ an area of 1 cm² would correspond to $1.5 \cdot 10^{-2}$ p⁻. If we use $\sigma_{p^-} = 2\sigma_{\pi^-}$, the scanning of 1 cm² would yield $4 \cdot 10^{-3}$ p⁻. In Berkeley 59 cm² and in Rome 131 cm² have been scanned in stack 64 by this method with a scanning efficiency that is difficult to estimate.

b) *Along-the-track scanning from the leading edge of the stack.* – This method was used for parts of stacks 62 and 65 of plan *B*. Here tracks entering the stack at the proper angle and grain density were picked up by scanning along the leading edge. These tracks were then followed to the end of their range and checked for interactions at rest or in flight.

The amount of scanning done by this method is best expressed in terms of the number of linear cm scanned in each 600 μm thick plate at the usable front edge of the stack. In each of the two stacks 62 and 65 there are 60 emulsions of 9 cm usable front edge and hence $2 \times 60 \times 9$ cm = 1080 cm that can be scanned along the leading edge of all the plates. In Section 2 above we have computed the total number of antiprotons expected in stacks 62 and 65 to be 10 for $\sigma_{p^-} = \sigma_{\pi^-}$ and 4 for $\sigma_{p^-} = 2\sigma_{\pi^-}$. This gives $9 \cdot 10^{-3}$ p⁻ per linear cm and $3.8 \cdot 10^{-3}$p⁻ per linear cm respectively. In Berkeley 290 linear cm of

(9) P. DUERR and E. TELLER: *Phys. Rev* (in press).

stacks 62 and 65 have been scanned by this method, with a scanning efficiency not fully determined.

c) *Along-the-track scanning from a region inside the emulsion stack.* – In this method all grey and black tracks going in a forward cone of $\pm 30^\circ$ are picked up at a position 7 cm from the leading edge and followed. It is clear that if this method is used in each plate of the stack, all antiprotons that have not undergone a nuclear interaction will be picked up and followed to the end of their range. This method was also used for parts of stacks 62 and 65.

The expected yield of antiprotons using this method of scanning can also be expressed in terms of number of antiprotons per linear cm. Due to the additional attenuation in the 7 cm of emulsion that an antiproton has to traverse before being picked up, the expected number of antiprotons is $8 \cdot 10^{-3}$ p^- per linear cm for $\sigma_{p^-} = \sigma_{\pi^-}$ and $3.1 \cdot 10^{-3}$ p^- per linear cm for $\sigma_{p^-} = 2\sigma_{\pi^-}$.

In Rome 50 linear cm of stack 62 have been scanned by this method with a scanning efficiency that is difficult to evaluate. The one star described below was found by this method.

For stack number 66 where this method was also applied the expected number of p^- is $3.4 \cdot 10^{-2}$ per linear cm and $1.1 \cdot 10^{-2}$ per linear cm respectively. In Berkeley 46 linear cm of stack 66 have been scanned by this method.

Following the procedures described above we estimate 7 antiprotons (assuming $\sigma_{p^-} = \sigma_{\pi^-}$) or 2.5 antiprotons (assuming $\sigma_{p^-} = 2\sigma_{\pi^-}$) should have been found whereas we have found only one. This might indicate a high value of σ_{p^-}.

4. – Description of the event.

In the scanning of plan *B* with method *c*), we observed a particle of protonic mass which came to rest and produced a large star.

The primary particle. – The track of the primary particle indicated in the following discussion by the letter *L*, enters emulsion number 62-12 from its front edge at a distance of 19 mm from the left hand corner. At this point the track forms an angle of 2° with the horizontal plane and is directed from emulsion 12 to emulsion 11 (i.e. downward). In the horizontal plane it makes an angle of 3° (from right to left) with the normal to the front edge of the emulsions.

These data permit us to determine that the trajectory of the particle remained inside the gap of the wedge magnet (see Fig. 3) when the particle was moving from the Cu absorber to the stack of emulsions. It is thus clear that the particle was not scattered on the magnet pole faces.

Proceeding from its entrance into the stack, track *L* goes to emulsion

umber 62-4 and then comes back to emulsion 62-9 where the star was pro-uced. The total range traversed by the primary particle from the entrance oint to the star is

$$R_L = (9.31 \pm 0.09) \text{ cm}$$

here the indicated error represents the standard deviation due to straggling. t a distance of 2.10 cm from the end of the range ($T = 80$ MeV) L under-oes an 8° scattering which does not show any recoil.

TABLE I. – *Mass measurements on the primary track.*

Method	Range Interval from the end (mm)	M/m_e	M/M_p
Ionization-scattering	82.0–66.0	1840 ± 250	1.00 ± 0.14
Ionization (mean gap length)-range	79.4–19.0	1810 ± 100	0.99 ± 0.06
Gap length-range	5–0	1740 ± 130	0.95 ± 0.07
Scattering-range	10–0	1635 ± 280	0.89 ± 0.15
Residual range-momentum (from orbit)	93.14 plus 132 g cm^{-2} copper	1865 ± 70	1.02 ± 0.04
Weighted average	—	1824 ± 51	0.99 ± 0.03

The determination of the particle's mass has been made by various methods whose results have been collected in Table I.

The scattering-grain density determination is based on the following experimental results:

$$p\beta = (305 \pm 30) \text{ MeV/c}$$

$$g/g_0 = 2.14 \pm 0.06,$$

which represent the coordinates of the center of the black rectangle marked as L in Fig. 4. Here g/g_0 is the ratio between the grain density and its plateau value. The open rectangles given

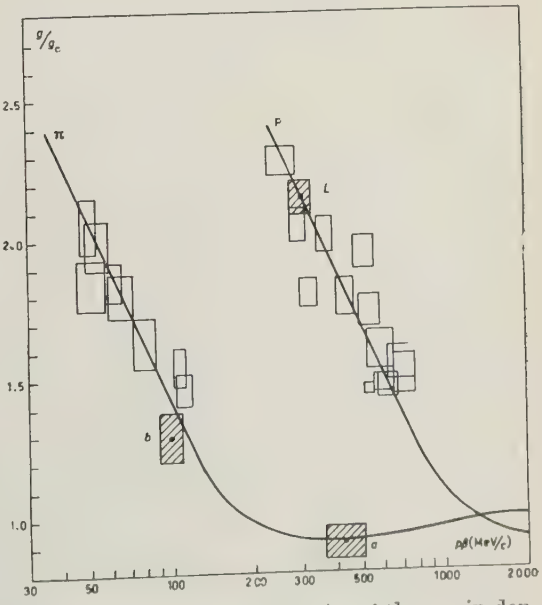

Fig. 4. – Plot of the ratio g/g_0 of the grain density to plateau value of grain density versus $p\beta$.

in the same figure represent the results of measurements on a few protons and pions used for calibration. The indicated curves represent the best fit (by means of the least square method) to the calibration points.

Some of the mass measurements are based on specific ionization and range determinations. The specific ionization has been determined either by grain count or by gap length measurement, depending upon which method was considered the more reliable in the velocity interval being studied ([10]).

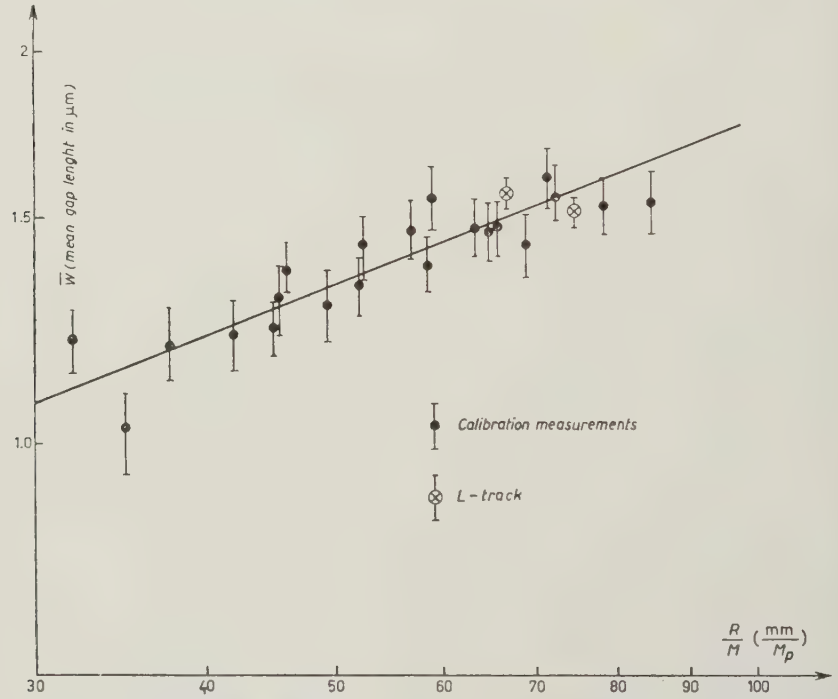

Fig. 5. – Plot of mean gap length versus R/M. R is the range in mm and M is the mass in units of the proton mass.

The calibration points of the mean gap length obtained by measuring a few pions in the same emulsions traversed by track L are shown in Fig. 5 where the straight line represents the best fit by means of the least square method. The two points relative to track L have been plotted in this figure under the assumption of a protonic mass, whereas in order to determine the value of the mass given in Table I, we have compared the measured value of R_L with the values of R/M deduced from the measured mean gap length and the straight line of Fig. 5.

The actual measurements were made in the following intervals of residual

([10]) C. CASTAGNOLI, G. CORTINI and A. MANFREDINI: *Nuovo Cimento*, **2**, 301 (1955).

O. Chamberlain, W. W. Chupp, G. Goldhaber, E. Segrè and C. Wiegand - *Berkeley*
E. Amaldi, G. Baroni, C. Castagnoli, C. Franzinetti and A. Manfredini - *Rome*

Fig. 6. – The star. *L* indicates the incoming antiproton track. Tracks *a* and *b* are pions, and *c* is a proton. The remaining tracks could be protons or α-particles.

range: 7.94 to 7.46 cm; 6.91 to 6.59 cm; 2.35 to 2.15 cm and 2.10 to 1.90 cm. The value given in Table I represents a weighted average.

Two determinations of the mass have been made near the end of the range. The first one by the gap-length-range method and the second by the scattering-range (constant sagitta) method.

Finally another determination of the mass was made by combining the total residual range in the Cu absorber and the emulsion with the magnetic rigidity of this particle as it is known from its trajectory.

The momentum of the particle has been measured on the trajectory of the particle by stretching a current carrying wire under known tension. Taking into account the absorption of the media traversed before entering the Cu absorber of Fig. 1 we find that at the entrance of this block the momentum was (1.090 ± 0.020) GeV/c. The particle traversed 132 g cm^{-2} of Cu and 9.31 cm of emulsion before coming to rest. Using standard range-energy relations we find from these data that its mass was $(1865 \pm 70)\, m_e$. The uncertainty arises mainly from the momentum measurement.

In the foregoing discussion we have tacitly assumed that the particle did not suffer a nuclear inelastic collision. This assumption is very likely correct because the angle of entrance into the emulsion is within the limits to be expected under such a hypothesis. Any inelastic collision would produce an apparent mass heavier than the true one.

From Table I one can conclude that the various measurements made with different methods are in satisfactory agreement and give a mass very close to the proton mass. Furthermore the agreement of the various mass measurements indicates that this particle came to rest before producing the star.

TABLE II. – *Individual measurements on the tracks of the star.*

Track	Range (μm)		Number of emulsions crossed	I/I_0	$p\beta$ MeV/c	Identity	T (MeV)	cos φ	θ
a	23 960	observed in em.	8	0.90 ± 0.06	430 ± 70	π	332	0.985	238° 26′
b	19 500	observed in em.	8	1.29 ± 0.09	98 ± 9	π	57.5	0.972	99° 35′
c	4 250	total	3	—	—	p	32.3	0.961	294° 40′
d	1 100	total	2	—	—	p(?)	15.0	0.860	350° 5′
e	340	total	1	—	—	p(?)	7.6	0.927	59° 45′
f	202	total	1	—	—	p(?)	5.5	0.800	124° 3′
g	4 050	total	6	—	—	p(?)	31.4	0.466	153° 22′
h	206	total	1	—	—	p(?)	5.5	0.208	129° 5′
i	100	total	1	—	—	p(?)	3.6	0.141	212° 44′

φ = angle of dip.
θ = angle in the plane of the emulsion.

The star. – Fig. 6 is a microphotograph of the star and Table II shows the pertinent data relative to its various prongs. Only tracks *a* and *b* go out of the stack.

The results of the measurements of the ionization and scattering of these two tracks are shown in Fig. 4 from which one can conclude with certainty that *b* is due to a pion whereas *a* had a mass certainly much smaller than that of a proton and most probably is due to a pion; this will be assumed in the following discussion.

Track *c* has been identified as a proton by means of gap measurements. The total energy release associated with these three identified particles amounts to 709 MeV as it is shown in Table III.

The tracks of all other particles, from *d* through *i*, are much too steep to allow an estimate of their masses.

The energy and momentum balance depends, of course, on the identification of all these tracks.

Various assumptions have been made on the nature of these particles; if we assume that they are all protons we obtain the minimum value of the visible energy (826 MeV) while if we assume that they are all alphas we get what we take as an upper limit since we consider it unlikely that any of these

TABLE III. – *Visible energy and momentum estimated under*

A) Identified particles

track	*a*	*b*	*c*
nature	π	π	p
T_i (MeV)	332	58	32

Kinetic energy of the two pions *a*) and *b*)	390 MeV
Rest energy of the two pions *a*) and *b*) . .	279 »
Kinetic energy of the proton *c*)	32 »
Binding energy of the proton	8 »
	709 MeV

Track	*d*
assumed identity	p
T_i (MeV)	15.0
assumed identity	p
T_i (MeV)	15.0
assumed identity	α
T_i (MeV)	59.2
assumed identity	α
T_i (MeV)	59.2

(*) The separation energy of the protons has been tak

tracks are due to particles heavier than an α-particle. Both these assumptions are probably too extreme. By tentative attributions of masses 1, 2, 3 and 4 to the particles d), ... i), we found that the minimum unbalanced momentum is obtained when tracks d) and i) are assumed to be alphas while all the others are protons (Table III).

But also such an assignment of masses seems rather unlikely because it implies the emission of an α-particle (track d) with an energy of 59 MeV, a circumstance which happens in less than 1 percent of the cases of α-emission.

The case that appears most likely to us is that given in the second line of Table III. There it is assumed that the four shortest tracks (e, f, h, i) are due to alphas while the others are due to protons. Such an assignment is made plausible by a comparison of the range spectra of both protons and alphas emitted in disintegrations of comparable excitation energy.

The visible energy is so high that independently of the determination of the mass of the primary, we can exclude the possibility that the observed star be due to any known particle except the antiproton.

On the other hand the determination of the mass of the primary confines its value to a rather narrow interval around the mass of the proton. There-

s regarding the nature of the unidentified particles.

identified particles						
/	h	i	Total kinetic energy (ΣT_i in MeV)	Unbalanced momentum (MeV/c)	Separation energy of protons (*) ($8N_p$ in MeV)	C) Total visible energy $709 + \Sigma T_i + 8N_p$ (MeV)
)	p	p				
.4	5.5	3.6	69	520	48	826
)	α	α				
.4	22	14.4	135	820	16	860
)	p	α				
.4	5.5	14.4	124	470	32	865
α	α	α				
26	22	14.4	274	982	—	983

ion energy of the α's has been neglected.

fore one can try to interpret the observed event as due either to the annihilation of an antiproton, or to the absorption of a new kind of particle whose mass is not far from that of the proton. This last assumption is clearly unlikely because it would imply that about 90 percent of the energy released is visible and it is very hard to balance the momentum with such a small energy margin.

Making use of the concept of strangeness ([11]) one can develop the two following arguments, kindly suggested to us by R. GATTO, which make the interpretation in terms of a boson of about protonic mass extremely unlikely, if the Gell-Mann scheme is correct and complete.

The first is based on the assumption that bosons with charge $\pm 2e$ do not exist in nature. From such an assumption it follows that a possible, yet undiscovered, negative meson X^- must have strangeness $S = -2$ and mass smaller than that of two K-mesons (i.e. $m_{X^-} \leqslant 986$ MeV) in order to be metastable; from the time of flight under the actual conditions of the experiment ($3.5 \cdot 10^{-8}$ s proper time) we know that the incident particle has a lifetime longer than 10^{-8} s. But such an X^- would rapidly be absorbed by nucleons with emission of any combination, allowed by conservation of energy, of new particles, which gives a total strangeness $S = -2$. The maximum energy release would be obtained in the reaction

$$X^- + p + n \rightarrow \Lambda^0 + \Lambda^0$$

and, considering the upper limit for m_{X^-}, the Q would be

$$Q = m_{X^-} - 353 \leqslant 986 - 353 = 633 \text{ MeV}$$

a value definitely lower than that observed in the present star.

The second argument avoids the assumption of the non-existence of particles of charge $\pm 2e$, and is based on the rule $\Delta S = \pm 1$ for weak interactions. A hypothetical negative boson X^- of mass close to that of the proton can not have strangeness $S = 0$, because it would decay into pions and/or gammas, nor strangeness $S = \pm 1$, because it would decay into K-mesons and/or pions and/or gammas. When X^- interacts with nucleons it is absorbed either rapidly or slowly. In the first case heavy mesons or hyperons must be emitted. The same will happen in the second case because of the assumption $\Delta S = \pm 1$. Therefore in all possible cases the Q-value would be definitely

([11]) M. GELL-MANN: *Proceedings of the Pisa Conference*, June 1955, in press in *Suppl. Nuovo Cimento*.

smaller than the visible energy observed in the star. Only in the very unlikely case that all the emitted particles with S different from zero were reabsorbed in the same nucleus could a boson as described above account for the observed star.

While no discussion has been given here of a possible fermion different from the antiproton but with mass very close to the proton mass, we consider it far more likely that the observed particle is a genuine antiproton.

Comparison with other events observerd in cosmic rays. – Finally it seems to us worthwhile to compare the event presented in this paper with those previously observed in cosmic rays and thoroughly discussed [5,6].

The comparison is straightforward in the case of the secondary star (star B) of the event observed a few months ago in the Rome Laboratory, also with emulsion technique [6]. From Table IV, where a few data relative to these two stars have been collected, it is clear that there is a remarkable similarity of their general features. Therefore one is strongly inclined to attribute both of them to the same type of primary and to interpret the differences between the two as due to accidental peculiarities and to statistical fluctuations inherent in phenomena involving the emission of many particles.

TABLE IV. – *Comparison between the main features of two stars, from which it is concluded that both stars were very likely caused by the same type of particle.*

	Pions		Protons		Tritons		Alphas		E_{vis} (MeV)	p MeV/c
	N_π	E_π (MeV)	N_p	T_p (MeV)	N_T	T_T (MeV)	N	T_α (MeV)		
Ro (cosmic rays)	2	$\geqslant 574$	4	331	1	114	—	—	$\geqslant 1050$	1500
Bk-Ro$_1$	2	669	3	78	—	—	4	89	860	820

In the case of the event observed in cosmic rays, it was concluded that, the probability of an accidental coincidence cannot be disregarded although it is rather small. If one excludes this possibility, the more likely interpretation seems to be that of an annihilation process of a heavy particle [6].

In the case of the star presented in this paper, the interpretation in terms of an accidental coincidence in space can be disregarded.

If the two events are to be interpreted as due to the same particle, the attribution of both stars to antiprotons is very strongly supported. All their general features are well consistent with the unique value of energy release which one has to assume for the annihilation of a negative proton. In looking for this type of star one has te bear in mind that even larger fluctuations have

to be expected owing to the possibility of emission of neutral pions which would most probably escape detection.

A comparison with the event observed in cosmic rays by the Massachusetts Institute of Technology group ([5]), by means of a cloud chamber, is more difficult. The multiplate cloud chamber may fail to show short prongs that are easily seen in an emulsion. Conversely, the emulsion may fail to show neutral mesons, which are observed in the cloud chamber through the electron showers they produce.

* * *

All of us, and in particular the group working in Rome, want to express their gratitude to those who have built and operated the Bevatron, especially to Dr. E. J. LOFGREN whose cooperation has been essential for the success of the experiment.

The group working in Rome wants to express thanks also to Prof. B. FERRETTI and Prof. G. CORTINI for various discussions.

Finally, all of us wish to thank the scanners both in Berkeley and Rome, for their keen interest and unselfish cooperation which has made this work possible.

The work at the University of California, Berkeley, was performed under the auspices of the U.S. Atomic Energy Commission.

APPENDIX

In order to be able to choose the more convenient experimental conditions it would be necessary to know the momentum and angular distribution of the antiprotons in the laboratory frame of reference (L.S.) produced in a nucleon-nucleon collision.

These are unknown and therefore we have to content ourselves with estimates made by considering statistical factors, and the movement of the nucleons inside the target nucleus.

For this last we have adopted the simplest model, namely a completely degenerated Fermi gas with a maximum kinetic energy $T_F = 25$ MeV, corresponding to the rather conservative value $1.38 \cdot 10^{-13}$ cm for the constant r_0 appearing in the radius formula of nuclei.

The probability $P(w_0)\,\mathrm{d}w_0$ that the total energy w_0 in the center of mass system of the incident nucleon and one nucleon of the target nucleus, lie between w_0 and $w_0 + \mathrm{d}w_0$, is given by the expression

$$P(w_0) = \frac{3w_0}{2B}\left\{1 - \left[\frac{B}{2A} - \sqrt{\left(\frac{B}{2A}\right)^2 + \frac{w_0^2 - C}{A}}\right]^2\right\} \tag{A.1}$$

$$A + C - B \leqslant w_0^2 \leqslant A + C + B$$

where

$$\text{(A.2)} \qquad \begin{cases} A = 2\mathcal{C}_F(\mathcal{C}+1) = 5.33\cdot 10^{-2}(\mathcal{C}+1) \\ B = 2\sqrt{2\mathcal{C}_F}(\mathcal{C}^2+2\mathcal{C})^{\frac{1}{2}} = 0.46(\mathcal{C}^2+2\mathcal{C})^{\frac{1}{2}} \\ C = 2(\mathcal{C}+2)\,. \end{cases}$$

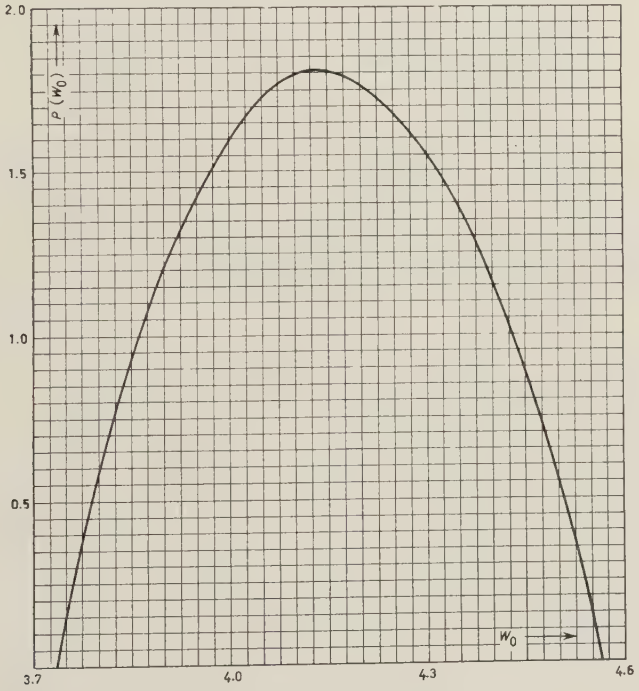

Fig. 7. – Probability distribution $P(w_0)$ as a function of w_0. Here w_0 is the total energy in the center-of-mass system of two nucleons divided by the proton rest energy. The beam energy is taken to be 6.1 GeV.

In these equations as well as in all the following, all energies (w_0 = total energy in the C.M.S.; $\mathcal{C}$ kinetic energy of the incident proton in the L.S.; $\mathcal{C}_F$ maximum kinetic energy of the nucleons in the target nucleus) and all momenta pc are expressed in units of $m_p c^2 = 938$ MeV.

Fig. 7 shows $P(w_0)$ as a function of w_0 for $\mathcal{C} = 6.5$ corresponding to $T = 6.1$ GeV.

We will now assume that the direct production of nucleon-antinucleon pairs in proton-nucleon collisions prevails, at the Bevatron energy, over the process going through the intermediary production of pions ([12]). In fact we know too little about the pion production at 6-7 GeV, to be able to consider quantitatively this last process.

([12]) G. Feldman: *Phys. Rev.*, **95**, 1697 (1954).

Then the threshold for production of a pair of nucleons is determined by the condition $w_0 = 4$.

The cross-section for production of pairs of nucleons can be written in the form

$$\sigma(w_0) = \sigma_r G(w_0 - 4) , \tag{A.3}$$

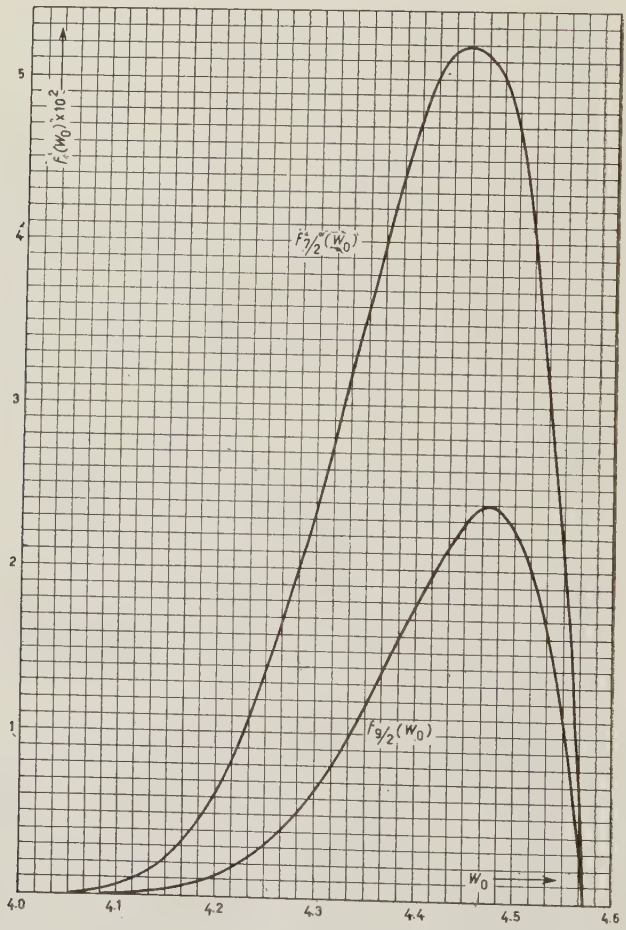

Fig. 8. – The functions $f_{7/2}(w_0)$ and $f_{9/2}(w_0)$ as functions of w_0.

where σ_r is the reaction cross-section corresponding to all possible processes with exception of the elastic scattering and $G(w_0 - 4)$ is a kind of branching ratio which is zero below the threshold $w_0 = 4$. σ_r is known, at 1.4 GeV from the measurement made at the Cosmotron ([13]) (for copper, 670 mb) and at

([13]) T. Coor, D. A. Hill, W. F. Hornyak, L. W. Smith and G. Snow: *Phys. Rev.*, **98**, 1369 (1955).

([14]) See for a collection of data R. W. Williams: *Phys. Rev.*, **98**, 1387 (1955).

cosmic rays energies from penetrating shower investigations ([14]) (for copper $\sim$ 800 mb) and therefore can be easily interpolated at the Bevatron energies.

$G(w_0 - 4)$ is unknown; we will assume in a rather arbitrary way that its dependence on the energy

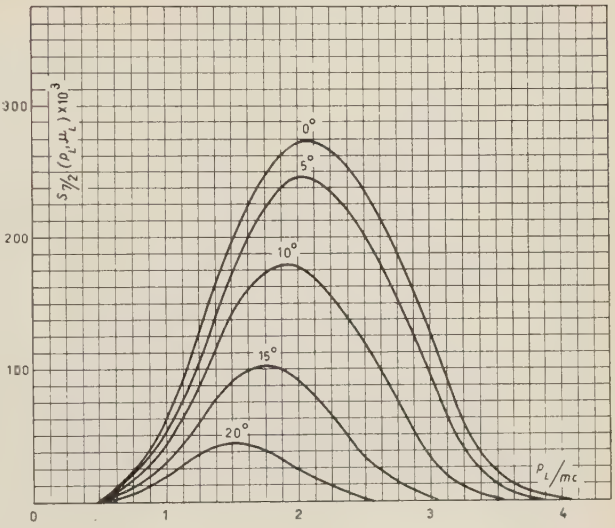

Fig. 9. – Calculated laboratory-system momentum distributions of antiprotons from p-n collisions inside the nucleus at various angles of observation at the target.

is determined by the statistical factor only. In other words we assume, near threshold

$$G(w_0 - 4) = A(w_0 - 4)^{7/2} \qquad (A = \text{constant}) \tag{A.4}$$

for the process

$$\mathrm{p} + \mathrm{n} \to \mathrm{p} + \mathrm{n} + \mathrm{p} + \bar{\mathrm{p}} \tag{A.5}$$

and

$$G(w_0 - 4) = B(w_0 - 4)^{9/2} \qquad (B = \text{constant}) \tag{A.6}$$

for the process

$$\mathrm{p} + \mathrm{p} \to \mathrm{p} + \mathrm{p} + \mathrm{p} + \bar{\mathrm{p}} \tag{A.7}$$

having introduced an extra factor $(w_0 - 4)$ in this second case in order to take into account the fact that, because of the Pauli principle, one of the three protons present in the final state must be in a state with $l = 1$.

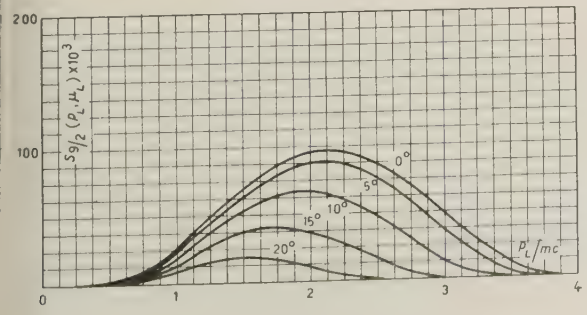

Fig. 10. – Calculated laboratory-system momentum distributions of antiprotons from p-p collisions inside the nucleus at various angles of observation.

Fig. 8 shows the quantities

$$f_n(w_0) = P(w_0)(w_0 - 4)^n \qquad n = \tfrac{7}{2}, \tfrac{9}{2} . \tag{A.8}$$

calculated for $\mathcal{T} = 6.5$.

From these figures we see that for the Bevatron conditions the most probable value for the energy available in the C.M.S. in the final states of the processes (A.5) and (A.7) is between 300 and 500 MeV.

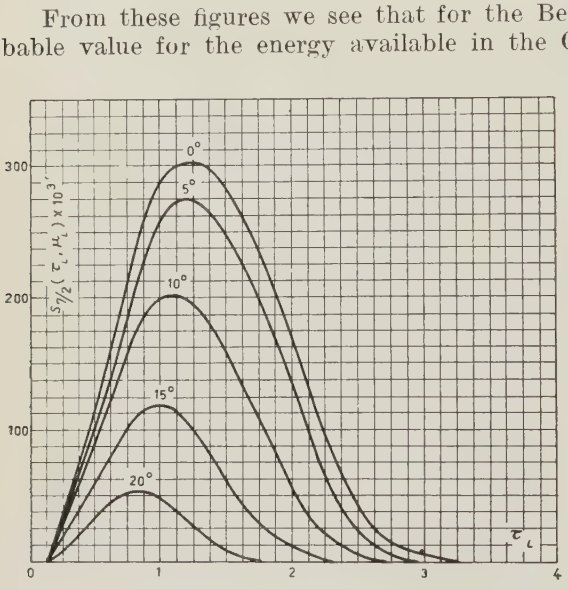

Fig. 11. – Calculated laboratory-system kinetic-energy distributions of antiprotons from p-n collisions inside the nucleus at various angles of observations. $\mathcal{T}_L$ is the antiproton kinetic energy divided by the proton rest energy.

We do not know how this energy is distributed between the 4 particles present in the final state: nor do we know how frequently they are produced all four, free or bound in groups of two or possibly three. In order to estimate these probabilities we had to introduce some very uncertain assumptions. We prefer to assume, in a rather arbitrary way, that the 4 particles are all produced free and that the available kinetic energy $w_0 - 4$ is distributed among them according to the statistical factors.

From the non-relativistic expression of these factors one obtains the normalized distribution function of the momentum of the antinucleon in the C.M.S.

$$S(p^*)\,\mathrm{d}p^* = \frac{105}{16}\{1 - v^{*2}\}^2 v^{*2}\,\mathrm{d}\mu^*\,\mathrm{d}v^* \tag{A.9}$$

where

$$v^* = \frac{p^*}{p^*_{\max}} ; \qquad \mu^* = \cos\theta^* . \tag{A.10}$$

The maximum value $p^*_{\max}$ of the momentum can be obtained immediately from the following relativistic expression of the corresponding maximum total energy

$$E^*_{\max} = \frac{1}{2}\left(w_0 - \frac{8}{w_0}\right) ; \qquad p^*_{\max} = \sqrt{E^{*2}_{\max} - 1} . \tag{A.11}$$

Finally one has to perform the Lorentz transformation of the distribution function (A.9) in the C.M.S. to the L.S. The relative velocity of the two systems

is given, with excellent approximation, by the expression

$$\beta = \left\{1 - \left(\frac{w_0}{\mathcal{T}+2}\right)^2\right\}^{\frac{1}{2}} \tag{A.12}$$

while in the substitution of the variables p^*, μ^* (in the C.M.S.), with the variables p, μ (in the L.S.) one has the relation

$$\frac{p^{*2}}{(p^{*2}+1)^{\frac{1}{2}}}\,\mathrm{d}p^*\,\mathrm{d}\mu^* = \frac{p^2}{(p^2+1)^{\frac{1}{2}}}\,\mathrm{d}p\,\mathrm{d}\mu\,. \tag{A.13}$$

In conclusion the distribution function with respect to p and μ is given by the expression

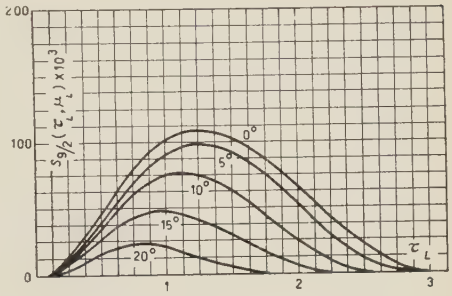

Fig. 12. – Calculated laboratory-system kinetic-energy distributions of antiproton from p-p collisions inside the nucleus at various angles of observation. $\mathcal{T}_L$ is the antiproton kinetic energy divided by the proton rest energy.

$$S_n(p,\mu)\,\mathrm{d}p\,\mathrm{d}\mu = \frac{105}{16}\,\frac{p^2}{(p^2+1)^{\frac{1}{2}}}\,\mathrm{d}p\,\mathrm{d}\mu \int_4^\infty \frac{P(w_0)(w_0-4)^n}{p^{*3}_{\max}}\,\sqrt{p^{*2}+1}\,\mathrm{d}w_0\,. \tag{A.14}$$

Figs. 9 to 12 show the momenta and energy spectra obtained from this equation for $\mathcal{T} = 6.5$.

The thickness of the copper absorber adopted in the experiment was chosen in such a way to make the number of antiprotons stopping in the emulsion stack maximum, assuming that their attenuation cross-section was geometric.

RIASSUNTO

In relazione con il piano di ricerca dell'antiprotone al Bevatrone, alcuni pacchi di emulsioni nucleari sono stati esposti ad un fascio di particelle negative separate magneticamente. Le particelle selezionate sono state prodotte in una targhetta di rame, bombardata da protoni di 6.3 GeV, ed avevano un momento di 1.09 GeV/c. L'esperimento è stato progettato allo scopo di osservare il processo di annichilazione provocato da un protone negativo che si arresti dentro l'emulsione. I dettagli della ricerca sono dati nel § 2. Il § 3 contiene una stima del numero delle stelle dovute a processi di annichilazione che ci si doveva aspettare in base a precedenti misure eseguite con contatori da Chamberlain, Segrè, Wiegand e Ypsilantis. Il § 4 contiene la descrizione del solo evento trovato finora. La massa della particella primaria che lo produce, calcolata da una media pesata su risultati ottenuta con diversi metodi indipendenti, è $(1824 \pm 51)\,m_e$. La stella prodotta è associata con una energia minima « visibile » di ~ 826 MeV mentre il corrispondente momento « visibile » è sbilanciato di ~ 520 MeV/c.

About the Capture and Annihilation of Antiprotons.

R. Gatto

Istituto di Fisica dell'Università - Roma
Istituto Nazionale di Fisica Nucleare - Sezione di Roma

(ricevuto il 5 Gennaio 1956)

Summary. — The mechanism of annihilation of antiprotons is discussed. It is shown that large multiplicities for the number of pions emitted should be infrequent and some considerations are reported concerning the average number of neutral pions to be expected. It is suggested that a $K\text{-}\overline{K}$ pair could also be emitted. An event recently found and interpreted as due to the annihilation of an antiproton is discussed, and it is shown that, using Gell-Mann's model, arguments, can be given against its interpretation in terms of a new long-lived heavy boson.

Recent results obtained at Berkeley [1] have shown the existence of negative particles of protonic mass, which have been interpreted as antiprotons. Previously, examples had been reported of cosmic ray events which could be attributed to antiprotons [2-4] although the interpretation was not so definite. Recently [5], in an emulsion stack exposed at the bevatron, a star has been found which is due to a negative particle of protonic mass interacting

[1] O. Chamberlain, E. Segrè, C. Wiegand and T. Ypsilantis: *University of California, Radiation Laboratory UCRL*-3172 (1955).

[2] E. Hayward: *Phys. Rev.*, **72**, 937 (1947).

[3] A. S. Bridge, H. Courant, H. De Staebler and B. Rossi: *Phys. Rev.*, **95**, 1101 (1954).

[4] E. Amaldi, C. Castagnoli, G. Cortini, C. Franzinetti and A. Manfredini: *Nuovo Cimento*, **1**, 492 (1955).

[5] O. Chamberlain, W. W. Chupp, G. Goldhaber, E. Segrè, C. Wiegand, E. Amaldi, G. Baroni, C. Castagnoli, C. Franzinetti and A. Manfredini: *Nuovo Cimento*, **3**, 318 (1956).

at rest and producing a visible energy release ~ 860 MeV. The star has been interpreted as due to the capture by an emulsion nucleus and subsequent annihilation of an antiproton produced by the bevatron. Two theoretical arguments have been given [5], which immediately follow from Gell-Mann's model [6], in order to exclude the interpretation of the event as due to the absorption of some new long-lived negative heavy boson (to be called x^-). For the first argument it is assumed that no particles with charge $\pm 2e$ exist —therefore x^- must have strangeness $S = -2$, and, when absorbed by nucleons, the maximum energy release would be ~ 630 MeV. The second argument uses the rule $\Delta S = \pm 1$ for weak interactions—because of the condition of metastability x^- can not have $S=0$ or ± 1, and, therefore, even if absorption is slow, new hyperons or heavy mesons must be emitted, what definitely reduces the energy release.

One of the simplest mechanisms of annihilation of an antinucleon interacting with matter would be

$$\overline{\mathrm{N}} + \mathrm{N} \to n \text{ pions}, \tag{1}$$

where only one of the constituent nucleons is taken to partecipate to the reaction. In a statistical theory the total probability of (1) will be proportional to

$$\omega_n \left(\frac{e^3}{6\pi^2 k^3}\right)^{n-1} \frac{m_N}{e} \int d\xi_1\, d\xi_2 \ldots d\xi_n\, \delta\Big(\sum_1^n \xi_i\Big)\, \delta\Big(1 - \sum_1^n \varepsilon_i\Big)\,; \tag{2}$$

where ω_n is a numerical factor which accounts for conservation of total isotopic spin and for the impossibility to distinguish among the n final pions; e is the total energy; k is the inverse length of the interaction region; m_N is the nucleon mass; and $\varepsilon_i = \eta^2 + \xi_i^2$, with $\eta = m_\pi/e$. To evaluate ω_n one has to distinguish two cases: (i) the two nucleons are one the charge conjugate of the other, and (ii), they are not. Case (i) ($\bar{\mathrm{p}}+\mathrm{p}$, $\bar{\mathrm{n}}+\mathrm{n}$) involves an equal admixture of $I = 1$ and $I = 0$; case (ii) ($\bar{\mathrm{p}}+\mathrm{n}$, $\bar{\mathrm{n}}+\mathrm{p}$) only involves $I = 1$. One easily finds

case (i): $\omega_2 = \frac{1}{2}$, $\omega_3 = \frac{1}{3}$, $\omega_4 = \frac{3}{16}$, $\omega_5 = \frac{7}{80}$;

case (ii): $\omega_2 = \frac{1}{2}$, $\omega_3 = \frac{1}{2}$, $\omega_4 = \frac{1}{4}$, $\omega_5 = \frac{1}{8}$.

In the case of annihilation at rest the total energy e will be $\cong 2m_N$. Let us call r the radius of the interaction region expressed in nucleon wavelengths

[6] M. Gell-Mann: *Proceedings of the Pisa Conference*, 1955.

The relative probabilities for the emission of 2, 3, 4, 5 pions are found to be

case (i):

$$(3)\qquad \begin{cases} 2 \text{ pions} & = 1 \\ 3 \text{ pions} & \sim 1.6 \cdot 10^{-2} r^3 \\ 4 \text{ pions} & \lesssim 0.56 \cdot 10^{-4} r^6 \\ 5 \text{ pions} & \lesssim 0.60 \cdot 10^{-7} r^9 \end{cases}$$

case (ii):

$$(3')\qquad \begin{cases} 2 \text{ pions} & = 1 \\ 3 \text{ pions} & \sim 2.5 \cdot 10^{-2} r^3 \\ 4 \text{ pions} & \lesssim 0.74 \cdot 10^{-4} r^6 \\ 5 \text{ pions} & \lesssim 0.86 \cdot 10^{-7} r^9 \end{cases}$$

From (3) and (3′) we see that multiple pion emission is very rare if the radius of the interaction region is of the order of the nucleon Compton wavelength ($r = 1$). If the radius of the interaction region is taken of the order of $\frac{1}{2}$ of the Compton wave length of the pion ($r = 3.35$), one gets from (3)

case (i):

$$\begin{cases} 2 \text{ pions} & = 1 \\ 3 \text{ pions} & \sim 0.6 \\ 4 \text{ pions} & \lesssim 0.79 \cdot 10^{-1} \\ 5 \text{ pions} & \lesssim 0.32 \cdot 10^{-2} \end{cases}$$

case (ii):

$$\begin{cases} 2 \text{ pions} & = 1 \\ 3 \text{ pions} & \sim 0.9 \\ 4 \text{ pions} & \lesssim 1.0 \cdot 10^{-1} \\ 5 \text{ pions} & \lesssim 0.46 \cdot 10^{-2} . \end{cases}$$

No valid arguments can be given to fix the value of r. However, from the figures reported one would conclude that the most frequent cases are the emission of two pions and of three pions, and large multiplicities should be infrequent.

The pions emitted in the primary annihilation act may suffer interaction with the remaining nucleons before escaping from the nucleus: scattering and reproduction processes by colliding against single nucleons, and absorption by pairs of nucleons. These various possibilities may give different aspects to the resulting stars. Either in the primary annihilation act, or in the pos-

sible successive interactions, charge independence will be satisfied. Therefore Watson's relation

$$n_+ + n_- = 2n_0 , \tag{4}$$

between the average numbers of pions produced of the various signs, is expected to hold. The relation (4) is rigorously satisfied for the sum of the mean numbers produced in annihilation against a proton and of the mean numbers produced in annihilation against a neutron. The validity of relation (4) may be only an approximate one owing to the slight neutron excess and to other causes. However, for the case of annihilation of $\bar{p}$ against n, one easily derives the general restriction

$$n_+ + n_- \geqslant n_0 . \tag{5}$$

Both (4) and (5) do not depend on the pion multiplicity. For the case of annihilation of $\bar{p}$ against an hydrogen nucleus leading to the emission of two pions the probability that the two pions are charged is at least a factor 2 larger than the probability that they are neutrals. In conclusion we may say that the probability that the annihilation event escapes detection due to the emission of neutral pions will not be very large.

From the occurrence of the reaction [7]

$$\pi + N \to N + K^+ + K^- ,$$

one would also suggest the possibility of annihilation processes of the kind

$$\bar{p} + p \to K^+ + K^- \tag{6}$$

$$\to K^0 + \bar{K}^0 \tag{6'}$$

$$\bar{p} + n \to K^0 + K^- . \tag{7}$$

Consider, for instance, the first of the above reactions, $\bar{p} + p \to K^+ + K^-$. One could assume the existence of a strong ($NK\Lambda^0$) interaction as the simplest trilinear charge-independent interaction to account for the strong Λ^0-N force. With such an interaction one can imagine the sequence of virtual processes

$$\bar{p} + p \to \bar{p} + (\Lambda^0 + K^+) \to K^- + K^+ .$$

A similar consideration would also hold for $\bar{p} + n \to K^0 + K^-$. The statistical weigth in both (6) and (6'), and (7) is only 0.85 times smaller than that for annihilation into two pions: however, one should consider, from the viewpoint

[7] M. Ceccarelli, M. Grilli, M. Merlin, G. Salandin and B. Sechi: *Nuovo Cimento*, **2**, 828 (1955).

of a statistical theory, that the radius of the interaction region is not necessarily the same in this case.

One could assume that more nucleons partecipate to the primary annihilation act, for instance, annihilation against a deuteron subunit, or an α-subunit of the capturing nucleus. Such a mechanism would in particular lead to the possibility of annihilations with emission of only one meson, and to the possibility of heavy very energetic secondaries in the annihilation star (4). However, as shown by ASHKIN, AVERBACH and MARSHAK (8), this mechanism should be improbable due to the smallness of the Fourier transform of the nuclear wavefunction for the large values of the momentum transfer to the nucleons.

As a general feature one would expect that slow antiprotons are captured at rest by the emulsion nuclei and then annihilated. As compared to the analogous case of π^- capture, the absorption from higher orbits would be more favoured in this case, due, at least partly, to the larger mass, although the calculation of such an effect would be very difficult at present. Similarly one would expect—on qualitative grounds—that an effect similar to the Panofsky effect for π-mesons does not occur in the case of antiprotons.

Antihyperons can only be produced in association with other new particles, what makes the thresholds for their production still higher. In collision between ordinary particles the lowest thresholds are for production of $\bar{\Lambda}+\Lambda$, $\bar{\Lambda}+\Sigma$, $\bar{\Sigma}+\Lambda$, $\bar{\Sigma}+\Sigma$, $\bar{\Lambda}+N+K^{\bar{0}}$, $\bar{\Sigma}+N+K^{\bar{0}}$, $\bar{\Xi}+\Xi$, etc. Antihyperons should have decay modes corresponding to those of their charge conjugates $\bar{\Lambda}^0 \to \bar{p} + \pi^0$, etc.). An interesting feature of their interaction with nucleons is that a K^0 or a K^+ (bound or free) should always emerge from the annihilation star.

* * *

I would like to thank Prof. E. AMALDI for many stimulating discussions on the subject.

(8) ASHKIN, AVERBACH and MARSHAK: *Phys. Rev.*, **79**, 266 (1951).

RIASSUNTO

Viene discusso il meccanismo di annichilamento di antiprotoni. Si fa vedere che grandi molteplicità per il numero dei pioni emessi dovrebbero essere infrequenti e vengono riportate alcune considerazioni circa i numeri medi di pioni neutri che possono venire emessi. Viene suggerita la possibilità che possano venire emesse coppie di $K\text{-}\bar{K}$. Un evento trovato di recente ed interpretato come dovuto all'annichilamento di un antiprotone viene discusso, e si fa vedere come, usando il modello di Gell-Mann, si possano dare argomenti contro la sua interpretazione in termini di un nuovo bosone pesante di vita media lunga.

Minimum Noise Pre-Amplifier for Fast Ionization Chambers.

C. Cottini, E. Gatti, G. Giannelli and G. Rozzi
Laboratori CISE - Milano

(ricevuto il 31 Dicembre 1955)

Summary. – A fast, low-noise, pulse amplifier is described, which has an input stage consisting of a cascode of two triode-connected E83F tubes. Its rms noise voltage is equivalent to a pulse of 280 electronic charges injected on an input capacity of 21 $\mu\mu$F, the frequency response of the amplifier being defined by two RC circuits having both a time constant of 1.5 μs. On a capacity of 34 $\mu\mu$F and a frequency response given by time constants of 3 μs, the rms noise is equivalent to a pulse of 380 electronic charges.

1. – Introduction.

In the study of energy spectra of particles, by means of ionization chambers, it is useful to reduce to a minimum the broadening of spectral lines due to the noise of the first stages of the electronic amplification.

The reduction of this broadening has particular importance in the researches that have for a purpose the study of the intrinsical width of the lines due, besides to the nuclear phenomena, to the mechanism of interaction of the ionizing particle with the filling gas [1].

It is well known that the signal generator (ionization chamber) may be considered as a current generator with a purely capacitive internal impedance and as such, completely noiseless.

Consequently the amplifier noise figure becomes in every case infinite; the noise at the output is entirely due to the internal noise of the amplifier.

Accordingly, in these applications, the noise figure is substituted by the number N of electronic charges to apply in an infinitesimal time at the input so as to obtain an output pulse of an amplitude equal to the rms voltage of the noise (likewise measured at the output). This value N has significance only if the value of capacity C_{ext} added at the amplifier input is simultaneously

[1] A. Bisi and L. Zappa: *Nuovo Cimento*, **2**, 988 (1955).

specified (output capacity of the ionization chamber and wiring capacity) [2].

The noise of the amplifier can be practically reduced to that due to the input stage. Under this hypothesis and using an amplifier that has the frequency response of the voltage amplification determined superiorly and inferiorly by two elementary RC circuits having equal time constants τ, N is given by the following formula [3].

$$N = \frac{C_{int} + C_{ext}}{e} \varepsilon \left\{ 4.84 \cdot 10^{-14} + \frac{kT_e}{2\tau} R_{eq} + \frac{e}{(4C_{int} + C_{ext})^2} I_g \tau \right\}^{\frac{1}{2}} \tag{1}$$

where e is the electron charge $1.59 \cdot 10^{-19}$ coulomb,

ε the natural logarithm base 2.718....

k Boltzmann constant $1.37 \cdot 10^{-23}$ joule/°K,

T_e absolute laboratory temperature 290°,

R_{eq} equivalent shot noise. In the case of pentodes R_{eq} is due also to the partition noise: in this paper reference is made only to triodes,

I_g the sum of the absolute values of the ionic and electronic components of the grid current: $I_g = |i_{g\,ion}| + |i_{g\,el}|$.

The three terms in brackets correspond respectively to the flicker noise, to the shot noise and to the noise due to the voltage developed by the grid current fluctuations across the input impedance.

In order to compare our results with those of other workers and for the experimental convenience of changing the frequency response by switching simple RC circuits, we have set up the experiment under the conditions where formula (1) is valid.

However, other shapes of frequency response have well known and calculable advantages and disadvantages [4-9].

It is worthwhile to point out that the input capacity C_{int} of formula (1) is the input capacity of the first stage, provided all the feedbacks driven by the output signal of the stage itself (Miller effect, feedback due to cathode resistor etc.) are rendered ineffective. In fact it is known that every feedback driven by the output signal modifies the transfer functions from any couples of terminals to the output by a common factor and hence, in particular, the amplifications of the signal and of the noise currents wherever they are injected.

From (1) it is easily deduced that N presents a minimum with respect to the variations of time constants τ, when

$$\tau = \sqrt{\frac{4kT_eR_{eq}}{2eI_g}} (C_{int} + C_{ext}) = 0.224(C_{int} + C_{ext}) \sqrt{\frac{R_{eq}}{I_g}} . \tag{2}$$

[2] A. B. Gillespie: *Signal Noise and Resolution in Nuclear Counter Amplifiers* (London, 1953), p. 81.

[3] A. B. Gillepsie: op. cit.

[4] J. M. W. Milatz and K. J. Keller: *Physica*, **9**, 97 (1942).

[5] K. J. Keller and H. J. A. Vesseur: *Physica*, **10**, 273 (1943).

[6] K. J. Keller: *Physica*, **13**, 326 (1947).

[7] Van Heerden: *Thèse Utrecht* (1945).

[8] R. Sherr and R. Peterson: *Rev. Sci. Instr.*, **18**, 567 (1947).

[9] G. Valladas and A. Levêque: *Rapport C.E.A.*, n. 141 (1952).

Under this condition the shot noise and the noise due to the grid current give equal contributions and

$$(3) \quad N_{\min} = \frac{\varepsilon}{e}\sqrt{C_{\text{int}} + C_{\text{ext}}}\left\{4.84\cdot 10^{-14}(C_{\text{int}} + C_{\text{ext}}) + \frac{1}{4}(2eI_g \cdot 4kT_e R_{\text{eq}})^{\frac{1}{2}}\right\}^{\frac{1}{2}} =$$

$$= 1.71\cdot 10^{19}\sqrt{C_{\text{int}} + C_{\text{ext}}}(4.84\cdot 10^{-14}(C_{\text{int}} + C_{\text{ext}}) + 178\cdot 10^{-22}\sqrt{R_{\text{eq}} I_g})^{\frac{1}{2}}.$$

The lowest values of $N_{\min}$ have been obtained till now with electrometer tubes having very low grid current and relatively high shot noise equivalent resistance: these minima were therefore obtained for high τ-values ([10-12]) which correspond to low resolving power and require careful precautions to avoid microphonic noise of the ionization chamber and of the amplifier itself.

Some attempts were made to achieve low $N_{\min}$ values for τ-values of a few microseconds, using high slope tubes ([13]) or reducing as much as possible the input capacitance C_{ext} ([14]). The N values so obtained were however superior to those reached using slow amplifiers (*).

Technical data of high slope tubes working at low plate voltage, now commercially available, have suggested the possibility of improving the preceding results and this has been the aim of our work.

2. – Choice of the tube type.

We carried out experiments with types of tubes, chosen either with view to compare the results of previous works, or from those which are characterized by a low plate voltage when operating with about 9 mA plate current and — 1.2 V of grid-cathode voltage.

This criterium was suggested by the strong dependence of the ionic grid current $i_{g\,\text{ion}}$ upon plate voltage v_p (a dependence, more or less quadratic, at a given plate current).

([10]) E. Baldinger, W. Hälg, P. Huber and A. Stebler: *Helv. Phys. Acta*, **19** 423 (1946).

([11]) A. B. Gillespie: op. cit., pp. 84-85.

([12]) G. Valladas: *L'onde électrique*, **33**, 615 (1953).

([13]) H. Guillon: *L'onde électrique*, **33**, 627 (1953).

([14]) G. Bertolini and A. Bisi: *Nuovo Cimento*, **9**, 1022 (1952).

(*) *Note added in proof.* – A result recently obtained by D. W. Engelkemeir and L. B. Magnusson, published on *Rev. Sci. Instr.*, **51**, 295 (1955) escaped our attention.

A preamplifier is there mentioned built around a Western Electric, triode connected, 6AK5.

The reported noise is equivalent to about 330 r.m.s. electronic charges with a pass band centered around 9 μs.

We disregarded after few tests the 6AK5 tubes as our samples presented scattered R_{eq}-values that were very high respecting the formula $2.5/g_m$ and sensitive to heater voltage.

For triodes the plate voltage is given with good accuracy by:

$$v_p = r_p i_p + \mu |v_g|, \tag{4}$$

where r_p is the plate resistance corresponding to the $v_g = 0$ anode characteristic.

In Table I the values of the choice parameter v_p for the tube types taken into account are given together with nominal data r_p and μ.

TABLE I.

Tube (triode connected)	Nominal Data (i_p=9 mA; v_g= — 1.2)			Experimental Data					
						R_{eq} (ohm)		$i_{g\,ion}$ (10^{-9} A)	
	μ	r_p (ohm)	v_p (volt)	i_p (mA)	v_g (volt)	R_{eq}	No. of samples	$i_{g\,ion}$	No. of samples
E83F	35	3100	70	10	— 1.5	250 260 270 280 290	4 1 1 1	1 1.5 2 2.5	2 3 2
EF42	80	6670	156	7	— 1.7	322 380 460	1 1 1	3.5 4 6 7	3 0 2
EF80	50	4680	102	10	— 1.9	325 350 375 400	1 1 2	5 10 15	2 2
EF91	80	8300	171	8	— 1.6	350 375 400 425	5 2 1	3 4 5 6 8 10	1 3 1 3 1
6AG5	55	6250	122	9.6	— 1.9	350 525 560	1 1 1	2.5 3 3.5 4	2 3 2

In the same table results are given of measured values of R_{eq} and $i_{g\,ion}$ for samples of these tubes working under the nearby specified conditions (details of experimental set-up for carrying out these measurements are reported in appendix).

The measurements have given very low grid current for the E83F tubes as was expected, considering the very low value of the parameter v_p taken as our standard for choice.

Furthermore the spread of measured values of $i_{g\text{ion}}$ and R_{eq} for the limited number of samples tested is particularly low for the type E83F; this has probably some connection with the fact that E83F is a long-life telephonic tube.

Qualitatively speaking, we can also say that in comparison with the other tubes, E83F was particularly insensitive to microphonic disturbances.

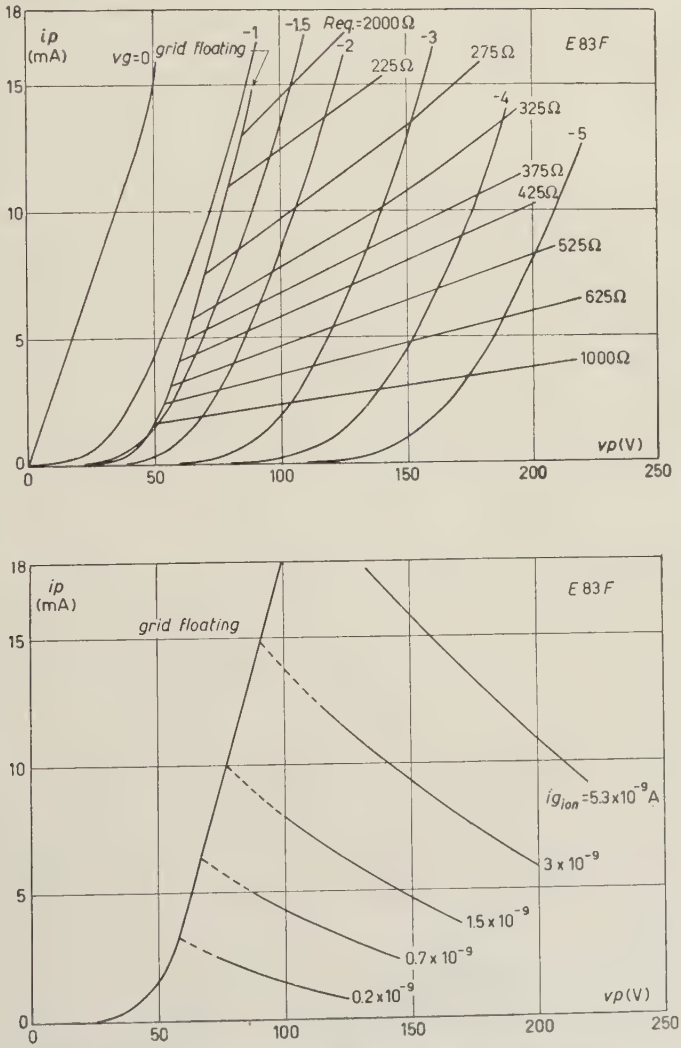

Fig. 1. – Tube E83F: *a*) constant R_{eq} curves in the plate characteristics plane; *b*) constant $i_{g\text{ion}}$ curves in the plate characteristics plane.

R_{eq} and $i_{g\text{ion}}$ have been measured for the best of samples of our E83F and EF42 under several working conditions and the results are plotted on the plate-characteristics plane in Fig. 1 and 2.

The E83F was accordingly chosen as the first stage of our preamplifier.

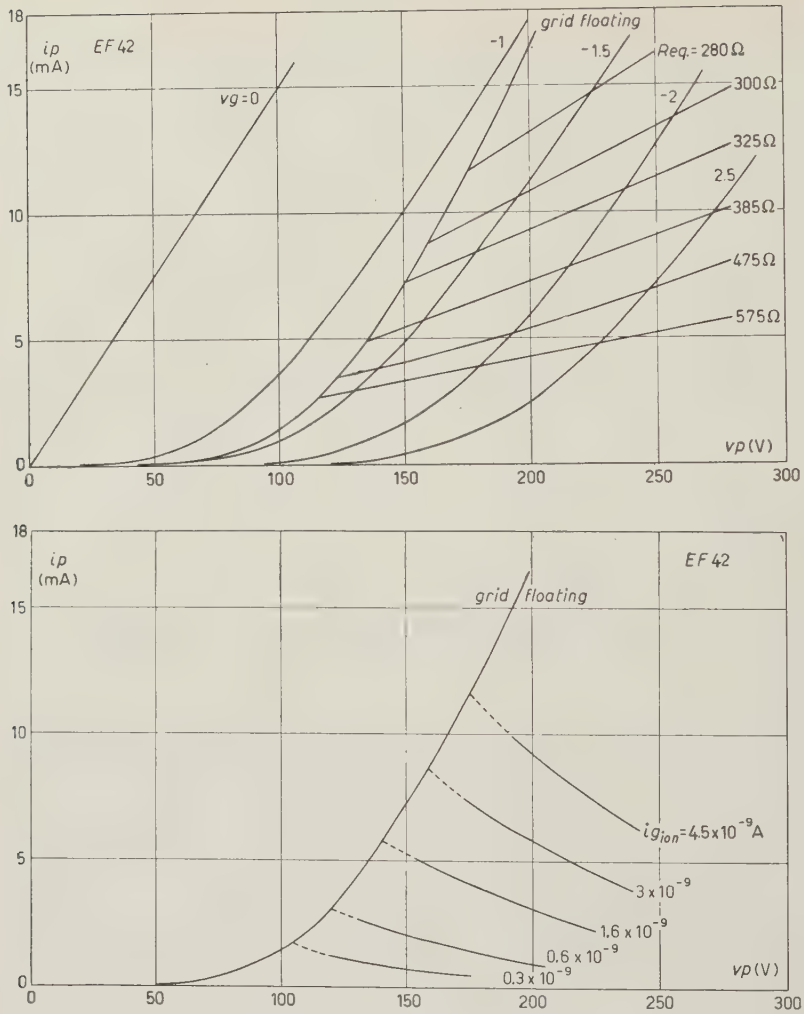

Fig. 2. – Tube EF42: *a*) constant R_{eq} curves in the plate characteristics plane; *b*) constant $i_{g\,ion}$ curves in the plate characteristics plane.

3. – Choice of working conditions.

The choice of working conditions requires at first the choice of one of the two following bias criteria:

a) grid bias $> |-1.6|$ V,
b) floating grid ($v_g \sim -1.2$ V) ([13]).

a) This bias reduces the grid current I_g to the ionic component ([15]). However the stability of the operating point poses a superior limitation to

([15]) A. B. GILLESPIE: op. cit., p. 31.

the grid resistance (partly obviated by a cathode bias resistor) which can eventually lead to a contribution of thermal noise by the grid resistor itself.

b) I_g is obtained by doubling $i_{g\text{ion}}$, as the electron grid current balances the ion grid current. This doubling is partly offset by the smaller values of $i_{g\text{ion}}$ (at the same plate current i_p) due to the smaller grid bias and consequently the smaller plate voltage; besides R_{eq} also becomes smaller (for same plate current i_p) by lowering v_p. As a result the product $I_g R_{eq}$, for constant i_p is slightly larger than in the corresponding case *a*) and consequently, according with (3), N_{min} also increases slightly: however the lower value of the ratio $R_{eq} I_g$ in case *b*), shifts the position of the minimum of N towards shorter time constants, in accordance with (2).

The values of $i_{g\text{ion}}$ on the floating grid characteristic have been obtained by extrapolating those measured in that range of plate characteristics where the electron component of grid current is negligible.

The voltage of the floating grid respecting the cathode has proved to be well determined and about — 1.2 V (for $i_p = 10$ mA) for all the tubes tested. This can be understood from the very fast variation of the electron grid current, according to the factor $\exp[ev_g/kT] = e^{11 v_g}$: a tenth of a volt compensates spreads of about a factor 3, in ionic current or in cathode emission.

Solution *b*) was chosen in order to reach N_{min} at low τ-values.

The operating point along the floating grid characteristics is selected using the corresponding $2i_{g\text{ion}}$ and R_{eq} values as deduced from Fig. 1 and calculating the position and value of N_{min} for every input capacity with formulas (2) and (3).

Selection of high i_p corresponds to low τ and viceversa; N_{min} slightly decreases with i_p.

4. – Amplifier. Description and performance.

The amplifier scheme is given in Fig. 3.

The input stage is a cascode of two triode–connected E83F and is followed by an EF91 pentode amplifier stage, followed in turn by an EF91 output

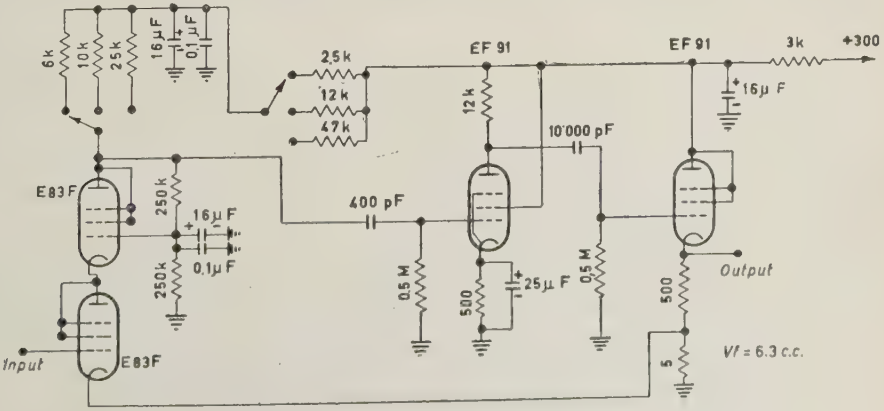

Fig. 3. – Preamplifier scheme.

cathode follower from which a resistive feedback is carried to the cathode of the first E83F.

The loop gain is of about 3000 while the feedback stabilizes the voltage gain to 100.

In Fig. 4 theoretical and experimental values of $N_{\min}$, for an input capacity $C_{ext} + C_{int} = 21\ \mu\mu F$ ($C_{ext} = 10\ \mu\mu F$) and cascode plate current $i_p = 8.8$ mA, are compared.

N has been experimentally measured by the conventional method of supplying a known charge to the amplifier input capacity through a calibrated small condenser of 0.1 $\mu\mu$F fed by a standard generator that gives calibrated voltage step functions. The pulse height at the output is measured with a conventional Shmitt discriminator.

The measurements of N have also been made with a large condenser of 1700 $\mu\mu$F which shunts the input so as to nullify the grid current noise contribution, and allows the evaluation of the shot and flicker contribution. These measurements have been carried out with different frequency responses of the amplifier (τ ranging from 1 to 50 μs) and in this way the contribution of the flicker noise alone has also been experimentally deduced ([16]) and found in good agreement with the theoretical term of formula (3).

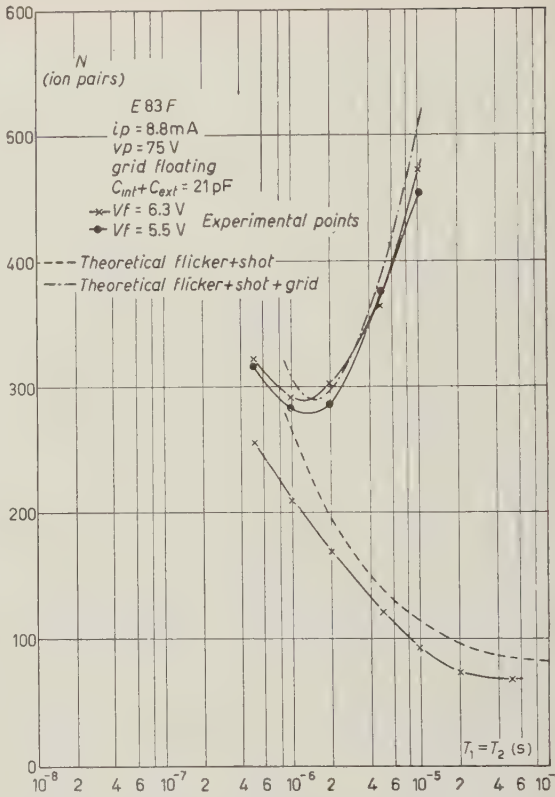

Fig. 4. – Total and shot+flicker noise in electronic charges; 8.8 mA plate current in the cascode input stage.

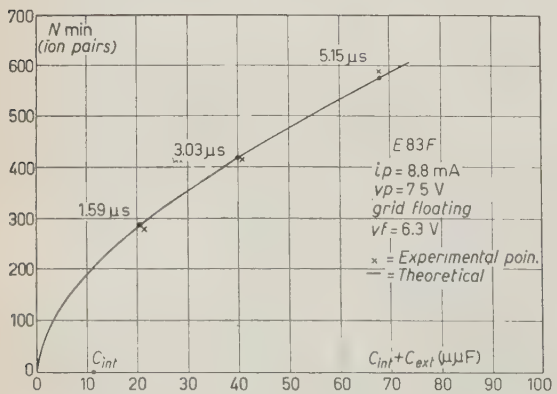

Fig. 5. – Total noise level measured at optimum time constants τ as a function of ($C_{int} + C_{ext}$) (8.8 mA plate current in the cascode input stage).

In order to compare flicker

([16]) A. B. GILLESPIE: op. cit., p. 43.

+shot noise with total noise, the values of N, as obtained in this set of measurements, have been reduced by the ratio of input capacitance 21/1722 and plotted on the same Fig. 4.

Fig. 5. shows the experimental values of N_{min} obtained for different values of input capacities in the same operating conditions of the input stage ($i_p = 8.8$).

In order to shift the position of N_{min}, a switch allows the selection of three values of cascode current i_p 8.8, 5 or 2 mA. For an input capacity $C_{ext} + C_{int} = 21$ $\mu\mu$F the minima of N occur respectively at 1.5, 4.5, 8.5 μs.

In Fig. 6, experimental and theoretical data for N are given when $i_p = 2$ mA.

The experimental value of N_{min} was found in this case to be higher than the theoretical one.

The spread of N for 6 different samples of E83F used as input stage has been measured. The operating conditions were: $C_{ext} = 10$ $\mu\mu$F, $i_p = 8.8$ mA, $\tau = 1$ μs.

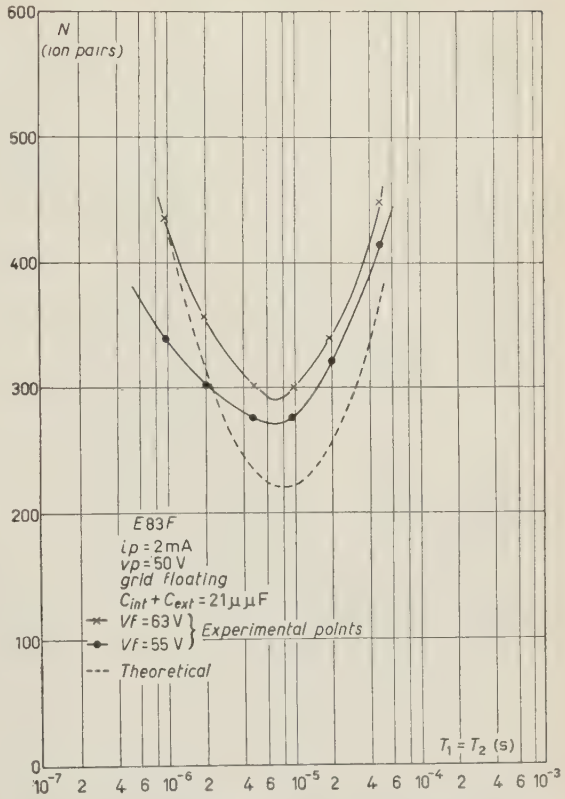

Fig. 6. – Total noise level in electronic charges. 2 mA plate current in the cascode input stage.

N turned out to be in the range of 330-340 electron charges for 3 of the samples, the others gave 298, 304, 365.

5. – Discussion of the feedback arrangement.

The feedback arrangement used is the conventional one which stabilizes the voltage amplification, which, however, does not seem to be the most convenient for an ionization chamber amplifier in which the transfer function which must be stabilized is the input current-output voltage gain. This could be achieved with a capacitive feedback such as that of Fig. 7: this kind of feedback is typical of analog computer integrators.

The conventional resistive feedback does not compensate the mentioned transfer function for drifts of the actual input capacitance (*), as due for in-

(*) I.e. the capacity measured under operating conditions and therefore affected by feedback, which makes it different from the previously defined $C_{ext} + C_{int}$.

stance to changes in the amount of Miller effect due to ageing of tubes and to space charge variations.

Nevertheless we have found that the reduction of 10% of the heater voltage affected the output pulse amplitude by less than 0.5% when C_{ext} was of 10 $\mu\mu$F and the input fed by equal charge pulses.

As a consequence we did not think it worthwhile as far as this application is concerned to develop further the proposed form of feedback.

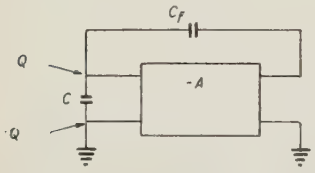

Fig. 7. – Proposed feedback for stabilizing input current – output voltage transfer function.

6. – Conclusions.

The E83F tube has proved to be suitable for the construction of minimal noise fast pulse preamplifiers as its low grid current and high slope makes it possible to achieve in the range of a few microseconds the same results that have been previously obtained in the range of the milliseconds with electrometer tubes.

Moreover the ascertained minimum spread of tube characteristics, grid current data included, allows the construction of amplifiers of optimum performance, with a minimum number of tubes rejected.

Appendix I

Grid current measurements.

The grid current measurements of the experimented tubes have been performed according to a well known method (Fig. 8) consisting in verifying by means of the galvanometer G that working conditions of the tube remain unaffected when operating the switch T: this obviously happens when the voltage V directly applied between grid and ground by means of the potentiometer P_1 is made equal to the voltage drop across the grid resistor R.

All tubes have been aged for at least 48 hours under working condition of about $i_p = 9$ mA and $V_g = -1.6$ V.

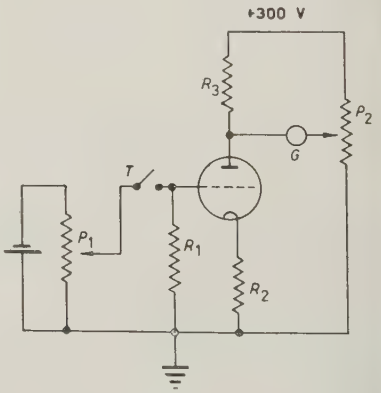

Fig. 8. – Grid current measurement arrangement.

Appendix II

Measurements of the equivalent shot noise resistance R_{eq}.

Known resistances R_{cal} (of the order of magnitude of R_{eq} to be measured) were used as calibrated thermal noise sources.

On a calibrated thermal instrument connected at the output of the amplifier two readings are taken: one P_1 due only to the shot and flicker noise, taken when the input grid is grounded, and another P_2 due to shot, flicker and the thermal noise, when the calibrated resistor is inserted between grid and ground.

The equivalent noise resistance of shot and flicker noise is:

$$R'_{eq} = R_{cal} \frac{P_1}{P_2 - P_1} .$$

R_{eq} is now deduced from R'_{eq} by subtracting the flicker noise contribution theoretically estimated with (1).

The frequency response of the amplifier used in the measurements was determined by a differentiating and an integrating RC circuit having equal time constants ranging between 1 and 50 μs. The rise time of the amplifier by itself was of 0.5 μs.

It has been also verified that the value of the equivalent shot noise resistance was practically indipendent of heater voltage variations of ± 5 %.

In order to check our results R'_{eq} was measured using several values of the calibrated grid resistance and several values of time constants that determine the band width of the amplifier; R'_{eq} was modified in order to account for the flicker noise contribution which become increasingly important for large τ's. All values of R_{eq} so obtained were in agreement within the experimental errors (5 %).

RIASSUNTO

Si descrive un amplificatore di impulsi rapido, a basso rumore, avente uno stadio di ingresso costituito da due tubi E 83 F, connessi a triodo, e montati a « cascode ». Il valore efficace della tensione di rumore è equivalente all'ampiezza di un impulso causato da 280 cariche elettroniche su una capacità di ingresso di 21 μμF, essendo la banda passante dell'amplificatore definita da due elementari circuiti RC di eguale costante di tempo pari a 1.5 μs. Su una capacità di 34 μμF e una banda definita da costanti di tempo di 3 μs la tensione di rumore è equivalente a un impulso di 380 cariche elettroniche.

LETTERE ALLA REDAZIONE

(La responsabilità scientifica degli scritti inseriti in questa rubrica è completamente lasciata dalla Direzione del periodico ai singoli autori)

Osservazioni sopra il processo di accrescimento a spirale in cristalli di bifosfato di ammonio (ADP).

L. Levi

Instituto de Investigaciones Científicas y Técnicas de las Fuerzas Armadas - Buenos Aires

(ricevuto il 22 Novembre 1955)

Studi recenti hanno dimostrato l'importanza che sulla struttura e sul comportamento delle sostanze cristalline hanno le imperfezioni che accompagnano la formazione di cristalli. È da ricordare in particolare l'ipotesi di F. C. Frank [1] (1949) sull'accrescimento a spirale confermata poi sperimentalmente dai risultati di varie osservazioni microscopiche [2], e in alcuni casi submicroscopiche [3].

Recentemente, dovendo curare una piccola produzione di cristalli piezoelettrici di bifosfato di ammonio ($NH_4H_2PO_4$; indicato nella tecnica come ADP), la mia attenzione è stata ripetutamente attratta dalla presenza di linee che, come si vede chiaramente nella fig. 1, si presentano sulle facce (100) e (010) di tali cristalli, e che ricordano, a parte le dimensioni qui decisamente macroscopiche, quelle riprodotte nelle tavole che accompagnano i lavori citati.

Nella riproduzione fotografica presentata qui, si notano infatti due serie di ombreggiature curvilinee, che si originano dove la cristallizzazione si è iniziata difettosa. Dette ombreggiature corrispondono a piccole ondulazioni della superficie, accompagnate da una lieve inclinazione di questa verso le estremità del cristallo, come può vedersi più chiaramente nella fig. 2 che riproduce lo stesso cristallo osservato per trasparenza in altra prospettiva (la superficie ondulata della fig. 1 coincide con la faccia superiore nella fig. 2). L'analogia osservata mi condusse quindi ad analizzare più attentamente il fenomeno per stabilire se una relazione esistesse effettivamente fra questo e il corrispondente fenomeno microscopico.

Allo scopo considerai conveniente completare le mie osservazioni mediante lo studio dei piccoli cristalli, delle dimensioni di pochi millimetri, che possono ottenersi in poche ore per la libera precipitazione di una soluzione soprasatura.

Le microfotografie delle fig. 3 e 4 offrono, in un ingrandimento $\times 90$, un

---

(1) F. C. Frank: *Disc. Faraday Soc.*, No. 5 (Crystal Growth), p. 48 (1949).

(2) S. Amelinckx: *Phil. Mag.* **43**, 562 (1952); A. J. Forty: *Phil. Mag.* **43**, 72, 377, 949 (1952); A. R. Verma: *Phil. Mag.*, **42**, 1005 (1951); **43**, 441 (1952); H. Rae e A. E. Robinson: *Proc. Roy. Soc.*, A **222**, 558 (1954).

(3) I. M. Dawson: *Proc. Roy. Soc.*, A **206**, 555 (1951); N. G. Anderson e I. M. Dawson: *Proc. Roy. Soc.*, A **218**, 255 (1953).

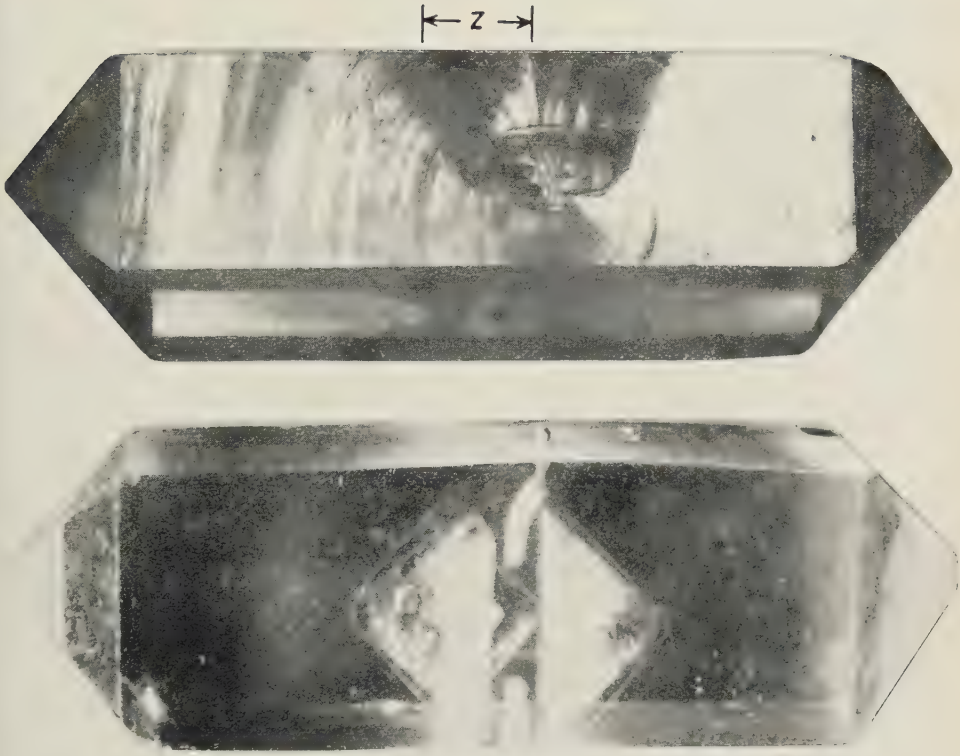

Fig. 1 (sopra) e fig. 2. – Lunghezza naturale del cristallo 9 cm.

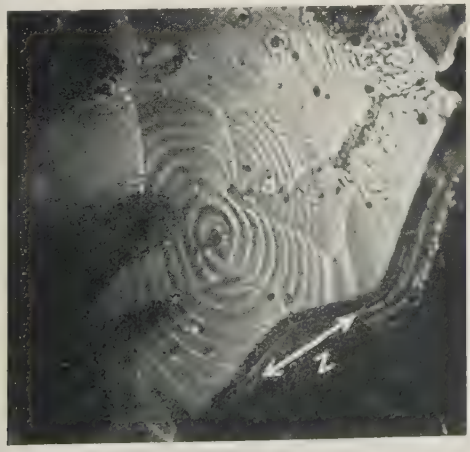

Fig. 3. – Ingrandimento · 90.

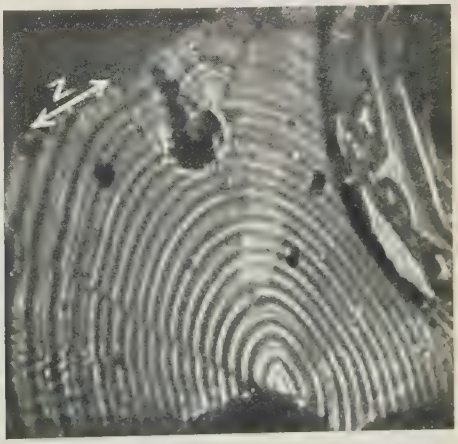

Fig. 4. – Ingrandimento ×90.

esempio dei risultati ottenuti. Nella fig. 3 può osservarsi il vero inizio di una spirale; a poca distanza dall'origine però il fenomeno si complica per la formazione di altri gruppi di linee dello stesso tipo, le quali formano arco attorno ad altri centri. Nella fig. 4 non può distinguersi chiaramente se gli archi hanno forma di spirale o di linee chiuse, ma essi si sviluppano sopra la maggior parte della superficie del piccolo cristallo, restando incompleti all'incontrare i margini.

Confrontando ora le fig. 3 e 4 con la fig. 1, pare debba concludersi che esse rappresentano veramente, in diverse dimensioni, lo stesso fenomeno: le curve presentano infatti tutte la stessa forma ovalata, con l'asse maggiore sempre orientato in direzione approssimativamente normale all'asse Z del prisma.

Il fatto che linee a spirale molto pronunciate si sono osservate con maggior frequenza in soluzioni invecchiate per il ripetuto uso, permette di supporre che le impurezze contenute nella soluzione influiscano sopra il fenomeno. Non si è potuto realizzare uno studio sistematico in questo senso. Ciò nonostante, nelle colonne I e II della tabella che qui si riproduce, riportiamo i risultati dell'analisi chimica rispettivamente della soluzione dalla quale si ottenne il cristallo delle fig. 1 e 2 (colonna I) e di un'altra soluzione, colla quale il fenomeno si presentò molto meno pronunciato (colonna II). Nella prima soluzione si osserva principalmente una maggior percentuale degli ioni metallici bivalenti Cu^{++} e Ba^{++}; il bario in particolare può essere stato ceduto dal vetro del cristallizzatore, il suo aumento risultando quindi una caratteristica naturale dell'invecchiamento della soluzione.

Dall'esame della fig. 2 risulta chiaramente che la crescita in sezione del cristallo (generalmente molto lenta rispetto alla crescita in lunghezza), viene favorita dalla formazione di spirali. Difatti la faccia dove si sono formate le spirali si trova assai più lontana dal nucleo di cristallizzazione che la sua simmetrica.

Le colonne III e IV della tavola riproducono rispettivamente i risultati dell'analisi chimica di parti del cristallo formate per crescita in lunghezza (colonna III) e di altre ottenute per deposizione sopra le facce laterali (colonna IV). È evidente la maggior inclusione di impurezze in queste ultime.

	I	II	III	IV
Fe^{+++}	2 mg %	2 mg %	0.1 mg %	0.2 mg %
Al^{+++}	1 »	4 »	1 »	4 »
Cu^{++}	5 »	0.1 »	—	5.1 »
Ba^{++}	20 »	10 »	2 »	10 »
SO_4^{--}	20 »	10 »	6 »	6 »

* * *

La serie di esperienze che ha dato luogo alla presente Nota si è svolta nel Laboratorio de Electronica y Comunicaciones, appartenente al Instituto de Investigaciones Científicas y Técnicas de las Fuerzas Armadas (República Argentina). Ringrazio quindi le corrispondenti autorità per avermi procurato i mezzi di lavoro; ringrazio pure i signori Sabato e Biloni della Comisión Nacional de la Energía Atómica per la collaborazione prestatami nell'ottenimento delle microfotografie.

The Solution of the Schrödinger Equation for an Approximate Atomic Field

T. Tietz

Department of Theoretical Physics University Łòdz - Łòdz (Poland)

(ricevuto il 29 Novembre 1955)

This note deals with the solution of the Schrödinger equation for an approximate atomic field. It is known [1] that the Schrödinger equation for the Fermi-Thomas potential can be written in atomic units as

$$\frac{\mathrm{d}^2\Phi}{\mathrm{d}r^2} + \left[-\eta^2 + \frac{2Z}{r}\varphi\left(\frac{r}{\mu}\right) - \frac{l(l+1)}{r^2}\right]\Phi = 0 \tag{1}$$

where

$$x = \frac{r}{\mu}, \qquad \mu = \frac{0.88534}{Z^{\frac{1}{3}}}, \qquad \eta^2 = \sqrt{2E},$$

and the Thomas-Fermi $\varphi(x)$ satisfies the equation

$$x^{\frac{1}{2}}\varphi'' = \varphi^{\frac{3}{2}}. \tag{2}$$

For a free neutral atom or a positive ion we know different approximate solutions [2], but for no approximate potential could one solve the Schrödinger equation in analytic form. The solution of the Schrödinger equation is given only in numerical form. Recently Kerner [3], taking into consideration his approximate potential has obtained a successful approximate analytic solution of the Schrödinger equation for a free neutral atom, but his final results for the eigenvalues and eigenfunctions are given only numerically. It seems that the problem at hand can be solved only by a special assumption. We shall limit ourselves to the free neutral atom. Taking into consideration Brinkman's [4] remarks, that $\sqrt{x\cdot\varphi}$

---

[1] P. Gombás: *Die statistische Theorie des Atoms und ihre Anwendungen* (Wien, 1949).

[2] A. Sommerfeld: *Zeits. f. Phys.*, **78**, 283 (1932); N. H. March: *Proc. Camb. Phil. Soc.*, **46**, 336 (1950); S. Rozental: *Zeits. f. Phys*, **98**, 742 (1935); E. H. Kerner: *Phys. Rev.*, **83**, 71 (1951); T. Tietz: *Journ. of Chem. Phys.*, **22**, 2094 (1955); *Ann. der Phys.*, **15**, 186 (1955); *Nuovo Cimento*, **1**, 955 (1955); **1**, 968 (1955); *Journ. of Chem. Phys.*, **23**, 1167 (1955); H. C. Brinkman: *Physica*, **20**, 44 (1954).

[3] E. H. Kerner: *Phys. Rev.*, **83**, 71 (1951).

[4] H. C. Brinkman: *Physica*, **20**, 44 (1954); T. Tietz: *Ann. der Phys.*, **15**, 186 (1955).

is a slowly varying function in some region, we can write

$$\mu \approx \frac{\varkappa}{x} \tag{3}$$

where $\varkappa$ is a constant. Bearing this in mind we write (1) as

$$\frac{\mathrm{d}^2\Phi}{\mathrm{d}r^2} + \left[-\eta^2 + \frac{1.7068\varkappa Z^{\frac{4}{3}} - cl(l+1)}{r^2}\right]\Phi = 0\,. \tag{4}$$

In equation (4) c is a disposable constant. Putting for brevity

$$1.7068\cdot\varkappa = 1 \tag{5}$$

we obtain

$$\frac{\mathrm{d}^2\Phi}{\mathrm{d}r^2} + \left[-\eta^2 + \frac{Z^{\frac{4}{3}} - cl(l+1)}{r^2}\right]\Phi = 0\,. \tag{6}$$

If

$$Z^{\frac{4}{3}} - cl(l+1) > \tfrac{1}{4} \tag{7}$$

the eigenvalues and eigenfunctions are known and were for the first [5] time obtained by CASE. Equation (6) shows, that the eigenvalues for the $1S$ states cannot be very accurate, because the eigenvalues depend on the behaviour of the potential near $r = 0$ and our potential for very small r does not behave as the potential of Fermi-Thomas. As we shall see later on, the determination of the eigenvalues for the $1S$ states can easily be done in another way. If (7) is fulfilled then according to CASE we have the following eigenvalues

$$\eta_n = \frac{Z}{a}\exp\left[\frac{B - (n+\frac{1}{2})\pi}{[Z^{\frac{4}{3}} - \frac{1}{4} - cl(l+1)]^{\frac{1}{2}}}\right], \qquad n = 1, 2, 3, \ldots \tag{8}$$

where B is any fixed factor common to all eigenfunctions for fixed Z and fixed l. Changing Z and l we must change generally B, in such a way that the new B becomes common to all eigenfunctions. We shall not write down the eigenfunctions for they are to be found in the paper of CASE. For brevity we determine the constant B so that the formula (8) for the eigenvalues will be of the following form:

$$\eta_n = \frac{Z}{a}\exp\left[\frac{(n-1)\pi}{[Z^{\frac{4}{3}} - \frac{1}{4} - cl(l+1)]^{\frac{1}{2}}}\right], \qquad n = 1, 2, 3, \ldots \tag{9}$$

where a is a new constant. We determine the constants a and c by trial and error so that the eigenvalues η_n for fixed Z and fixed l should be placed nearly on a common correct straight line. We can admit for a and c the following values:

$$a = 1.26263\,; \qquad c = 0.45\,. \tag{10}$$

---

(5) K. M. CASE: *Phys. Rev.*, **80**, 797 (1950).

Table I shows the eigen-η computed from (9) and (10) in comparison with Hartree's values and Kerner's values computed from an infinite determinant for the mercury atom ($Z = 80$).

TABLE I. – *Comparison of the eigenvalues of η for $Z=0$.*

n	l	HARTREE	KERNER from infinite determinant	From equation (9)
1	S	74.48	74.40	63.36
2	S	30.41	30.46	30.41
2	P	29.87	29.98	29.88
3	S	14.76	15.29	14.60
3	P	14.19	14.73	14.06
3	D	13.08	13.57	12.92
4	S	6.87	8.08	7.01
4	P	6.34	7.61	6.62
4	D	5.27	6.69	5.84
4	F	3.09	5.18	4.60

In Table II we have the $2S$ and $2P$ levels split with increasing Z.

TABLE II. – *$a\cdot\eta$ as a function of Z for the $2S$ and $2P$ states. $\Delta = a(\eta_{2S} - \eta_{2P})$ shows the splitting of the states with increasing Z.*

Z	10	20	30	40	50	60	70	80	90
$2S$	2.23325	6.16082	10.77027	15.80450	21.14280	26.71544	32.47720	38.39640	44.45052
$2P$	1.86137	5.67387	10.21596	15.20285	20.50490	26.04830	31.78570	37.68420	43.71996
Δ	0.37188	0.48695	0.55431	0.60165	0.63790	0.66714	0.69150	0.71220	0.73056

Tables I and II show that the simple assumption (3) gives relatively good eigenvalues and that it can explain the splitting of levels with increasing Z. The formula (9) will not give good eigenvalues for n greater than 5, because the approximate potential is not suitable for such states. In practice, it is not necessary to compute the eigen-η for quantum numbers n larger than 5 except for states corresponding to optical states. The computation of the eigen-η for another approximate potential than the potential considered above is connected with extra mathematical complexity and this is too great for any but the simplest of atomic calculations. As mentioned before we see from Table I that for $n=1$ the $1S$ states are too inaccurate. One can give a simple formula for the $1S$ states if we assume that the Fermi-Thomas function $\varphi(x)$ near $x=0$ behaves as the following function

$$\varphi(x) = \frac{ax}{e^{ax} - 1}, \tag{11}$$

which one can always do through the matching of the constant a. We know that in this case the Schrödinger equation (1) for $l=0$ can be solved exactly. When we take $a=1.8508$ we obtain after some calculations the following formula for the $1S$ state

$$\eta_1 = Z - 1.04561 \cdot Z^{\frac{1}{3}}. \tag{12}$$

For the mercury atom we obtain for the $1S$ state, the value 74.48 in this case the Hartree's value is 74.48. The approximate Fermi-Thomas function of the author ([6])

$$\varphi(x) = \frac{1}{(1+b\cdot x)^{\alpha}}, \quad \alpha > 1/5 \tag{13}$$

as it was shown before gives a good approximation fo the Fermi-Thomas function. The following table gives us the values of the constant b for different α.

TABLE III. – *The values of b for different α.*

α	7/5	3/2	2
b	0.881206	0.80812	0.569272

The exactness of this approximation is visible if we calculate the mean excitation energy E_M

$$E_M = (2/5) v_M \cdot e, \tag{14}$$

where v_M is ([1])

$$v_M = 10^{\gamma} \frac{Ze}{\mu} \tag{15}$$

and the constant γ is

$$\gamma = \int_0^{\infty} \varphi^{\frac{1}{2}} \cdot x^{\frac{1}{2}} \log_{10} \frac{\varphi}{x} \, \mathrm{d}x. \tag{16}$$

The numerical value of γ is $-0{,}968$.

In the approximation (13) after some calculation we obtain for γ following formula

$$\gamma = \left[C + \Psi(\alpha) - 2 - \frac{\alpha}{\alpha + 1} \right] \log_{10} e + \log_{10} b \tag{17}$$

where $e=2.7182...$, $C=0.5772...$, and $\mathrm{d}\Gamma(z)/\mathrm{d}z$ is denoted by $\Psi(z)$. The following table gives us the values of the constant γ for different α.

([6]) T. TIETZ: *Journ. of Chem. Phys.*, **23**, 1560 (1955).

TABLE IV. – *The values of γ for different α.*

α	7/5	3/2	2
γ	— 0.95520	— 0.95516	— 0.96848

We compare the values of the excitation energy E_M for Fe, Ag, Pb in our case with the numerical values, the experimental values, and the Sommerfeld values.

TABLE V. – *Comparison of the excitation energy E_M for* Fe, Ag, Pb *in* eV.

	Fe	Ag	Pb
experimental	104	224	402
numerical	102	226	474
Sommerfeld's values	173	303	635
for $\alpha = 7/5$	105	232	486
for $\alpha = 3/2$	105	232	485
for $\alpha = 2$	102	226	474

The solution of the Schrödinger equation from the potential derived from (1) can be obtained only numerically. We have calculated the eigen-η for the approximate Fermi-Thomas function (13) for $\alpha=2$. More details will be published later on.

* * *

In conclusion, the writer wishes to thank Professor Dr. F. J. WISNIEWSKI for friendly discussion and criticism.

IL NUOVO CIMENTO Vol. III, N. 2 1° Febbraio 1956

Some Considerations on the Phase-Shift Analysis in the (p^+-p^+) Scattering.

G. Puppi and A. Stanghellini

Istituto di Fisica dell'Università - Bologna

(ricevuto il 27 Dicembre 1955)

Although we have a rather satisfactory global description of the pion-nucleon scattering processes, the situation ought to be improved in order to clear the following fundamental points:

1) Determination of the properties of the isotopic spin states, independently, from the results relative to different charge states.

Such a determination in fact, would show, from comparison, up to what degree of approximation the charge-independence is true.

2) Improvement of the numerical definition of the various phase shifts, particularly the small ones. This information would show more clearly the nature of the nuclear forces. To contribute to this achievement, we have examined the state $T = \frac{3}{2}$, as it results from the pion-nucleon properties in the p^+ charge state and we have studied its behaviour with energy. The experimental results give several determinations of total cross-sections ([1,2]) and some angular distributions. Considering the first datum as the most reliable from the point of view of experimental errors, we have normalized on it the results of the angular distributions of 6 experiments at 113 ([3]), 120 ([4]), 150 ([5]), 165 ([6]), 170 ([5]), 189 ([7]), MeV chosen according to the energy interval we wanted to investigate, and to the completness of the results.

Let us remember the form of angular distribution with 2 waves:

$$\frac{\mathrm{d}\sigma}{\mathrm{d}\omega} = a + b\cos\vartheta + c\cos^2\vartheta = \frac{1}{4K^2}\{|A + B\cos\vartheta|^2 + |C\sin\vartheta|^2\}$$

where

$$A = \exp[i2\alpha_3] - 1\,,$$

$$B = 2\exp[i2\alpha_{33}] + \exp[i2\alpha_{31}] - 3\,,$$

$$C = \exp[i2\alpha_{33}] - \exp[i2\alpha_{31}]\,.$$

([1]) J. Ashkin, J. P. Blaser, F. Feiner, J. G. Gorman and M. O. Stern: *Phys. Rev.*, **96**; 1104, (1954).

([2]) S. J. Lindenbaum and L. C. L. Yuan: *Phys. Rev.*, **100**; 306, (1955).

([3]) J. Orear: *Phys. Rev.*, **96**; 1417, (1954).

([4]) L. Ferretti, E. Manaresi, G. Puppi, G. Quareni and A. Ranzi: *Nuovo Cimento*, **1**, 1238, (1955).

([5]) J. Ashkin, J. P. Blaser, F. Feiner, and M. O. Stern: Private communication.

([6]) H. L. Anderson and M. Glicksman: *Phys. Rev.* **100**, 268, (1955).

([7]) H. L. Anderson, W. C. Davidson, M. Glicksman and V. E. Kruse: *Phys. Rev.* **100**, 279 (1955).

Now we have fitted with trial functions the coefficients a, b, c, in the energy interval considered and we have prolonged the fit through zero, joining it smoothly with analytical forms suggested by the hypothesis that at low energies, the S-phase varies linearly with the momentum in C.M., and p-phases with the cube of the momentum.

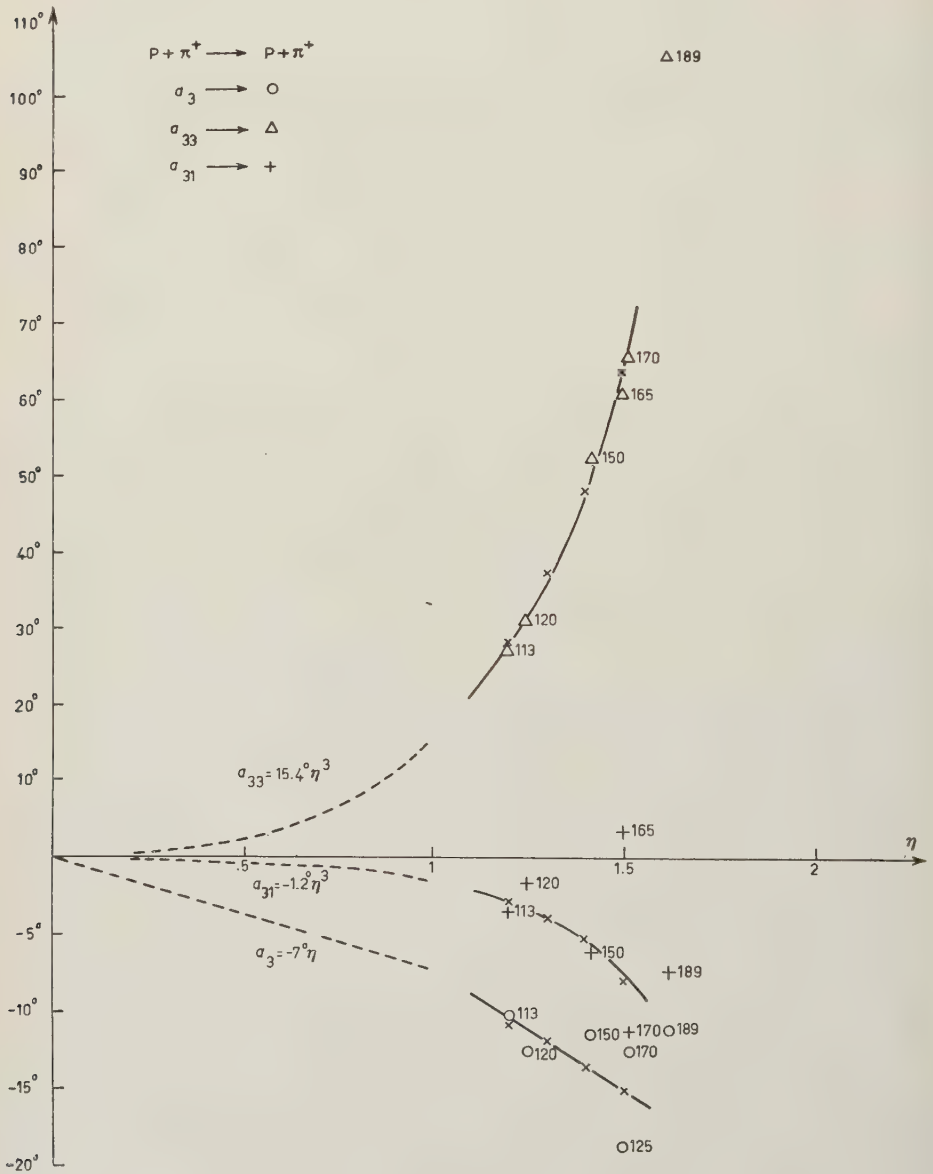

Fig. 1.

These forms are chosen by general considerations on the scattering theory and because they are suggested by the

behaviour in the region where the experiments take place.

The matter gets more complicated for the S-phase and the choice of linearity spoils the detail of the behaviour. This choice gives one set of Fermi-type phase-shifts and one of Yang-type, with their simmetrics in signs.

Solutions of Steinberger-type do not appear, because they have different analytical behaviour through zero. Table I shows the results obtained, relative to the reckoning of the phases in the interval investigated and to the definition of the behaviour through zero. Fig. 1 shows the behaviours obtained of the Fermi-type phases and the results of the authors in each experiment.

We note:

a) The behaviours at low energies are consistent with OREAR's [8] research in these regions and with STEINBERGER's [9] direct determination.

b) The behaviour of phase α_3 agrees with the average of the results obtained with negative mesons, which gives for the mesic-atom, Panosky's effect, photoproduction, charge-exchange scattering, whole

$$\alpha_3 = (-\,6.2^\circ \pm 1.2^\circ)\eta\,.$$

c) Phase α_{31} seems to assume a definite aspect. It is negative, small and its order of magnitude is a few degrees in the interval considered.

d) On the behaviour of α_3 towards the resonance, we get a line more inclined than that obtained at low energy.

e) α_{33} presents nothing new, because as it is well known, it practically originates from the total cross-section.

The set of Fermi-type phase shifts drawn in Fig. 1 agrees both with the experimental results on the Coulomb-interference and with the conditions imposed by the causality principle. In fact, an examination of the phase-shift behaviours, performed with an analytical method equivalent to Askin-Vosko's graphic method, shows that around 120 MeV, there is only one set of phase-shifts affected by the Fermi-Yang ambiguity and sign ambiguity. The ambiguity of sign can be resolved with the Coulomb interference observed in this region [3-4-10] and therefore allows one to choose a track affected by Fermi-Yang's ambiguity only which, as it is well known, can be resolved by a polarization experiment.

We realise that the choice of the positive sign for α_{33} can be justified at such energies, considering that the derivative

TABLE I.

	Fermi-type			Yang-type	
η	α_3	α_{33}	α_{31}	α_{33}	α_{31}
1.2	$-\,10.6^\circ$	27.8°	$-\,2.8^\circ$	8.4°	38.8°
1.3	$-\,11.7^\circ$	37.6°	$-\,3.5^\circ$	12.9°	53.9°
1.4	$-\,13.5^\circ$	48°	$-\,5^\circ$	20°	70.2°
1.5	$-\,15^\circ$	64.1°	$-\,7.9^\circ$	37.8°	108.7°
1 (*)	$-\,7^\circ$	15.4°	1.2°	4.2°	20.5°

(*) Obtained from the definition of the behaviour through zero as described in the text.

(8) T. OREAR: *Phys. Rev.*, **96**, 176 (1954).

(9) D. BODANSKI. A. SACHS and J. STEINBERG: *Phys. Rev.*, **93**, 1367, (1954).

(10) E. PEDRETTI, A. STANGHELLINI, G. QUARENI: *Nuovo Cimento*, **2**, 450 (1955).

of the phase α_{33} if it were negative, would not agree with the non-relativistic formulation of the principle of causality given by WIGNER [11], who pointed out that the derivative of the phase ought not to overcome a certain negative limit, namely:

$$\frac{d\alpha_{33}}{d\eta} < -1 .$$

With the behaviours obtained near zero, we see, « a posteriori », that the solution with reversed signs, must already be disregarded at 100 MeV.

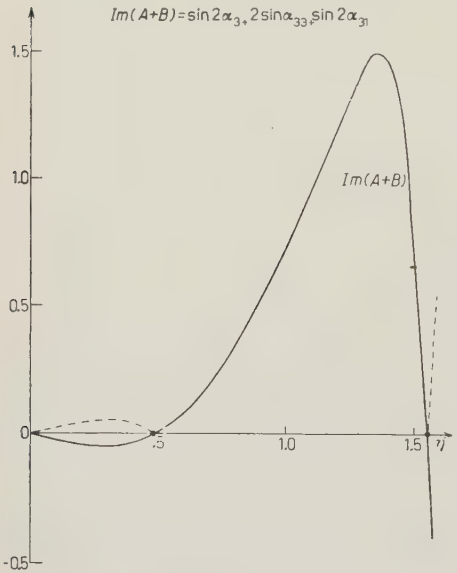

Fig. 2.

Besides, ANDERSON [12] has found the causal form of the real part of the forward scattering which is equal to Im $(A+B)$. Such quantity has been drawn from our data (Fig. 2) and agrees with ANDERSON's very well.

This quantity once fixed, the sign of the phases is fixed too. The experimental data give $|A-B|$, Re $(A+B)$ and Im $(A+B)$. If of this last term we take the causal form shown in Fig. 2, we can make an analysis of the spurious solutions. These appear when Im $(A+B)$ is small, i.e. in the $\eta=0 \div 0.6$ and $\eta \sim 1.5$ intervals.

In the first interval it is called Steinberger's solution; it has α_3 positive and positive derivative. Therefore it is not likely to be taken for the good solution and it is to be neglected because discontinuous. For Im $(A+B)=0$ the spurious solutions coincide with the symmetrics of the good solutions. In such case it may happen to follow up this spurious symmetrical solution (Im > 0 instead of Im < 0) in the first interval, and the good solution (Im > 0 and big) in the second interval, and in the last one, again the spurious symmetric solution (Im > 0).

FERMI-METROPOLIS [13] found this last chance, as it was recognized by BETHE [14]. It is therefore obvious that once the causal form of Im $(A+B)$ is given, there is no other choice but Fermi-Yang's solutions.

We have also determined, by the value obtained in our research, the parameters of the formula given by Chew for α_{33}:

$$\frac{4}{3}\frac{\eta^3}{\omega^*}\operatorname{cotg}\alpha_{33} = \frac{1}{f^2}\left(1-\frac{\omega^*}{\omega_0}\right)$$

and we have got:

$$f^2 = 0.087$$

$$\omega_0 = 2.19$$

in agreement with the preceding determinations [15].

[11] E. P. WIGNER: *Phys. Rev.*, **98**, 145 (1955).

[12] H. L. ANDERSON, W. C. DAVIDON and V. E. KRUSE: *Phys. Rev.*, **100**, 339 (1955).

[13] E. FERMI, N. METROPOLIS and FELIX ALEI: *Phys. Rev.*, **95**, 1581 (1955).

[14] F. DE HOFFMAN, N. METROPOLIS, E. F. ALEI and H. A. BETHE: *Phys. Rev.*, **95**; 1586, (1955).

[15] *Proceedings of the Fifth Rochester Conference.*

For α_{31} the following formula is given:

$$-\frac{2}{3}\frac{\eta^3}{\omega^*}\operatorname{cotg}\alpha_{31}=\frac{1}{f^2}\left(1+X\frac{\omega^*}{\omega_0}\right)$$

From the cut-off theory one may calculate X, which results fairly small. We have therefore determined α_{31} using the same coupling constant found for α_{33}, and putting $X=0$.

In this way one obtains a behaviour of α_{31} which is not inconsistent with the results of our fit.

* * *

We wish to thank Dr. F. Fattorini, who friendly collaborated with us in this research, and Miss A. Vignudelli for the numerical calculations.

A Remark on Quantum Electrodynamics with Non-Vanishing Photon Mass and Lamb Shift Calculations.

B. Nagel

CERN Theoretical Study Division
at the Institute for Theoretical Physics, University of Copenhagen

(ricevuto il 9 Gennaio 1956)

When treating quantum electrodynamics as the limiting case $\mu \to 0$ of a neutral vector meson theory with meson mass μ [1-3], it is generally assumed that the contribution of the longitudinal mesons vanishes in the limit. This statement should, however, be applied with some care, and it is the purpose of this note to show that the longitudinal mesons give a non-vanishing contribution to the cross-section for bremsstrahlung with emission of soft photons. This is of some interest in connection with the calculation of the Lamb shift [4,5], as the relation $\log(2k_{\min}/\mu) = \frac{5}{6}$ between the photon mass and an infrared non-covariant momentum cut-off $k_{\min}$; necessary to join the covariant and non-covariant parts of the Lamb shift calculation as performed by Feynman, is conveniently derived by calculating the bremsstrahlung cross-section with the two methods and equating the results [6,7].

Incidentally, the contribution of the longitudinal mesons turns out to be the number $\frac{1}{6}$, which is rather famous in this connection; if we take only the transversal mesons into account we get the incorrect relation $\log(2k_{\min}/\mu) = 1$.

The probability for scattering of an electron by a static field with emission of photons with momenta smaller than ΔE (assumed to be small compared with the kinetic energy of the electron) is given by [8]

$$W = \frac{e^2 |M_0|^2}{(2\pi)^3} \cdot \int_0^{\Delta E} \frac{\mathrm{d}^3 k}{2k_0} \cdot \left\{ \sum_i \left(\frac{p \cdot e_i}{p \cdot k} - \frac{p' \cdot e_i}{p' \cdot k} \right)^2 \right\}, \tag{1}$$

(1) F. J. Belinfante: *Phys. Rev.*, **75**, 1321 (A) (1949); *Prog. Theor. Phys.*, **4**, 165 (1949).
(2) F. Coester: *Phys. Rev.*, **83**, 798 (1951).
(3) R. J. Glauber: *Prog. Theor. Phys.*, **9**, 295 (1953).
(4) R. P. Feynman: *Phys. Rev.*, **74**, 1430 (1948) and **76**, 769 (1949).
(5) J. B. French and V. F. Weisskopf: *Phys. Rev.*, **75**, 1240 (1949).
(6) R. H. Dalitz: *Proc. Roy. Soc.*, A **206**, 521 (1951).
(7) L. R. B. Elton and H. H. Robertson: *Proc. Phys. Soc.*, A **65**, 145 (L) (1952).
(8) See e.g. J. M. Jauch and F. Rohrlich: *Helv. Phys. Acta*, **27**, 613 (1954), eqns. (2–5).

M_0 is the matrix element for elastic scattering, p and p' are the initial and final four-momenta of the electron, $k_0=\sqrt{|\bar{k}|^2+\mu^2}$, and the summation is to be performed over three (in the case $\mu=0$ two transversal) polarization directions e_i satisfying $k\cdot e_i=0$.

As we have to do with vector mesons, that is $k^2=-\mu^2$, this formula implies that we have neglected some terms in μ^2 in the numerator and denominator as compared with the original exact expression (eq. (2) in ref. [8]). The omission in the numerator is trivially justified. As for the denominator, the remaining term $p\cdot k$ is of order μ at least, and a correction μ^2 will give a contribution to the final result of order $\mu\cdot\log\mu$ at most, and is thus of no consequence.

It is well known (and can easily be verified by direct calculation) that because of the Lorentz condition the summation over the three (or two) polarization directions is equivalent to summation over all four directions [9], and thus the sum becomes

$$\frac{2m^2+q^2}{(p\cdot k)(p'\cdot k)}-\frac{m^2}{(p\cdot k)^2}-\frac{m^2}{(p'\cdot k)^2}$$

where $q=p'-p$, $m=$ electron mass.

If we perform the integral, assuming $q^2/m^2\ll 1$ and $\Delta E/\mu\gg 1$, we obtain

$$W=\frac{e^2|M_0|^2}{(2\pi)^3}\cdot\frac{4\pi}{3}\cdot\frac{q^2}{m^2}\cdot\left(\log\frac{2\Delta E}{\mu}-5/6\right)+\dots . \tag{2}$$

If we instead put $\mu=0$ and integrate down to some lower limit $k_{\min}$; we have

$$W=\frac{e^2|M_0|^2}{(2\pi)^3}\cdot\frac{4\pi}{3}\cdot\frac{q^2}{m^2}\cdot\log\frac{\Delta E}{k_{\min}}+\dots . \tag{3}$$

In this case it is easier to use the expression with summation over the two transversal directions only.

We are now especially interested in the longitudinal mesons. If we write

$$W=\frac{e^2|M_0|^2}{(2\pi)^3}\cdot\int_0^{\Delta E}\frac{\mathrm{d}^3k}{2k_0}\sum_i S_i\,,$$

the longitudinal contribution S_3 is given by

$$S_3=\left(\frac{p\cdot e_3}{p\cdot k}-\frac{p'\cdot e_3}{p'\cdot k}\right)^2 \quad \text{with} \quad e_3=\left(\frac{k_0}{\mu|\bar{k}|}\cdot\bar{k},\ i\frac{|\bar{k}|}{\mu}\right),$$

and is

$$S_3=\frac{\mu^2}{|\bar{k}|^2}\cdot\left(\frac{p_0^2}{(p\cdot k)^2}+\frac{p_0'^2}{(p'\cdot k)^2}-\frac{2p_0p_0'}{(p\cdot k)(p'\cdot k)}\right)-\frac{\mu^2}{|\bar{k}|^2\cdot k_0^4}\cdot\frac{(q\cdot k)^2}{m^2}+\dots \tag{4}$$

(in the last expression we have assumed $q^2/m^2\ll 1$).

(9) Actually, as we have made some approximations, we should perhaps not expect this equivalence to be valid exactly; nevertheless it turns out to be so.

The approximation involved by putting $p_0 = p_0'$ can be justified by means of an argument similar to the discussion in connection with equation (1).

Integration gives the probability for emission of longitudinal mesons with momenta smaller than ΔE (still $\Delta E/\mu \gg 1$):

$$W_3 = \frac{e^2 |M_0|^2}{(2\pi)^3} \cdot \frac{4\pi}{3} \cdot \frac{q^2}{m^2} \cdot \frac{1}{6} + \dots . \tag{5}$$

A comparison of S_3 with the corresponding expression for a transversal meson shows that the probability for emission of a longitudinal meson with momentum $|\bar{k}|$ is equal to $\mu^2/(|\bar{k}|^2 + \mu^2)$ times the probability for emission of a transversal meson (2). Though this ratio goes to zero with μ for every finite $|\bar{k}|$, it is of order one for $|\bar{k}| \leqslant \mu$, and, as the integral

$$\int_0^{\mu} \frac{|\bar{k}|^2 \cdot \mathrm{d}|\bar{k}|}{(|\bar{k}|^2 + \mu^2)^{\frac{3}{2}}} = \int_0^1 \frac{x^2 \,\mathrm{d}x}{(1 + x^2)^{\frac{3}{2}}},$$

giving the contribution from transversal mesons with momenta smaller than μ, stays different from zero as $\mu \to 0$, it is obvious that also the longitudinal mesons do give a finite contribution.

It may be pointed out that S_3 is not Lorentz invariant. A vector meson with a specified polarization is, of course, not an invariant concept.

* * *

It is a pleasure to thank Dr. G. Källén for valuable advice and discussions.

IL NUOVO CIMENTO Vol. III, N. 2 1° Febbraio 1956

About the Λ^0-Nucleon Force.

R. Gatto

Istituto di Fisica e Scuola di Perfezionamento in Fisica Nucleare dell'Università - Roma
Istituto Nazionale di Fisica Nucleare - Sezione di Roma

(ricevuto il 16 Gennaio 1956)

The existence of Λ^0-nuclei with lifetimes of the order of that of the free Λ^0 implies that a Λ^0-nucleon force exists, sufficiently attractive to produce the binding of the Λ^0 to the nucleons.

As to the strong interactions from which this force may originate, one can speculate as follows.

— Interactions such as $(\Lambda^0, N\pi)$ (it would produce an exchange Λ^0-N force) which would lead to the rapid decay of the Λ^0 are to be excluded as strong.

A possible $(\Lambda^0, \Lambda^0\pi^0)$ interaction would produce a direct Λ^0-N force through virtual processes of the kind $\Lambda^0 + N \to (\Lambda^{0\prime} + \pi^0) + N \to \Lambda^{0\prime} + N'$. However it does not conserve total isotopic spin — the Λ^0 has isotopic spin zero — and the resulting Λ^0-N force would therefore be charge-dependent. As Dalitz [1] has emphasized, the resulting Λ^0-p and Λ^0-n forces would be of opposite sign (this follows from the charge independence of the ordinary π-N interaction which requires the $p\pi^0$ interaction to be opposite in sign to the $n\pi^0$ interaction). On the other hand present experimental data suggest that total isotopic spin is approximately a good quantum number for the lightest Λ^0-nuclei.

— Higher order interactions as for instance $(\Lambda^0, \Lambda^0\pi\pi)$ [1] cannot be excluded by similar considerations.

— A strong $(\Lambda^0, N\overline{K})$ interaction ($\overline{K}$ is a K^0 or a K^-) would lead to an exchange Λ^0-N force through virtual processes of the kind $\Lambda^0 + N \to (N' + \overline{K}) + N \to N' + \Lambda^{0\prime}$. This strong $(\Lambda^0, N\overline{K})$ interaction would also explain: (i) the associated production of $\Lambda^0 + K$ (K is a K^+ or a K^0) in N-N and π-N collisions; (ii) the production of a Λ^0 after the capture of a K^- by a nucleus; (iii) the many cases observed of K-N scatterings (by the virtual sequence $K + N \to K + (\Lambda^0 + K') \to N' + K'$. Pais and Serber [2] have remarked that such a scattering would have an exchange character, and therefore it would frequently be associated with large momentum transfers).

— Other more indirect contributions cannot be excluded: (for instance, through

[1] R. H. Dalitz: *Phys. Rev.*, **99**, 1475 (1955).
[2] A. Pais and R. Serber: *Phys. Rev.*, **99**, 1551 (1955).

a possible strong (Λ^0, $\Sigma\pi$) interaction the Λ^0 goes over into a Σ which again transforms into a Λ^0, the two virtual pions being absorbed by the nucleon, etc.).

It seems to be a general conclusion from the foregoing discussion that the Λ^0-N force should in any case have a range smaller than $1/m_\pi$. In the following we shall mainly consider the exchange force arising from the suggested (Λ^0, $N\overline{K}$) interaction — no arguments are given to conclude that this force must be the dominant one among the many possible contributions: however, there is presently a large number of data which could be explained by a strong (Λ^0, $N\overline{K}$) interaction. This Λ^0-N force would result from the virtual exchange of K-mesons among the two baryons and it should have a range $\sim 1/m_K$. According to the present ideas both the θ- and τ-mesons could contribute to this exchange.

It is expected that the Λ^0 has not to satisfy the exclusion principle in nuclear matter, contrary to the ordinary nucleons. Therefore the Λ^0 binding energy will generally increase with increasing A and will not exhibit the typical saturation character of the nucleon binding energies in ordinary nuclei. This general trend is fairly confirmed by the recent investigation of Fry, Schneps and Swami [3]. However we expect that, due to the short range of the Λ^0-N force (of the order $\sim 1/m_K$), the Λ^0 binding energies will again exhibit a saturation limit for larger mass numbers. This would follow from the fact that only those nucleons which are not very outside the range of the force will contribute to the resulting potential acting on the Λ^0. The possible exchange character of the Λ^0-N force should also contribute to this effect, but presumably in a less important way — roughly speaking, the exchange character would mean a reduction of the effective force for distances larger than, about, the internucleon distance, which is larger than the range of the force $\sim 1/m_K$.

We can only give here approximate estimates — a more rigorous treatment would not perhaps be justified in view of our insufficient knowledge about the Λ^0-N force.

Let us call B the total number of baryons of the Λ^0-nucleus, and A the total number of nucleons, so that $B=A+1$. We consider the limiting case of a very massive Λ^0-nucleus. In this large nucleus the Λ^0 occupies states of very small momentum since it is not subject to the restrictions of the exclusion principle. If we neglect the polarization of the system of the nucleons due to their interaction with the Λ^0, we can approximately write for the binding energy of the Λ^0 in the Λ^0-nucleus, assuming a spin-space exchange potential with a spatial dependence given by $u(|\boldsymbol{x}-\boldsymbol{x}'|)=u(r)$

$$B_\Lambda \cong A\big(\psi^*(\boldsymbol{x}'s't',\,2,\ldots,A)\varphi^*(\boldsymbol{x}s)u(r)\psi(\boldsymbol{x}st',\,2,\ldots,A)\varphi(\boldsymbol{x},\,s)\big), \tag{1}$$

where ψ describes the nucleons and φ the bound Λ^0, $\boldsymbol{x}$, s, t are space, spin, and isotopic spin coordinates respectively, and $r=|\boldsymbol{x}-\boldsymbol{x}'|$.

Expression (1) can be put in the form

$$\sum_{ss'}\int \mathrm{d}\boldsymbol{x}\,\mathrm{d}\boldsymbol{x}'u(r)\varphi^*(\boldsymbol{x}s)\eta(\boldsymbol{x}s\boldsymbol{x}'s')\varphi(\boldsymbol{x}'s'), \tag{2}$$

where

$$\eta(\boldsymbol{x}s\boldsymbol{x}'s') = A\sum_{t'}\mathrm{d}(2)\,\mathrm{d}(3)\ldots\mathrm{d}(A)\psi(\boldsymbol{x}'s't',\,2,\ldots A)\psi(\boldsymbol{x}st',\,2,\ldots A)\,. \tag{3}$$

[3] W. F. Fry, J. Schneps and M. S. Swami: *Phys. Rev.*, **99**, 1561 (1955), and II (preprint).

The quantity $\eta(\boldsymbol{x}s\boldsymbol{x}'s')$ can be calculated for any given nuclear model. In a Fermi gas model, carrying out the spin and isotopic-spin summations we obtain for (1)

$$B_\Lambda = \frac{c^3}{\pi^2}\int \mathrm{d}\boldsymbol{x}\,\mathrm{d}\boldsymbol{x}'\varphi^*(\boldsymbol{x})\varphi(\boldsymbol{x}')(cr)^{-1}j_1(cr)u(r), \tag{4}$$

where $j_1(cr)$ is a spherical Bessel function and c is the maximum nucleon momentum.

Let us assume

$$u(r) = u_0\,\frac{e^{-\nu r}}{\nu r}, \tag{5}$$

where ν is the K-meson mass. For the limiting case considered, by evaluating the integral, we find

$$B_\Lambda = -\frac{4}{\pi}u_0(\xi - \operatorname{arctg}\xi), \tag{6}$$

where

$$\xi = \left(\frac{9\pi}{8}\right)^{\frac{1}{3}}\frac{1}{r_0\nu}, \tag{7}$$

where r_0 is defined by, radius of the Λ^0-nucleus $= r_0 A^{\frac{1}{3}}$.

The limiting value (6) does not depend on A, as already remarked.

We cannot trust on quantitative estimations based on (6) in view of the numerous hypotheses introduced. However it may be instructive to see what limitation follows for the Λ^0 binding energies from the assumption — which seems to be clearly substantiated by the experimental data — that the Λ^0-N system has no bound states.

For the Λ^0-N potential which we are considering, the assumption of no bound states for the Λ^0-N system leads to the restriction [4]

$$\frac{2m_N m_\Lambda}{m_N + m_\Lambda}\,\frac{u_0}{\nu^2} < 1.68\,, \tag{8}$$

where m_N is the nucleon mass and m_Λ is the mass of the Λ^0.

Taking for r_0 a value of $1.4\cdot 10^{-13}$, from (8) we get for our limiting B_Λ the restriction $B_\Lambda < \sim 14$ MeV. This result however depends rather strongly on the value assumed for r_0 — if we take $r_0 \simeq 1.2\cdot 10^{-13}$ the corresponding value would be $B_\Lambda < \sim 22$ MeV.

In the quoted paper by FRY, SCHNEPS abd SWAMI [3] a very accurate measurement of B_Λ for $^9\mathrm{Be}_\Lambda$ is reported: B_Λ (in $^9\mathrm{Be}_\Lambda$) $= 6.5 \pm 0.6$ MeV. This value is consistent with the minimum value required to have nuclear stability (i.e. for times of the order of $10^{-20} \div 10^{-22}$ s) against disintegration into $^4\mathrm{He} + {}^5\mathrm{He}_\Lambda$ [5].

---

[4] See, for instance, L. ROSENFELD: *Nuclear Froces* (Amsterdam, 1948).

[5] If the binding energy of $^9\mathrm{Be}_\Lambda$ were less than the sum of the binding energy od $^5\mathrm{He}_\Lambda$ and of that of ^{4}He, it would rapidly (in a time $\sim 10^{-20} \div 10^{-22}$ s) disintegrate into these particles. Therefore, from its existence for a much longer time ($\sim 10^{-10} \div 10^{-11}$ s), we obtain

$$B_\Lambda(^9\mathrm{Be}_\Lambda) > 2B(^4\mathrm{He}) - B(^8\mathrm{Be}) + B_\Lambda(^5\mathrm{He}_\Lambda)$$

$= 2.1 \pm 0.6$ MeV, taking for $B_\Lambda(^5\mathrm{He}_\Lambda)$ the value reported by FRY, SCHNEPS and SWAMI.

In the case of $^{11}C_\Lambda$ FRY, SCHNEPS and SWAMI report a B_Λ (in $^{11}C_\Lambda$) of 13 ± 6 MeV. Further measurements of the binding energies in the heavier hyperfragments would be of great interest — however they are rendered very difficult by the presence of neutrons among the secondaries.

In the preceding discussion the treatment of the Λ^0 as a spin $\frac{1}{2}$ particle was implicit — and it is difficult to see how much the results would be altered by a different assumption. Growing evidence based on angular correlation data substantiates the opinion that the Λ^0 may have an higher spin ([6]). The angular and energy distributions in the decay of the lightest Λ^0-nuclei could be used in some cases to derive evidence on the spins. For instance, it is very reasonable to assume that $^5He_\Lambda$ (formed by an α-particle and a Λ^0) has a spin $\frac{1}{2}$ if the Λ^0 has spin $\frac{1}{2}$, a spin $\frac{3}{2}$ if the Λ^0 has spin $\frac{3}{2}$, etc. The value of the spin of $^5He_\Lambda$ will be reflected in the angular and energy distributions of the decay mode (probably the most frequent)

$$^5He_\Lambda \to {}^4He + p + \pi^- .$$

However, it should be remarked that in a Λ^0-nucleus the non-mesonic decay mode would result much more frequent than the mesonic one if the Λ^0 were assumed to have a very high spin. This conclusion follows from the same argument which was given last year ([7]) to demonstrate the inconsistency at the high spin hypothesis to explain the long lifetimes. The transition probability for the mesonic decay mode $\Lambda^0 \to N + \pi$ is strongly weakened, from angular momentum considerations, if the Λ^0 has an high spin. On the other hand, the transition probability for the non-mesonic decay mode $\Lambda^0 + N \to N + N$ is much less weakened, because of the higher Q-value, because of the larger masses of the final particles which entrain larger relative momenta, and also due to the tail of the momentum distribution of the bound Λ^0 and N, which may thus collide with higher relative momenta. It seems that a value higher than $\sim \frac{7}{2}$ for the Λ^0 spin would be inconsistent with the observed lifetimes of the Λ^0-nuclei (which could result much smaller, due to the predominance of the non-mesonic decay mode), and with the observed mesonic to non-mesonic ratio.

* * *

I would like to thank Prof. W. F. FRY and his collaborators who have kindly sent a preprint of their work prior to publication.

([6]) See, for instance WALKER amd SHEPHERD (preprint).
([7]) R. GATTO: *Il Nuovo Cimento* **1**, 375 (1955).

IL NUOVO CIMENTO Vol. III, N. 2 1° Febbraio 1956

A Quantum Theory of Refractive Index, Čerenkov Radiation and Ionization Loss.

D. A. Tidman

The F.B.S. Falkiner Nuclear Research and Adolph Basser Computing Laboratories School of Physics (*), The University of Sydney - Sydney N.S.W.

(ricevuto il 16 Gennaio 1956)

The effect of polarisation on the energy loss of a fast charged particle passing through matter was first treated classically by Fermi [1], who found that the ionization loss reached a plateau value at some very high energy. He also obtained a flux of radiation at large distances from the path of the particle which he identified with Čerenkov radiation. The classical theory of Čerenkov radiation had previously been worked out by Frank and Tamm [2].

Several authors [3] have attempted a quantum mechanical theory of Čerenkov radiation but none have given a quantum treatment of the effect of polarisation on the ionization loss. We describe here a new approach to these related problems. This was arrived at by first writing in hamiltonian form the equations of the classical electromagnetic field in a medium of extended induced dipoles [4].

Consider the transformation

$$(1) \qquad \begin{cases} \bar{q} = \mu_\lambda^{-1} \bar{Q}_\lambda \\ \bar{p}_\lambda = \mu_\lambda \bar{P}_\lambda \end{cases}$$

of the classical canonical variables $\bar{q}_\lambda$ and $\bar{p}_\lambda$ of the radiation field. μ_λ is the index of refraction. This transformation enables one to describe the total field in the medium as a superposition of oscillators each with the correct time dependence of the field in the refracting medium.

We now apply a transformation of the same form to the usual quantum mechanical Hamiltonian H of the radiation field in interaction with a medium of atoms. Leaving μ_λ undefined for the moment we find the following expression

(*) Also supported by the Nuclear Research Foundation within the University of Sydney.

(1) E. Fermi: *Phys. Rev.*, **57**, 485 (1940).

(2) I. Frank and I. Tamm: *Compt. Rend.*, **14**, 109 (1937).

(3) J. M. Jauch and K. M. Watson: *Phys. Rev.*, **74**, 950 and 1485 (1948); **74**, 1249 (1949); S. M. Neamtan: *Phys. Rev.*, **92**, 1362 (1953); **94**, 327 (1954).

(4) M. Born: *Optik*, p. 313.

for the transformed Hamiltonian:

$$(2)\qquad \bar{H}=\left[H_M+\tfrac{1}{2}\sum_\lambda(\bar{P}_\lambda^2+\bar{\nu}_\lambda^2\bar{Q}_\lambda^2)\right]-$$
$$-\sum_{i,\lambda}e_i\alpha\mu_{-\lambda}^{-\frac{1}{2}}(Q_\lambda A_{-\lambda}+Q_\lambda^* A^*_{-\lambda})+$$
$$+\tfrac{1}{2}\sum_\lambda(\mu_\lambda^2-1)\bar{P}_\lambda^2=$$
$$=\bar{H}_0+\bar{H}_{\lambda M}+\tfrac{1}{2}\sum_\lambda(\mu_\lambda^2-1)\bar{P}_\lambda^2\dots .$$

Here H_M is the Hamiltonian of the medium, $\bar{Q}_\lambda=Q_\lambda+Q_\lambda^*$, $\bar{\nu}_\lambda=\nu_\lambda\mu_\lambda^{-1}$ and $\sum_i$ sums over all the electrons of the medium.

Consider the state of the system in which the medium is in quantum state A and only one real photon is present in state λ. We can compute the excitation energy of this state (compared to no real photons present) to some order of perturbation theory. Let this energy be $E_{A\lambda}+\hbar\nu_\lambda$. We now fix the parameter μ_λ in (1) by demanding that the zero-order transformed Hamiltonian $\bar{H}_0$, applied to this state, have the eigenvalue $E_A+\hbar\nu_\lambda+E_{A\lambda}$ where E_A is the eigenvalue of H_M. This is the standard way of treating secular perturbations, and gives

$$\mu_\lambda=\frac{\hbar\nu_\lambda}{\hbar\nu_\lambda+E_{A\lambda}}.$$

Now consider quantum states in which several radiation oscillators have occupation numbers $n_\lambda\neq 0$. The transformation (1) with μ_λ defined by (3) now fails to satisfy the condition we imposed. However the eigenvalues of $\bar{H}_0$ differ from the eigenvalues of H (as found by the perturbation method) only by terms of the fourth order.

In order to fix the physical meaning of μ_λ consider the time dependence of the operators Q_λ^* in our new zero-order system.

We obtain

$$(4)\qquad \langle A;\bar{0}\dots\bar{1}_\lambda\dots\bar{0}|Q_\lambda^*|A;\bar{0}\dots\bar{0}\dots\bar{0}\rangle+$$
$$+\frac{\nu_\lambda^2}{\mu_\lambda^2}\langle A;\bar{0}\dots\bar{1}_\lambda\dots\bar{0}|Q_\lambda^*|A;\bar{0}\dots\bar{0}\dots\bar{0}\rangle=0$$

This shows that μ_λ is the refractive index of the medium in state A. Equation (3) is therefore our quantum mechanical definition of the refractive index. It agrees with a definition proposed on formal grounds by Neamtan [3].

Eigenvalues of the new zero-order oscillators $\frac{1}{2}(\bar{P}_\lambda^2+\bar{\nu}_\lambda^2\bar{Q}_\lambda^2)$ include the polarization energy of the medium. We have

$$(5)\qquad \bar{E}_\lambda=\hbar\bar{\nu}_\lambda=\hbar\nu_\lambda+E_{A\lambda}.$$

We call these quanta of the field in interaction with the medium « physical photons ». They have a self energy deriving from polarisation of the medium in which they are propagated. The momentum of a « physical photon » of energy $\bar{E}_\lambda$ is

$$(6)\qquad |P_{-\lambda}|=\frac{\bar{E}_\lambda\mu_\lambda}{c}.$$

We have applied the transformation (1) to the Hamiltonian for a fast charged particle passing through a medium of atoms. The particle is then accompanied by its field of virtual « physical photons ». A particle in free space cannot radiate photons because of the conservation laws, but in passing through matter it may radiate « physical photons » as a consequence of the changed energy momentum relation (6). This process is the Čerenkov radiation. In addition, combination of the relation (6) and radiation damping theory leads directly to the Fermi saturation of the ionization loss at high energies.

These calculations will be reported more fully in a later paper.

* * *

I am grateful to Dr. J. Blatt who suggested the approach to this problem, and to Dr. M. R. Schafroth, Mr. J. E. Moyal and Dr. S. T. Ma for useful discussions. I am also indebted to the University of Sydney Research Committee for the provision of a research grant.

Production d'un hyperfragment par capture d'un hypéron négatif.

Ph. Rosselet, R. Weill et M. Gailloud

Laboratoire de Recherches Nucléaires
École Polytechnique de l'Université de Lausanne

(ricevuto il 23 Gennaio 1956)

L'évènement décrit ci-dessous a été observé dans un stack de 108 émulsions pelées Ilford G5 ($12'' \times 8'' \times 600$ μm) exposé au rayonnement cosmique à 30 km d'altitude (Vol du Texas 1955).

Une particule (*a*) issue d'une étoile 10+5n parcourt 2310 μm avant d'être capturée à l'arrêt puis absorbée par un noyau de l'émulsion, avec destruction de ce noyau. Une des branches (*b*) de l'étoile de capture présente l'aspect caractéristique d'un fragment excité se désintégrant au repos en un méson π négatif (*f*) et un noyau de recul (*e*).

Caractéristiques des diverses traces.

	Nature	Longueur (μm)	Energie (MeV)	Temps de Vol (s)
a	Σ^-	2310	25	$5 \cdot 10^{-11}$
b	$^4H^*$	375	15	$2 \cdot 10^{-11}$
c	^4He	11.5	3.3 (*)	—
d	^4He	24.9	5.9 (*)	—
e	^3He	3.2	0.9 (*)	—
f	π^-	15500	30.0 (+)	—

(*) Relation Energie – Parcours de Steigert. [1]
(+) Relation Energie – Parcours de Baroni [2].

[1] R. Steigert: *Phys. Rev.*, **83**, 474 (1951).
[2] G. Baroni, C. Castagnoli, G. Cortini, C. Franzinetti et A. Manfredini: *Publications du CERN* BS9.

Désintegration de l'Hyperfragment.

La trace (*b*), d'après le nombre de lacunes, peut être identifiée à celle d'une particule de charge 1 en fin de parcours.

La trace (*f*) s'arrête dans l'émulsion après un parcours, pratiquement horizontal, de 15 500 μm, et produit une étoile σ caractéristique d'un méson π négatif. Quant au noyau de recul (*e*) sa trace est trop courte pour fournir directement le moindre renseignement.

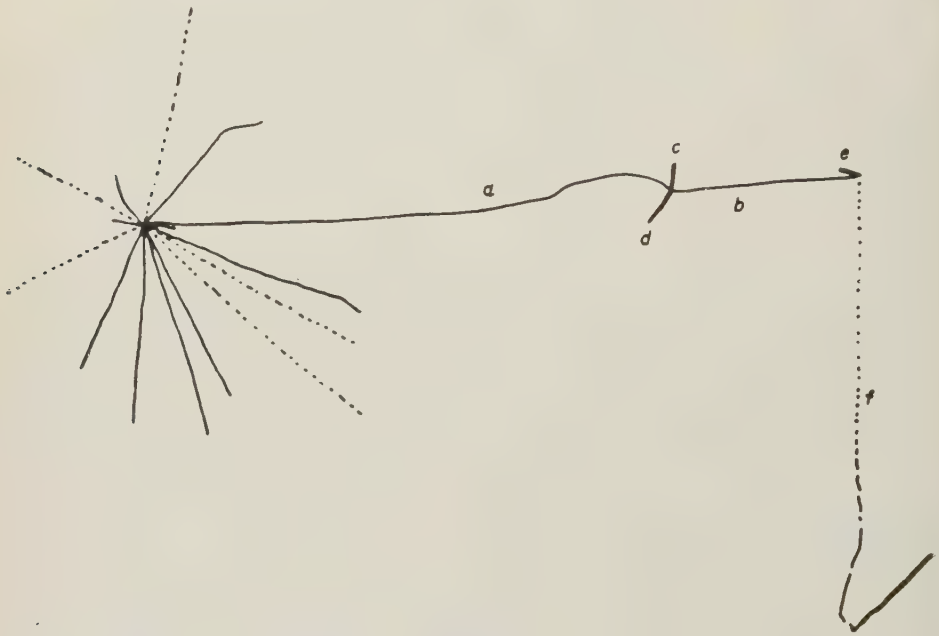

Fig. 1.

Les traces (*e*) et (*f*) ne sont pas colinéaires, ce qui implique, pour l'équilibre des quantités de mouvement, qu'un neutron ait été émis simultanément. Il ne peut s'agir d'une désintégration en vol en 2 particules, les deux traces étant dirigées vers l'arrière par rapport à la direction de (*b*).

Le seul schéma possible de désintégration d'un hyperfragment de charge 1, présentant l'aspect décrit, est:

(1) $\quad {}^4\mathrm{H}^* \rightarrow {}^3\mathrm{He} + \mathrm{n} + \pi^- .$

L'énergie du neutron, calculée de manière à satisfaire la condition de conservation des quantités de mouvement, est de 4 MeV, ce qui donne pour le bilan énergétique total de la désintégration:

$$Q = 30 + 0.9 + 4.0 = 34.9 \pm 0.5 \text{ MeV} .$$

Cette valeur est tout à fait compatible avec l'hypothèse d'un Λ^0 lié à un fragment nucléaire, à un triton dans le cas particulier.

L'énergie de liaison de l'hypéron est alors:

$$B_{\Lambda^0} = B_{^3\mathrm{He}} - B_{^3\mathrm{H}} + Q_{\Lambda^0} - Q$$

où Q_Λ est l'énergie libérée par la désintégration du Λ^0 libre

$$(\Lambda^0 \rightarrow \mathrm{p} + \pi^- + 36.9 \pm 0.2 \text{ MeV})$$

$$B_{\Lambda^0} = -0.8 + 36.9 - 34.9 = 1.2 \pm 0.7 \text{ MeV}.$$

Étoile de capture.

L'hyperfragment considéré ci-dessus est créé dans un phénomène d'absorption d'une particule négative par un noyau de l'émulsion. Plusieurs cas ont été observés de production d'un fragment instable par capture d'un méson K négatif et, à notre connaissance, un seul cas par capture d'un hypéron [3]. Ces deux phénomènes sont conformes aux prévisions théoriques de GELL-MANN et PAIS.

La masse de la particule absorbée a été déterminée par diffusion multiple (méthode de la flèche constante) et d'après le nombre de lacunes en fonction du parcours restant. La première méthode ne donne qu'un ordre de grandeur et permet seulement d'affirmer que la masse est supérieure à celle du proton ($(2 \pm 0.5)\ m_p$). Le comptage de lacunes donne une masse de 2270 ± 110 masses électroniques, l'étalonnage ayant été fait par rapport aux protons et aux deutérons.

Nous sommes donc en présence du phénomène élémentaire suivant:

$$(2) \qquad \Sigma^- + p \rightarrow n + \Lambda^0 ,$$

le Λ^0 restant lié à un fragment du noyau capteur. Des considérations énergétiques vont nous permettre de préciser davantage la masse de la particule capturée.

L'examen des traces (*c*) et (*d*) nous fournit peu de renseignements sur leur nature; on peut tout au plus affirmer que la charge de ces particules n'est pas supérieure à 2. Supposons que nous ayons affaire à deux particules α; ceci nous suggère l'interprétation suivante du phénomène:

$$(3) \qquad \Sigma^- + {}^{12}C \rightarrow n + 2\,{}^4He + {}^4H^* ,$$

hypothèse la plus simple, le carbone étant le noyau le plus léger présent dans l'émulsion, à part l'hydrogène.

Les trois particules chargées ont une quantité de mouvement totale de 225 MeV/c, qui est équilibrée par un neutron de 26,9 MeV. Le bilan énergétique de la réaction (3) est ainsi de 51 ± 3 MeV. Compte tenu des énergies de liaison, celui de la réaction (2) est 76.5 ± 3 MeV, d'où pour la masse du Σ^-:

$$m_{\Sigma^-} = m_{\Lambda^0} + 76.5 + m_n - m_p =$$

$$= 2181 + \frac{76.5 + 1.3}{0.51}$$

$$\boxed{m_{\Sigma^-} = 2333 \pm 7\ m_e} .$$

Rappelons que la valeur trouvée pour les Σ^+ se désintégrant au repos est $2327 \pm 3\ m_e$. Ce résultat confirme nos hypothèses concernant la nature de la particule capturée et celle du noyau capteur, car il est très peu probable qu'un tel accord soit fortuit.

Étoile-mère de l'Hypéron.

Toutes les branches de cette étoile ont été suivies jusqu'à leur point d'arrêt ou, sur plusieurs centimètres, jusqu'à leur sortie du stack, afin de déceler la présence éventuelle d'un méson lourd.

Aucune des traces s'arrêtant ne présente un secondaire visible.

Des mesures de diffusion multiple et de densité de grains sur les traces sortantes nous conduisent aux deux résultats important suivants:

1) Aucune de ces particules n'a une masse inférieure à celle du proton, donc aucun méson lourd chargé n'est produit dans le phénomène.

2) Aucune n'est assez énergique pour être le primaire de l'étoile dont l'énergie totale est supérieure à 1 GeV. Le primaire est donc une particule neutre, vraisemblablement un neutron, qui produit la réaction suivante avec un neutron appartenant à un noyau lourd de l'émul-

[3] M. CECCARELLI, N. DALLAPORTA, M. GRILLI, M. MERLIN, G. SALANDIN, B. SECHI et M. LADU: *Nuovo Cimento*, **2**, 542 (1955).

sion:

$$n + n \rightarrow \Sigma^- + K^0 + p$$

selon les règles de GELL-MANN de la production associée.

Conclusions.

Nos observations confirment que la particule connue par sa désintégration en vol $\Sigma^- \rightarrow n + \pi^- + \sim 110$ MeV est susceptible, lorsqu'elle arrive à l'arrêt dans l'émulsion photographique, d'être absorbée par un noyau, avec production d'un Λ^0 qui peut rester lié.

Nous ne pouvons pas exclure l'existence d'un état intermédiaire Σ^0 qui réagirait rapidement suivant

$$\Sigma^0 + N \rightarrow \Lambda^0 + N .$$

Il est intéressant de remarquer que, si la masse du Σ^+ est connue avec grande précision ($\pm 3\ m_e$), celle du Σ^- n'était jusqu'à présent qu'assez mal déterminée

Notre mesure est sans doute la plus précise parmi celles où la charge est connue avec certitude.

Il semble que le phénomène d'absorption du Σ^-, comme celui des mésons π^- et K^-, n'affecte pas un seul, mais simultanément plusieurs nucléons du noyau capteur, sinon la probabilité serait dérisoire de voir le Λ^0 rester lié sous forme d'hyperfragment.

La valeur trouvée pour l'énergie de liaison du Λ^0 est comparable à celle mesurée par LADU, LEVI SETTI et SCARSI [4] pour un phénomène identique (1.2 MeV) ainsi qu'aux valeurs trouvées dans les 3 cas observés de désintégration d'un $^4H^*$ suivant le schéma:

$$^4H^* \rightarrow {}^4He + \pi^- \quad [5] [6] [7]$$

Elle est aussi pratiquement identique à l'énergie de liaison du Λ^0 dans $^4He^*$ (8 cas observés) ce qui constitue un argument en faveur de l'identité des interactions (p, Λ^0) et (n, Λ^0), et confirme la valeur 0 pour le spin isotopique du Λ^0 [8]. La valeur moyenne de B_{Λ^0} pour tous les cas observés de $^4H^*$ et $^4He^*$ est de 1.5 MeV.

Addenda: Interprétation possible de l'événement Y-Br_{12}.

En plus des deux exemples mentionnés ci-dessus, l'événement Y-Br_{12} décrit par FRIEDLANDER, KEEFE et MENON (*Nuovo Cimento*, **1**, 482 (1955)) présenté comme la capture d'un hypéron négatif, nous paraît pouvoir s'interpréter plus simplement par la désintégration d'un hyperfragment, suivant le schéma:

$$^4H^* \rightarrow {}^3He + n + \pi^- .$$

Sur la base de cette interprétation, nous avons calculé les valeurs suivantes des énergies:

^3He	3.6 MeV
π^-	29.6
n	2.6

soit $Q = 34.8$ MeV, valeur tout-à-fait comparable à celles trouvées dans les deux cas précités, et sans doute même plus précise. L'énergie de liaison du Λ^0 dans le fragment serait de 1.3 ± 0.6 MeV.

(4) M. LADU, R. LEVI SETTI et L. SCARSI: *Comptes-Rendus du Congrès de Pise*, p. 487 éd. miméographique (1955).

(5) M. W. FRIEDLANDER, D. KEEFE et M. G. K. MENON: *Nuovo Cimento*, **2**, 663 (1955).

(6) J. CRUSSARD, V. FOUCHÉ, G. KAYAS, L. LEPRINCE-RINGUET, D. MORELLET, F. RENARD et J. TREMBLEY: *Comptes-Rendus du Congrès de Pise*, p. 481 éd miméographique (1955).

(7) OSLO et COPENHAGUE: *Comptes-Rendus du Congrès de Pise*, p. 505 éd. miméographique (1955).

(8) R. H. DALITZ: *Phys. Rev.*, **99**, 1475 (1955).

* * *

Nous adressons nos remerciements à Monsieur le Professeur CH. HAENNY, Directeur du Laboratoire, pour ses encouragements et pour l'intérêt qu'il a pris à notre travail. Nous remercions également Mr. LEHMANN pour la part qu'il a prise à certaines mesures.

Nous avons bénéficié du vol du Texas, généreusement organisé par l'Office of Naval Research, grâce au Dr. A. ROBERTS, à qui nous exprimons notre reconnaissance, ainsi qu'au Centre Européen de Recherches Nucléaires, à Genève,

Nous remercions le Prof. HOUTERMANS ainsi que plusieurs de ses collaborateurs, le Dr. TEUCHER en particulier, pour le traitement des émulsions qui a été poursuivi et organisé dans son Institut.

Ce travail a été effectué grâce à l'appui financier du Fonds National Suisse pour la Recherche Scientifique.

ADDENDUM

TO

On the Masses and Modes of Decay of Heavy Mesons Produced by Cosmic Radiation.

(G. STACK COLLABORATION)

Nuovo Cimento, Vol. 2, 1063-1103 (1955).

The Authors of the above article regret their omission from Appendix II, pag. 1101, *of the following Section:*

« 3*b*) *Error.* The error on $p\beta$ measured by scattering was determined from the formulae of Molière-d'Espagnat [1], modified to take into account the non-normal distribution of the angles of scattering [2]. The relative curves and experimental values can be found in two contributions on scattering [3,4], to the Pisa Conference ».

---

[1] B. d'ESPAGNAT: *Journ. de Phys. et Rad.*, **13**, 74 (1952).

[2] M. HUYBRECHTS: *Thèse de Doctorat*, Université Libre de Bruxelles.

[3] M. DI CORATO, D. HIRSCHBERG and B. LOCATELLI: *Pisa Conference*, June 1955, cyclostiled report, p. 275.

[4] R. K. W. JOHNSTON: *Pisa Conference*, June 1955, cyclostiled report, p. 287.

LIBRI RICEVUTI E RECENSIONI

M. Goeppert Meyer and J. H. D. Jensen – *Elementary theory of nuclear shell structure*, pp. XVI+ +269, J. Wiley & Sons Inc. New York e Chapman & Hall, London, 1955.

La fisica nucleare procede, da alcuni anni, lungo due distinte strade. Il punto di partenza comune è costituito dalle cosidette « regole di Mattauch » che sintetizzano le conoscenze relative alla stabilità dei nuclei. Dall'analisi di queste regole si ricavano le proprietà delle forze nucleari quali, ad esempio, la saturazione e l'indipendenza dalla carica. Stabilite tali caratteristiche generali, si cerca di soddisfarle facendo ricorso a tutti i tipi di forze che possono agire fra nucleoni, naturalmente tenendo presenti i risultati delle esperienze di diffusione.

Una seconda via per inquadrare i fenomeni è quella del modello « a shell », detto anche « a particelle indipendenti ». In questo caso, per mezzo di un accurato esame statistico delle proprietà dei nuclei, si elencano, per prima cosa, tutte le regolarità che esistono nei fenomeni nucleari. Subito dopo si cerca di stabilire una analogia tra il caso di un atomo a molti elettroni, trattato col metodo di Hartree-Fock e un nucleo, supponendo che un nucleone si muova nel campo medio generato da tutti i rimanenti nucleoni. Si introduce, anche in questo caso, sia il concetto di momento orbitale con numero quantico l, che l'accoppiamento tra spin e orbita dei nucleoni. Il tipo di accoppiamento scelto è quello *jj*, in contrasto col caso atomico, in cui si ha normalmente l'accoppiamento Russel-Saunders.

Un tale modello, relativamente semplice, riesce a inquadrare una grande massa di dati sperimentali, con rare eccezioni, per nuclei con numeri di massa A fino a 140.

I problemi trattati in particolare in questo libro riguardano in primo luogo la giustificazione dei « numeri magici » e, inoltre, le proprietà dei nuclei nello stato fondamentale, i momenti di quadrupolo nucleare, lo spostamento spettrale isotopico, il decadimento beta, i momenti magnetici dei nuclei. La trattazione è svolta in un complesso di tredici capitoli e di quattro appendici matematiche. Ogni capitolo in cui venga esposta una applicazione della teoria « a shell » è generalmente seguito da un riassunto in cui sono indicati in breve i risultati acquisiti e i limiti della teoria. Completano il libro estese tabelle in cui sono posti a confronto i dati sperimentali e le previsioni teoriche; la notazione usata è tale da stabilire immediatamente gli eventuali punti di disaccordo.

Malgrado la formulazione del titolo, questo libro è tutt'altro che elementare; è vero che in esso buona parte del formalismo matematico è racchiuso in una appendice a sè, ma accade frequentemente che risultati teorici e sperimentali vengano richiamati così sommariamente da disorientare un lettore che non abbia già una buona conoscenza della fisica nucleare. Questa critica può essere solo in parte annullata dall'avvertimento contenuto nella prefazione del libro, quando si dice che « elementare » va inteso nel senso che si fa uso solo di concetti elementari di fisica teorica.

Una seconda critica è legata alla mancanza di sufficienti giustificazioni

della cattiva prova del modello « a shell » quando esso venga applicato alla trattazione dei nuclei di numero di massa elevato. Nel caso, per esempio, del decadimento beta, sono tabulati, con grande dettaglio, i nuclei fino ad $A = 143$, mentre per quanto riguarda numeri di massa superiori, le poche osservazioni contenute alla fine del capitolo sono insufficienti a stabilire se si ha una discordanza tra teoria ed esperienza e in quale misura.

È molto probabile che la causa della rapidità di esposizione, a volte eccessiva, vada ricercata nel desiderio degli Autori di non sovraccaricare troppo il libro con digressioni dall'argomento fondamentale.

A parte queste osservazioni, che, come si è già detto, perdono il carattere di appunti al libro qualora si supponga nel lettore una buona conoscenza della fisica nucleare non disgiunta da senso critico, la lettura del volume è utilissima. I successi ottenuti dal modello a particelle indipendenti, infatti, sono tali che anche in avvenire non si potrà prescindere dalle idee che sono alla base di questa teoria. Ciò è provato del resto, anche dai recenti sviluppi del cosiddetto « modello collettivo », che, partendo dalle posizioni del modello a shell è riuscito a inquadrare molti fatti sperimentali relativi ai nuclei pesanti.

G. Cortellessa

Direttore responsabile: G. Polvani Tipografia Compositori - Bologna

Questo fascicolo è stato licenziato dai torchi il 10-II-1956